This electronic thesis or dissertation has been downloaded from the King's Research Portal at https://kclpure.kcl.ac.uk/portal/

A functional investigation of human regulatory T cell subsets in health and pregnancy related diseases

Harris, Ffion

Awarding institution:
King's College London

The copyright of this thesis rests with the author and no quotation from it or information derived from it may be published without proper acknowledgement.

END USER LICENCE AGREEMENT

Unless another licence is stated on the immediately following page this work is licensed

under a Creative Commons Attribution-NonCommercial-NoDerivatives 4.0 International

licence. https://creativecommons.org/licenses/by-nc-nd/4.0/

You are free to copy, distribute and transmit the work

Under the following conditions:

- Attribution: You must attribute the work in the manner specified by the author (but not in any way that suggests that they endorse you or your use of the work).
- Non Commercial: You may not use this work for commercial purposes.
- No Derivative Works - You may not alter, transform, or build upon this work.

Any of these conditions can be waived if you receive permission from the author. Your fair dealings and other rights are in no way affected by the above.

Take down policy

If you believe that this document breaches copyright please contact librarypure@kcl.ac.uk providing details, and we will remove access to the work immediately and investigate your claim.

Download date: 31. Oct. 2023

A functional investigation of human regulatory T cell subsets in health and pregnancy related diseases

Submitted by Ffion Harris

Thesis submitted to King's College London for the degree of Doctor of Philosophy

Department of Immunobiology

School of Immunology & Microbial Sciences

December 2022

Abstract

Regulatory T cells (Tregs) have been implicated in the pathogenesis of many human diseases from classical autoimmune diseases to cancer, and their role in inducing tolerance in transplantation and at the foetal-maternal interface is increasingly recognised. Tregs can express a huge variety of surface markers giving rise to phenotypically diverse subsets. This thesis therefore aimed to carry out a phenotypic and functional analysis of subsets of Tregs in healthy donors and in the context of pregnancy. In the first experimental chapter, our key hypothesis was that Treg subsets with differing surface phenotypes would display differing functional properties. Flow cytometric analysis was carried out in 10 healthy donors using both manual gating and unbiased clustering methods. Using manual gating, we identified several previously reported Tregs subsets, while unbiased analyses enabled us to identify novel populations. We then simultaneously compared the function of several Treg subsets in healthy donors using an *in vitro* Treg suppression assay optimised for small cell numbers. Results from this assay showed that naïve Tregs expressing CD31 were significantly more suppressive than bulk Tregs and memory Treg subsets. We also found preliminary evidence suggesting an enhanced ability of these cells to suppress IL-2 production. The second experimental chapter then further investigated the *ex vivo* expansion properties of this subset. We found that naïve $CD31^+$ Tregs had an equal expansion potential to bulk, memory, or naïve Tregs. As analysed by flow cytometry, this subset also had stable FoxP3 expression throughout expansion, and expressed significantly higher Helios than all the other expanded Tregs at 28 days of expansion. A large proportion of naïve Tregs co-expressed CD45RA and CD95 at the end of 6 weeks of expansion involving

strong TCR stimulation. Therefore, in the following chapter we hypothesised that Tregs with stem cell-like memory potential could exist in the Treg compartment. As analysed by a 16-marker flow cytometry panel, we observed FoxP3^{+}Helios^{+} Tregs with a stem cell-like memory phenotype. However, we saw no conclusive evidence of stem cell-like memory function in these Tregs after expanding the cells in culture. In the final experimental chapter, we investigated the phenotype and prevalence of Treg subsets in healthy pregnancy compared to pregnant women with pre-eclampsia and gestational diabetes mellitus (GDM) stratified for 3 different treatment interventions. Through manual gating and unbiased clustering analyses we found that Tregs from GDM and pre-eclampsia mothers were skewed towards a memory phenotype, expressing surface markers such as CD45R0, CCR4, and CD95. Additionally, all GDM groups had a significantly reduced frequency of CXCR5^{+} Tregs, and unbiased Treg clusters which were significantly more abundant in healthy pregnant women compared to GDM groups and pre-eclampsia were predominantly of a naïve CD73^{+} phenotype. Finally, we found that the *in vitro* suppressive capacity of bulk Tregs from GDM and pre-eclampsia mothers was significantly reduced compared to healthy pregnant controls and an inverse correlation between CD45R0 expression and suppression was found. Collectively data from this thesis show that the surface phenotype of Tregs dictates the functional properties of Treg subsets and that the balance of frequencies of Treg subsets may differ in immune pathologies.

Acknowledgements

First and foremost, I would like to thank my supervisor Professor Tim Tree for giving me the opportunity to undertake this PhD in his lab. On both an academic and pastoral level, Tim has been a constant source of support, guidance, and endless positivity over the past 4 years, and I am forever grateful for his mentorship and kindness. Also, thank you to the KCL MRC-DTP for funding this PhD studentship.

Thank you to my second supervisor and thesis committee members Shahram Kordasti, Georgina Ellison, Giovanna Lombardi, and Alberto Sanchez-Fueyo for your valuable advice and thoughtful recommendations. I am also very grateful to Panicos Shangaris for providing the pregnancy study samples.

Thank you to all the members of the Tree lab for teaching me your technical expertise, for lending a helping hand with my experiments, and for making this lab a great place to work. A special thank you to Jennie Yang from whom I've learned so much. Thanks also to Semah Abdu for your friendship throughout our PhDs and for the fun we had together during our graduate teaching activities.

I am so fortunate to have a supportive family, Mum, Dad, Rhiannon, and Dad Cu, who have always encouraged me to pursue my ambitions. Thank you to my closest friends Catrin and Eve who have helped me to feel proud of every milestone, no matter how small. Finally to Jon, thank you for being a source of peace, happiness, and steadfast support throughout our PhD journeys.

Table of Contents

List of abbreviations

ADP – adenosine diphosphate

AIRE – autoimmune regulator

AMP – adenosine monophosphate

ANOVA – analysis of variance

APC – antigen presenting cell

APECED – autoimmune polyendocrinopathy-candidiasis-ectodermal dystrophy

AS – ankylosing spondylitis

ATP – adenosine triphosphate

CAR – chimeric antigen receptor

CFSE – carboxyfluorescein succinimidyl ester

CIA – collagen-induced arthritis

CNS – central nervous system

CPM – counts per minute

cTECs – cortical thymic epithelial cells

CTLA-4 – cytotoxic T-lymphocyte associated protein 4

CTV – CellTrace violet

CyTOF – mass cytometry

CV – coefficient of variance

DCs – dendritic cells

DN – double negative thymocytes

DP – double positive thymocytes

DPBS – Dulbecco's phosphate-buffered saline

EAE – experimental autoimmune encephalomyelitis

EDTA – ethylenediaminetetraacetic acid

FACS – fluorescence-activated cell sorting

FBS – foetal bovine serum

FoxP3 – forkhead box protein P3

GDM – gestational diabetes mellitus

GFP – green fluorescent protein

GMP – good manufacturing practice

GvHD – graft versus host disease

GWAS – Genome wide association studies

HLA-DR – human leukocyte antigen-DR

IBD – inflammatory bowel disease

ICOS – inducible T cell co-stimulator

IDO – Indoleamine 2,3-dioxygenase

IFN-γ – interferon-γ

IL – interleukin

IL-2 – interleukin-2

IL-2R – interleukin-2 receptor

IL-2Rα – interleukin-2 receptor α-chain

IL-2Rβ – IL-2 receptor β-chain

IL-2Rγc – IL-2 receptor γ-chain

ILCs – innate lymphoid cells

IPEX – immune dysregulation polyendocrinopathy enteropathy X-linked syndrome

IVF – *in vitro* fertilisation

JAK – Janus kinase

LAG3 – lymphocyte activation gene-3

MFI – mean fluorescence intensity

MHC – major histocompatibility complex

MS – multiple sclerosis

mTECs – medullary thymic epithelial cells

NK – natural killer cells

PBMCs – peripheral blood mononuclear cells

PD – percentage divided

PD-1 – programmed death-1

PD-L1 – programmed death ligand-1

PET – pre-eclampsia

PHA – phytohaemagglutinin

PIH – pregnancy-induced hypertension

PTEN – phosphate tensin homolog

PTPN2 – protein tyrosine phosphate N2

pTreg – peripheral Tregs

RA – rheumatoid arthritis

RTE – recent thymic emigrant

Sca-1 – stem cell antigen-1

SCID – severe combined immunodeficiency

SD – standard deviation

SEB – staphylococcal enterotoxin B

SEM – standard error or the mean

SOM – self-organising maps

SP – single positive thymocytes

SLE – systemic lupus erythematosus

SNP – single nucleotide polymorphism

SS – systemic sclerosis

STAT5 – signal transducer and activator of transcription 5

T1D – type 1 diabetes

T_{CM} – central memory T cells

Tconv – conventional T cell

TCR – T cell receptor

T_{EM} – effector memory T cells

Tfh – T follicular helper

Tfr – T follicular regulator

TGF-β – transforming growth factor-β

TIGIT – T-cell immunoreceptor with immunoglobulin and ITIM domains

T_N – T naïve

TNF – tumour necrosis factor

TRAIL – TNF-related apoptosis inducing ligand

TREC – TCR rearrangement excision circles

Treg – regulatory T cell

Tscm – stem cell-like memory T cells

TSDR – Treg-specific demethylated region

tSNE – t-distributed stochastic neighbour embedding

tTreg – thymic Tregs

V(D)J – variable, diversity, joining

1. Chapter 1. Introduction

1.1 T cells in Immune Regulation

1.1.1 Regulation vs autoimmunity

The adaptive immune system has evolved to recognise foreign antigens and provide the host with immune memory whilst simultaneously preventing an autoreactive immune response towards self-antigens. This balance between activation and regulation is essential to maintaining a state of health. However, the prevalence and number of different autoimmune diseases in the human population are testament to the many pitfalls which can result in loss of tolerance towards self-peptides.

T cells are a subset of lymphocyte which have crucial roles in both protection against infection and immune regulation. T lymphocytes are thus named as they develop in the thymus in early life (Hozumi & Tonegawa, 1976). Characterised by expression of CD3 and either CD4 or CD8 co-receptors, T cells use T cell receptors (TCR) expressed at their cell surface to recognise antigens presented in the context of major histocompatibility complexes (MHC) by antigen presenting cells (APCs). A T cell becomes activated when its TCR binds its cognate antigen presented on MHC molecules and adequate co-stimulation is provided by the APC.

The $CD4^+$ T cell pool largely consists of conventional T cells (Tconv) which differentiate into ‘helper’ subsets and aid in the activation of the immune system towards potential threats. However, approximately 5-10% of peripheral blood $CD4^+$ T cells are comprised of Regulatory T cells (Tregs) (Sakaguchi, Sakaguchi,

Asano, Itoh, & Toda, 1995) which are specialised to control the activation and proliferation of immune cells and play a crucial role in preventing autoimmunity.

1.1.2 Early T cell development and TCR diversity

During T cell development, bone marrow-derived progenitor cells are recruited to the thymus where they undergo a series of maturation stages before being released into the periphery. The role of the thymus in T cell development is evidenced in complete DiGeorge syndrome patients. This rare developmental disorder characterised by absence of the thymus leads to depletion of nearly all peripheral T cells and severe immune deficiency (Bastian et al., 1989). Allografts of infant thymic tissue have been shown to rescue T cell development in some patients (Markert et al., 1999).

Cord-blood progenitor cells expressing the haematopoietic stem cell marker CD34 begin to populate the thymus by week 9 of foetal development (Haynes & Heinly, 1995) (figure 1.1). $CD34^+$ precursors which upregulate CD1A are committed to the T cell lineage (Blom et al., 1999). Thymocytes then undergo a mechanism of somatic recombination known as V(D)J recombination (Blom, Res, Noteboom, Weijer, & Spits, 1997; Hozumi & Tonegawa, 1976). During this tightly regulated process (reviewed in Schatz & Ji, 2011), germline genes encoding the antigen-binding domains of the α and β TCR chains known as V(variable), D(diversity), and J(joining) gene segments are randomly rearranged, producing T cell progeny with a highly diverse TCR repertoire of up to 10^{15} unique TCRs (Zarnitsyna, Evavold, Schoettle, Blattman, & Antia, 2013).

This process has evolved to generate distinct T cell clones which can recognise a huge array of antigens derived from bacterial, viral, and parasitic pathogens. However due to the random nature of V(D)J recombination, this process also yields TCRs that are reactive to peripheral self-antigens. Therefore, these cells must be eliminated during thymic development to prevent systemic autoimmunity.

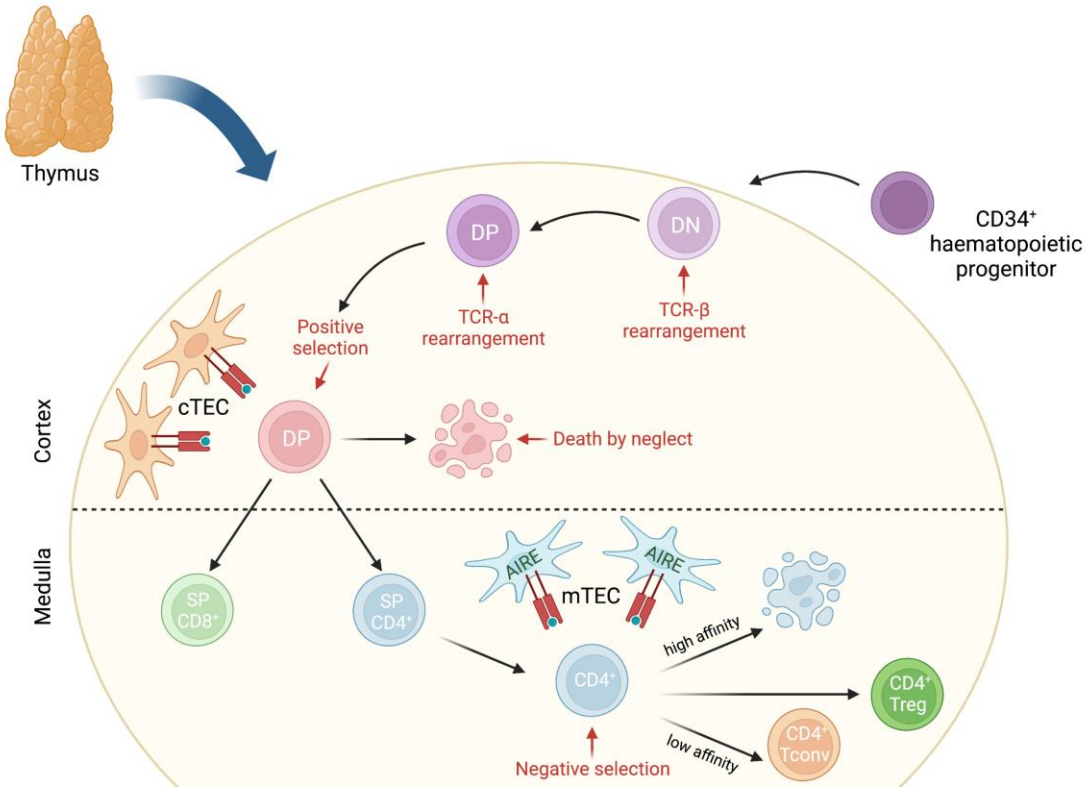

Figure 1.1: T cell development in the thymus. T cells are thus named as they develop from haematopoietic progenitor cells in the thymus. CD34+ haematopoietic progenitors migrate from the bone marrow to the thymic cortex. TCR-β chain rearrangement occurs during the double negative (DN) stage in which T cell progenitors express neither CD4 or CD8 co-receptors. TCR-α chain rearrangement occurs during the double positive (DP) stage in which T cell progenitors express both the CD4 and CD8 co-receptors simultaneously. Following this, double positive thymocytes survey self-MHC proteins expressed by cortical thymic epithelial cells (cTECs) and thymocytes bearing TCRs which are not able to bind self MHC undergo death by neglect in a process known as positive selection. Surviving thymocytes then migrate to the thymic medulla and downregulate either CD4 or CD8 coreceptors to become single-positive (SP) CD4+ or CD8+ thymocytes. Both CD4+ and CD8+ single positive thymocytes then undergo negative selection. Medullary thymic epithelial cells expressing the transcription factor autoimmune regulator (AIRE) allowing expression and presentation of peripheral antigens in the context of MHC. Thymocytes which experience strong TCR-self peptide-MHC binding affinity are deleted to prevent T cells with a potential to cause autoimmunity from reaching the periphery. T cells which experience intermediate TCR-peptide-MHC interactions can develop into regulatory T cells (Tregs) and those with a low binding affinity develop into conventional T cells (Tconvs). Created using BioRender.com

1.1.3 Central tolerance

Once developing thymocytes have undergone recombination of the TCR-β chain, the cells enter the double positive thymocyte stage by upregulation of both CD4 and CD8 co-receptors followed by subsequent TCR-α chain recombination (Trigueros et al., 1998) (figure 1.1). These double positive thymocytes then undergo a series of selection processes to deplete TCRs which are unable to interact with self-MHC proteins or TCRs which have the potential to cause autoimmunity.

Firstly, thymocytes scan MHC-self peptide complexes expressed by cortical thymic epithelial cells (cTECs). If low affinity interactions between the TCRαβ and MHC-peptide complexes occur, these cells are stimulated to survive and commit to either the $CD8^+$ or $CD4^+$ lineage depending on their affinity to MHC-I and II, respectively (reviewed by Klein, Kyewski, Allen, & Hogquist, 2014). As V(D)J recombination is a random process, over 90% of immature thymocytes bear TCRs which fail to recognise self-MHC and would be incapable of binding antigen in the periphery. Therefore these cells undergo 'death by neglect' (Klein et al., 2014). These two processes are known as positive selection which promotes the survival of T cells with TCRs which are capable of binding MHC-peptide complexes in the periphery.

The process of negative selection deletes T cells with TCRs which bind to self-peptide-MHC complexes with too high an affinity and have the potential to cause autoimmune activation in the periphery. $CD4^+$ and $CD8^+$ positively selected thymocytes express CCR7 allowing them to migrate into the thymic medulla

(Ueno et al., 2004). Here, medullary thymic epithelial cells (mTEC) express and present peripheral tissue-restricted antigens such as insulin and α-fetoprotein, a process which is mediated by the unique expression of the transcription factor autoimmune regulator (AIRE) by mTECs (Derbinski, Schulte, Kyewski, & Klein, 2001). Thymocytes which bind peripheral antigens with high affinity are deleted.

Thymocytes which bind self-antigen-MHC with intermediate affinity can develop into Tregs. This is evidenced by studies which show that the Tconv and Treg TCR repertoires only partially overlap (Pacholczyk, Ignatowicz, Kraj, & Ignatowicz, 2006) and the Treg TCR repertoire is skewed towards peripheral self-antigens (Hsieh et al., 2004). Moreover, autoimmune polyendocrinopathy-candidiasis-ectodermal dystrophy (APECED) is a primary autoimmune disorder caused by loss of function mutations in the AIRE gene. A significantly reduced Treg TCR repertoire and mean FOXP3 expression has been shown in these patients (Kekäläinen et al., 2007), consistent with failed thymic Treg selection and differentiation. In addition to thymically derived Tregs, sometimes referred to as 'natural' Tregs, Tregs can also be induced from naïve $CD4^+$ T cells in the periphery under tolerogenic conditions (Apostolou & Von Boehmer, 2004). These peripheral Tregs (pTregs) have a similar phenotype and suppressive capacity but are considered to be distinct and separate linages which play different roles in establishing tolerance, which is described in more detail below.

The mature thymocytes are then ready to exit the thymus. It is thought that only 3% of total thymocytes survive the selection processes and enter the periphery (Egerton, Scollay, & Shortman, 1990). Despite this stringent process, up to 40%

of low-affinity autoreactive Tconv cells can escape negative selection (Bouneaud, Kourilsky, & Bousso, 2000) and autoreactive Tconvs can be detected in the peripheral blood of healthy individuals (Danke, Koelle, Yee, Beheray, & Kwok, 2004; Snir et al., 2011). However, these cells are kept in a functionally suppressed state by Tregs in the periphery as evidenced in a study by Kim, Rasmussen, & Rudensky (2007) which showed that ablation of Tregs in both neonatal and adult mice leads to systemic autoimmunity.

1.2 Treg Discovery

1.2.1 Suppressive immune cells

Although the concept of suppressive cells in the immune system has existed since the 1970s, for at least 20 years this was a topic of controversy amongst immunologists. An early study by Gershon and Kondo was the first to demonstrate that the T cell compartment had a dual role in both activation and dampening of the immune response and suggested a distinct subset of T cells was responsible for inducing tolerance (Gershon & Kondo, 1970). However the field was limited by factors such as a lack of definitive markers characterising suppressive cells and no evidence of mechanisms which mediate suppression (Reviewed in Sakaguchi, 2011).

Many early studies showed that the thymus plays a key role in preventing autoimmunity. These studies demonstrated that day-3 neonatal thymectomy caused autoimmune inflammation targeting different organs such as the gut, ovaries, thyroid gland, and prostate gland depending on the strain of mouse used (Kojima & Prehn, 1981). Furthermore, Penhale *et al.* (1990) showed that

thymectomy and irradiation in adult rats caused rapid onset of type 1 diabetes and islet autoantibody production. Crucially, autoimmune destruction of targeted organs following thymectomy could be prevented through inoculation with normal $CD4^+$ T cells (Sakaguchi, Takahashi, & Nishizuka, 1982a), and $CD4^+$ T cells transferred from diseased mice were able to recapitulate autoimmune phenotypes in recipient nude mice (Sakaguchi, Takahashi, & Nishizuka, 1982b). These results collectively suggested that the $CD4^+$ T cell pool consists of subsets which act as opposing forces in driving and preventing autoimmunity and that disruption of thymic output tips the balance towards autoimmunity.

1.2.2 CD25 as a Treg biomarker

Research interests then turned to identifying a biomarker that distinguished suppressive $CD4^+$ T cells from self-reactive $CD4^+$ T cells. Sakaguchi *et al.* (1985) were the first to demonstrate that spontaneous multi-organ autoimmunity could be induced by adoptively transferring splenic T cells depleted of $CD4^+CD5^{hi}$ cells into athymic nude mice. Similar adoptive transfer studies were carried out using other biomarkers for *ex vivo* depletion such as $CD4^+CD45RC^{lo}$ T cells in rats (Powrie & Mason, 1990) and $CD4^+CD45RB^{lo}$ T cells in mice (Morrissey, Charrier, Braddy, Liggitt, & Watson, 1993; Powrie, Leach, Mauze, Caddie, & Coffman, 1993).

A seminal paper by Sakaguchi *et al.* (1995) then identified that the $CD5^{hi}$ and $CD45RB^{lo}$ $CD4^+$ T cell compartments were both encompassed in the $CD25^+$ $CD4^+$ T cell population, comprising 10-15% of mouse $CD4^+$ T cells. This study showed that depleting splenic $CD4^+$ T cell suspensions of $CD25^+$ cells caused

rapid, spontaneous, multiorgan autoimmunity when transferred into athymic nude mice. Histological evidence of gastritis, oophoritis, thyroiditis, sialoadenitis, adrenalitis, insulitis, glomerulonephritis, and arthritis was accompanied by autoantibody production in recipient mice. Depleting $CD25^+$ cells affected more target organs and disease occurred at a higher prevalence than depletion of $CD5^{hi}$ or $CD45RB^{lo}$ $CD4^+$ T cells in previous studies. This autoimmune phenotype could be prevented if an additional inoculum of $CD4^+CD25^+$ T cells was administered within days of the first (figure 1.2).

Subsequent studies then linked this population to previously published observations made in day-3 neonatal thymectomised mice. $CD4^+CD25^+$ cells are detectable in the periphery in 3-day old mice (Asano, Toda, Sakaguchi, & Sakaguchi, 1996), whereas $CD4^+CD8^-CD25^+$ thymocytes are detectable in the thymus but not the spleen in 2-day old mice (Itoh et al., 1999). Removal of the thymus at day-3 was shown to diminish $CD4^+CD25^+$ T cells in peripheral blood, allowing a window for autoimmune disease development (Asano et al., 1996). Inoculation of $CD4^+$ single positive thymocytes depleted of $CD25^+$ cells also lead to autoimmune disease in nude mice, further supporting the notion that these cells are thymically derived (Asano et al., 1996).

These $CD4^+CD25^+$ 'suppressor' cells then took on the name of regulatory T cells or Tregs. CD25, otherwise known as the interleukin-2 (IL-2) receptor α-chain, remains the most important cell surface receptor for identifying Tregs. The seminal studies from Sakaguchi and colleagues enabled the isolation and culture of Tregs, which further enhanced the understanding of their biology e.g., the

importance of IL-2 to the survival and function of Tregs and their suppressive mechanisms. Development of assays to measure the ability of mouse Tregs to suppress Tconv ($CD4^+CD25^-$) proliferation *in vitro* (Takahashi et al., 1998; Thornton & Shevach, 1998) finally enabled the confirmation that the human $CD4^+$ T cell compartment also contained Tregs, as shown by several different groups in 2001 (Baecher-Allan, Brown, Freeman, & Hafler, 2001; Dieckmann, Plottner, Berchtold, Berger, & Schuler, 2001; Jonuleit et al., 2001; Levings, Sangregorio, & Roncarolo, 2001; Stephens, Mottet, Mason, & Powrie, 2001; Taams et al., 2001).

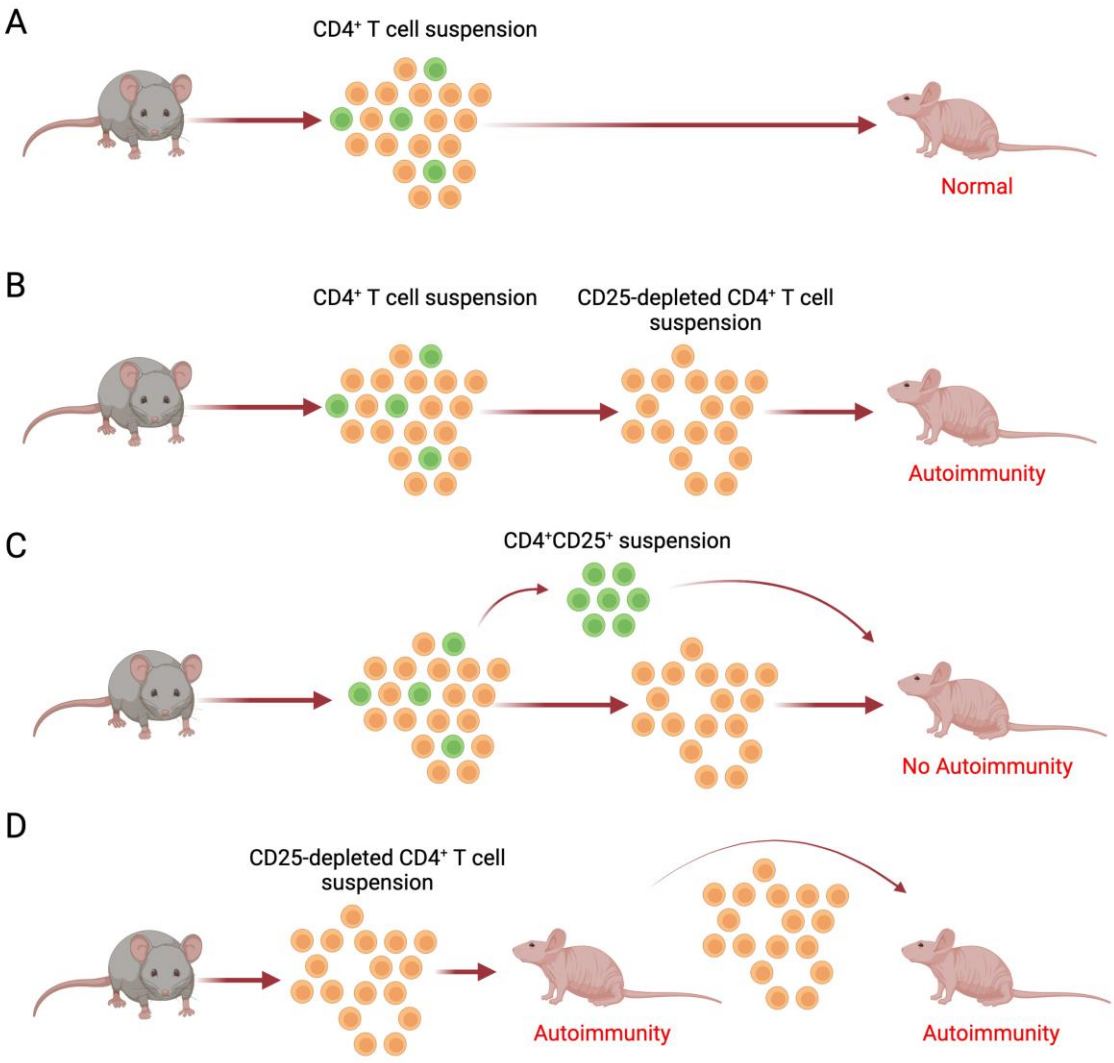

Figure 1.2: Adoptive T cell transfer used by the Sakaguchi group. In the seminal paper by Sakaguchi et al. (1995), $CD4^+CD25^+$ cells were first characterised as suppressive immune cells which had the capacity to prevent autoimmune disease. (A) Total $CD4^+$ T cells did not cause autoimmune symptoms when transferred into athymic nude mice. (B) $CD4^+$ T cell suspensions depleted of $CD25^+$ cells caused multi-organ autoimmunity when adoptively transferred into athymic nude mice. (C) When CD25-depleted T cell suspensions were transferred into athymic nude mice, autoimmunity did not develop when the recipient mice were reconstituted with $CD25^+$ cells within a limited time period (<10 days) after the initial T cell transfer. (D) CD25-depleted T cell suspensions caused autoimmune disease when transferred to athymic nude mice, and this autoimmune phenotype could be transferred through inoculation of T cell suspensions into secondary athymic nude mice. Created using BioRender.com.

1.2.3 FoxP3 as a Treg master regulator

The transcription factor Forkhead box protein P3 (Foxp3) was later identified as a master regulator of Treg development and function (Fontenot, Gavin, & Rudensky, 2003; Hori, Nomura, & Sakaguchi, 2003). Loss of function mutations in the FoxP3 gene were found to cause the previously described systemic autoimmune disease immune dysregulation polyendocrinopathy enteropathy X-linked (IPEX) syndrome in humans (Bennett et al., 2001) and causes a similar phenotype in the Scurfy mouse (Brunkow et al., 2001). Ectopic expression of FoxP3 in Tconv cells through retroviral transduction induces a suppressive function and phenotype (Hori et al., 2003). Tconv cells are also known to transiently upregulate FoxP3 upon activation (Wang, Ioan-Facsinay, van der Voort, Huizinga, & Toes, 2007), however Tregs constitutively express this protein. Liu et al. (2006) then described that the expression of intracellular FoxP3 in $CD4^+$ T cells is inversely correlated with expression of the IL-7 receptor CD127 at the cell surface, meaning that the $CD4^+CD25^{hi}CD127^{lo}$ surface phenotype yields a highly enriched Treg population.

It is thought that during thymic Treg development, initial intermediate TCR stimuli induce the activation of super-enhancers such as Satb1 prior to FoxP3 expression (Kitagawa et al., 2017). This leads to hypomethylation and expression of Treg-specific genes such as *IL2RA* (CD25), *Ikzf2* (Helios), *CTLA4*, and *FoxP3*, and this Treg-specific DNA hypomethylation pattern can be used to distinguish bona fide Tregs from activated Tconv cells (Ohkura et al., 2012). Many Treg signature genes such as *Ikzf2* (Helios) peak in expression before FoxP3 (Reviewed in Ohkura & Sakaguchi, 2020), and indeed $CD4^+CD25^+FoxP3^-$

thymocytes can differentiate into Tregs in culture (Lio & Hsieh, 2008). This suggests that the Treg lineage is established independently of FoxP3. However ablation of FoxP3 from fully differentiated Tregs causes loss of their suppressive capacity (Williams & Rudensky, 2007), and *ex vivo* expanded Tregs can also undergo a loss of FoxP3^{+} phenotype stability and suppressive activity in culture (Marek et al., 2011). This demonstrates that FoxP3 provides reinforcement and stabilisation of Treg gene signatures while repressing the expression of activating cytokines such as IL-2, interferon-γ (IFN-γ), and IL-4 (Reviewed in Vent-Schmidt, Han, Macdonald, & Levings, 2014).

1.2.4 Treg development in the thymus and the role of the TCR in Treg selection and function

As described above, the thymus has long been considered to be essential in generation of Tregs as Asano *et al.* (1996) showed that removal of the thymus up to 3 days after birth gives rise to spontaneous autoimmunity in mice, and CD4^{+}CD25^{hi} cells are readily detectable in the periphery after 3 days. Itoh *et al*. (1999) also showed that CD4^{+}CD25^{hi} cells are detectable in the thymus in day-2 neonatal mice, demonstrating that migration of these cells from the thymus at day 3 is essential for prevention of autoimmunity. As these cells arise from the same common progenitors as Tconvs and express productive TCRs at their cell surface, Tregs must be subjected to the same thymic selection processes which occur during central tolerance.

TCR transgenic mice have been a powerful tool in understanding the importance of TCR engagement and specificity during thymic development of Tregs. Itoh *et*

al. (1999) showed that while DO11.10 TCR transgenic mice expressing OVA-peptide-specific TCRs had similar frequencies of $CD4^{+}CD25^{hi}$ thymocytes and peripheral T cells to wild type mice, DO11.10 transgenic mice on a RAG-2 deficient background had a significantly depleted proportion of cells with a $CD4^{+}CD25^{hi}$ Treg phenotype within the total thymocyte and peripheral CD4+ T cell pools. A study by Jordan *et al.* (2001) also showed that in hemagglutinin (HA)-specific transgenic mice, HA-specific Tregs only arose when this antigen was ectopically expressed in the thymus. These studies suggest that developing thymocytes must experience TCR-cognate antigen engagement in the thymus for Treg development. Furthermore, it is known that the Treg TCR repertoire does not fully overlap with the Tconv repertoire and is skewed towards self-peptides; a study by Hsieh *et al.* (2004) showed that Tconvs transduced with Treg-derived TCRs readily reacted to self-antigens leading to autoimmune *manifestations in vivo*. However, these Treg-TCR-transduced Tconvs could mount only a weak response to self-peptides presented on syngeneic APCs. Moreover, a study by Cozzo Picca *et al.* (2011) using TCR-transgenic mouse lines specific to HA peptides showed that treatment with low affinity HA-peptides could drive negative selection but were not sufficient to induce Treg differentiation. Collectively, these studies have led to an interpretation that TCR-self-antigen engagement is crucial to thymic Treg development, and therefore thymocytes which give rise to Tregs must bind self-peptide-MHC complexes with an intermediate affinity allowing a survival advantage over highly self-reactive thymocytes which are deleted during negative selection.

There is now a body of evidence suggesting that TCR specificity plays a role in selecting thymocytes for Treg development. For example, in a mouse model in which negative selection was partially abrogated through reduced expression of self-peptide-MHC-II complexes on mTECs, the frequencies of Tregs were found to be increased (Hinterberger *et al.,* 2010). Moreover, studies by Bautista *et al.* (2009) and Leung *et al*. (2009) showed that higher clonal frequencies of single positive $CD4^+$ thymocytes expressing the same Treg-derived TCRs unexpectedly led to a significant reduction in the frequency of thymic Tregs arising from this population, whereas lower clonal frequency yielded higher Treg numbers. In support of this, a study using Nur77-GFP reporter mice, which express green fluorescent protein (GFP) upon TCR stimulation, showed that GFP expression was higher in $FoxP3^+$ thymocytes compared to $FoxP3^-$ which implies that Treg precursors require strong TCR stimulation (Moran *et al.,* 2011). Additionally, in agreement with the previous study, a higher precursor $CD4^+$ clonal frequency gave rise to fewer GFP^+ thymic Tregs. Therefore, the selection of Tregs is thought to be dependent on TCR specificity, possibly owing to limited thymocyte-self-antigen encounters, which creates intra-clonal competition giving rise to a Treg population with high TCR diversity. Despite this evidence for an instructive role for TCR specificity in Treg development, Pennington *et al*. (2006) also showed that events which influence Treg lineage commitment may begin prior to genetic rearrangement of the TCR during the double negative thymocyte stage, suggesting that TCR specificity may not be the only factor which determines Treg differentiation. Finally, following TCR-peptide-MHC encounters, Tregs are thought to arise from $CD4^+CD25^+FoxP3^-$ thymocyte precursors during a TCR-

independent step through IL-2 stimulation, which induces FoxP3 expression (Lio and Hsieh, 2008).

As well as supporting Treg thymic development, stimulation of Tregs by TCR-cognate antigen binding also appears to play an important role in maintenance of Tregs in the periphery. A study by Seddon and Mason (1999) demonstrated that $CD4^+$ T cells from rats lacking thyroid glands caused autoimmune thyroiditis when transferred into recipient rats, suggesting that presence of thyroid antigens in the periphery is crucial for continual antigen-stimulation and survival of thyroid-specific Tregs. Additional findings from Itoh *et al.* (1999) showed that Tregs from DO11.10 transgenic mice functionally suppressed in vitro proliferation of OVA-peptide stimulated Tconv cells, however Tregs from non-transgenic littermates were unable to exert suppression of Tconvs in response to this antigen.

To demonstrate the importance of downstream TCR signalling, Schmidt *et al.* (2015) generated Tregs deficient in several TCR signalling proteins such as phospholipase C γ, and showed that in vitro suppressive function was ablated in these cells. A more recent study from the Palmer group has demonstrated that in TCR-transgenic mice which have monoclonal Treg populations, exposure to cognate antigen is an essential requirement for suppressive function *in vitro* and *in vivo* (Gubser *et al.,* 2016). Furthermore, the authors showed that the level of TCR-binding affinity of cognate antigens positively correlated with the level of Treg-mediated suppression of Tconv proliferation and Treg CD25 expression in vitro. These results suggest that TCR specificity and cognate antigen exposure also play a crucial role in Treg suppressive mechanisms. This concept is

increasingly recognised as a clinically relevant factor in the generation of Treg therapies (described in more detail in 1.4.5) as several studies have now demonstrated that monoclonal therapeutic Tregs with disease-relevant TCR specificities are more efficacious at suppressing inflammation than polyclonal Tregs (Lee *et al.*, 2014; NCT02711826). In support of this, a recent study by Boardman *et al.* (2023) has demonstrated that Tregs with engineered-specificity towards Escherichia coli-derived flagellin peptides preferentially migrated to and expanded within humanised mouse colons, and these Tregs were significantly more suppressive than control Tregs *in vitro* in the presence of flagellin peptides. Collectively, these studies show that Tregs require TCR stimulation for optimal suppressive function *in vivo*.

1.3 Tregs and IL-2

1.3.1 CD25, IL-2, and Treg homeostasis

Identifying CD25 as a key marker of Tregs highlighted the importance of IL-2 in Treg homeostasis. IL-2 is a potent immune-activating cytokine which consists of 133 amino acids and forms a four-alpha-helix bundle structure (Brandhuber, Boone, Kenney, & McKay, 1987) which is primarily secreted by Tconvs (Gillis, Ferm, Ou, & Smith, 1978) and B cells (Kindler, Matthes, Jeannin, & Zubler, 1995) upon activation. One defining feature which distinguishes Tregs from Tconvs is that Tregs cannot produce IL-2 upon activation (Thornton, Donovan, Piccirillo, & Shevach, 2004).

IL-2 has pleiotropic effects on many immune cell types dependent on their expression of IL-2 receptors at their cell surface. IL-2 receptors can be composed

of up to 3 subunits; the IL-2 receptor α-chain (IL-2Rα; CD25), the IL-2 receptor β-chain (IL-2Rβ; CD122), and the common gamma-chain (IL-2Rγc; CD132) (Hatakeyama et al., 1989; Takeshita et al., 1992). These subunits can form heterodimeric or heterotrimeric complexes giving rise to IL-2 receptors with differing binding affinities. The intermediate affinity IL-2 receptor (*K*d ≈ 1 nM) is formed through association of the IL-2Rβ and IL-2Rγc chains and is expressed by non-activated Tconvs and other non-T cell immune cells e.g. natural killer (NK) cells. The high affinity IL-2 receptor complex (*K*d ≈ 10 pM) is formed of all 3 subunits and is constitutively expressed at a high level on Tregs giving them a competitive binding advantage for IL-2 over Tconvs which can only transiently express this receptor after activation (reviewed by Ye, Brand, & Zheng, 2018). The IL-2Ra subunit can also be expressed alone as the low affinity receptor, however due to its short cytoplasmic tail which lacks kinase binding sites, signal transduction cannot be initiated without the IL-2Rβ and IL-2Rγc chains (Ye et al., 2018) (figure 1.3).

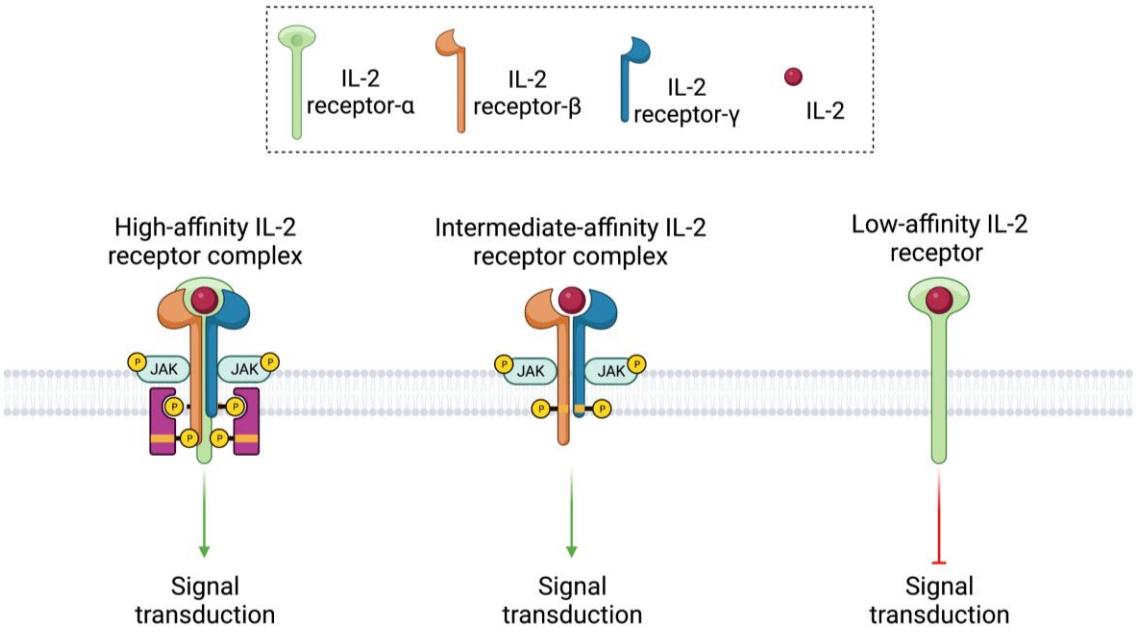

Figure 1.3: IL-2 receptor complexes. The 3 IL-2 receptor complexes, the IL-2 receptor-α, IL-2 receptor-β, and the IL-2 receptor-γ (common gamma chain), can form IL-2 receptor complexes on the surface of T cells and other immune cells. The high affinity IL-2 receptor complex consists of a heterotrimer of all 3 subunits and is constituently expressed by Tregs and transiently expressed by activated Tconvs. The intermediate affinity IL-2 receptor complex is formed of a heterodimer of the IL-2 receptor-β and -γ subunits and is constitutively expressed by Tconvs. Both the high and intermediate affinity IL-2 receptors can initiate signal transduction upon binding of IL-2. The low affinity IL-2 receptor consists of the IL-2 receptor-α subunit only and cannot initiate signal transduction. Created using BioRender.com.

Historical studies showed that IL-2 is a potent T cell growth factor *in vitro* (Morgan, Ruscetti, & Gallo, 1976), therefore lack of IL-2 signalling was expected to restrict T cell proliferation *in vivo.* However, contrary to prior expectations, deficiency of *IL2* (Sadlack et al., 1993), the *IL2RB* (Suzuki et al., 1995), or the *IL-2RA* (Willerford et al., 1995) genes were all later shown to cause autoimmune manifestations and lymphoproliferation in mice. It has since been shown that *IL-2RA* (CD25) knockout has a profound effect on Treg survival in mice, causing them to die by apoptosis leading to uncontrolled proliferation of Tconvs (Barron et al., 2010). Point mutations in the *IL2RA* and *IL2RB* genes have also been reported in humans, both causing autoimmune disease, a reduction in circulating Treg numbers, and decreased Treg suppressive capacity *in vitro* (Roth et al., 2018; Sharfe, Dadi, Shahar, & Roifman, 1997; Zhang et al., 2019). More recently, using CRISPR-Cas9 technology, Van Zeebroeck et al. (2021) showed that *IL2RA*-knockout-human Tregs exhibit a reduced suppressive capacity. Collectively, these studies demonstrate that IL-2 is essential to Treg function and that loss of IL-2 signalling prevents Treg survival, leading to loss of control of Tconv proliferation.

IL-2 is essential for Treg development. A seminal study by Malek, Yu, Vincek, Scibelli, & Kong, (2002) showed that thymic Treg development fails in mice deficient for the *IL2RB*, however transgenic re-expression of IL-2Rβ specifically in the thymus rescues Treg development. *IL2RA* knockout mice also have a dramatically reduced Treg compartment relative to Tconv cells, and these Tregs display a significantly lower expression of FoxP3 (Fontenot, Rasmussen, Gavin, & Rudensky, 2005). IL-2 is also essential for maintenance and survival of Tregs

after normal development, as shown by studies in which IL-2 neutralising antibody treatment completely ablates Tregs in the periphery in both neonatal and adult mice (Bayer, Yu, Adeegbe, & Malek, 2005; Setoguchi, Hori, Takahashi, & Sakaguchi, 2005). Continuous IL-2 signalling is necessary to maintain FoxP3 expression, which in turn reinforces the characteristic Treg gene expression signature (Ono et al., 2007).

1.3.2 Differential IL-2 signalling in Tregs and Tconvs

Ligand binding to the high affinity IL-2 receptor causes the cytoplasmic tails of the IL-2Rβ and γ chains to dimerise, allowing for recruitment of the Janus kinases (JAK) JAK1 and JAK3 (Russell et al., 1994) (figure 1.4). These non-receptor tyrosine kinase proteins then phosphorylate residues on the IL-2Rβ and γ cytoplasmic tails, and in Tregs this predominantly leads to signal transduction through the signal transducer and activator of transcription 5 (STAT5) pathway (Bensinger et al., 2004), which has been shown to promote Treg signature gene expression by binding non-coding sequences in the FoxP3 gene (Zheng et al., 2010). STAT5 mutations which reduce signal strength through this pathway in humans can lead to autoimmune symptoms and defects in Treg function (Bernasconi et al., 2006; Cohen et al., 2006).

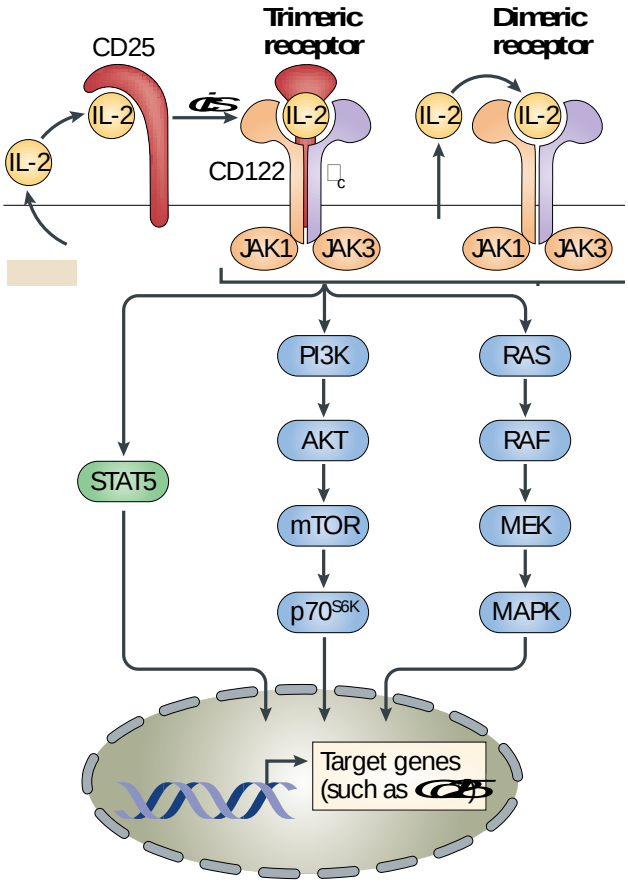

Figure 1.4: IL-2 receptor signalling. In T cells, signalling through the trimeric (high affinity) and the dimeric (intermediate affinity) IL-2 receptor complexes can induce signal transduction through 3 pathways; the STAT5 pathway which is predominantly used by Tregs, and the PI3K/Akt/mTOR and Ras/Raf/MEK/MAPK pathways used in Tconvs (adapted from Boyman & Sprent, 2012).

In Tconvs, following phosphorylation of tyrosine residues by JAK1/3 proteins, this can also drive signal transduction through the Ras/Raf/MAPK and the PI3K/Akt/mTOR pathways, giving these cells a high proliferative capacity in response to IL-2 (Reviewed in Gaffen, 2001). In Tregs however, constitutive expression of phosphate tensin homolog (PTEN) strongly inhibits activation of the PI3K/Akt/mTOR pathway, and this appears to be crucial to maintaining the Treg phenotype as ectopic activation of Akt leads to loss of Treg suppressive capacity (Crellin, Garcia, & Levings, 2007). This inability to signal through this pathway also prevents IL-2-induced proliferation (Walsh et al., 2006) and thus gives Tregs resistance to the macrolide immunosuppressant drug rapamycin, which potently inhibits Tconv proliferation and promotes a suppressive phenotype in these cells (Reif, Burgering, & Cantrell, 1997; Sabatini, Erdjument-Bromage, Lui, Tempst, & Snyder, 1994; Valmori et al., 2006). For these reasons, when culturing and expanding Tregs *in vitro,* IL-2 and rapamycin are often added to culture media to suppress the outgrowth of any contaminating Tconvs (Strauss et al., 2007).

As detailed above, Tregs have a competitive binding advantage over Tconvs to IL-2 in their environment due to their constitutively high expression of the high affinity IL-2 receptor complex (containing CD25). Consequently, Tregs can sequester IL-2 which promotes their suppressive phenotype, while restricting the proliferation of adjacent Tconvs (Reviewed by Cheng, Yu, & Malek, 2011). In addition to this, a study by Yu et al. (2015) showed that Tregs have a heightened intracellular sensitivity to IL-2 which is independent of CD25 expression. This study showed Tregs required a 10-fold lower concentration of extracellular IL-2

to achieve full STAT5 phosphorylation, and a 100-fold lower IL-2 concentration to activate IL-2 response genes than Tconvs or T cell blasts expressing high levels of CD25. As Tregs can respond to concentrations of IL-2 *in vivo* which are too low to stimulate Tconvs, this principle has allowed for the development of low-dose IL-2 therapy which is currently in phase I and II trials for the treatment of several autoimmune diseases (reviewed by Klatzmann & Abbas, 2015).

1.4 Tregs in health and disease

In order to achieve a state of health, the number and function of Tregs and Tconvs must exist in a state of dynamic flux whereby appropriate immune activation is permitted to prevent infection and cancer while fully functional Tregs are necessary to prevent autoimmune diseases and also in induction of tolerance towards grafted organs and during pregnancy (figure 1.5).

1.4.1 Treg dysfunction in autoimmunity

As detailed above, autoreactive T cells are readily detectable in the peripheral blood of healthy individuals, meaning functional Tregs are essential to maintaining these cells in a suppressed state in order to avoid onset of autoimmune disease. A large body of *in vitro* and *in vivo* evidence suggests that a lack of fully functional Tregs can be a driver of autoimmune disease in humans.

Several studies have shown that the absolute number of Tregs can be altered in autoimmune disease patients. In some autoimmune diseases such as systemic lupus erythematosus (SLE) there is evidence that Tregs may be reduced in number in patients (Li, Deng, Yang, & Wang, 2019). In rheumatoid arthritis (RA)

there are conflicting studies which cite either an increase (Moradi et al., 2014) or a decrease (Zhang et al., 2018) in Treg numbers in the synovial tissue or peripheral blood, respectively.

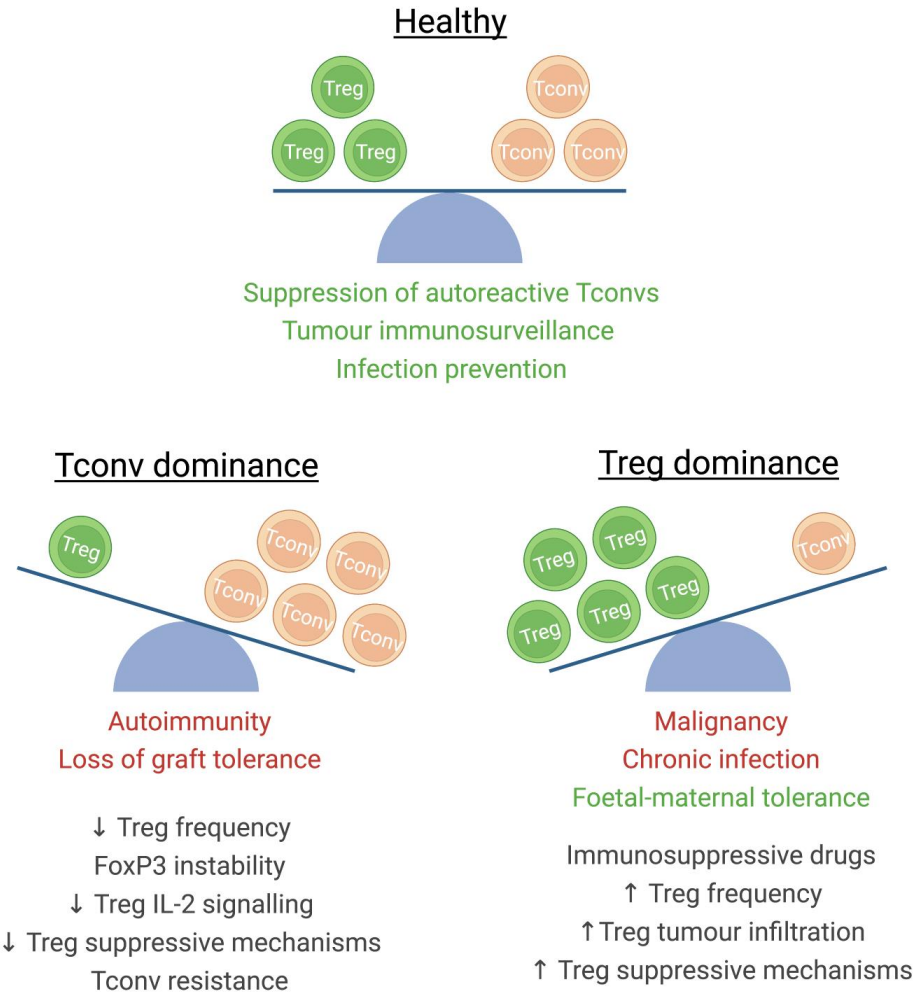

Figure 1.5: Tregs in health and disease. In a state of health, Tregs and Tconvs should exist in a state of numerical and functional balance whereby appropriate Tconv activation to prevent infection and malignancy are permitted while Tregs prevent autoimmunity. In a state of Tconv dominance, the risk of autoimmunity and failure of tolerance towards grafted organs prevails. In a state of Treg dominance, the risk of malignancy and infection increases, however this is a necessary process to promote tolerance to the semi-allogeneic foetus during pregnancy. Created using BioRender.com.

Despite this, it is generally agreed that irrespective of their frequency, Tregs are functionally impaired in many autoimmune and inflammatory diseases such as SLE (Valencia, Yarboro, Illei, & Lipsky, 2007), RA (Flores-Borja, Jury, Mauri, & Ehrenstein, 2008), multiple sclerosis (MS) (Sambucci et al., 2018), ankylosing spondylitis (AS) (Guo et al., 2016), systemic sclerosis (Wang et al., 2014), and Type 1 Diabetes (T1D) (Brusko, Wasserfall, Clare-Salzler, Schatz, & Atkinson, 2005; Lindley et al., 2005; Long et al., 2010; Yang et al., 2015). Many mechanisms of Treg dysfunction have been reported in different autoimmune diseases including an over-active OX40/OX40L immune checkpoint axis (Jacquemin et al., 2018), over-expression of the receptor for the Treg-inhibitory hormone prolactin (Legorreta-Haquet et al., 2016), reduced cytotoxic T-lymphocyte associated protein 4 (CTLA-4) expression (Flores-Borja et al., 2008) and loss of FoxP3 (Valencia et al., 2007). This 'Treg instability' model whereby bona fide Tregs can downregulate FoxP3 and transdifferentiate into inflammatory T helper subsets has been shown to arise in mouse models of T1D (Zhou et al., 2009) and experimental autoimmune encephalomyelitis (EAE) (Bailey-Bucktrout et al., 2013).

Defects in components of the IL-2 signalling pathway causing reduced Treg responsiveness to IL-2 have been widely reported across several different autoimmune diseases. For example, a study by Koga *et al.* (2012) showed that Tconvs from SLE patients had a reduced ability to produce the IL-2 protein. Additionally, a study from our group and collaborators demonstrated that Tregs from T1D patients have a diminished response to IL-2 compared to healthy controls leading to lower Treg numbers, reduced FoxP3 expression, and impaired

suppressive function (Yang et al., 2015). These Tregs were enriched in patients bearing single nucleotide polymorphisms (SNPs) in the protein tyrosine phosphatase N2 gene (*PTPN2*). Many genes encoding proteins which form components of the IL-2 signalling pathway, including *PTPN2* and *IL2,* have been identified in genome wide association studies (GWAS) as genes which associate with autoimmune diseases such as RA, Crohn's disease (Burton et al., 2007), and T1D (Barrett et al., 2009; Todd et al., 2007). These GWAS studies show that defects in IL-2 signalling are part of the primary cause of autoimmune disease development rather than a later consequence of ongoing disease.

1.4.2 The role of Tregs in transplant tolerance

Despite the major advances in the field of solid organ transplantation, long-term graft survival is limited by alloimmune activation of the recipient immune system towards the organ graft which in some cases can lead to graft versus host disease (GvHD). In order to limit this risk, transplant patients rely heavily on a strict treatment regimen of potent immunosuppressive drugs, often calcineurin inhibitors, which carry a long-term risk of renal toxicity, chronic infection, and malignancy (reviewed by Webber & Vincenti, 2016). For this reason, several other immunosuppressive therapies are being investigated which may give more targeted regulation and lead to fewer side effects.

Tregs are known to play an important role in both induction and maintenance of tolerance towards the transplanted organ. Pre-clinical animal models have shown that infusion of Tregs can protect against allograft reactivity and lengthen graft survival (Joffre et al., 2008; Lee, Nguyen, Lee, Kang, & Tang, 2014) and depletion

of Tregs leads to rapid graft rejection (Hu et al., 2013). Tregs have been shown to migrate into the donor organ and upregulate suppressive effector molecules, followed by migration to the lymph nodes to inhibit dendritic cell migration which in turn suppressed Tconv proliferation within the allografts (Zhang et al., 2009). Additionally, further evidence suggests that induced Tregs with TCR specificity towards donor alloantigens can be induced within donor grafts (Hu et al., 2013) and are 5-10 fold more effective at inducing graft tolerance than polyclonal Tregs (Lee et al., 2014). These pre-clinical studies have paved the way for development of adoptive Treg therapies to enhance graft survival in humans and several safety trials have been completed (Sánchez-Fueyo et al., 2020; Sawitzki et al., 2020). Moreover, combinations of low-dose IL-2 and polyclonal Treg treatment have been trialled in T1D, however this trial failed to meet its primary endpoint (Dong et al., 2021). A trial in kidney transplant patients comparing the efficacy of polyclonal and donor alloantigen-specific Tregs is now underway (NCT02711826: Treg Therapy in Subclinical Inflammation in Kidney Transplantation; TASK).

1.4.3 Tregs in the tumour microenvironment

Contrary to the protective role that Tregs play in autoimmunity and transplant tolerance, Tregs are known to infiltrate tumours and play a role in tumour immune evasion. This was originally evidenced by studies which showed that Treg depletion by administration of anti-CD25 antibodies or T cell suspensions depleted of $CD25^{hi}$ cells increased tumour rejection rates in mice (Onizuka et al., 1999; Shimizu, Yamazaki, & Sakaguchi, 1999). Tumours are known to be heavily infiltrated by Tregs, which can make up between 10-50% of $CD4^+$ T cell infiltrates in the tumour microenvironment (Saito et al., 2016). Moreover, a higher infiltration

of Tregs is associated with poor prognosis in many cancers (Curiel et al., 2004; Sasada, Kimura, Yoshida, Kanai, & Takabayashi, 2003; Schaefer et al., 2005). Many successful immune checkpoint inhibitor therapies such as the anti-CTLA4 monoclonal antibody ipilimumab and the anti-PD-1 monoclonal antibody pembrolizumab are thought to work through targeting Tregs within the tumour microenvironment (Reviewed by Togashi, Shitara, & Nishikawa, 2019).

1.4.4 Tregs in foetal-maternal tolerance

During pregnancy, a state of heightened immune tolerance must ensue to protect the developing foetus expressing paternal antigens from the maternal immune system and Tregs play a crucial role in regulating this process (Mjösberg, Berg, Ernerudh, & Ekerfelt, 2007). During healthy pregnancy, the frequency of maternal Tregs increases both in the peripheral blood (Somerset, Zheng, Kilby, Sansom, & Drayson, 2004a) and the decidua, and failure of decidual Treg infiltration is associated with recurrent spontaneous abortion (Sasaki et al., 2004) and preterm birth in humans (Gomez-Lopez et al., 2020). In addition, human decidual Tregs are more efficient at suppressing self-cord blood Tconvs than third party Tconvs suggesting a role for antigen specificity (Tilburgs et al., 2008).

There is evidence that peripherally induced Tregs are enriched at the foetal-maternal interphase as CNS2$^{-/-}$ mice which cannot produce pTregs experience depletion of decidual Tregs, immune infiltration, and foetal resorption when mated with allogeneic males (Samstein, Josefowicz, Arvey, Treuting, & Rudensky, 2012). An *in vitro* study using human cord blood mononuclear cells showed that the presence of progesterone, which is highly expressed in the

placenta, skewed the differentiation of naïve $CD4^+$ T cells into induced, highly suppressive $FoxP3^+$ Tregs and blocked the production of Th17 Tconvs in a STAT5-dependent manner (Lee, Ulrich, Cho, Park, & Kim, 2011). This supports the notion that the foetal-maternal interphase environment is conducive to pTreg induction.

On the other hand, a recent study has also highlighted the importance of thymically-derived Tregs in pregnancy; deletion of the receptor-activator of NF-κB (RANK) from thymic epithelial cells prevents the expansion of Tregs in pregnant mice and leads to a reduced number of placental Tregs and gestational diabetes mellitus (GDM)-like symptoms (Paolino et al., 2021). In addition to immune regulation, Tregs are proangiogenic and promote the formation of healthy placental architecture as defects in formation of spiral arteries have been shown in mice depleted of Tregs (Care et al., 2018; Nadkarni et al., 2016; Samstein et al., 2012).

There is a growing body of evidence which suggests that Treg dysfunction during pregnancy is involved in the pathogenesis of many pregnancy-related diseases such as recurrent miscarriage, pre-eclampsia, and GDM (Green et al., 2021; Sasaki et al., 2007, 2004; Yang et al., 2018). Several studies have shown an imbalance in frequencies of Treg subsets compared to those in healthy pregnancies (Boij et al., 2015; Kisielewicz et al., 2010; Steinborn et al., 2012; Wagner et al., 2016). Moreover, many groups have shown that Treg suppressive function may be altered in these conditions due either to intrinsic defects in Treg function or due to a skewed pro-inflammatory environment associated with these

disorders (Green et al., 2021; Toldi et al., 2012; Yang et al., 2018). A more detailed discussion of the role of Tregs in pre-eclampsia and GDM is featured in chapter 6.1.

1.4.5 Treg therapies and impact of subsets

As Tregs are known to be dysfunctional in several autoimmune diseases, the notion of treating patients with large numbers of autologous, suppressive Tregs is being explored in clinical trials. A number of phase I trials to date have demonstrated that infusion of autologous, polyclonal, *ex vivo* expanded Tregs is safe and well tolerated in GvHD (Brunstein et al., 2011), T1D (Bluestone et al., 2015a; Marek-Trzonkowska et al., 2014), and organ transplantation patients (Sánchez-Fueyo et al., 2020; Sawitzki et al., 2020). While the efficacy of these therapies has not yet been shown by means of phase III clinical trials, there is potential to further tailor these Treg therapies to enhance their efficacy.

It is crucial that therapeutic Tregs used possess properties such as good *ex vivo* expansion potential, stability of FoxP3 expression and suppressive capacity both during expansion and also *in vivo* once infused into the patient. The protocol for generating therapeutic Tregs usually involves *ex vivo* expansion by stimulating the cells with anti-CD3/CD28 beads in the presence of high doses of IL-2 (Safinia et al., 2016). Most clinical trials to date have used polyclonal, bulk Tregs as their expansion material, however studies have now shown that use of tissue sources which are enriched for naïve Tregs (e.g. umbilical cord blood) or purified naïve Tregs yield higher cell numbers which have superior suppressive capacity and FoxP3 stability than memory Tregs (Canavan et al., 2016; Hoffmann et al., 2009, 2006; Scottà et al., 2013). Furthermore, non-autologous umbilical cord blood has

been used in early clinical trials to treat GvHD which were well-tolerated (Brunstein et al., 2011). A study by Seay et al. (2016) showed that Tregs from umbilical cord blood cells cryopreserved after birth expanded more efficiently than Tregs from adult peripheral blood. A more recent study has also shown that Tregs isolated from the discarded paediatric thymus following cardiac surgery are an excellent source of naïve Tregs which expand to form a highly pure and suppressive product (Bernaldo-de-Quirós et al., 2022).

Although peripheral blood naïve Tregs do not tend to express high levels of chemokine receptors which may allow migration to inflammatory tissues *in vivo,* Donnelly et al. (2018) showed that naïve expanded Tregs could be manipulated to express surface glycans which promote endothelial migration, showing the potential for ectopic expression of other tissue-specific homing molecules. Other methods adopted to increase cell yield, expansion efficiency, and expression of homing receptors include expansion in the presence of multipotent adult progenitor cells which promotes expanded Tregs to express a gut-homing phenotype (Reading et al., 2021).

In summary, understanding how the surface phenotype of Tregs affects their functionality has important implications not just *in vivo* in disease settings but also when considering which Tregs may be the best candidates for future, disease-specific Treg therapies.

Collectively, the above sections show that Tregs can play a protective or an antagonistic role in a wide range of human pathologies, therefore a deeper

understanding of the phenotype and function of this cell type could support our understanding of the pathogenesis of many human diseases and how Treg therapies could be improved.

1.5 Mechanisms of Treg suppression

Although *in vivo* mouse studies have demonstrated that Tregs have a potent suppressive effect on Tconv proliferation and activation, it is known that Tregs can exert regulatory effects on a range of immune cell types, and also play other non-immunological roles such as tissue repair and regeneration. Other immune cell targets of Tregs include antigen presenting cells such as B cells, dendritic cells (DCs), and monocytes, $CD8^+$ T cells, and NK cells. Tregs can alter the activation and proliferation state of Tconvs either directly or through inducing APCs into a tolerogenic state (figure 1.6).

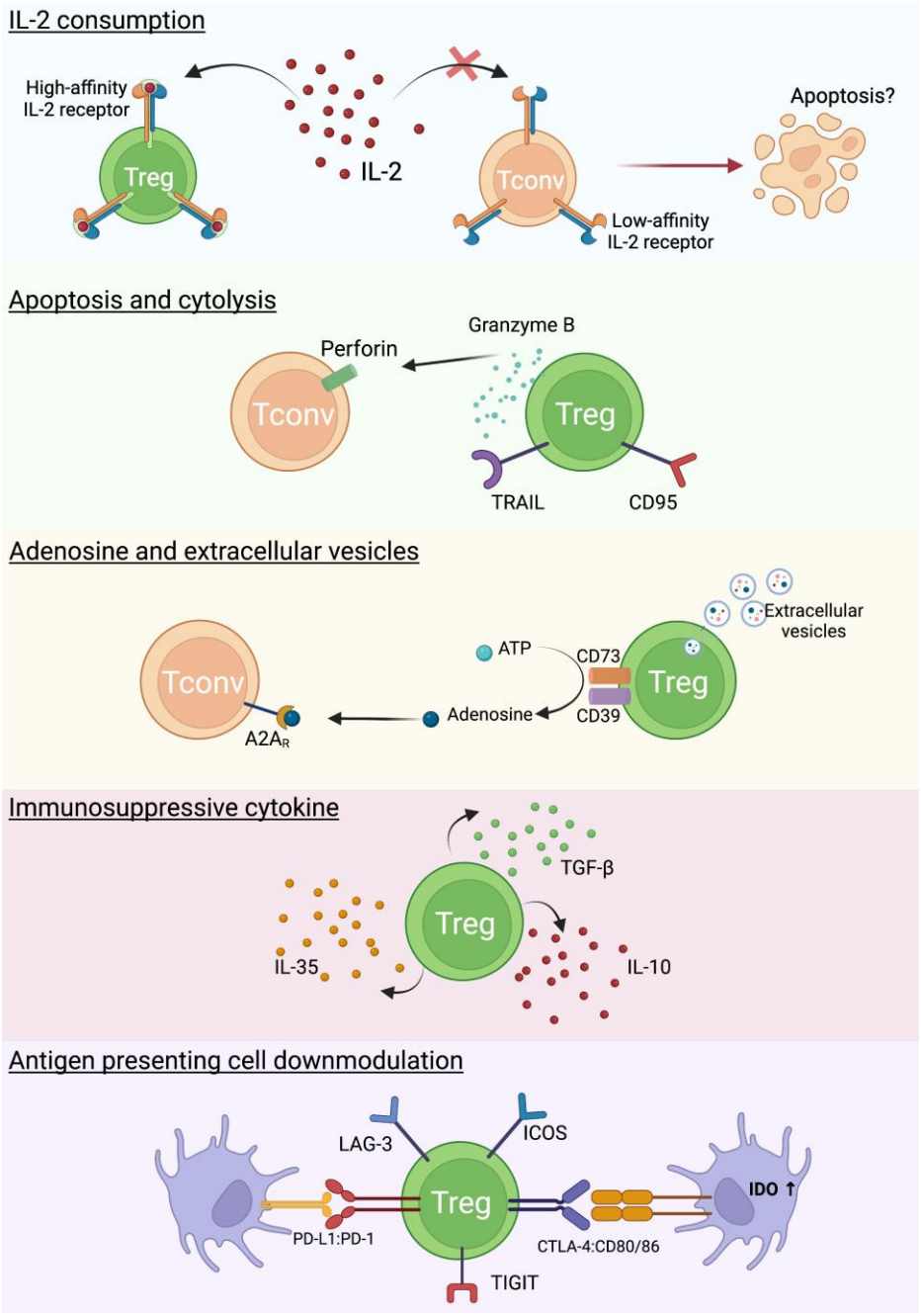

Figure 1.6: Mechanisms of Treg-mediated suppression. Tregs have a broad range of suppressive mechanisms which they can use to regulate the activation of Tconvs and antigen-presenting cells. IL-2 consumption involves sequestering IL-2 from the environment by use of the high affinity IL-2 receptor containing CD25. Some reports have shown that this causes Tconvs to die by apoptosis. Apoptosis in target cells can also be induced by release of cytolytic granules such as granzyme B, and expression of death receptors such as TRAIL and CD95 (Fas) by Tregs. Metabolic disruption of Tconvs can be caused by generation of extracellular adenosine by Tregs which binds the A2A receptor on Tconvs. Adenosine is catabolised from ATP using the extracellular ectonucleotidases CD73 and CD39. Tregs can secrete immunosuppressive cytokines such as IL-10, IL-35, and TGF-β. Antigen presenting

cells can be induced into a tolerogenic state by Tregs through Treg surface expression of molecules such as LAG-3, ICOS, CTLA-4, TIGIT, and PD-1. Created using BioRender.com.

1.5.1 IL-2 consumption and apoptosis

As outlined above, IL-2 is an essential cytokine for T cell survival and promotes the proliferation of Tconvs through the Ras/MAPK and PIK3/Akt/mTOR pathways. The constitutively high expression of CD25 on the surface of Tregs allows these cells to act as 'IL-2 sinks' thus outcompeting Tconvs for available IL-2. Barthlott et al. (2005) showed that in mice, Tregs further upregulate expression of CD25 in the presence of IL-2 generating a positive feedback loop for IL-2 consumption.

In vitro Treg suppression assays commonly involve the co-culture of Tconvs, Tregs, and a source of APC (three-cell assay), and mechanisms indicating that either the Tconvs or the APCs (or both) are the cellular targets of Tregs have been described. Early studies in murine and human Tregs showed that upon activation via anti-CD3 antibodies, IL-2 consumption is an important mechanism which directly targets Tconvs and inhibits their proliferation *in vitro,* and addition of IL-2 inhibits suppression (Baecher-Allan et al., 2001; de la Rosa, Rutz, Dorninger, & Scheffold, 2004; Thornton & Shevach, 1998).

Tregs actively suppress the production of IL-2 mRNA by Tconvs as early as 1 hour after stimulation (Oberle, Eberhardt, Falk, Krammer, & Suri-Payer, 2007), however this is unaffected by addition of exogenous IL-2. This has led some investigators to believe that Treg-mediated suppression of IL-2 at protein level and mRNA level occur by different mechanisms, and while IL-2 sink/consumption

could play a part in Tconv suppression, Tregs are likely to use several suppressive mechanisms simultaneously to inhibit proliferation (reviewed by Scheffold, Hühn, & Höfer, 2005; Shevach, 2018a). In further support of this theory, in a trans-species suppression assay whereby human Tregs can efficiently suppress murine Tconvs, addition of a blocking human CD25 antibody had no effect on suppression showing loss of the 'IL-2 sink' can be compensated by other mechanisms (Tran et al., 2009). Additionally Sojka *et al.* (2005) demonstrated that inhibition of IL-2 mRNA production by responder cells could be overcome through CD28 engagement on Tconvs by prolonging the half-life of IL-2 mRNA in responder cells.

A study by Pandiyan *et al.* (2007) indicated that consumption of IL-2 by Tregs can induce Bim-dependent apoptosis of Tconvs both *in vitro* and *in vivo* in a murine model of inflammatory bowel disease (IBD). However apoptosis driven by IL-2 consumption is a debated suppressive mechanism as in contrast to this study, Szymczak-Workman *et al.* (2011) showed no change in suppression of $Bim^{-/-}$ apoptosis-resistant Tconvs, therefore the link between IL-2 deprivation of Tconvs and apoptosis requires further clarification.

Killing of Tconvs via apoptosis induction has been reported in some studies independently of IL-2 consumption. Pre-activated Tregs have been shown to utilise the death receptor TNF-related apoptosis inducing ligand (TRAIL) against Tconvs *in vitro* and *in vivo* (Ren et al., 2007). Involvement of cytolytic granules such as perforin and granzyme have also been reported in Treg suppression of

Tconvs, monocytes, DCs (Boissonnas et al., 2010; Grossman et al., 2004) and B cells (Iikuni, Lourenço, Hahn, & Cava, 2009).

1.5.2 Adenosine generation

Hydrolysis of free adenosine triphosphate (ATP) to adenosine in the extracellular space is a Treg-mediated suppressive mechanism known to disrupt the metabolism of Tconvs. As ATP has a high concentration gradient across cell membranes, extracellular ATP acts as a signal for tissue damage and thus has proinflammatory effects on immune cells (Reviewed by Bours, Swennen, Di Virgilio, Cronstein, & Dagnelie, 2006). Tregs express the ectonucleotidases CD39 and CD73 at their surface which convert ATP to adenosine diphosphate /adenosine monophosphate (ADP/AMP) and adenosine, respectively (Deaglio et al., 2007). Adenosine is known to have inhibitory effects on T cell activation through engagement with the A2A cell surface receptor, and Tconvs which lack this receptor are resistant to Treg suppression in murine colitis models (Huang, Apasov, Koshiba, & Sitkovsky, 1997; Naganuma et al., 2006). A2A receptor engagement on both Tconvs and DCs inhibits the secretion of pro-inflammatory cytokines such as TNF-α, IFN-γ, IL-12, and IL-2 (Reviewed by Ernst, Garrison, & Thompson, 2010).

$CD39^+$ Tregs in humans have been identified as a highly suppressive subset (Mandapathil, Lang, Gorelik, & Whiteside, 2009). $CD39^{-/-}$ mice failed to protect skin allografts from rejection (Deaglio et al., 2007) and dysfunctional circulating $CD39^+$ Tregs have been reported in human diseases such as MS (Borsellino et al., 2007), SLE (Loza, Anderson, O'Rourke, Wood, & Khan, 2011) and

autoimmune hepatitis (Grant et al., 2014). Likewise, Tregs from $CD73^{-/-}$ mice have a significantly limited ability to protect against gastritis compared to wild type Tregs (Alam et al., 2009). Blocking the function of CD73 is currently being investigated in several anti-cancer trials (NCT03616886; NCT03611556; NCT03334617) as pre-clinical evidence suggests that CD73 contributes to tumour immune evasion (Stagg et al., 2010).

Evidence has also shown that Tregs can secrete extracellular vesicles containing suppressive immune-modulatory molecules. A study by Smyth et al. (2013) showed that Tregs can release extracellular vesicles containing CD73, and these isolated extracellular vesicles alone had adenosine-producing and suppressive functions independently of Tregs themselves.

1.5.3 Immunosuppressive cytokines

Tregs secrete a repertoire of suppressive cytokines which have immune regulatory effects on a range of target cell types. These include IL-10, transforming growth factor-β (TGF-β), and IL-35 and there is evidence that these cytokines play a role in Treg development and autoimmune disease prevention.

A broad range of immune cells can express IL-10 including Tregs, Tconv helper subsets, DCs, NK cells, B cells, and $CD8^+$ T cells. Early studies investigating the function of IL-10 unveiled that this cytokine can downregulate the expression of pro-inflammatory cytokines and MHC-II complexes by APCs which in turn reduces Tconv activation (Fiorentino, Zlotnik, Mosmann, Howard, & O'Garra, 1991; Fiorentino, Bond, & Mosmann, 1989; Wakkach et al., 2003). For example,

IL-10 can activate tolerogenic pathways in DCs which trigger the differentiation of IL-10-producing peripherally-induced Tregs, leading to a reinforcement of the tolerogenic niche (Gregori et al., 2010). IL-10 has a direct effect on Th17 Tconvs by inhibiting their proliferation in *vivo* (Huber et al., 2011) and promotes the survival and suppressive phenotype of Tregs under inflammatory conditions (Murai et al., 2009).

IL-10 deficient mice demonstrate that this cytokine plays an important role in mucosal immune regulation as these animals suffer severe colitis (Asseman, Mauze, Leach, Coffman, & Powrie, 1999; Kühn, Löhler, Rennick, Rajewsky, & Müller, 1993) and airway inflammation (Rubtsov et al., 2008). GWAS studies have identified SNPs in the *IL10 and IL10R* genes which confer increased risk of inflammatory bowel disease in humans (Franke et al., 2008; Moran et al., 2013). Moreover, studies by the Powrie group demonstrated that FoxP3^{+} Tregs expressing IL-10 are enriched in the murine colonic lamina propria of during colitis recovery and IL-10-deficient Tregs fail to protect against colitis in T cell-induced colitis murine models, highlighting Tregs as an important source of IL-10 for gut immune homeostasis (Asseman et al., 1999; Uhlig et al., 2006).

TGF-β is fundamental to regulation of T cell activation as TGF-β1-null mice develop lethal multi-organ inflammatory disease (Kulkarni et al., 1993), however crossing these mice with MHC-II-deficient or β2-microglobulin-deficient animals ameliorates this inflammation (Kobayashi et al., 1999; Letterio et al., 1996). The role of this cytokine as a Treg suppressive mechanism is more controversial. Some studies have shown that blocking active TGF-β production/function

reduces Treg-mediated suppression of Tconv proliferation *in vitro* (Marie, Letterio, Gavin, & Rudensky, 2005) and in *in vivo* models of colitis and GvHD (Cuende et al., 2015; Nakamura et al., 2004). However, many studies show that Treg-derived TGF-β-1, the subclass most abundantly expressed by Tregs, is largely redundant in Treg suppression (Edwards et al., 2013; Fahlén et al., 2005; Kullberg et al., 2005) and that inhibition of Tconv proliferation by TGF-β-1 can be overcome by addition of CD28 co-stimulation (Sung, Lin, & Gorham, 2003).

TGF-β family cytokines are widely expressed by an array of different cell types, and therefore there is conflicting evidence as to whether specifically Treg-derived TGF-β is required for Treg function *in vivo* (Kullberg et al., 2005; Li, Wan, & Flavell, 2007). A study by Fahlén et al., (2005) showed that transferred Tregs from TGF-β-1$^{-/-}$ mice were fully functional in protecting against colitis, but surprisingly, administration of a TGF-β-blocking antibody abrogated this protection, suggesting that TGF-β from non-Treg sources may support Treg function or that colitogenic Tconvs are directly regulated by non-Treg derived-TGF-β. In support of this, expression of a dominant negative form of TGF-βRII specifically in T cells leads to aggressive, systemic autoimmunity and accumulation of Th1 and Th2 Tconvs (Gorelik & Flavell, 2000). Furthermore, deletion of the *Tgfb1* gene from Tregs alone has no effect on development of EAE, however deletion from all CD4^{+} T cells significantly reduces Th17 differentiation and EAE development, suggesting that Treg-derived TGF-β has no impact on pathogenic Tconv differentiation in this model (Gutcher et al., 2011).

Despite debate over the role of TGF-β as a Treg suppressive mechanism, it is known that TGF-β is crucial for the development of thymic Tregs by promoting the survival of low/intermediate affinity self-reactive T cells (Ouyang, Beckett, Ma, & Li, 2010) and also of induction of peripherally induced Tregs (Chen et al., 2003). Induction of oral tolerance is one of the best-characterised *in vivo* models of peripheral Treg generation in which tolerogenic DCs present oral antigens to naïve $CD4^+$ T cells in the presence of retinoic acid and TGF-β (Coombes et al., 2007). Recent studies have shown that Treg-derived TGF-β is indispensable for generation of *in vivo* peripheral Tregs (Edwards et al., 2016; Turner et al., 2020).

IL-35 is a recently characterised member of the IL-12 family of cytokines with immune regulatory properties. In 2007, Collison et al. (2007) showed that this cytokine is secreted mostly by $FoxP3^+$ Tregs and not Tconvs, and that its deficiency in Tregs leads to decreased *in vitro* suppressive capacity and loss of protection against inflammatory bowel disease in mice. Additionally, the authors showed that ectopic expression of IL-35 in naïve $CD4^+$ T cells (or IL-35 treatment (Collison et al., 2010)) induces a regulatory phenotype, and that Tconvs fail to proliferate in the presence of this protein, thus demonstrating the polarising regulatory effects of this cytokine. Niedbala et al. (2007) showed in the same year that IL-35 treatment could inhibit Th17 differentiation and collagen-induced arthritis in mice. It is now known that IL-35 is secreted but regulatory B cells (Shen et al., 2014), tolerogenic DCs (Dixon, van der Kooij, Vignali, & van Kooten, 2015), and monocytes (Li et al., 2012).

1.5.4 Downmodulation of antigen presenting cells

Tregs are capable of influencing Tconv activation via APCs such as B cells and DCs by altering maturation and inducing a tolerogenic phenotype in these cells. One of the best-characterised mechanisms of APC modulation is through CTLA-4, an inhibitory immune checkpoint molecule constitutively expressed by Tregs. Blocking of CTLA-4 function both *in vitro* and *in vivo* can be associated with reduced Treg function (Read, Malmström, & Powrie, 2000; Takahashi et al., 2000) and *Ctla4*$^{-/-}$ mice experience a lethal lymphoproliferative disease similar to IPEX/Scurfy mice (Tivol et al., 1995). In humans, heterozygous mutations in the *CTLA4* gene can hinder expression of this protein on Tregs, which limits their suppressive function and gives rise to an immune dysregulation syndrome (Schubert et al., 2014).

CTLA-4 competes with its co-stimulatory homologue CD28 for binding to CD80/86 on the surface of APCs (Van Der Merwe, Bodian, Daenke, Linsley, & Davis, 1997). A seminal study by Qureshi et al. (2011) showed that CTLA-4 on the surface of Tregs can remove CD80/CD86 from APC surfaces by transendocytosis, thus preventing co-stimulation of Tconvs by depleting CD28 ligands on APCs. In addition, Treg-CTLA-4-CD80/86 engagement leads to APC production of the enzyme Indoleamine 2,3-dioxygenase (IDO) which catabolises tryptophan leading to Tconv cell cycle arrest and apoptosis (Grohmann et al., 2002), and induced Treg production (Curti et al., 2007; Fallarino et al., 2006).

However, despite the compelling evidence that CTLA-4 plays an immune-suppressive role, this pathway does not appear to be Treg specific and blocking

CTLA-4 on human Tregs has given mixed results. Some studies have described that deletion of CTLA-4 specifically in Tregs promotes Treg proliferation leading to enhanced suppressive capacity via other mechanisms e.g. IL-10 *in vivo* (Paterson et al., 2015). Schmidt et al. (2011) found only a partial abrogation of Tconv proliferation and no change in Tconv IL-2 secretion during co-culture of Tconvs, Tregs, and APCs with anti-CTLA-4 *in vitro.* This again suggests that Tregs can simultaneously use multiple suppressive mechanisms which can compensate for redundancies in specific pathways.

Treg-derived CTLA-4 can also act in combination with other contact-dependent suppressive molecules which modulate APC function. For example, Tregs can express both the immune checkpoint inhibitor PD-1 (programmed death) and it's ligand PD-L1 which can act to promote Tconv anergy (Treg PD-L1:Tconv PD-1) and tolerogenic DCs (DC PDL-1:Treg PD-1) (Reviewed by Gianchecchi & Fierabracci, 2018). T-cell immunoreceptor with immunoglobulin and ITIM domains (TIGIT) binds CD155 on DCs which enhances their secretion of IL-10 (Yu et al., 2009). Interaction of inducible T cell co-stimulator (ICOS) with ICOS-L on the surface of APCs reinforces Treg FoxP3 expression (Landuyt, Klocke, Colvin, Schoeb, & Maynard, 2019) and prevents apoptosis in Tregs (Kornete, Sgouroudis, & Piccirillo, 2012). Finally, lymphocyte activation gene-3 (LAG-3), a CD4 homologue which binds MHC-II, inhibits DC maturation (Liang et al., 2008).

Therefore, Tregs have an arsenal of different suppressive mechanisms which equip them with the ability to regulate the activation of all manner of immune cells. As eluded to above, it is likely that Tregs can simultaneously use a number of

different mechanisms at once rather than choosing individual mechanisms where appropriate, which may help to explain the discrepancies between studies in which individual mechanisms have been blocked.

1.6 How is Treg suppression measured *in vitro?*

1.6.1 Readouts of suppression

As outlined above, Tregs can use a plethora of different suppressive mechanisms to bring about peripheral tolerance. *In vivo*, loss of Treg suppressive capacity is often measured in the context of clinical manifestations in murine models of disease, some examples of which are lymphoproliferation and tissue immune infiltration, inflammation of disease sites, wasting disease, peripheral Tconv/Treg ratios, and autoantibody production.

However, in *in vitro* suppression assays, while adaptations can be made to the assay to disable the function of specific suppressive mechanisms (e.g anti-CTLA-4 antibodies as discussed above), Treg suppression is most widely measured by proliferation of Tconvs which are co-cultured with Tregs and stimulated either in the presence of a source of APC or by anti-CD3/CD28-coated beads, an assay which was originally developed by the Shevach (Thornton & Shevach, 1998) and Sakaguchi groups (Takahashi et al., 1998). Numerous dilutions of Tregs are often used while the number Tconvs remains constant, and proliferation is then compared to wells in which no Tregs are present. Other common readouts of suppression include Tconv cytokine production, although it is of note that cytokine regulation can occur via independent mechanisms to proliferation regulation (Thornton et al., 2004; Thornton & Shevach, 2000), and more recently

upregulation of early activation markers on Tconv surfaces such as CD25, CD134, CD69, and CD154 (Canavan et al., 2012; Long, Tatum, Mikacenic, & Buckner, 2017). While the latter has the advantage of being a shorter assay than the standard 5-6-day proliferation assay, some commentators have questioned the validity of this method. Wendering et al. (2019) showed that when anti-CD3/CD28 beads were adjusted to the total cell number (Tconvs and Tregs) rather than Tconvs only, differences in the percentage of $CD69^{+}CD154^{+}$ Tconvs between decreasing Treg dilutions were lost suggesting that differences in activation markers were due to competition for beads rather than suppression.

For these reasons, Tconv proliferation remains the most robust readout for suppressive capacity *in vitro.* Although it can always be asked whether *in vitro* suppression assays represent Treg suppression *in vivo,* proliferation assays are sensitive enough to detect functional differences in suppression and Tconv refraction to suppression between Tregs from healthy donors and autoimmune diseases (Lawson et al., 2008) and between active and quiescent disease stages (Schneider et al., 2013).

1.6.2 Treg co-culture and isolation

There are several technical considerations for suppression assays measuring Tconv proliferation and the exact setup of the assay may be influenced by the research question at hand, cellular composition of the sample and number of cells available. Firstly, as described above, the assay can be carried out in a two-cell or three-cell manner whereby Tconvs and Tregs are cultured in the absence or presence of an APC, respectively. The source of APCs can vary from irradiated

T cell-depleted splenocytes or PBMCs (Tran et al., 2009), *in vitro* monocyte-derived DCs (Hou et al., 2015) or B cells (Camu et al., 2020; Gubser, Schmaler, Rossi, & Palmer, 2016).

Tregs and Tconvs can either be isolated through magnetic enrichment of the $CD25^{hi/low}$ fraction of $CD4^+$ T cells, respectively, or by fluorescence-activated cell sorting (FACS). As intracellular FoxP3 staining requires fixation/permeabilisation of cells, it is not possible to select $FoxP3^+$ cells for functional assays. FACS sorting allows incorporation of more surface markers and therefore isolation of more specific cell populations e.g. $CD4^+CD25^{hi}CD127^{lo}$ Tregs, or indeed, subsets of Tregs. Liu et al. (2006) showed that >85% of $CD4^+CD25^{hi}CD127^{lo}$ are $FoxP3^+$ cells compared with 22.9% in the $CD4^+CD25^{hi}CD127^+$ fraction. Therefore, although magnetic enrichment offers a cheaper and more time efficient alternative, Treg isolation by FACS sorting can yield a purer population of Tregs. Moreover, our lab has developed a Treg micro-suppression assay, a miniaturised version of traditional suppression assays (described in detail in chapter 3 materials and methods), in which cells are sorted directly into 96-well plates which enhances precision of cell counts compared to manually plating the cells (Camu et al., 2020; Todd et al., 2016; Yang et al., 2015).

1.6.3 Stimulation and detection of proliferation

The method of stimulation used in Treg suppression assays is a topic of much debate. As mentioned above, *in vitro* Treg suppression assays are often set up by stimulating the Tconv/Treg co-culture with anti-CD3/CD28 beads (two-cell assay, no APC), however a ratio of 1:1 Tregs to Tconvs is often needed to

achieve significant suppression (Reviewed by Shevach, 2018b). This is unsurprising as multiple studies have shown that many Treg suppressive mechanisms can be overcome *in vitro* by use of anti-CD28 co-stimulation (Schmidt et al., 2011; Sojka et al., 2005; Sung et al., 2003; Thornton et al., 2004). A strong TCR and co-stimulatory signal delivered by plate-bound anti-CD3/CD28 can completely overcome suppression (Baecher-Allan, Viglietta, & Hafler, 2002).

Unpublished work from our lab has shown that results of assays using anti-CD3/CD28 beads are not comparable to use of B cells as APCs in the same donors and that inter-donor variation is significantly reduced using beads. Therefore, use of APCs may provide a more physiological stimulus and given the wide range of suppressive mechanisms which target APCs, presents an opportunity for more Treg mechanisms to be investigated. However, if sourcing of APCs is not possible (e.g. if T cells are tissue-derived), or if research questions pertaining specifically to Tconvs as the target cells are being investigated then use of the two-cell assay may be preferable. When using the three-cell assay, the source of cell stimulus can also vary but usually involves either soluble or plate-bound anti-CD3 antibody (Baecher-Allan et al., 2002) or phytohaemagglutinin (PHA) (Camu et al., 2020; Todd et al., 2016; Yang et al., 2015).

Finally, measuring the proliferation of Tconvs is usually carried out after 5 days by either a dye-dilution flow cytometric assay (Venken et al., 2007) or by tritiated thymidine incorporation (Thornton & Shevach, 1998) (figure 1.7). The former carries the advantage of being able to track the proliferation and phenotype of the different cells within the co-culture by labelling the Tconvs, Tregs, and APCs

with different tracer dyes in combination with fluorescently labelled antibodies. However the thymidine incorporation method, which relies on the principle that Tregs remain anergic *in vitro* unless stimulated with very high doses of IL-2 (Levings et al., 2001), gives robust readouts from far fewer cells which is ideal when analysing rare populations of Tconv responders or even rarer subsets of Treg.

(A) Tritiated thymidine incorporation

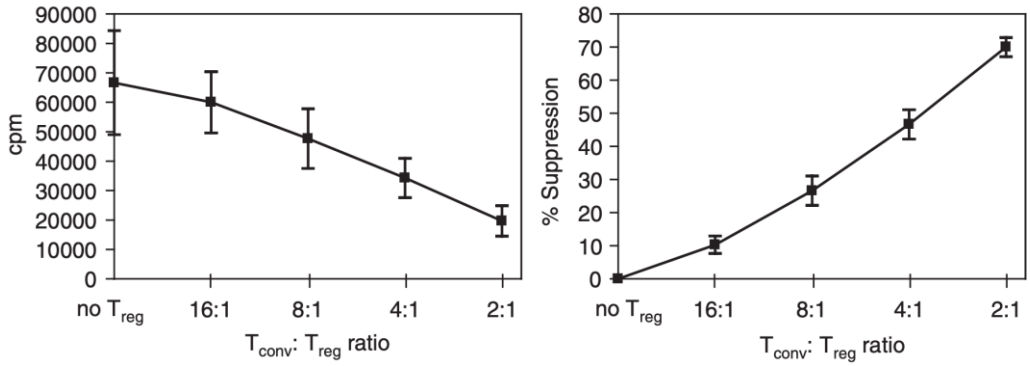

(B) Dye dilution

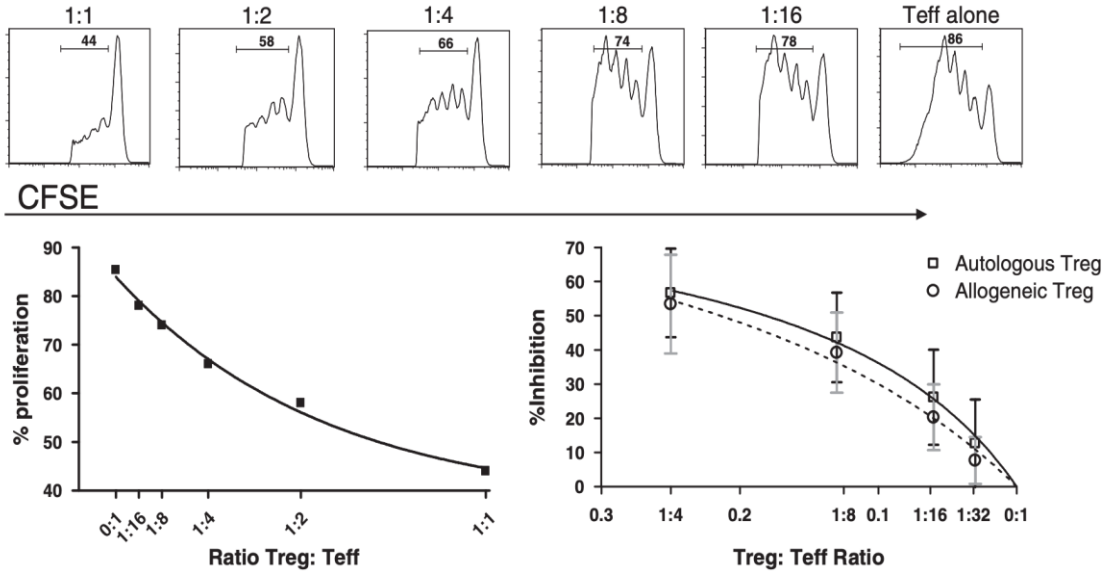

Figure 1.7: Measuring Tconv proliferation in Treg suppression assays. When measuring Treg *in vitro* suppressive capacity, the proliferation of Tconvs is commonly measured by (A) tritiated thymidine incorporation whereby radioactive counts per minute (CPM) are the readout from which percentage suppression can be calculated, or (B) dye dilution in which the percentage of proliferated cells is measured by flow cytometry. Different ratios of Tconvs and Tregs are commonly used. (Collison & Vignali, 2011; Schneider & Buckner, 2011).

There is an increasing body of evidence showing that Tregs are not a homogenous population of cells, but rather a phenotypically diverse lineage and therefore assessing the frequency and suppressive capacity of different subsets of Tregs may uncover important implications not only for disease states but also for the use of Tregs as cellular therapies.

1.7 Treg diversity and subsets

1.7.1 Thymic vs Peripheral Tregs

The cardinal phenotype which characterises Tregs has long been held as surface $CD4^{+}CD25^{hi}CD127^{low}$ and FoxP3 expression. Over the years attempts have been made to divide Tregs into subsets based on factors such as their site of development, surface phenotype, and function.

As described in section 1.1.3, thymic Tregs (tTregs) can develop from thymocytes bearing TCRs with an intermediate affinity for self-antigens. Conversely, pTregs differentiate under tolerogenic conditions from naïve $CD4^{+}$ T cells (Apostolou & Von Boehmer, 2004; Lafaille, Lino, Kutchukhidze, & Lafaille, 2004) and are largely present at mucosal interphases such as the gut. tTregs and pTregs have largely non-overlapping TCR repertoires as pTreg TCRs are often found to recognise foreign antigens (Lathrop et al., 2011).

It was previously proposed that the transcription factor Helios could be used to differentiate tTregs from pTregs as this marker is highly expressed by Tregs in the thymus (Thornton et al., 2010). However it has since been shown that pTregs can express Helios (Gottschalk, Corse, & Allison, 2012) and that like FoxP3,

Tconvs can transiently express Helios upon activation (Akimova, Beier, Wang, Levine, & Hancock, 2011). It was then found that Helios^{+} and Helios^{-} Tregs exist within the tTreg compartment, thus discrediting Helios as a tTreg marker (Himmel, MacDonald, Garcia, Steiner, & Levings, 2013). It has also been suggested in the past that tTregs have a more stable FoxP3 expression owing to a fully demethylated Treg-specific demethylated region (TSDR) whereas some studies showed that *in vivo* pTregs harboured some methylated CpG motifs within the TSDR (Haribhai et al., 2011). Subsequent studies have shown that while *in vitro* induced Tregs do not display Treg-specific demethylation patterns, *in vivo* pTregs and tTregs have comparable patterns (Ohkura et al., 2012).

Distinguishing tTregs from pTregs could have important implications for research and clinical purposes as it has been hypothesised that highly suppressive Tregs which infiltrate tumours are largely peripheral in origin owing to the tolerising tumour microenvironment, whereas Tregs which protect against autoimmunity are thymically derived owing to their self-antigen skewed TCR repertoire (Reviewed by Adeegbe & Nishikawa, 2013). In addition, a study by Samstein, Josefowicz, Arvey, Treuting, & Rudensky (2012) utilised CNS1$^{-/-}$ mice which fail to develop pTregs to show the importance of pTregs in pregnancy; when mated with allogeneic males, these mice failed to develop decidual pTregs which led to heightened immune infiltration and foetal resorption. This suggests that pTregs are instrumental in promoting tolerance to paternal antigens presented by the developing foetus.

1.7.2 Human naïve, memory, and individual marker Treg subsets

A landmark study by the Sakaguchi group (Miyara et al., 2009) demonstrated that human FoxP3-expressing cells in peripheral blood can be divided into 3 main subsets based on their expression of the markers FoxP3, CD25, and CD45RA; fraction I $CD45RA^{+}FoxP3^{low}CD25^{low}$ naïve/resting Tregs, fraction II $CD45RA^{-}FoxP3^{hi}CD25^{hi}$ effector Tregs, and fraction III $CD45RA^{-}FoxP3^{low}CD25^{low}$ cytokine-secreting cells although these cells were largely non-Tregs owing to their low TSDR hypomethylation, poor suppression of Tresp proliferation, and relatively high production of IL-2 and IFN-γ. Both naïve and effector Tregs (Fraction I + II) had demethylated TSDR regions (figure 1.8). During *in vitro* suppression assays involving plate bound anti-CD3 stimulation in the presence of irradiated accessory cells, both the naïve and effector Tregs potently suppressed the proliferation of carboxyfluorescein succinimidyl ester (CSFE)-labelled responder cells. Although data from only a single donor was shown, the effector Tregs showed a trend towards better suppression than naïve Tregs. In addition, effector Tregs died during the suppression assays, while naïve Tregs upregulated CD45R0 and were able to differentiate into effector Tregs *in vitro*. In support of this, a previous study by Fritzsching et al. (2006) had shown that human umbilical cord blood Tregs are mostly composed of naïve Tregs and could be stimulated *in vitro* to upregulate markers of memory such as CD95 showing the developmental trajectory of naïve and memory Treg subsets.

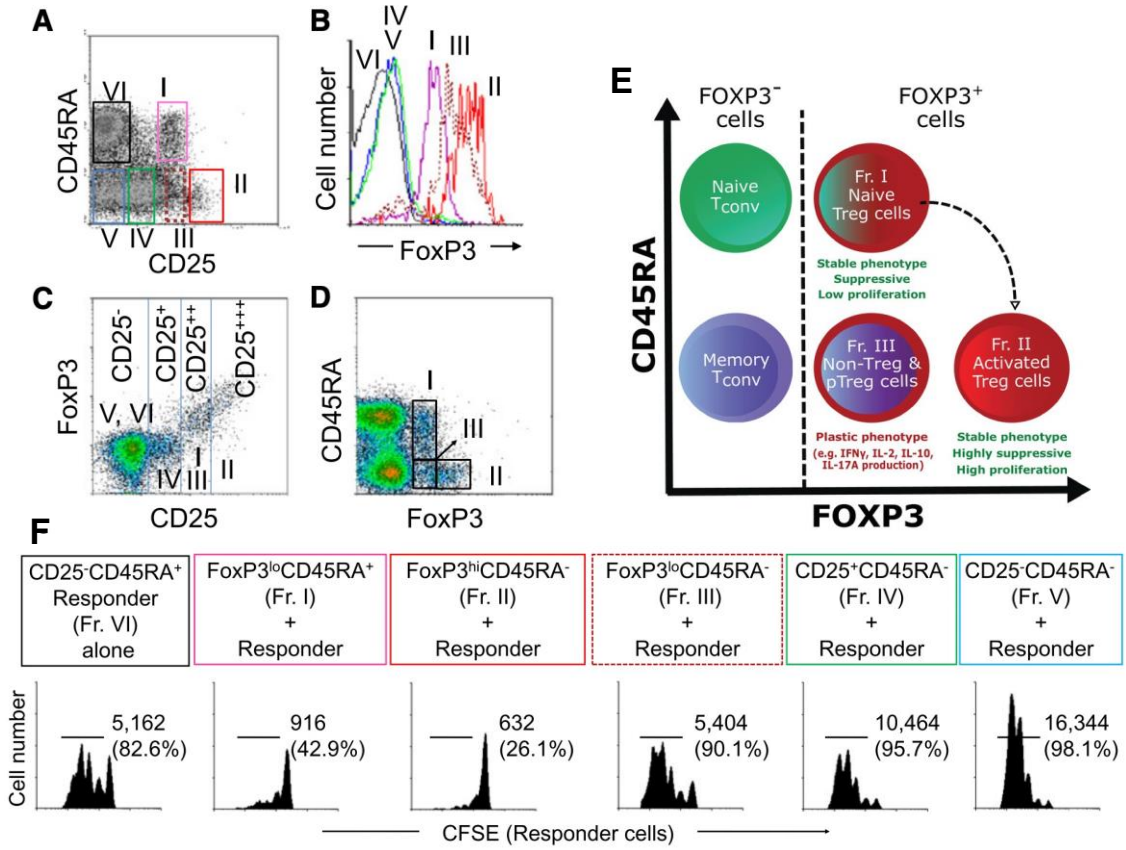

Figure 1.8: The Miyara Treg fractions. Miyara *et al.* showed that FoxP3^{+} CD4^{+} T cells can be divided into 6 fractions, 3 of which are CD25^{hi} Tregs; fraction I are naïve CD45RA^{+} Tregs, fraction II are CD45RA^{-} FoxP3^{hi} Tregs, and fraction III which are cytokine producing (A-E). (F) Fractions I and II have good suppressive capacity while fraction III has minimal suppressive capacity (Giganti et al., 2021; Miyara et al., 2009).

The Treg subset phenotypes in this paper by Miyara et al. (2009) have been extensively investigated in different disease contexts. A subsequent study by the same group showed that CD15s expression in CD45RA^{-}FoxP3^{+} Tregs could be used as a marker to differentiate fraction II from fraction III (Miyara et al., 2015). However, the authors were not the first to report that Tregs express differential surface markers of naivety and memory (figure 1.8). Early studies of Tregs in human peripheral blood showed that the CD25^{hi} fraction of CD4^{+}CD25^{+} human Tregs were CD45R0^{+} and exhibited potent suppressive capacity *in vitro* (Baecher-Allan et al., 2001). Subsequent studies showed that CD45RA^{+} naïve Tregs showed equivalent suppressive capacity to memory Tregs when directly compared *in vitro* (Booth et al., 2010; Miyara et al., 2015; Seddiki et al., 2006; Valmori, Merlo, Souleimanian, Hesdorffer, & Ayyoub, 2005). However, a more recent study analysing unbiased subsets of Tregs based on RNA-sequencing data showed two memory subsets, each expressing high levels of FoxP3 and MKI67, were significantly better suppressors than subsets displaying a naïve phenotype, however 4 other memory/effector subsets showed no difference in suppression (Luo et al., 2021). This highlights the internal differences in Treg subsets and, also of note, that different stimulation conditions of Tconvs between suppression assays can yield different results.

Alterations in the frequencies of naïve CD45RA^{+} and memory CD45R0^{+} Treg subset have been implicated in several disease states in humans. For example, several studies have showed that CD45RA^{+} Tregs are significantly reduced in peripheral blood of MS patients compared to healthy controls (Ciccocioppo et al., 2019; Verma et al., 2021), accompanied by a reciprocal increase in CD45R0^{+}

memory Tregs. Balint et al. (2013) also demonstrated that naïve Tregs which co-express CD31, a marker of recent thymic emigrant (RTE) T cells, are also reduced in MS and that reduced $CD45RA^{+}CD31^{+}$ numbers or depletion of these cells from the Treg pool gave significantly worse *in vitro* suppressive capacity (Haas et al., 2007b). In addition to MS, reduced numbers of circulating $CD45RA^{+}CD31^{+}$ Tregs compared to healthy donors have been reported in idiopathic pulmonary fibrosis, which correlated with increasing disease severity (Hou et al., 2017), atherosclerosis (Huang et al., 2017), and in pre-eclampsia (Steinborn et al., 2012; Wagner et al., 2015). In these *in vivo* human studies, it is difficult to know if a reduction in the frequency of naïve Treg subsets is a causative factor of disease initiation/progression or if this is due to an expansion of the Treg memory compartment as a consequence of ongoing systemic inflammation. However, the studies which show reduced $CD45RA^{+}CD31^{+}$ RTE Tregs give more compelling evidence that reduced thymic output of naïve Tregs rather than solely an expansion of memory Tregs could be contributing to immune dysregulation.

Several other individual cell surface molecules have been utilised to delineate distinct subsets of Tregs with potent suppressive capacity. These include human leukocyte antigen-DR (HLA-DR) (Baecher-Allan, Wolf, & Hafler, 2006a; Schaier et al., 2012), CD39/CD73 (Borsellino et al., 2007; Deaglio et al., 2007), CD161 (Afzali et al., 2013; Pesenacker et al., 2013), CCR4 (Iellem, Colantonio, & D'Ambrosio, 2003; Sugiyama et al., 2013), TIGIT (Fuhrman et al., 2015; Joller et al., 2014), and ICOS (Ito et al., 2008; Kälble et al., 2021). Conversely, $CD49d^{+}$ Tregs, otherwise known as the α4-integrin subunit, are almost always associated

with poor *in vitro* suppressive capacity (Kraczyk, Remus, & Hardt, 2014). Although CD49d is known as a central nervous system (CNS) homing molecule on T cells (Glatigny, Duhen, Oukka, & Bettelli, 2011), the proportion of $CD49d^+$ Tregs in peripheral blood is significantly increased in both MS (Venken et al., 2008) and Parkinson's disease patients compared to healthy controls (Karaaslan et al., 2021) and *in vitro* Tregs from Parkinson's disease patients have impaired *in vitro* suppressive capacity (Saunders et al., 2012).

1.7.3 T helper-like Treg subsets and stability

In addition to classifying Treg subsets based on their expression of individual surface markers, suppressive $FoxP3^+$ Tregs which mirror the chemokine receptor and cytokine expression of Tconv T helper subsets have been described in the literature. A study by Duhen, Duhen, Lanzavecchia, Sallusto, & Campbell (2012) showed that subsets of Tregs with an activated, memory-like phenotype ($CD45RA^-CD45R0^+$) can differentially express the chemokine receptors CCR4, CXCR3, CCR6, and CCR10 which colocalise to Th1, Th2, Th17, and Th22 Tconv cells. In addition, these so-called T helper-like Tregs were found to express the same cytokine (IL-17, IFN-γ) and transcription factor (RORC, TBX21, GATA-3) profiles as known T helper subsets. A more recent study from the same authors showed that although at the cell surface these Tconv and Treg helper-like subsets are phenotypically similar, they are transcriptionally distinct, with the Treg-helper-like subsets all expressing an overlapping immunosuppressive gene signature controlled by FoxP3 between subsets, whereas the gene signatures of the Tconv helper subsets were much more diverse (Höllbacher et al., 2020). Therefore, the authors proposed that the chemokine receptor profiles expressed

by the different T helper-like Tregs do not alter their suppressive mechanisms but allow different helper subsets to home to tissue sites where their Tconv helper counterparts reside such as the skin.

It is of course well documented that while chemokine receptor repertoire can be used to characterise subsets of lymphocytes, the biological function of these receptors on T cells is to facilitate homing and migration from peripheral blood into tissues. To name some examples, CCR7 and CD62L are crucial lymphoid homing molecules (Venturi, Conway, Steeber, & Tedder, 2007; Zhang et al., 2009). Loss of Treg-CCR4 expression in mice leads to severe inflammation of the skin and lungs (Sather et al., 2007), while expression of CCR6 on Tregs allows suppression of Th17 responses e.g. in synovial joints and the CNS (Hirota et al., 2007; Yamazaki et al., 2008). Both CXCR3 and CCR10 expressing Tregs are enriched in livers of chronic liver disease patients (Eksteen et al., 2006). Finally, CXCR5 enables homing of T follicular regulatory cells (Tfr) to B cell follicles and germinal centres and this well-defined Treg subset has a role in regulating germinal centre responses (Wollenberg et al., 2011).

Previously, there has been much debate as to whether Treg helper-like subsets have evolved to specifically target and suppress their matched Tconv helper counterparts. However a study by Halim et al. (2017) showed that Th1, Th2, Th17.1, and Th17 helper-like Tregs suppressed Tconv helper subset proliferation and cytokines without preference for their equivalent Tconv subset. Moreover, they found that Th2-like Tregs were highly migratory and enriched in melanoma and colorectal tumours.

While some authors argue an immune protective role for these cells with enhanced trafficking capabilities, others believe that T helper-like Tregs are not stable lineages and are more of a hindrance to immune regulation. Fate mapping studies in inducible murine models of inflammatory disease have shown that FoxP3$^+$ Tregs can lose their expression of FoxP3 and trans-differentiate into pathogenic 'ex-Treg' Tconv helper subsets under inflammatory conditions (Komatsu et al., 2013; Zhou et al., 2009). However other similar studies have shown that these ex-Tregs could be derived from Tconv cells which transiently upregulate FoxP3 upon activation and only a small fraction of <5% of Tregs tended to lose FoxP3$^+$ expression (Miyao et al., 2012). Others have argued that the extreme inflammatory conditions in some of these murine models would not occur in humans. However, some studies do support the notion that T helper-like Treg subsets could be relevant to human disease. For example, a study by Noval Rivas et al. (2015) showed that Th2-like Tregs expressing GATA-3 and IL-4 were increased in children with food allergies, and that these cells fail to suppress food allergy in mice. In addition, IFN-γ^+FoxP3$^+$ Tregs which express T-bet and CXCR3 upon *ex vivo* expansion were significantly increased in T1D patients compared to healthy controls (McClymont et al., 2011). Conversely, Th17-like Tregs have been shown to be protective in murine SLE models and removal of these cells led to enhanced tissue Tconv Th17 expansion (Kluger et al., 2016). Therefore the definitive biological role of helper-like phenotypes in Tregs remains unclear.

1.7.4 Unbiased clustering analysis of Tregs

Technological advances in cytometry have allowed for an ever-increasing number of markers to be analysed simultaneously. This has made analysing data

via standard Boolean gating more challenging and has driven a trend towards using dimensionality reduction and clustering algorithms to identify unbiased clusters of cells; a method which has been used in analysing RNA sequencing data for many years.

Feuerer et al., (2010) undertook a gene expression analysis of murine Tregs isolated from different tissue locations such as spleen, lymph node, gut lamina propria and compared these to Tregs which had been induced *in vivo* (pTregs) or *ex vivo* by different mechanisms. The findings revealed considerable variation not only in expression of genes encoding effector molecules (e.g. CTLA-4 and Granzyme B) and chemokine receptors (e.g. CCR4, CCR6, CCR10, CXCR3, CXCR5), but also in "bedrock" Treg signature genes such as *IL2RA* and *FoxP3* thus confirming the internal heterogeneity and overlapping phenotypic states which Tregs can acquire under different environmental cues. A more recent study by Luo et al. (2021) used RNA sequencing to identify subsets of Tregs and showed that similar subsets of Tregs can be found in human peripheral blood and bone marrow and pseudotime analysis revealed 2 distinct developmental trajectories from naïve Tregs can give rise to either cytokine secreting or $CD25^{hi}CTLA\text{-}4^{hi}$ memory Tregs.

A study by our group and collaborators showed that by using a comprehensive mass cytometry panel of 26 markers expressed at the Treg cell surface, bulk Tregs could be divided into 22 unbiased clusters (Mason et al., 2015). This approach was also used to identify differences in Treg subset frequencies in treatment responders and non-responders in idiopathic aplastic anaemia patients

(Kordasti et al., 2016). Having a further understanding of how the surface phenotype of Tregs effects their functional properties could have important implications when considering Treg dysfunction and deficiencies of certain subsets in different autoimmune diseases. Profiling the Treg compartment based on their surface heterogeneity rather than gene expression profiles or intracellular molecules (e.g. FoxP3) is important when carrying out *in vitro* functional assays as this requires sorting of live, unfixed cells. Additionally, Tregs are now being considered not only as pharmacological drug targets for the treatment of autoimmune diseases but also as cellular therapies themselves (Reviewed by Duggleby, Danby, Madrigal, & Saudemont, 2018). Establishing the most suitable Treg subsets for therapeutic purposes will require thorough analysis of Treg subsets based on their surface phenotype in order to sort and expand live cells with the best therapeutic properties.

1.8 Aims of this thesis

In the following experimental chapters, we aimed to use flow cytometry, *in vitro* suppression assays, and long-term expansion in order to identify Treg subsets based on their surface expression, and to compare their functional properties to test the following hypotheses:

1. The surface phenotypes of Treg subsets can give rise to differential capacities to suppress the proliferation of Tconvs when compared directly *in vitro*.
2. Tregs with potent *in vitro* suppressive capacity will have the capacity to expand *ex vivo* while maintaining their Treg phenotype.

3. Cells with a stem cell-like memory phenotype and function exist within the Treg pool which become prominent during expansion.
4. Immune dysregulation in pre-eclampsia and gestational diabetes mellitus disease backgrounds are associated with changes in Treg phenotype and function compared to Tregs from healthy pregnant women.

2 Chapter 2. General Materials and Methods

A detailed description of methods used in each experimental chapter is included within each chapter, therefore this section serves as a general description of methodology for reference.

2.1 Equipment

Biological safety cabinet

Measuring balance

Centrifuge with microplate swinging bucket rotor

Tissue culture incubator

Waterbath at 37°C

Block heater

Haemocytometer

Inverted microscope

BD FACSAria IIu

BD FACSCanto II

BD LSRFortessa

Cytek Aurora

DynaMag-15 cell isolation Magnet

Microwave

Packard Filtermat Cell Harvester

Wallac Trilux 1450 Microbeta Liquid scintillation counter

2.2 Tissue culture

All cultured cells were incubated at 37°C at 5% $C0_2$ in a humidified incubator.

2.2.1 Cell culture media preparation

Penicillin-streptomycin and fungizone

Penicillin-streptomycin (Sigma) and amphotericin B (fungizone; Thermo Fisher) combined and stored in 10ml aliquots at -20°C. When a new 500ml bottle of media is opened, 1x10ml aliquot is thawed and added to media.

Sera

Foetal bovine serum (FBS; Gibco) and human AB serum (Sigma) stocks were thawed at room temperature (RT) and heat inactivated at 56°C in a waterbath for 45 minutes, then cooled and stored in aliquots at -20°C.

RPMI

Roswell Park Memorial Institute 1640 medium (Gibco) containing penicillin-streptomycin and fungizone.

X-VIVO 15

X-VIVO 15 media (Lonza) containing penicillin-streptomycin and fungizone.

Thaw media

RPMI supplemented with 10% FBS and sterile filtered using a 0.45μm syringe filter (Appleton Woods).

Culture media

X-VIVO 15 media supplemented with 10% human AB serum and sterile filtered using a 0.45μm syringe filter.

Treg feeding media

X-VIVO 15 media supplemented with 5% human AB serum containing 1200U/ml of IL-2 (Proleukin; Novartis) and 250ng/ml of rapamycin (Rapamune; Pfizer) and sterile filtered using a 0.45μm syringe filter.

2.2.2 Buffers

FACS buffer for washing prior to cell culture

Dulbecco's phosphate-buffered saline (DPBS; Gibco) containing 2mM of Ethylenediaminetetraacetic acid (EDTA; Sigma), supplemented with 1% human AB serum, passed through a 0.45μm syringe filter.

FACS buffer for washing prior to flow cytometry

DPBS containing 2mM of EDTA, supplemented with 1% FBS.

Cell isolation buffer for magnetic enrichment

DPBS containing 2mM of EDTA and 1% FBS, sterile filtered through a 0.45μm syringe filter.

Fixation/Permeabilisation buffer

For intracellular staining, the FoxP3/transcription factor staining buffer set (eBioscience) was used. Working buffer was prepared by combining the

fixation/permeabilisation concentrate and diluent buffer at a 1:4 ratio, respectively, after allowing both buffers to come to room temperature.

Permeabilisation Wash buffer

Wash buffer was also prepared using the FoxP3/transcription factor staining buffer set. Permeabilisation buffer was diluted 1:10 in distilled water.

2.2.3 Cell isolation methods

Peripheral blood mononuclear cell isolation

PBMCs were isolated from whole blood or from leukocyte cones where indicated. Whole blood was collected into 9ml sodium heparin tubes. Blood was poured into 50ml falcon tubes and diluted 1:1 in warm RPMI. For leukocyte cones, blood was collected into 50ml falcon tubes and diluted 1:4 in warm RPMI. Diluted blood was then layered carefully onto lymphoprep density gradient media (Axis shield) and centrifuged at 1000xg for 15 minutes without the break. PBMC layer was then harvested and transferred to a 30ml universal tube and resuspended in 15ml of RPMI before centrifuging at 300xg for 10 minutes. Cell pellets were then resuspended in 10ml of RPMI and centrifuged at 200xg for 10 minutes. PBMC counting was then carried out using a Türk's solution (Merck Millipore) counterstain and a haemocytometer.

Magnetic enrichment of $CD4^+$ T cells

$CD4^+$ T cells were negatively enriched using the Dynabeads™ Untouched™ Human CD4 T Cells Kit (Invitrogen). Briefly, cells were washed in isolation buffer and incubated at 4°C for 20 minutes with an antibody cocktail containing

antibodies specific to non-$CD4^+$ T cells. During the incubation, Dynabeads™ magnetic beads were washed in isolation buffer using a DynaMag-15 magnet. Cells were then washed and incubated with magnetic beads for 15 minutes at room temperature, then suspensions were placed in the magnet allowing negative enrichment and collection of $CD4^+$ T cells.

Cryopreservation and thawing of cells

Following PBMC isolation or $CD4^+$ T cell enrichment, cells were counted and then centrifuged at 400xg for 5 minutes. Cryovials were labelled and cooled to 4°C by placing in a refrigerated CoolRack placed in a CoolBox (Biocision). Pellets were then resuspended in cold FBS before gradually adding an equal volume of FBS containing 20% dimethyl sulfoxide (DMSO) dropwise until a cell suspension of $10x10^6$/ml was achieved. 1ml of this cell suspension was then transferred to cryovials and moved to CoolCell cryogenic storage containers and placed in a -80°C freezer. The following day, cells were transferred to liquid nitrogen tanks.

On day 0 of subsequent experiments, thaw media was prepared and placed in a waterbath at 37°C. Cryovials were then placed in the waterbath until a small amount of ice remained. Warm thaw media was then added to each vial, dropwise, while gently shaking the vials. Cells were then collected into 15ml falcon tubes and thaw media was added before centrifuging at 400xg for 5 minutes.

Cell culture

For suppression assays, Tregs co-cultures were prepared as described in Chapter 3 materials and methods and incubated at 37°C in 5% $C0_2$ for 5 days prior to proliferation analysis.

For Treg expansion, Tregs were plated in 96-well round-bottom plates in X-VIVO 15 media containing 5% human AB serum. Tregs were then cultured in Treg feed media containing IL-2 and rapamycin and half the media was replenished every 48 hours. As Tregs expanded, Tregs were transferred sequentially to 48, 24, and 12 well plates then cultures were split at 90% confluency.

2.2.4 General flow cytometry sample preparation

Specific methods and lists of antibodies used in flow cytometry experiments are detailed in methods sections of the following results chapters. A generalised protocol for preparation of samples for flow cytometry experiments is described below. For viability staining, a working solution of 1μL/mL of Live/Dead fixable stain was prepared by diluting the stock solution in plain DBPS. Cells were transferred to 5ml FACS tubes and washed twice in plain DPBS. An aliquot of $0.5x10^6$ cells was taken to prepare the live/dead compensation single stain; half the cells were killed by heat treatment by placing the cells on a heat block warmed to 70°C for 10 minutes. These cells were then returned to the tube with the live cells. The viability stain solution was then added to the sample tubes and live/dead compensation single stain tubes and tubes were incubated for 15 minutes at room temperature in the dark. Cells were then washed twice with FACS buffer.

All fluorescently labelled antibodies were titrated in panel optimisation experiments at first use. Staining of cell surface antigens was divided into two incubations where applicable; staining of chemokine receptors was performed by resuspending pellets in the residual volume in the FACS tube after removing supernatants (~100uL), antibody mastermix was added, and tubes were incubated at 37°C by placing tubes in the waterbath. Staining of all other surface antigens was then carried out by adding the second antibody mastermix and incubating the cells at 4°C for 30 minutes. Cells were then washed in FACS buffer.

When staining intracellular transcription factors such as FoxP3 and Helios, cells were resuspended well then fixed and permeabilised by adding 1ml of diluted fixation/permeabilisation buffer (described above) and incubating for 40 minutes at room temperature. Cells were then washed twice with permeabilisation buffer before pelleting, adding the intracellular antibody mastermix, and incubating for 40 minutes at room temperature in the dark. Two final washes were then carried out using permeabilisation buffer, then pellets were resuspended in FACS buffer prior to acquisition.

Compensation singles when using BD FACSCanto II, BD LSRFortessa, and BD FACSAria II analysers were prepared using the anti-mouse Ig, κ/Negative control compensation particles set (BD) for anti-mouse antibodies or UltraComp eBeads Compensation beads (Invitrogen) for anti-hamster antibodies. 1uL of antibody was added to FACS tubes containing beads, and beads were resuspended in FACS buffer. When using the Cytek Aurora spectral analyser, compensation

singles were prepared using cells which were stained, fixed and permeabilised using an identical protocol to the sample tubes.

All cell sorting was carried out using a BD FACSAria IIu cell sorter. Cells were sorted directly into plates containing culture media for suppression assays, and sorted into 5ml FACS tubes containing 2.5ml of culture media for bulk sorting of Treg subsets prior to expansion.

3 Chapter 3. Identification of reproducible Treg subsets in healthy donor peripheral blood and direct comparison of their *in vitro* suppressive capacity

3.1 Introduction

As discussed in chapter 1, it is now known that Tregs are highly heterogeneous at their cell surface and differing frequencies of Treg subsets have been detected in patients of several disease states (Hou et al., 2017; Steinborn et al., 2012; Verma et al., 2021). It is assumed by some authors that differences in the frequency of Treg subsets between healthy donors and patients may be a driver of immune dysregulation, however it is difficult to know whether changes in Treg activation, differentiation, and expression of functional surface markers is a causative factor in autoimmunity or a consequence of insidious inflammation. Moreover, investigation of Treg subsets in the blood may be irrelevant in autoimmune diseases in which specific tissues are targeted such as T1D and RA as the frequencies at these tissue sites may differ from blood.

Many studies have shown differential suppressive capacity of Treg subset populations when the subsets are defined using a small number of markers (Baecher-Allan et al., 2001; Booth et al., 2010; Deaglio et al., 2007; Joller et al., 2014; Miyara et al., 2009; Schaier et al., 2012). However, differences in cell isolation methods (magnetic enrichment or FACS sorting), markers used to gate on Tregs during cell sorting (e.g. inclusion of CD127), the inability to use intracellular FoxP3 to identify Tregs, and the setup of suppression assays (two-

cell vs three-cell; source of cell stimulus; duration of assay; phenotype of responder Tconv) mean that direct comparison of suppressive capacities of Treg subsets between studies is challenging and unreliable. For example, the Sakaguchi (Miyara et al., 2015, 2009) group commonly use a suppression assay co-culturing Tregs with $CD4^+CD25^-CD45RA^+$ naïve Tconvs in the presence of irradiated 'accessory' cells (containing B cells) and stimulated with plate-bound αCD3, previously shown to be a very strong method of proliferation stimulation (Baecher-Allan et al., 2002). In these studies, the authors found that naïve Tregs were inferior suppressors to memory Tregs in suppression assays from a single donor. Other studies using αCD3/CD28 beads have shown similar results (Baecher-Allan, Wolf, & Hafler, 2006b; Joller et al., 2014). Conversely, studies using total Tconvs rather than naïve Tconvs as responder cells and those using PHA as a method of stimulation have shown equal or superior suppressive capacity of naïve Tregs compared to memory Treg subsets (Booth et al., 2010; Seddiki et al., 2006; Valmori et al., 2005). Therefore, a comparison of the suppressive capacity of Treg subsets in multiple healthy donors is needed to resolve these differences between studies.

A study from our group using a 26-marker mass cytometry (CyTOF) panel to analyse the surface phenotype of Tregs from 4 individual donors combined with unbiased clustering analysis, demonstrated that up to 22 subsets of Tregs can be identified in healthy donor blood (Figure 3.1) (Mason et al., 2015). Despite showing the wide heterogeneity in Treg cell surface phenotypes, it was not possible to assess the function of these subsets in this study. Following this study, we hypothesised that phenotypic diversity can also lead to functional diversity

between human Treg subsets and therefore we aimed to design a compressed Treg surface marker panel which could be used in FACS sorting to isolate live Treg subsets while still capturing much of the same internal diversity within the Treg pool as the original CyTOF panel.

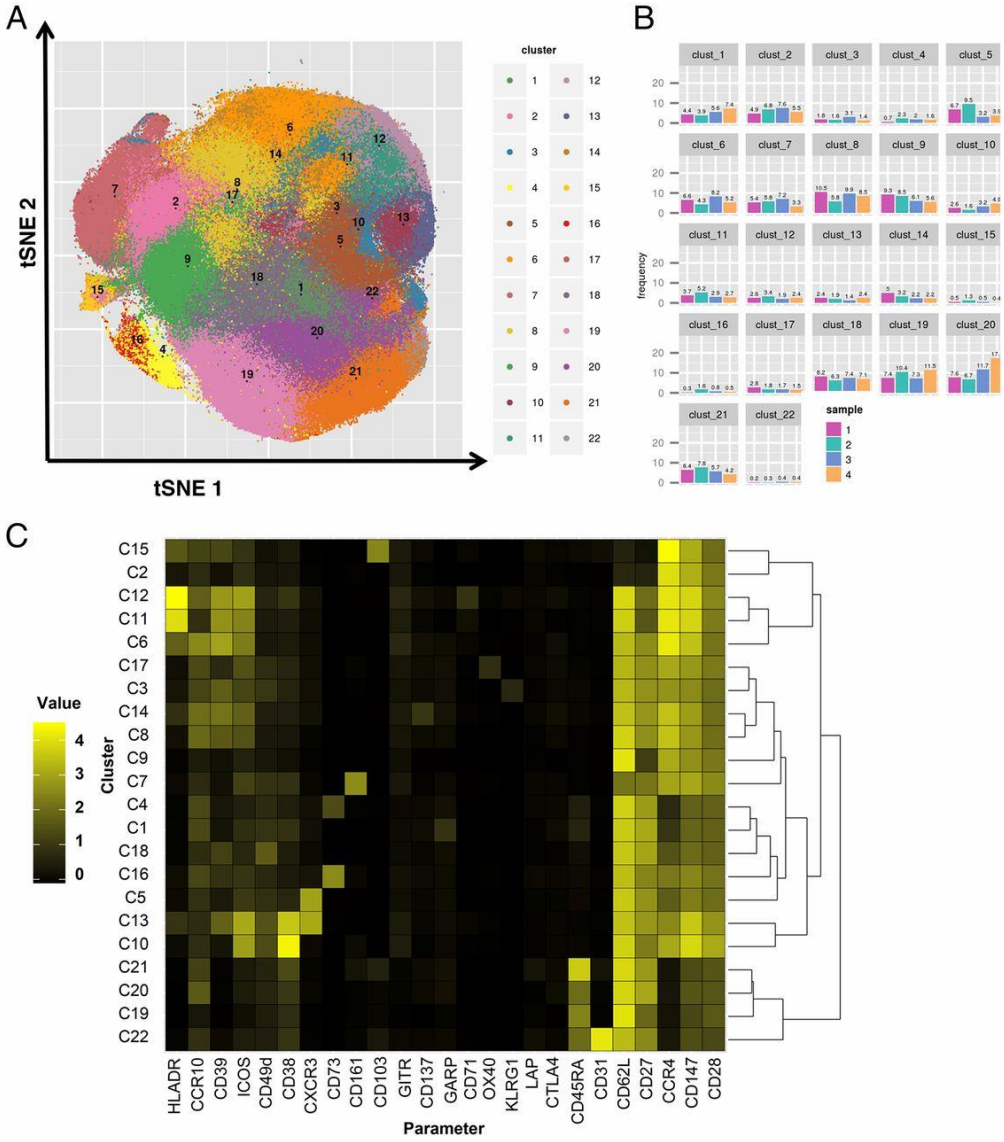

Figure 3.1: Human Tregs can be divided into subsets using their surface phenotypes. (A) 26 surface markers and t-distributed stochastic neighbour embedding (tSNE) 1 and 2 parameters were used to generate Treg clusters. The frequency (B) and median expression intensity of parameters (C) in each cluster was then determined. Figure from (Mason et al., 2015).

Several factors were taken into account when considering appropriate markers for this flow cytometry Treg surface marker panel. For example, as sorting strategies are based on Boolean gating schemes, any markers which appeared to be diffusely expressed across several Treg clusters were excluded e.g. CD28, CD147, CD62L. In the case of surface markers which have a mutually exclusive or co-expressed counterpart, such as CD45RA and CD45R0 or CD39/CD73 respectively, only one marker from these pairs was chosen. Moreover, we aimed to include markers which encompass many of the Treg subsets which have previously been reported on in the literature. These include a range of chemokine receptors to identify T helper-like Treg subsets and CXCR5 to identify T follicular regulatory cells (Duhen et al., 2012; Halim et al., 2017; Wollenberg et al., 2011) and 'mechanistic' surface markers which play a role in Treg suppressive function such as CD73, ICOS, and CD95 (Landuyt et al., 2019; Mandapathil et al., 2010; Weiss et al., 2011). Finally, as this panel was designed for FACS sorting of live cells to carry out functional assays, it was of utmost importance that for each marker selected, there are commercially available fluorescently-conjugated monoclonal antibodies which do not block the function of their target receptor and diminish the suppressive function of the Tregs in culture.

The experimental work in this chapter will test the following hypotheses:

1. Previously reported Treg subsets can be reproducibly identified in peripheral blood from multiple healthy donors.
2. In addition to previously reported subsets, our Treg surface marker panel can capture new unbiased Treg subsets which have not been reported in the literature.

3. Treg subsets with differing surface phenotypes will have differing suppressive capacities *in vitro* as determined by proliferation and cytokine inhibition.

In order to identify subsets of Tregs we adopted both manual 'Boolean' gating and unbiased clustering analysis approaches. Although Boolean gating in flow cytometry is a useful tool to identify cells with a pre-determined phenotype, identifying phenotypically complex subpopulations by this method while using high dimensional panels can be inefficient and results can be difficult to interpret. Therefore, use of dimensionality reduction tools and unbiased clustering algorithms enhances the ability to identify novel cell subsets.

3.2 Materials and methods

Methods pertaining to cell culture media and buffers, PBMC isolation, $CD4^+$ magnetic enrichment, cell cryopreservation and thawing were carried out as described in chapter 2.

3.2.1 Surface staining only used for flow cytometry

Cell suspensions were transferred to FACS tubes and centrifuged at 400xg for 5 minutes. For acquisition only, up to $10x10^6$ PBMCs were used per healthy donor. Cell pellets were resuspended in the residual volume in the FACS tubes after discarding the supernatants (~100μL). Cells were first stained with a mastermix of CCR6 BV711, ICOS BV650, CCR4 BV605, CXCR3 BV510, CXCR5 PE-Cy7, CCR10 PerCP-Cy5.5, and CD73 FITC at 37°C for 15 minutes (Table 3.1). A second staining mastermix of CD45RA BV786, CD31 BV421, CD127 PE-Cy5, CD95 PE-CF594, CD25 PE, CD4 AF700, and CD49d APC was then added, and

cells were incubated at 4°C for 30 minutes. Cells were washed with 2ml of cold FACS buffer to remove any free antibody, and suspensions were pelleted by centrifugation at 400xg for 5 minutes. Finally, pellets were resuspended in FACS buffer, passed into new FACS tubes through a 35μm cell strainer cap, and kept at 4°C prior to acquisition.

Table 3.1: Fluorochrome-conjugated antibodies used in Treg surface marker flow cytometry panel

Fluorochrome	Marker	Clone	Supplier	μL/10x10^6 cells
Master Mix 1				
BV711	CCR6	G034E3	BioLegend	2
BV650	ICOS	DX29	BD Biosciences	5
BV605	CCR4	L291H4	BioLegend	2
BV510	CXCR3	G025H7	BioLegend	2
PE-Cy7	CXCR5	J252D4	BioLegend	2
PerCP-Cy5.5	CCR10	1B5	BD Biosciences	1
FITC	CD73	AD2	BioLegend	5
Master Mix 2				
BV786	CD45RA	HI100	BioLegend	0.5
BV421	CD31	WM59	BioLegend	2.5
PE-Cy5	CD127	A019D5	BioLegend	2.5
PE-CF594	CD95	DX2	BD Horizon	1
PE	CD25	2A3	BD Biosciences	5
PE	CD25	M-A251	BD Biosciences	5
AF700	CD4	OKT4	BioLegend	2
APC	CD49d	9F10	BioLegend	5

3.2.2 Viability, surface, and intracellular staining used for flow cytometry

In experiments where the intracellular transcription factors FoxP3 and Helios were analysed, a separate staining procedure was followed. Following thawing

and counting, up to $10x10^6$ PBMCs were transferred to FACS tubes, washed with 2ml of plain PBS (containing no EDTA or serum) and centrifuged at 400xg for 5 minutes. This wash and centrifugation were then repeated with a further 2ml of plain PBS. A working solution of 1μL/mL of Live/Dead fixable near infrared dead cell stain (ThermoFisher) was prepared. Pellets were resuspended well in 500μL of plain PBS and 500μL of working Live/Dead stain solution was added to each tube. Tubes were incubated for 30 minutes at 4°C. Two washes were then performed by adding 2ml FACS buffer, centrifuging at 400xg for 5 minutes, and resuspending the cell pellets. Staining for Treg surface markers was carried out as described above using the panel shown in table 3.2. Mastermix 1 was added, and cells were incubated at 37°C for 15 minutes. In this panel, the following markers were moved to different fluorochromes to accommodate for inclusion of additional intracellular antibodies; CCR10 BUV395, CD49d BUV737. Mastermix 2 was then added and a 30-minute incubation at 4°C was carried out. After staining of surface markers was completed, cells were fixed and permeabilised by adding 1ml of fixation/permeabilisation buffer, and tubes were vortexed and incubated for 40 minutes at room temperature in the dark. PBMCs were then washed twice with 2ml of permeabilisation buffer. A third master mix containing antibodies for the intracellular transcription factors FoxP3 AF647 and Helios PerCP-eFlour 710 were added and cells were incubated for 40 minutes at room temperature in the dark. Two final washes with 2ml of permeabilisation buffer were carried out and following centrifugation cells were resuspended in 500μL and kept on ice prior to acquisition. Data were acquired using a BD LSR Fortessa flow cytometer.

Table 3.2: Fluorochrome-conjugated antibodies used in Treg surface marker and intracellular staining flow cytometry panel

Fluorochrome	Marker	Clone	Supplier	µL/10x10^6 cells
Master Mix 1				
BV711	CCR6	G034E3	BioLegend	2
BV650	ICOS	DX29	BD Biosciences	5
BV605	CCR4	L291H4	BioLegend	2
BV510	CXCR3	G025H7	BioLegend	2
PE-Cy7	CXCR5	J252D4	BioLegend	2
BUV395	CCR10	1B5	BD Biosciences	1
FITC	CD73	AD2	BioLegend	5
Master Mix 2				
BV786	CD45RA	HI100	BioLegend	0.5
BV421	CD31	WM59	BioLegend	2.5
PE-Cy5	CD127	A019D5	BioLegend	2.5
PE-CF594	CD95	DX2	BD Horizon	1
PE	CD25	2A3	BD Biosciences	5
PE	CD25	M-A251	BD Biosciences	5
AF700	CD4	OKT4	BioLegend	2
BUV737	CD49d	9F10	BioLegend	5
Master Mix 3				
AF647	FoxP3	259D	Beckman Coulter	10
PerCP-eFluor 710	Helios	22F6	eBioscience	5

3.2.3 Treg *in vitro* micro-suppression assay setup

A schematic diagram demonstrating the workflow of the Treg micro-suppression assay is shown in figure 3.14. Cryopreserved PBMCs and enriched CD4$^+$ T cells were isolated and stored as described above. For sorting of Treg subsets, 60x10^6 CD4$^+$ T cells were thawed and washed twice with FACS buffer. These cells were then stained with the Treg surface marker panel as shown in Table 3.1 and as described above in the 'surface staining only' section. 10x10^6 PBMCs from the

same donor were also thawed, washed twice with FACS buffer, and stained with a smaller mastermix of antibodies used to identify Tconvs and B cells (Table 3.3) including CD4 AF700, CD127 PE-Cy5, CD25 PE, CD19 APC-Cy7 for 30 minutes at 4°C. At the end of these incubations, the enriched $CD4^+$ T cell tube and PBMC tube were washed twice with FACS buffer, and pellets were then resuspended in 600μL and 400μL of FACS buffer, respectively. Cells from both tubes were then passed through a 35μm cell strainer into new polypropylene FACS tubes and kept on ice until cell sorting.

All FACS sorting was carried out using a BD FACS Aria-IIu cell sorter (BD). Sorting of Tconvs and B cells from the PBMC tube was first carried out using the gating strategy in figure 3.16. Subsequently, sorting of Treg subsets was carried out from the enriched $CD4^+$ T cell tube using the strategy shown in figure 3.17. 1000 B cells, 500 Tconvs, and 250 Tregs of a single subset of interest were sorted directly into a single well on a 96-well v-bottom plate containing culture media (4:2:1 ratio). Wells containing B cells and Tconvs only were also sorted as comparators to calculate the maximum proliferation potential per donor. 5 replicate wells were established per experimental condition. When sorting the rarest Treg subset, the $CXCR5^+$ $CD45RA^+$ (naïve) Tregs, it was not always possible to carry out 5 replicate wells for this condition before running of out sample and therefore this subset was excluded from further analysis. On completion of sorting of each plate, culture media containing phytohaemagglutinin (PHA) was added to each well to stimulate proliferation (final concentration within each well 4μg/ml) and plates were centrifuged at 400xg for 4 minutes to ensure contact between cells. RPMI media was added to the

outer wells of the plate to minimise evaporation. Plates were incubated at 37°C in 5% CO_2 for 5 days.

3.2.4 Treg *in vitro* micro-suppression assay read-out

On day 5 of co-culture, half the media from each well was removed carefully with a multi-channel pipette and stored in labelled 96-well NUNC maxisorp plates (VWR) at -80°C. This was replaced with pre-warmed culture media containing 0.5μCi/well of tritiated thymidine (Perkin Elmer) and plates were returned to the incubator for a further 18 hours. Finally, uptake of tritiated thymidine, a surrogate marker for cell proliferation, was measured as the number of radioactive counts per minute within each well. Briefly, cells from each well were harvested onto glassfibre filter papers (Perkin Elmer) and dried in a microwave. Filters were then placed into sealed plastic bags containing 5ml of BetaPlate Scint (Perkin Elmer) and the number of counts per minute in each well was read using a Wallac Trilux 1450 Microbeta plate reader (Wallac). In analysing the counts per minute in each well, any wells containing B cells and Tconvs only with readouts of fewer than 3000 counts per minute were excluded, and outliers were identified as any values which were less than half or more than double any of the other 4 replicates values per condition. The mean values were calculated for each condition and percentage suppression was calculated using the following formular, as previously described:

$$Percentage\ Suppression = 100 - \left[\left(\frac{Sum\ of\ counts\ from\ wells\ containing\ Tregs}{Sum\ of\ counts\ from\ wells\ containing\ no\ Tregs}\right) \times 100\right]$$

3.2.5 Measurement of cytokines in culture supernatant

The LEGENDPlex Human T-helper cytokine 13-plex panel (Biolegend) cytokine array kit was used to assess the concentration 13 cytokines within the culture supernatants collected at day 5 of co-culture, according to the manufacturer's instructions. The cytokines included IL-2, IL-4, IL-5, IL-6, IL-10, IL-9, IL-13, IL-17a, IL-17F, IL-21, IL-22, IFN-γ, and TNF-α. Data from this bead-based assay were acquired on a BD FACS Canto II analyser and LEGENDPlex software was used to analyse the data and determine cytokine concentrations. IL-17A, IL-17F, IL-21, IL-22 and IL-10 were below the level of detection within the supernatants.

Table 3.3: Fluorochrome-conjugated antibodies used to identify Tconvs and B cells prior to cell sorting in the micro-suppression assay.

Fluorochrome	Marker	Clone	Supplier	μL/10x10^6 cells
PE-Cy5	CD127	A019D5	BioLegend	2.5
PE	CD25	2A3	BD Biosciences	5
PE	CD25	M-A251	BD Biosciences	5
AF700	CD4	OKT4	BioLegend	2
APC Cy7	CD19	9F10	BioLegend	2

3.2.6 Data analysis

Total Tregs ($CD4^+CD25^{hi}CD127^-$) were gated manually for each donor using FlowJo software. Histogram overlays and heatmaps showing MFI of all markers expressed by naïve and memory Tregs were generated after importing exported Tregs into OMIQ software. Manual gating of previously reported Treg subsets, analysis of their FoxP3 and Helios expression, and MFI of surface markers was carried out within FlowJo software. Unbiased analyses were all performed using OMIQ (https://app.omiq.ai). Imported Treg files were down sampled to 20,000

events to ensure a maximal but equal number of events was analysed per donor. Opt-SNE dimensionality reduction analysis was then carried out using the following parameters: CD45RA BV786, CCR6 BV711, ICOS BV650, CCR4 BV605, CXCR3 BV510, CD31 BV421, CXCR5 PE-Cy7, CD95 PE-CF594, CD25 PE, CCR10 PerCP-Cy5.5, CD73 FITC, CD49d APC.

For FlowSOM clustering analysis, the number of appropriate meta-clusters must be pre-determined by the analyst. Determining the correct number of clusters for this dataset was guided by Phenograph clustering analysis, which automatically determines the number of clusters, setting the number of nearest neighbours to k=200. Following this, the number of clusters determined by Phenograph (33) was input into FlowSOM using the following parameters: CD45RA BV786, CCR6 BV711, ICOS BV650, CCR4 BV605, CXCR3 BV510, CD31 BV421, CXCR5 PE-Cy7, CD95 PE-CF594, CD25 PE, CCR10 PerCP-Cy5.5, CD73 FITC, CD49d APC, opt-SNE-1 and opt-SNE-2. Histogram overlays for each marker were used to ensure that each cluster consisted of a single population of cells. In clusters where histograms revealed heterogeneous expression of individual markers, these clusters were reviewed and split into 2 separate clusters.

Dot plots showing differences in the frequencies of previously reported subsets and of MFIs of individual markers in Tregs and Tconvs were generated using GraphPad Prism software. Statistical differences in MFIs of individual markers between Tregs and Tconvs were analysed by paired students t-tests. Box and scatter plots shown in suppression assay figures were generated using Graphpad prism software. Normalised suppression values were calculated using the

formula =100x(subset percentage suppression value/bulk percentage suppression value). Normality of the data was tested using a Shapiro-Wilk test. Paired one or two-way ANOVA with either a Turkey's or Dunnet's multiple comparisons test were used where indicated in figure legends.

3.3 Results

3.3.1 Expression patterns of memory and naïve Tregs

Using the Treg surface marker panel described above, we aimed to characterise which subsets of Tregs could be identified in healthy donor blood. Firstly, PBMCs from 10 healthy donors, differing in age and sex, were isolated and surface staining was carried out as described in 3.2.1 using the Treg surface marker panel. Total Tregs were manually gated as $CD4^{+}CD25^{hi}CD127^{low}$ and events from different donors were concatenated for analysis. We observed that many of the surface markers were differentially expressed by naïve Tregs ($CD45RA^{+}CD95^{-}$) and memory Tregs ($CD45RA^{-}CD95^{+}$) in accordance with previous studies (figure 3.1 and figure 3.4). As expected, all Tregs were $CD25^{hi}$ and memory Tregs had a higher MFI for CD25 than naïve Tregs, and memory Tregs expressed high levels of characteristic memory markers such as CCR4 and CD95, whereas naïve Tregs expressed low levels of these markers and were CD45RA high. Expression of the chemokine receptors CCR6, CXCR3, and CCR10 was enriched in the memory Treg population, although there was heterogeneous expression of these markers within memory Tregs, and expression of CCR10 was low. CXCR5, a characteristic T follicular helper/regulator marker (Tfh/Tfr), was expressed at a similar but low level by both memory and naïve Tregs. The extracellular ectonucleotidase CD73 was

expressed at a very minimal level by memory and naïve Tregs. Memory Tregs expressed higher levels of ICOS than naïve Tregs, and there was heterogeneous expression of CD49d by memory Tregs. Finally, both memory and naïve Tregs displayed expression of CD31, a marker of recent thymic emigrants (RTEs), although a higher proportion of naïve Tregs were positive for this marker than memory Tregs.

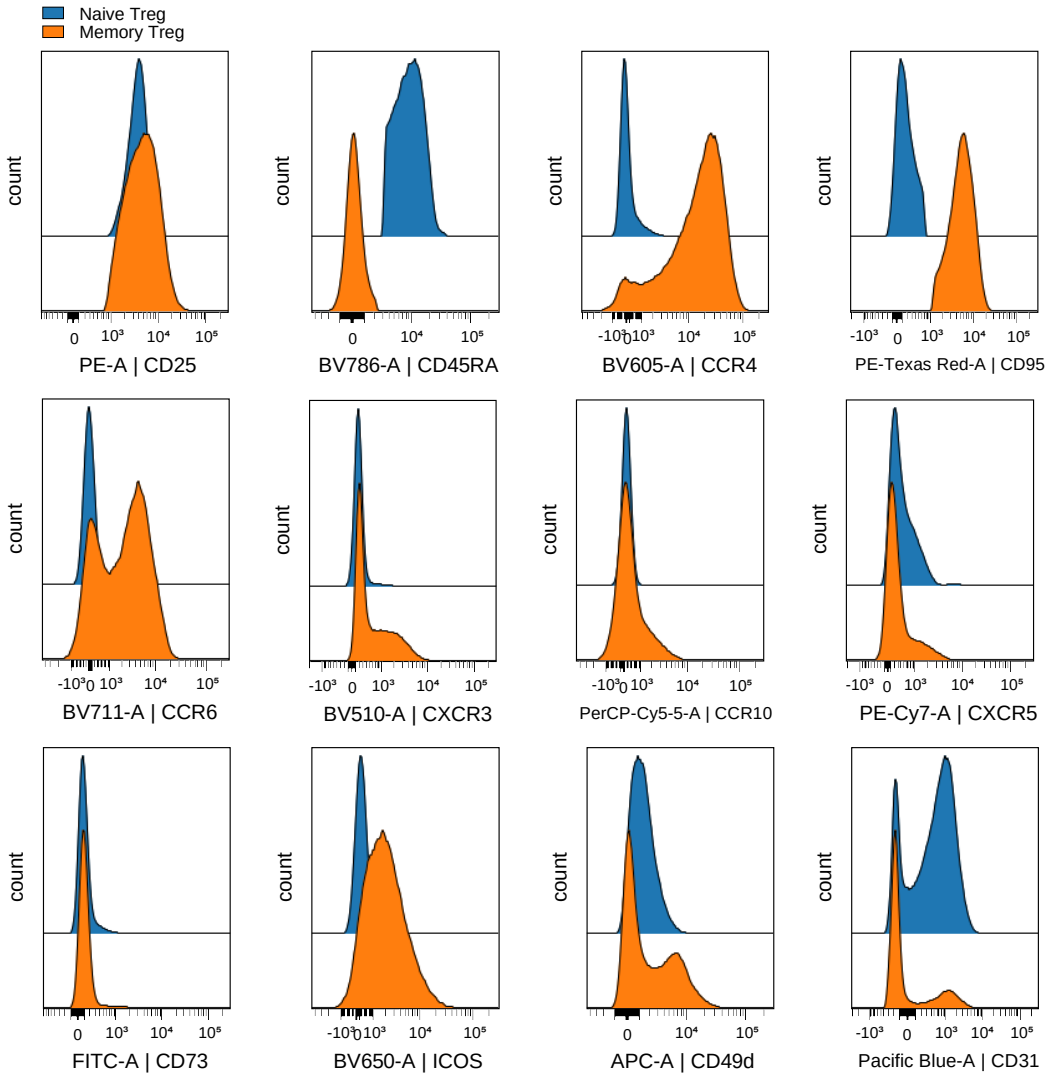

Figure 3.2: Human healthy donor peripheral Naïve and Memory Tregs had different surface phenotypes. Tregs from 10 healthy donors (n=10) were stained with the Treg subset surface marker panel and data acquisition carried out on a BD FACS Aria-IIu cell sorter. Naïve Tregs were gated as $CD4^{+}CD25^{hi}CD127^{lo}CD45RA^{+}$ cells and memory Tregs as $CD4^{+}CD25^{hi}CD127^{lo}CD95^{+}$ cells. Data from 10 donors were concatenated to show the mean fluorescence intensity of the above markers.

OMIQ software was used to generate a heatmap and dendrogram of agglomerative hierarchical clustering of naïve and memory Tregs from each individual based on mean expression of surface markers. The heatmap shown in figure 3.3 (A) shows that memory Tregs (gated as $CD95^{+}CD45RA^{-}$) and naïve Tregs (gated as $CD95^{-}CD45RA^{+}$) from all donors clustered separately, showing that these expression patterns in naïve and memory Tregs were consistent from donor to donor. The dendrogram on this heatmap also shows how expression of these markers are related to one another. For example, as eluded to in figure 3.2, markers such as CCR6 and ICOS clustered together as markers which were most highly expressed by memory Tregs, whereas CD31 was most highly expressed in naïve Tregs. From this heatmap, it is also evident that CD25 was more highly expressed by memory Tregs than naïve Tregs, and subsequently high CD25 expression was related to that of CCR4. The remaining markers CCR10, CD73, CXCR3, CXCR5, and CD49d had more diffuse expression patterns across memory and naïve Tregs. It should be noted that the data shown in the heatmap are scaled by column to maximise the visualisation of differences in expression of each marker, and therefore the expression of markers such as CD73 and CCR10 are still low when compared to markers such as CD49d. As shown in figure 3.3 (B) naïve and memory Tregs also cluster together based on expression of 'mechanistic' receptors alone, which is largely driven by the differential expression of CD95 and ICOS by memory and naïve Tregs. Differences in expression in CD49d and CD73 seem to be more driven by inter-donor variation than memory/naïve status.

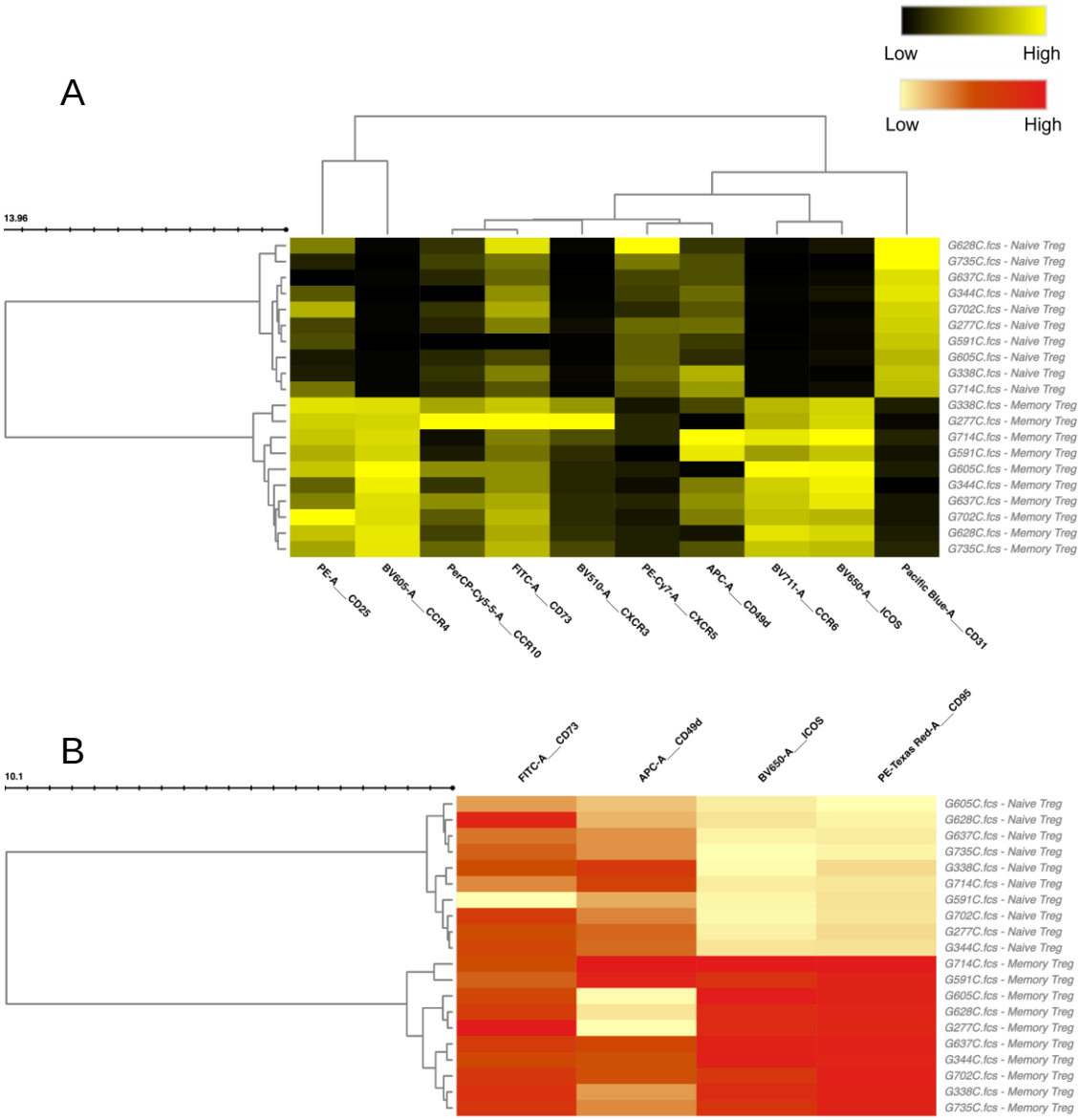

Figure 3.3: Naïve and memory Tregs from human healthy donors cluster separately based on their surface phenotype..Tregs from 10 healthy donors (n=10) were stained with the Treg subset surface marker panel and data acquisition carried out on a BD FACS Aria-IIu cell sorter. Naïve Tregs were gated as $CD4^{+}CD25^{hi}CD127^{lo}CD45RA^{+}$ cells and memory Tregs as $CD4^{+}CD25^{hi}CD127^{lo}CD95^{+}$ cells. (A) Heatmap shows the mean fluorescence intensity of the above markers in 10 naïve and memory Tregs from 10 donors. (B) Heatmap shows expression of 'mechanistic receptors' by naïve and memory Tregs. Agglomerative hierarchal clustering is shown by dendrograms on the left of each heatmap. Scales show low to high MFIs of each marker.

3.3.2 Identification of previously reported Treg subsets by Boolean gating

As described in detail in chapter 1.7, many Treg subsets have been reported in the literature based on their expression of surface receptors. We next aimed to use our Treg surface marker panel to confirm that these subsets could be consistently identified in all donors using the Treg surface marker panel. Figure 3.4 (A) shows the Boolean gating strategy designed to identify several previously reported Treg subsets within individual donors, and a comparative gating strategy showing their Tconv counterparts (B).

Tregs were gated as $CD4^{+}CD25^{hi}CD127^{low}$ cells, and naïve and memory Tregs were gated as $CD45RA^{+}CD95^{-}$ and $CD45RA^{-}CD95^{+}$, respectively, as described above. Using the expression pattern data described above and in figure 3.2 to guide our analysis, we found that within the naïve Treg pool the most highly expressed markers were CD31 and CXCR5, and these markers correspond to naïve RTE Tregs and naïve T follicular regulatory cells which are commonly reported in the literature (Balint et al., 2013; Haas et al., 2007a; Wollenberg et al., 2011). As shown in representative plots (A) and (B) in figure 3.4, subsets of naïve Tregs were detected with $CD31^{+}$, $CXCR5^{+}$, or $CD31^{+}CXCR5^{+}$ double positive phenotypes, however naïve Tconvs expressing CXCR5 were present at low frequencies in these donors. Within the memory Treg pool it was possible to identify several helper-like Treg populations based on the differential expressions of the chemokine receptors CCR4, CXCR3, CCR6 and CCR10. As previously reported by Duhen et al. (2012) and Halim et al. (2017) memory Tregs can be identified expressing a Th2, Th17, Th22, Th1, and Th17.1 helper-like surface

phenotype as observed in the Tconv compartment. We also identified Tregs with a similar surface phenotype to Th9 Tconvs. The table in figure 3.4 (C) summarises the surface chemokine receptor and cytokine profiles of each helper subset.

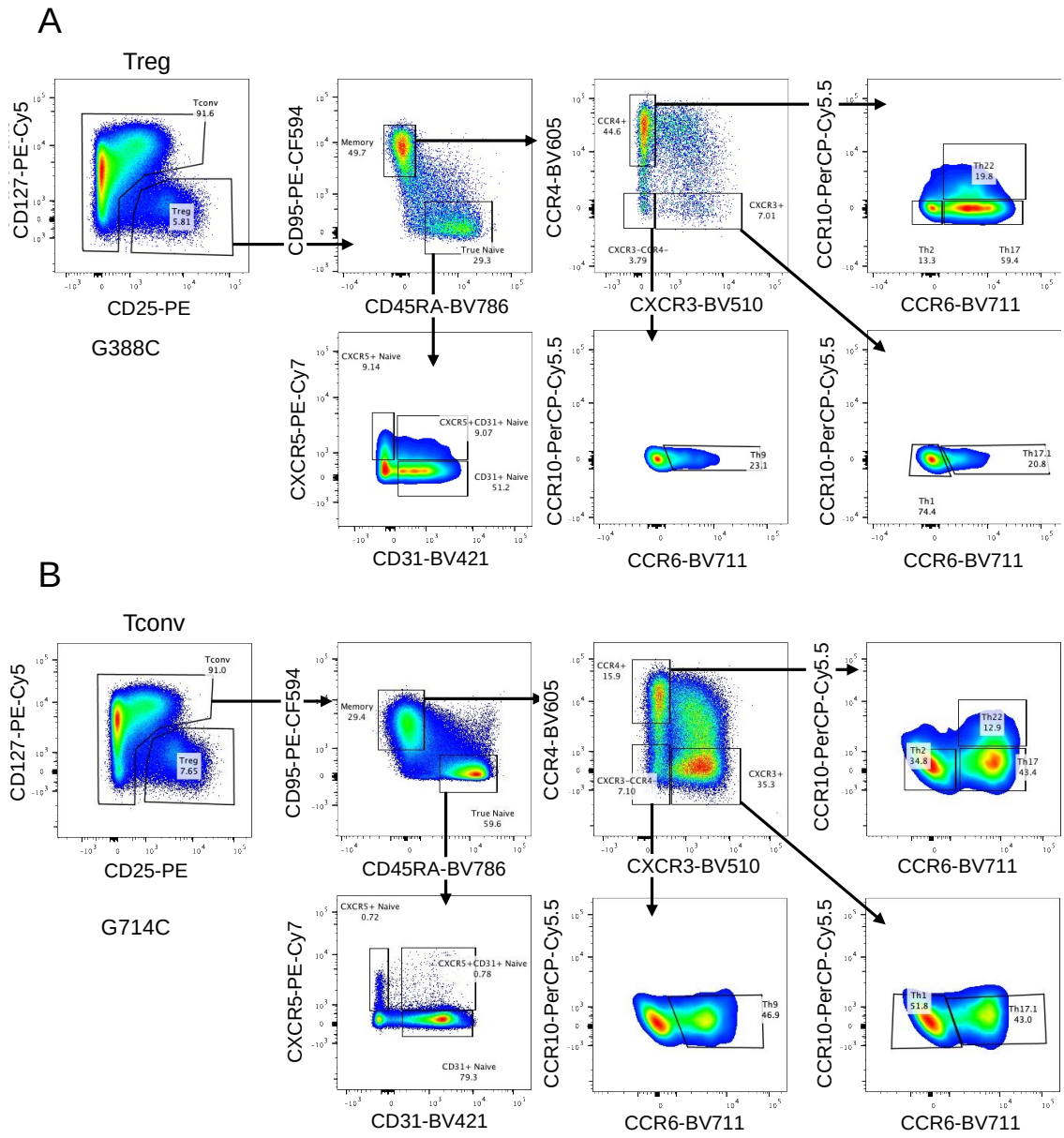

C

T-helper Subtype	Chemokine Receptor	Key Cytokine Profile
Th1	CXCR3$^+$	IFN-γ
Th2	CCR4$^+$CCR6$^-$	IL-4, IL-5, IL-13
Th9	CCR4$^-$CCR6$^+$	IL-9
Th17	CCR4$^+$CCR6$^+$	IL-17, IL-22
Th17.1	CCR3$^+$CCR6$^+$	IFN-γ, IL-17
Th22	CCR4$^+$CCR6$^+$CCR10$^+$	IL-22, IL-13
Tfh	CXCR5$^+$	IL-21

Figure 3.4: Recent thymic emigrant Tregs and T helper-like Treg subsets could be identified using surface expression of CD31 and of the chemokine receptors CCR4, CXCR3, CCR6 and CCR10.(A) Representative plots showing the gating strategy of subsets which have previously been reported in the literature and can be detected using our Treg surface marker panel; Th1, Th17.1, Th2, Th17, Th22, and Th9-like Tregs and naïve CD31$^+$ and CXCR5$^+$ Tregs (B) Gating strategy showing the equivalent subsets within the Tconv pool

in a healthy donor. (C) Table showing the surface phenotypes and cytokine profiles of helper subsets (Reviewed by Askar et al., 2014). Data acquisition carried out on a BD FACS Aria-IIu cell sorter.

Activated Tconvs can upregulate CD25 and downregulate CD127 giving them a similar surface phenotype to Tregs. It could therefore be hypothesised that some of the subsets within the $CD4^{+}CD25^{hi}CD127^{low}$ gate could be contaminated by Tconv cells, especially within memory Treg subsets which express higher CD25 than naïve subsets (figure 3.3). Therefore, it was important to determine whether these Treg subsets expressed FoxP3 and Helios intracellularly, although it is of note that both FoxP3 and Helios can also be upregulated on activation in Tconvs. An amended staining panel and protocol was used as described in 3.2.2 to analyse the expression of these transcription factors by each subset. Figure 3.5 shows representative histogram overlays from a single donor showing the MFI of FoxP3 and Helios within each Treg subset. Memory Treg subsets on average had a higher expression of FoxP3 than naïve Tregs (figure 3.5 A and B) which is in agreement with previous studies (Miyara et al., 2009). Notably, within each memory helper subset shown in 3.5 (A), there were some cells expressing similar levels of FoxP3 as Tconvs (red histogram), suggesting the presence of some contaminating Tconvs within these subsets. Naïve Treg subsets, however, showed no evidence of contaminating Tconvs (B). Therefore, it is possible that when isolating Tregs based on expression of surface markers alone that memory Treg subsets may contain more contaminating Tconvs than naïve Tregs. All memory and naïve Treg subsets contained cells expressing Helios (figure 3.5 C and D), although all subsets contained a mixture of Helios positive and negative cells. This was to be expected as not all Tregs express Helios.

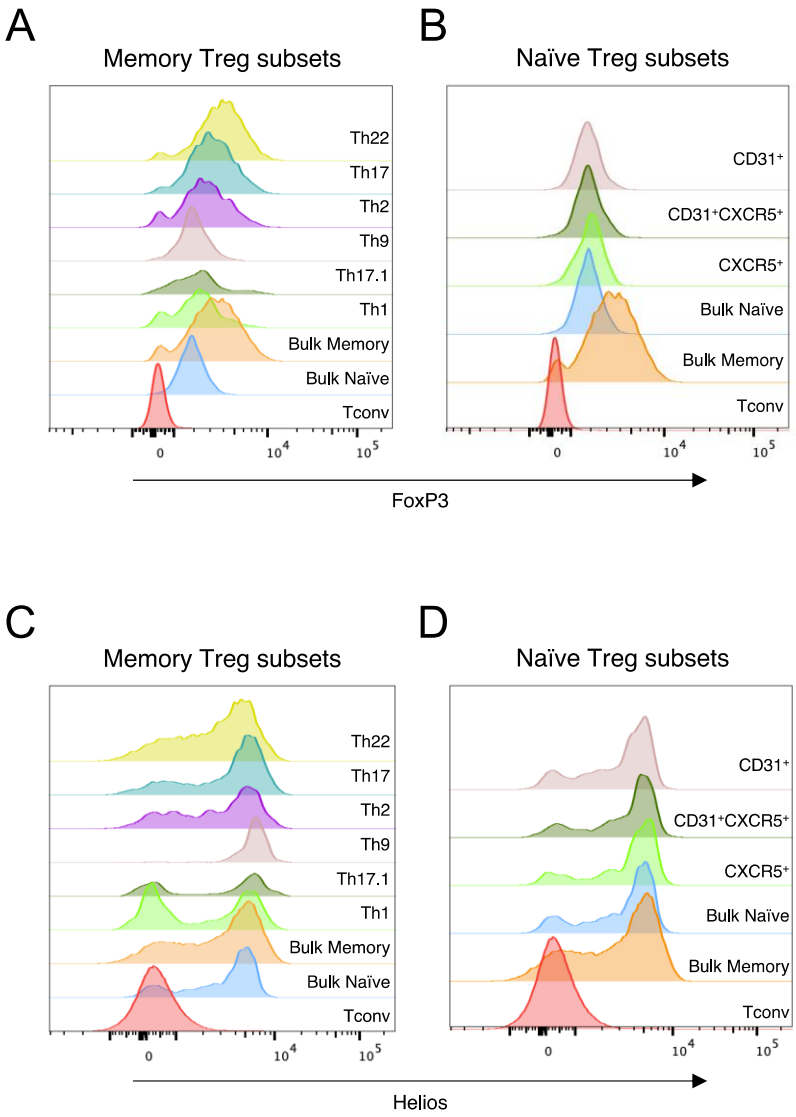

Figure 3.5: Human peripheral Treg subsets expressed varying levels of intracellular FoxP3 (A-B) and Helios (C-D). Representative histogram plots from a single healthy donor showing the mean fluorescence intensities (MFI) of FoxP3 (top panels) and Helios (bottom panels) within subsets of peripheral memory (left panels) and naïve (right panels) Tregs. Healthy donor PBMCs were stained with the Treg surface marker panel, followed by fixation and permeabilisation, and staining with FoxP3 and Helios antibodies and analysed by flow cytometry. Tconvs were also stained as comparators. Data acquired on a BD LRS Fortessa analyser.

As shown in figure 3.6, the balance of cells in each subpopulation differed in frequency in Tregs and Tconvs using the gating strategy shown in figure 3.4. Firstly, memory and naïve Tconvs existed at mean frequencies of 39.56% and 48.47%, respectively, within peripheral blood from 10 healthy donors. However, within the Treg pool in the same donors, memory Tregs made up a mean of 54.35% of total Tregs with naïve Tregs occupying 23.9% of the Treg pool (figure 3.6 A). The frequencies of the memory helper-like subsets did not show consistent patterns of frequencies between Tconvs and Tregs. Within Tconvs, the most frequent memory subset was Th1 helper cells (15.68% of memory Tconvs) and the least frequent subset was Th22-like Tconvs at 2.246% (figure 3.6 B). Within the memory Treg compartment, Th1-like Tregs were among the least frequent subsets at 3.835% of memory Tregs, with the most frequent subset being Th17-like Tregs at 27.51% of memory Tregs. Th17.1 and Th9-like Tregs were very rare subsets with mean frequencies of 0.87% and 0.618% of memory Tregs, respectively. There was also considerable variation in the frequencies of memory subsets within both the Tconv and Treg pools from donor to donor as indicated by the coefficient of variance (CV) values which were greater than 25% for most subsets (figure 3.6 B).

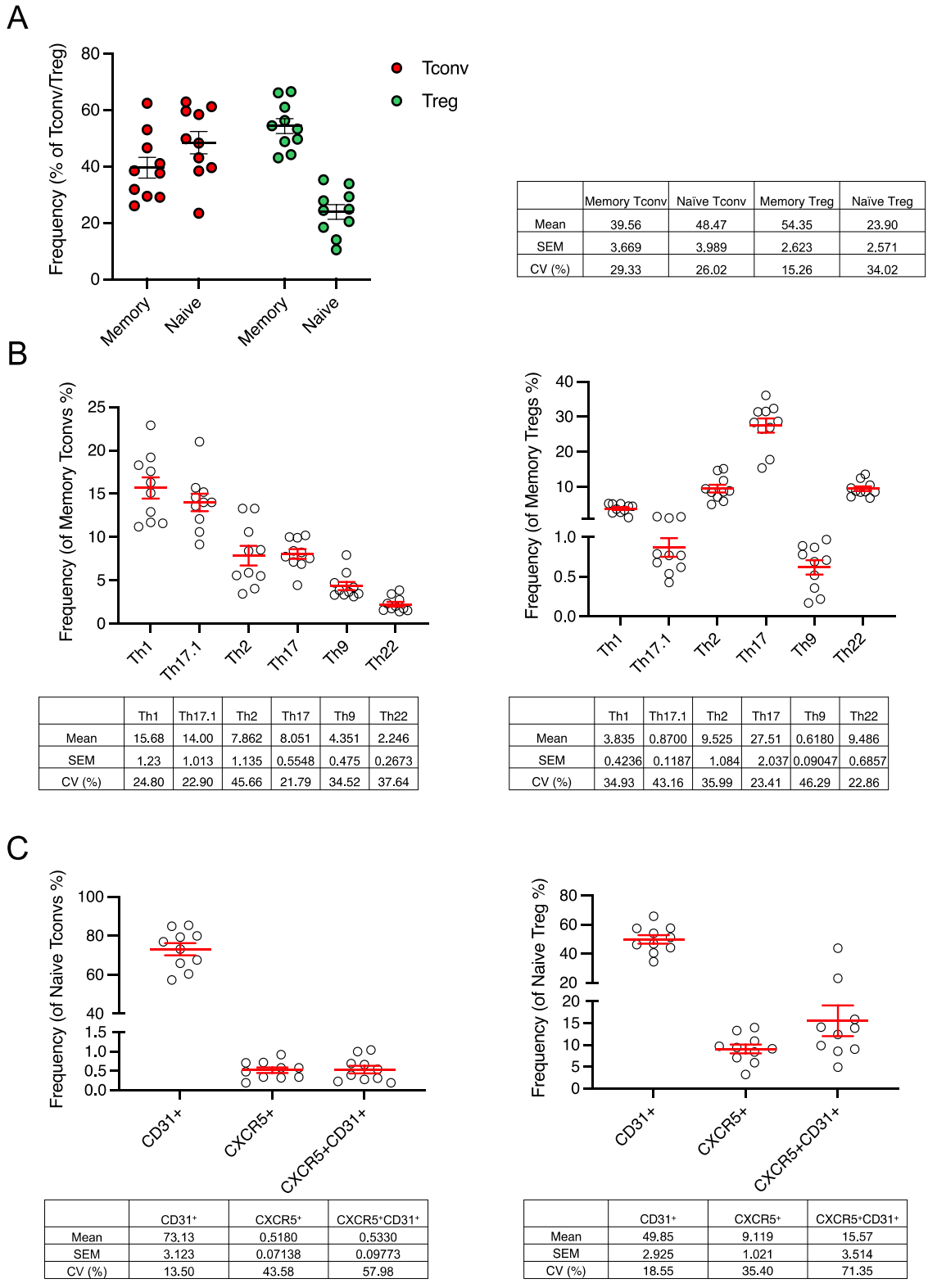

	Memory Tconv	Naïve Tconv	Memory Treg	Naïve Treg
Mean	39.56	48.47	54.35	23.90
SEM	3.669	3.989	2.623	2.571
CV (%)	29.33	26.02	15.26	34.02

	Th1	Th17.1	Th2	Th17	Th9	Th22
Mean	15.68	14.00	7.862	8.051	4.351	2.246
SEM	1.23	1.013	1.135	0.5548	0.475	0.2673
CV (%)	24.80	22.90	45.66	21.79	34.52	37.64

	Th1	Th17.1	Th2	Th17	Th9	Th22
Mean	3.835	0.8700	9.525	27.51	0.6180	9.486
SEM	0.4236	0.1187	1.084	2.037	0.09047	0.6857
CV (%)	34.93	43.16	35.99	23.41	46.29	22.86

	CD31+	CXCR5+	CXCR5+CD31+
Mean	73.13	0.5180	0.5330
SEM	3.123	0.07138	0.09773
CV (%)	13.50	43.58	57.98

	CD31+	CXCR5+	CXCR5+CD31+
Mean	49.85	9.119	15.57
SEM	2.925	1.021	3.514
CV (%)	18.55	35.40	71.35

Figure 3.6: Helper-like subsets and naïve CD31⁺ and CXCR5⁺ subsets occurred at different frequencies in peripheral Tregs and Tconvs from matched healthy donors. Tregs from 10 healthy donors (n=10) were stained with the Treg subset surface marker panel and data acquisition carried out on a BD FACS Aria-IIu cell sorter. Naïve Tregs were gated as $CD4^+CD25^{hi}CD127^{lo}CD45RA^+$ cells and memory Tregs as $CD4^+CD25^{hi}CD127^{lo}CD95^+$ cells. (A) Frequencies of memory and naïve cells within the Tconv and Treg compartments.

(B) Frequencies of helper subsets within the memory compartments of Tconvs and Tregs. (C) Frequencies of naïve cells expressing (or co-expressing) CXCR5 and CD31 within Treg and Tconv pools. Error bars represent mean +/- standard error of the mean. SEM = standard error of mean; CV= coefficient of variance.

Within the naïve compartments, a mean of 73.13% and 49.85% of Tconvs and Tregs respectively were single positive for CD31 (figure 3.6 C). As suggested in figure 3.4, CXCR5-expressing naïve Tconvs were rare, existing at a mean frequency of 0.518% of naïve Tconvs in comparison with 9.119% of naïve Tregs. Furthermore only 0.533% of naïve Tconvs co-expressed CXCR5 and CD31, while these cells were more frequent in the Treg pool at 15.57% of naïve Tregs. However, the frequency of this naïve Treg subset had a high inter-donor variation (CV = 71.35%).

Some of the large differences in frequencies of the memory subsets in Tconvs and Tregs can be explained by observing the comparative MFIs of the individual surface markers expressed by these subsets (figure 3.7). Namely, memory Tregs expressed significantly lower levels of CXCR3 at their cell surface than memory Tconvs (figure 3.7 A). In support of this, the gating strategy shown in figure 3.4, shows that $CXCR3^{+}$ cells represent 7.01% of memory Tregs in this donor, whereas $CXCR3^{+}$ cells represent 35.3% of memory Tconvs. It is evident that this reduced expression of CXCR3 causes reduced frequencies of Th9, Th1, and Th17.1-like Tregs compared to Tconvs. In addition, memory Tregs displayed a significantly higher MFI of CCR4 and CCR6 than in memory Tconvs which explains the higher frequencies of Th17 and Th22-like Tregs in Tregs compared to Tconvs. No difference in expression of CCR10 was observed between memory Tregs and Tconvs. Figure 3.7 B shows as expected that naïve Tconvs had a

significantly higher MFI of CD31 than naïve Tregs, and conversely, naïve Tconvs had a significantly lower MFI of CXCR5 than naïve Tregs. In conclusion, all previously reported Treg subsets can be reproducibly found in healthy donor blood using our Treg surface marker panel. Differences in levels of expression of markers used to identify these subsets and therefore frequencies of these subsets differ between Tconvs and Tregs.

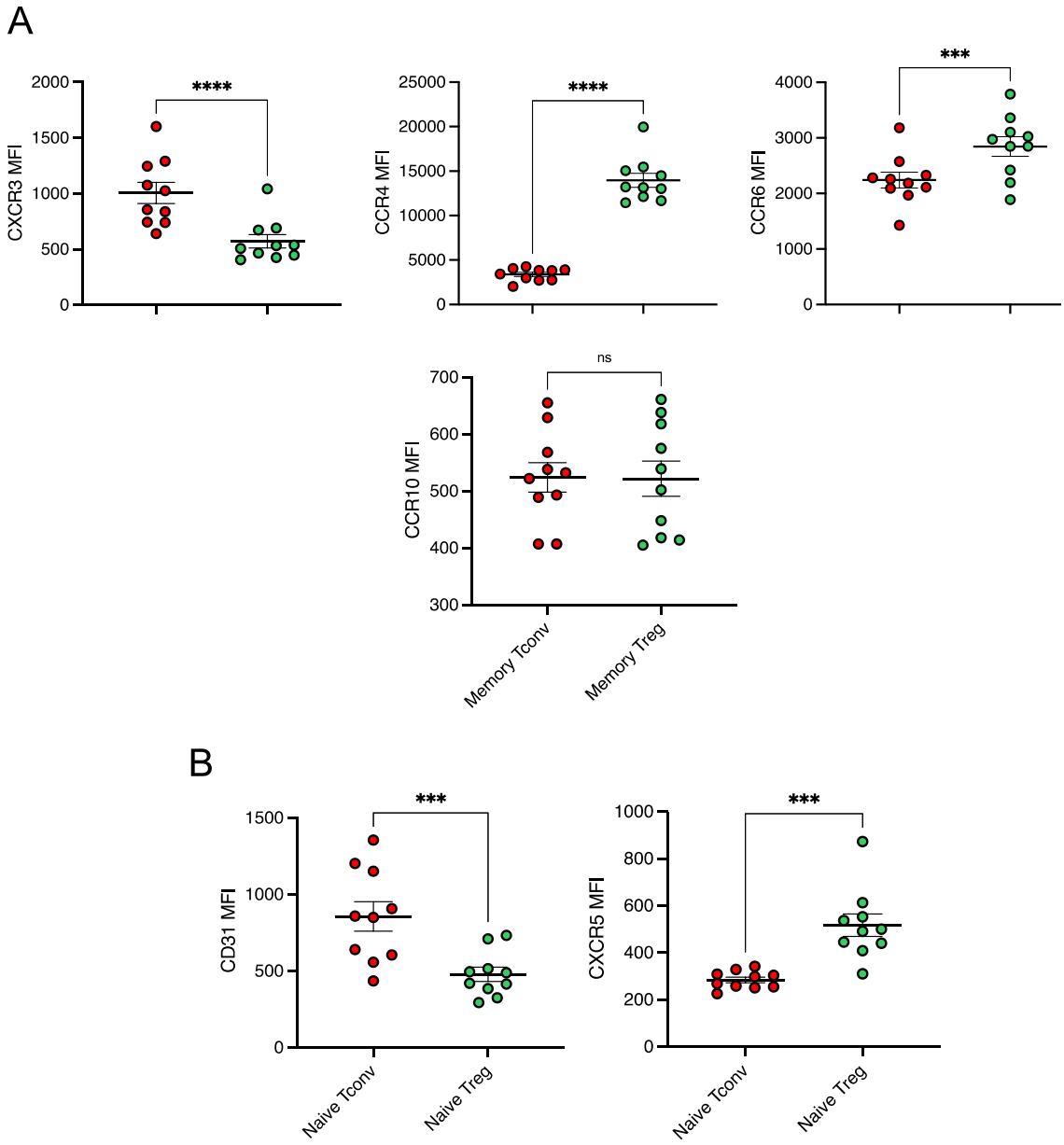

Figure 3.7: Mean fluorescence intensities (MFIs) of CXCR3, CCR4, CCR6, CD31, and CXCR5 were significantly different in memory and naïve Tregs and Tconvs. Tregs from 10 healthy donors (n=10) were stained with the Treg subset surface marker panel and data acquisition carried out on a BD FACS Aria-IIu cell sorter. Naïve Tregs were gated as $CD4^{+}CD25^{hi}CD127^{lo}CD45RA^{+}$ cells and memory Tregs as $CD4^{+}CD25^{hi}CD127^{lo}CD95^{+}$ cells. (A) MFIs of CXCR3, CCR4, CCR6, and CCR10 in memory Tconvs and Tregs. (B) MFIs of CD31 and CXCR5 in naïve Tconvs and Tregs. Tconv and Treg data were derived from matched donors. Significant differences were determined by paired student t-tests (***= $p < 0.0005$; ****= $p < 0.0001$) Error bars represent mean +/- standard error of the mean. Data acquisition carried out on a BD FACS Aria-IIu cell sorter.

3.3.3 Unbiased analysis of Treg subsets

As well as taking a literature-based approach using previously reported Treg subsets to direct our analysis, we also opted to use *in silico* clustering tools to identify subsets of Tregs. Using the same dataset derived from PBMCs from 10 healthy donors stained with our Treg surface marker panel, Tregs were first manually gated as $CD4^{+}CD25^{hi}CD127^{low}$ for each donor and data from each donor were combined. Dimensionality reduction was then carried out using the optSNE algorithm. As shown in figure 3.8, by overlaying the colour-axis of each marker onto the optSNE plot, it was clear that dimensionality reduced events have been resolved on a vertical axis dependent on their expression of typical naïve/memory markers such as CD45RA, CCR4, and CD95 shown in the top row of panels. Events enriched for CD45RA also co-localised with events with a high CD31 MFI, and additionally, a separate clade within the memory population was also enriched for CD31. Similarly, CXCR5 expression was observed within both memory and naïve-rich areas. As expected, regions enriched for chemokine receptors CXCR3, CCR10, and CCR6 and also ICOS mostly co-localised with regions enriched for memory markers towards the bottom of the y-axis. Events with high expression of CD49d mostly occurred within memory regions but lower expression was also observed within naïve regions. Finally, small and distinct regions of events expressing CD73 occurred. Therefore, the manner in which the unsupervised dimensionality reduction algorithm spatially separated high dimensional events was reminiscent of how data were manually visualised in the previous data figures using histogram overlays and heatmaps of MFI data (figures 3.2 and 3.3) thus showing that the optSNE parameters were well optimised.

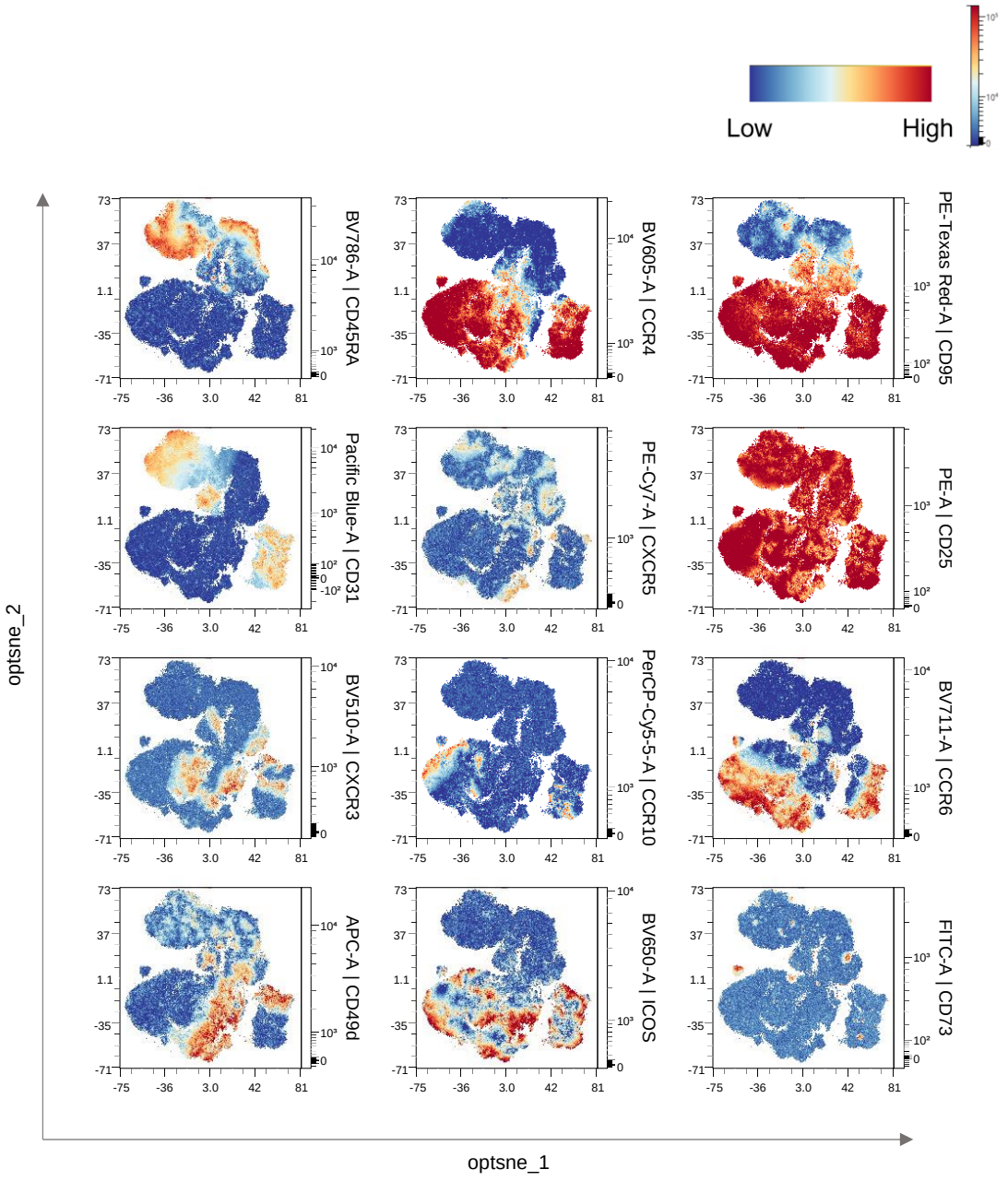

Figure 3.8: optSNE colour-axis overlays showing that dimensionality reduction of Treg surface markers was driven predominantly by naïve/memory status. Tregs from 10 healthy donors (n=10) were stained with the Treg subset surface marker panel and data acquisition carried out on a BD FACS Aria-IIu cell sorter. Gated bulk Tregs ($CD4^{+}CD25^{hi}CD127^{lo}$) were down sampled to 20,000 events per donor. The optimised t-distributed stochastic neighbour embedding (optSNE) algorithm was used for dimensionality reduction analysis of the concatenated Treg dataset giving rise to optsne_1 and optsne_2 parameters. The mean fluorescence intensities of CD45RA, CCR4, CD95, CD31, CXCR5, CD25, CXCR3, CCR10, CCR6, CD49d, ICOS, and CD73 are indicated by colour axis scales (red=high, blue=low.)

Clustering was then carried out using the FlowSOM clustering algorithm. As described in the methods, the Phenograph clustering algorithm was also used to guide the number of clusters which was appropriate for this dataset. Phenograph found 33 clusters when the number of nearest neighbours was set to k=200, and 33 clusters was then input as the target number of clusters in the FlowSOM algorithm. The FlowSOM clusters were then individually analysed to ensure that each cluster consisted of a unique and homogenous population of cells. As shown in figure 3.9, histograms of each marker within each cluster were used for this analysis. Figure 3.9 A is an example of where the FlowSOM algorithm under-clustered the dataset as the events within FlowSOM cluster 8 were heterogeneous for CCR4 and CXCR3 expression, and therefore under-clustered populations such as these were split. Figure 3.9 B then shows a representation of over-clustering as FlowSOM clusters 14 and 19 had a very similar phenotype. The only differences seen between these two clusters were subtle differences in the MFI of CD31, however both were $CD31^{+}$ and therefore clusters such as these were merged.

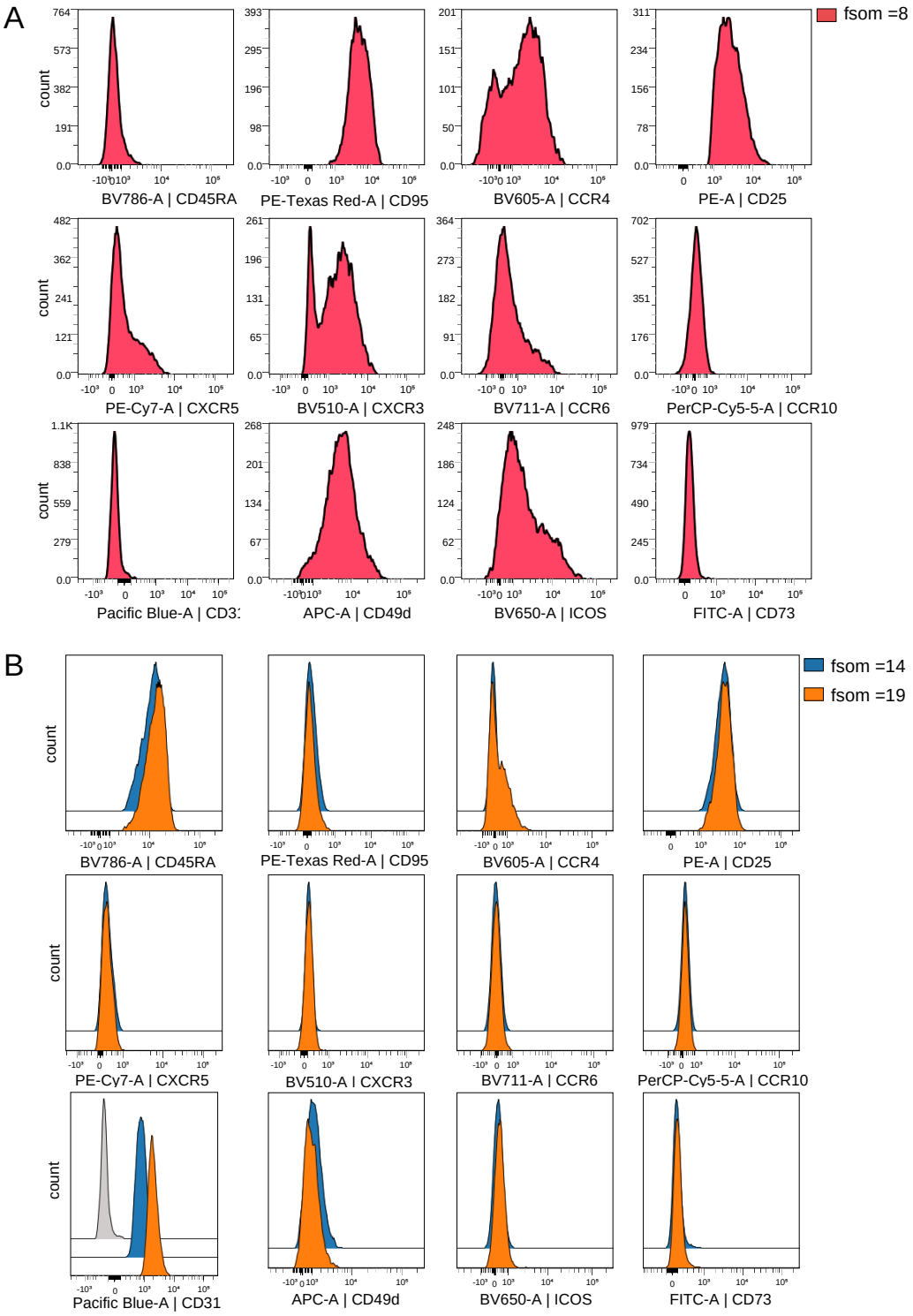

Figure 3.9: The FlowSOM clustering algorithm could give rise to under and over-clustering of Tregs. Tregs from 10 healthy donors (n=10) were stained with the Treg subset surface marker panel and data acquisition carried out on a BD FACS Aria-IIu cell sorter. Following $CD4^{+}CD25^{hi}CD127^{lo}$ Treg gating, down sampling, and dimensionality reduction using optSNE, phenograph and flowSOM (self-organising map) clustering algorithms were used to identify unbiased subsets of Tregs. The number of clusters as determined by phenograph was input into FlowSOM (33) and histograms showing the MFI for each marker

were used to determine any under or over-clustering. (A) Example of under-clustering in FlowSOM cluster 8. (B) Example of over-clustering in FlowSOM clusters 14 and 19.

Following this close analysis of the phenotypes of each cluster of cells, 26 Treg clusters were found based on the expression of the parameters CCR4, CD25, CD95, CD31, CD45RA, CXCR5, CD73, CCR10, CCR6, CD49d, CXCR3, and ICOS (figure 3.10 A). The heatmap shown in figure 3.10 B shows the expression profiles of each of these surface markers within the 26 unbiased Treg populations. As in the previous heatmap of raw MFI data shown in figure 3.3, CCR4, CD25, and CD95 were highly related as memory markers according to the dendrogram on this heatmap, as were CD45RA and CD31. Figure 3.11 shows the relative frequencies of each of these clusters as a percentage of total Treg events. As show here, the naïve Treg subsets expressing CD45RA such as clusters 23, 24, 25, and 26 were often the most frequent. This is perhaps owing to the increased diversity in surface markers within the memory Treg population which increases the number of potential clusters.

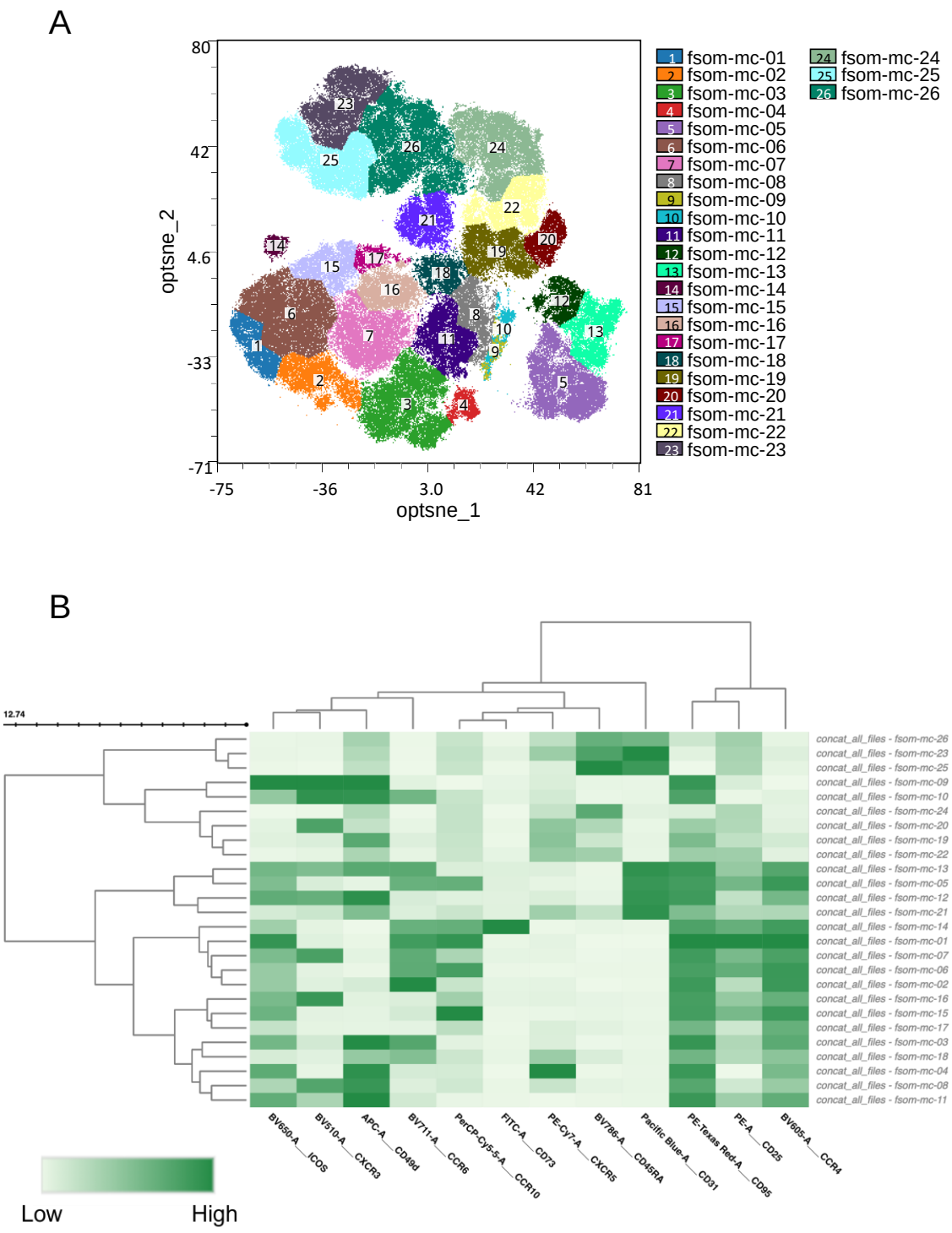

Figure 3.10: Human Tregs could be divided into 26 unbiased subsets using FlowSOM clustering of Treg surface phenotypes. Tregs from 10 healthy donors (n=10) were stained with the Treg subset surface marker panel and data acquisition carried out on a BD FACS Aria-IIu cell sorter. Following $CD4^{+}CD25^{hi}CD127^{lo}$ Treg gating, down sampling, and dimensionality reduction, the flowSOM clustering algorithm was used to identify unbiased subsets of Tregs based on mean fluorescence intensities of surface markers. (A) Treg FlowSOM clusters indicated by distinctly coloured regions overlaid on the optSNE dimensionality reduction plot. (B) Heatmap showing the fluorescence intensities of Treg

surface markers within 26 unbiased FlowSOM clusters. The dendrogram to the left of the histogram indicates the agglomerative hierarchal clustering of Treg clusters, whereas the dendrogram above indicates agglomerative hierarchal clustering of surface markers.

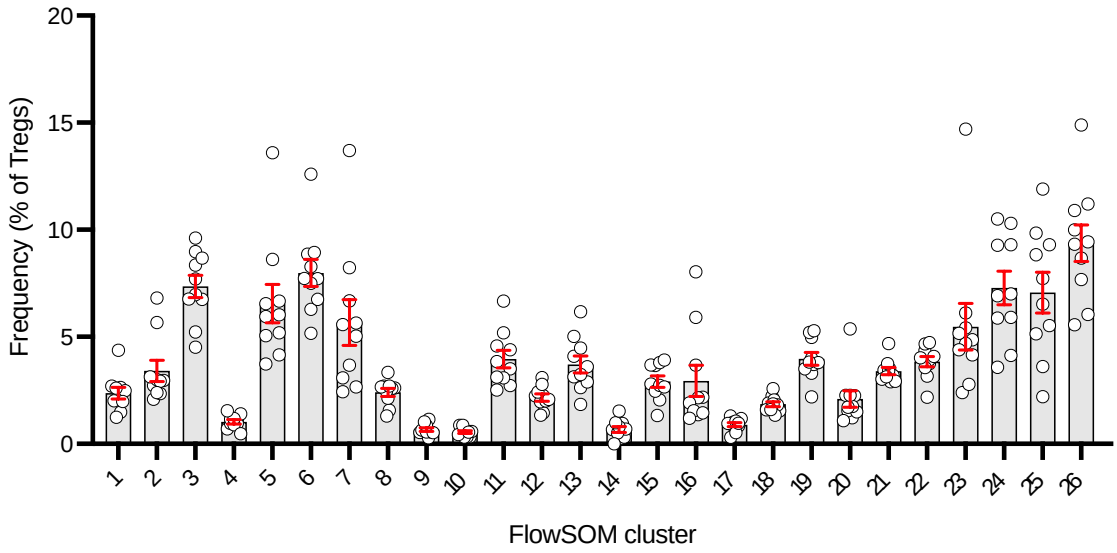

Figure 3.11: The 26 Treg clusters as determined by FlowSOM clustering occurred at varying frequencies in 10 healthy donors. Tregs from 10 healthy donors (n=10) were stained with the Treg subset surface marker panel and data acquisition carried out on a BD FACS Aria-IIu cell sorter. Following $CD4^{+}CD25^{hi}CD127^{lo}$ Treg gating, down sampling, and dimensionality reduction, the FlowSOM clustering algorithm was used to identify unbiased subsets of Tregs. Box plots show the mean frequencies of each FlowSOM cluster as a percentage of total Tregs within each donor.

Next we sought to characterise the phenotype of each unbiased Treg cluster. By closely analysing the surface phenotype of each subset, we then aimed to decipher whether any of these unbiased subsets overlapped with the previously reported Treg subsets discussed in the above figures, and conversely whether any of these subsets represented novel Treg subsets which have not previously been reported in the literature. Table 3.4 shows a table with the comprehensive surface phenotype of each Treg subset identified by FlowSOM. We identified several subsets which seemed to overlap with the previously reported Treg subsets described earlier in this chapter. For example, as also shown in figure 3.12, FlowSOM cluster 2 showed a clear Th17-like Treg phenotype and FlowSOM cluster 9 had a Th1-like Treg phenotype according to our previously reported Treg gating strategy. Cluster 25 also showed a clear naïve $CD31^+$ Treg phenotype, cluster 24 had a naïve $CXCR5^+$ phenotype, and clusters 26 and 23 had naïve $CXCR5^+CD31^+$ phenotypes, respectively. Unbiased FlowSOM clustering did not identify any clusters which resembled Th9-like Tregs.

We also found that several FlowSOM clusters represented previously reported Treg subsets in combination with different effector molecules on their surface such as Clusters 10 which had a Th17.1-like $ICOS^+CD49d^+$ phenotype and cluster 14 which had a Th22-like $CD73^+$ phenotype.

Table 3.4: Phenotypes of each unbiased Treg subset identified by FlowSOM

FlowSOM cluster	CD49d	CXCR3	CCR4	ICOS	CCR6	CD45RA	CD73	CD25	CXCR5	CD95	CD31	CCR10	Main Phenotype	Previously reported?
1	-	-	+	+	+	-	-	+	-	+	-	+	Th22 with ICOS	Th22-like
2	-	-	+	low/-	+	-	-	+	-	+	-	-	Th17	Th17-like
3	+	-	+	+	+	-	-	+	low/-	+	-	-	Th17 ICOS+ CD49d+	Th17-like
4	-	-	+	+	-	-	-	+	+	+	-	-	memory Tfr	T-follicular regulatory
5	-	low/-	+	low	+	-	-	+	-	+	+	+	Th22 without ICOS with CD31	Th22-like
6	-	-	+	low/-	+	-	-	+	-	+	-	+	Th22	Th22-like
7	-	+	+	+	+	-	-	+	-	+	-	low/-	CXCR3hi CCR4hi CCR6+	Novel
8	+	+	low	low/-	-	-	-	+	low	+	-	-	CXCR3+ CCR4lo CD49d+	Novel
9	+	+	-	+	-	-	-	+	low	+	-	-	Th1 with CD49d and ICOS	Th1-like
10	+	+	-	low	+	-	-	+	low	+	-	low/-	Th17.1 with CD49d and ICOS	Th17.1
11	+	low/-	+	+	-	-	-	+	-	+	-	-	CXCR3lo CCR4+ CCR6+ CD49d+ ICOS+	Novel
12	+	+	low	+	-	-	-	+	low/-	+	+	-	CXCR3+ CCR4lo CD49d+ ICOS+ CD31+	Novel
13	+	low/-	+	low/-	+	-	-	+	low/-	+	+	-	CXCR3lo CCR4+ CCR6+ CD49d+CD31 +	Novel
14	-	-	+	low	+	-	+	+	-	+	-	+	Th22 with CD73	Th22-like
15	-	-	+	+	-	-	-	+	-	+	-	+	CCR4+ CCR10+ ICOS+	Novel
16	-	+	+	+	-	-	-	+	-	+	-	low/-	CXCR3 hi CCR4+ ICOS+	Novel
17	-	-	+	-	-	-	+	+	-	+	-	-	Th2 CD73+	Th2-like
18	low/-	-	low	-	+	low	-	+	+	low	-	-	transitioning CXCR5+ CCR6lo	Novel
19	+	-	low/-	-	-	low	-	+	+	low	-	-	transitioning CXCR5+ CD49d+	Novel
20	-	+	-	-	-	low	-	+	+	low	-	-	transitioning CXCR5+ CXCR3+	Novel
21	low	low/-	-	-	-	low	-	+	+	low	+	-	transitioning CXCR5+ CXCR3lo CD49dlo CD31+	Novel
22	low/-	-	-	-	-	low	-	+	+	low	-	-	transitioning CXCR5+ CD49dlo	Novel
23	low/-	-	-	-	-	+	-	+	+	-	+	-	Naïve CXCR5+ CD31+	Naïve CXCR5+ CD31+
24	low/-	-	-	-	-	+	-	+	low/-	-	-	-	Naïve CXCR5lo	Naïve CXCR5+
25	-	-	-	-	-	+	-	+	-	-	+	-	Naïve CD31+	Naïve CD31+
26	-	-	-	-	-	+	-	+	low/-	-	+	-	Naïve CXCR5lo CD31+	Naïve CXCR5+ CD31+

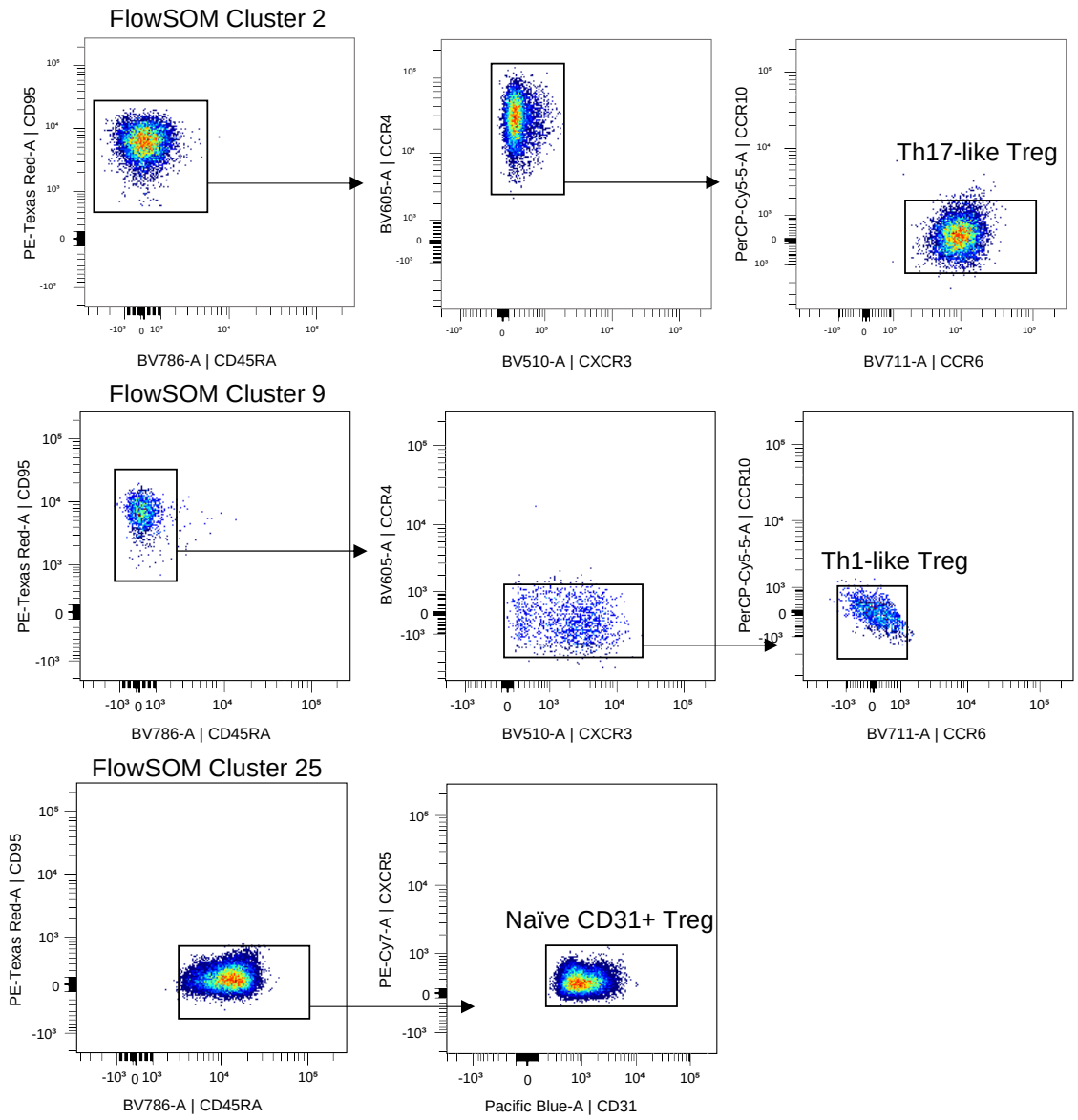

Figure 3.12: Individual Treg unbiased clusters identified by FlowSOM clustering had overlapping surface phenotypes with previously reported Treg helper-like and naïve CD31⁺ subsets. Tregs from 10 healthy donors (n=10) were stained with the Treg subset surface marker panel and data acquisition carried out on a BD FACS Aria-IIu cell sorter. Following $CD4^{+}CD25^{hi}CD127^{lo}$ Treg gating, down sampling, and dimensionality reduction, the FlowSOM clustering algorithm was used to identify unbiased subsets of Tregs. Representative plots showing examples of clusters which fall into helper-like and naïve $CD31^{+}$ Treg gating strategies. FlowSOM cluster 2 had an overlapping surface phenotype with memory Th17-like Tregs (top panel). FlowSOM cluster 9 had an overlapping surface phenotype with memory Th1-like Tregs (middle panel). FlowSOM cluster 25 had an overlapping surface phenotype with naïve $CD31^{+}$ Tregs (bottom panel).

As well as the previously reported Treg subsets, FlowSOM was able to identify several novel clusters as indicated in the right-hand column of table 3.4. These included several memory clusters (indicated as white rows in table 3.4) expressing various levels of chemokine receptors such as CCR4, CXCR3, CCR6, and CCR10 and different combinations of the effector molecules CD49d and ICOS, such as clusters 7, 8, 11, 12, 13, 15, and 16. In addition to the memory clusters shown as white rows on table 3.4 and naïve clusters shown in blue, FlowSOM also identified 5 clusters (18, 19, 20, 21, 22) co-expressing low levels of CD45RA and CD95 which seemed to be Tregs which were in the differentiation process of transitioning between a naïve and memory phenotype (yellow rows in table 3.4). Most of these clusters also expressed CXCR5, CD31, and CD49d which can be expressed by naïve Tregs and some had early signs of upregulating CCR6 and CXCR3. As these Treg subsets had not previously been reported, we surmised that these would be exciting populations of cells to isolate and subject to functional assays if they could be reproducibly found with a consistent phenotype from donor to donor.

We then sought to investigate the inter-donor variation within these clusters. As clustering was carried out on a virtually concatenated dataset from 10 donors, OMIQ software allowed us to de-concatenate this 10-donor dataset and analyse the same FlowSOM clusters within each individual donor. Figure 3.13 shows flow cytometry data of examples of 4 FlowSOM clusters each within 3 individual donors which present several problems relating to inter-donor variation within the novel clusters. Firstly, FlowSOM cluster 19, an example of a transitioning naïve

to memory Treg cluster, had inter-donor variation in the number of $CD45RA^+$ events. In donor G277C most events within this cluster were $CD95^+CD45RA^-$, however in donors G714C and G388C there were more $CD95^+CD45RA^+$ events. A similar scenario is shown in FlowSOM cluster 7 in which donor G591C seems to express no CCR10, however donors G388C and G277C do express CCR10. When analysing the phenotypes of FlowSOM cluster 13 in individual donors there was also a visible disparity in the number of CXCR3 positive events. Additionally, while analysis of CXCR3 in the concatenated dataset showed a single homogenous peak for CXCR3 expression for this cluster, in some donors such as G277C and G605C there seemed to be two distinct populations of cells which were either positive or negative for CXCR3 within this cluster. Finally, FlowSOM cluster 14 which represented Th22-like Tregs co-expressing CD73 had a large variation in frequency between donors, and in some donors such as G591C, no events fell into this cluster which is likely a consequence of CD73 expression being variable between donors as shown in figure 3.3 A.

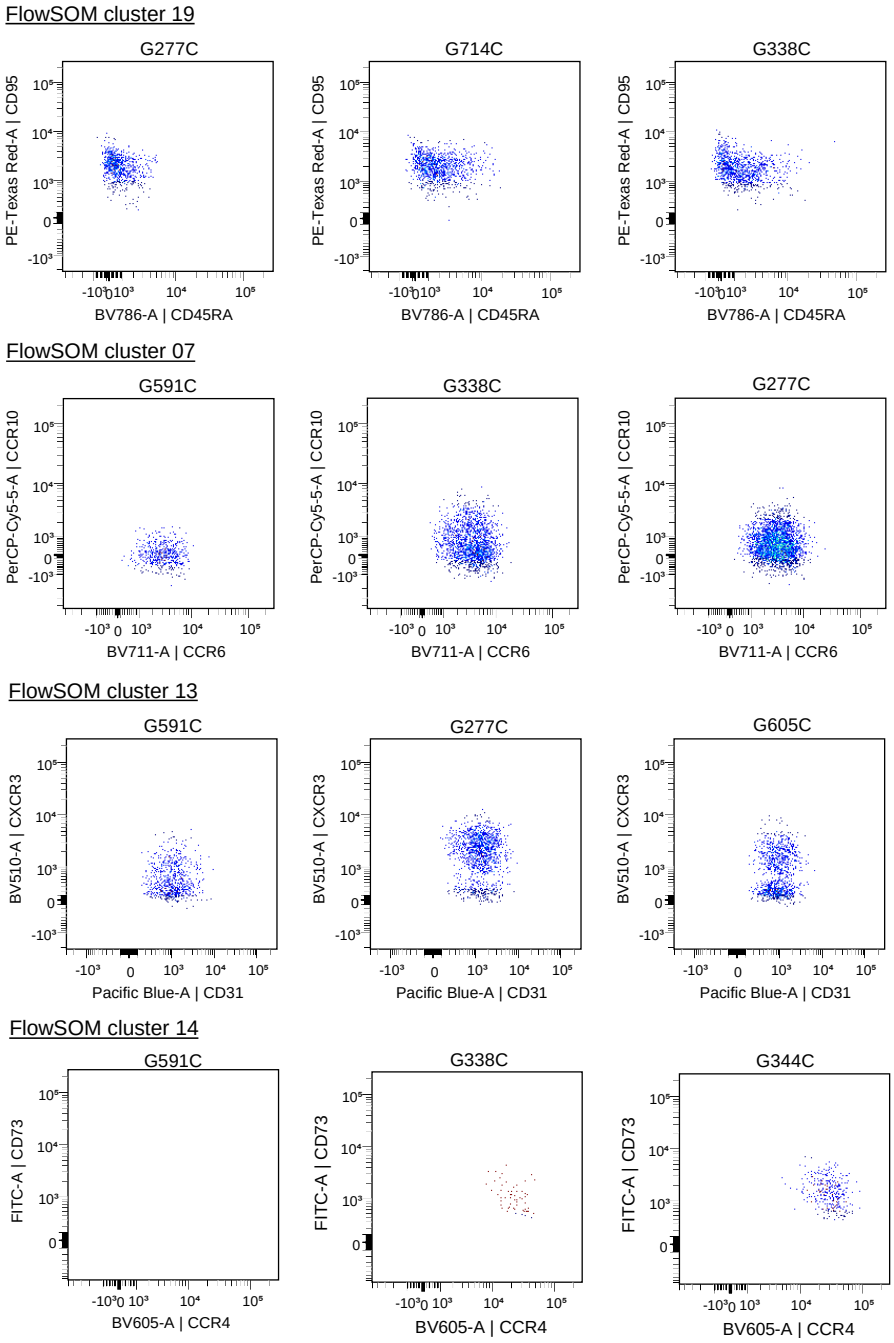

Figure 3.13: Some Treg unbiased clusters identified by FlowSOM did not display consistent phenotypes in all 10 donors. Tregs from 10 healthy donors (n=10) were stained with the Treg subset surface marker panel and data acquisition carried out on a BD FACS Aria-IIu cell sorter. Following $CD4^{+}CD25^{hi}CD127^{lo}$ Treg gating, down sampling, and dimensionality reduction, the FlowSOM clustering algorithm was used to identify 26 unbiased subsets of Tregs. Flow cytometry data above show data from 3 individual donors (columns) for each FlowSOM cluster described (rows); FlowSOM clusters 19, 07, 13, and 14 had intra-donor phenotypic inconsistencies.

These findings show that while these unbiased subsets seemed robust in the concatenated dataset from 10 donors, there was significant inter-donor variation within many of these novel Treg clusters. These novel FlowSOM clusters had complex surface phenotypes and factors which defined different clusters were often based on very subtle differences in the level of expression of chemokine receptors and CD45RA/CD95. Therefore, we concluded that the subtle differences in the level of expression of surface molecules on both an inter and intra-cluster level would make it very difficult to devise consistent gating schemes based on Boolean operators to isolate these Treg subsets during FACS sorting. Due to inter-donor variation, this would likely have a negative effect on reproducibility of functional analyses. In addition, as differing expression of 'mechanistic' receptors such as CD49d, ICOS, and CD73 often defined otherwise very similar clusters, inclusion of these molecules in the panel massively increased the number of potential clusters within the Treg pool and it was unlikely that it would be possible to FACS sort this many clusters from a single biological sample. For these reasons, we decided to focus our comparison of the *in vitro* suppressive function of Treg subsets on the previously reported Treg subsets described in figures 3.4-3.6, as these subsets could be reproducibly identified in all donors.

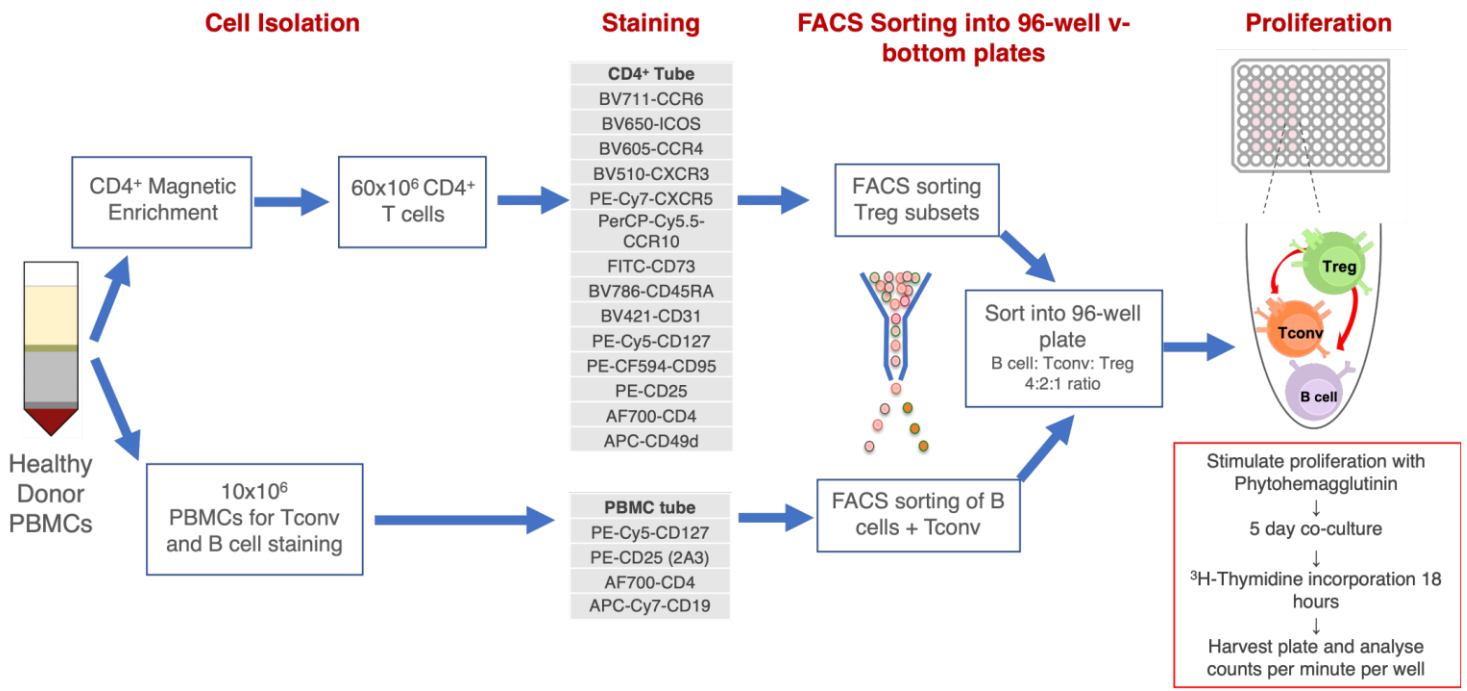

Figure 3.14: Schematic diagram of the Treg subset micro-suppression assay. PBMCs were isolated from healthy donor blood. 10 million cells were reserved and stained with a small panel of fluorescently conjugated antibodies to identify Tconvs and B cells. The remaining PBMCs were subjected to magnetic enrichment of $CD4^+$ T cells and stained with the Treg surface marker antibody panel. FACS sorting was then used to sort B cells, Tconvs and individual Treg subsets directly into 96-well v-bottomed plates at a 4:2:1 ratio. At least 5 replicate wells of each condition were carried out. Post-sorting, the cells were stimulated with 4μg/ml of phytohaemaglutinin and cultured for 5 days. At day 5, half of the culture supernatants were collected and media containing tritiated thymidine was added to the wells. 18 hours later, plates were harvested and numbers of radioactive counts per minute per well were read.

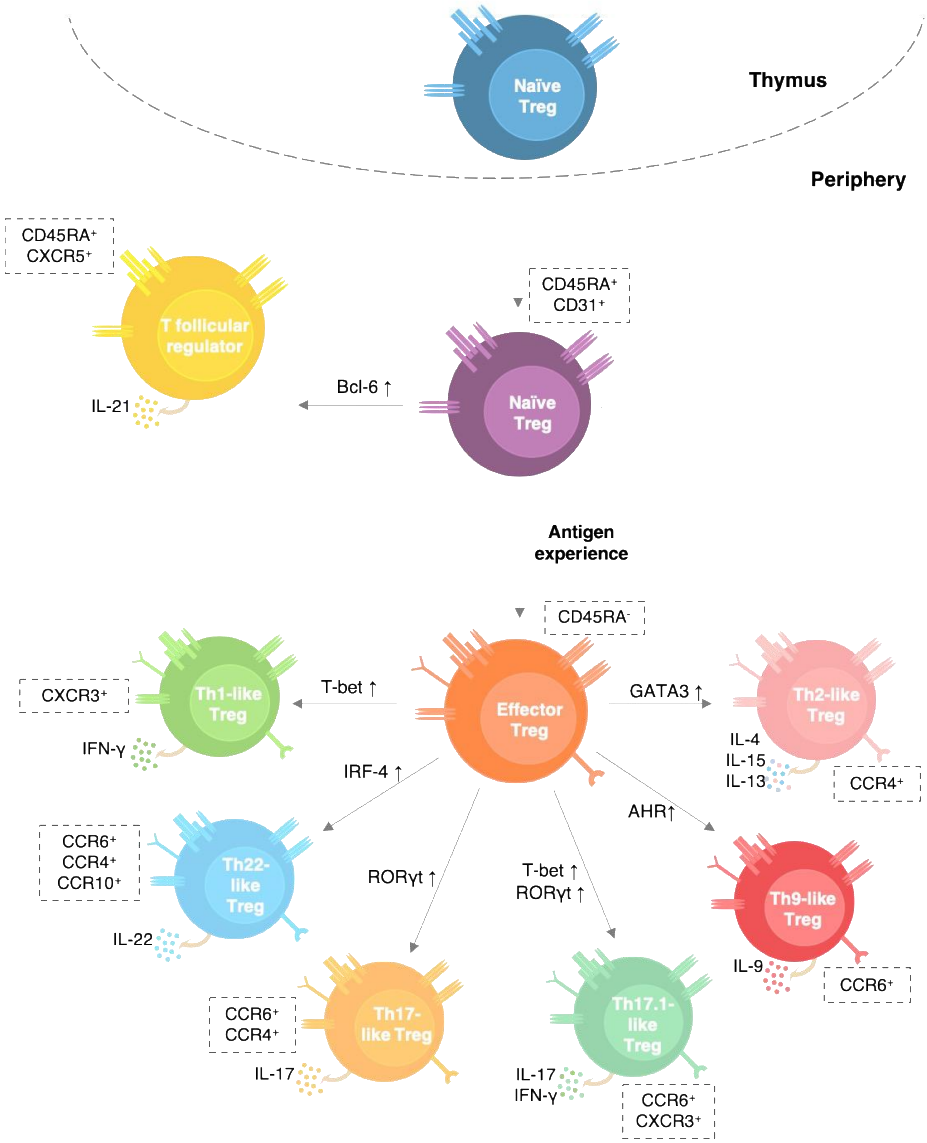

Figure 3.15: Schematic diagram showing the Treg subsets chosen to compare using the *in vitro* Treg micro-suppression assay. Tregs were evaluated for their surface phenotype by flow cytometry and the above previously-reported subsets were found. Naïve Tregs expressing CD45RA leave the thymus and upregulate CD31, a marker of recent thymic emigrant (RTE) Tregs. Naïve RTE Tregs could also co-express CXCR5, a marker of T follicular regulatory cells. Upon antigen experience, naïve Tregs then downregulate CD45RA and upregulate memory markers such as CD95. Memory Tregs can then take on cell surface phenotypes which mirror those of T helper subsets, such as Th1, Th2, Th9, Th17.1, Th17, and Th22-like Tregs through differential expression of the chemokine receptors CCR4, CXCR3, CCR6, and CCR10.

3.3.4 Analysing the *in vitro* suppressive capacities of Treg subsets

Treg subsets were isolated from healthy donor PBMCs and subjected to the Treg micro-suppression assay as described in 3.2.3 and as shown in figure 3.14. In summary, this method consisted of immunofluorescent staining and FACS sorting of Treg subsets along with B cells and Tconvs into plates, followed by a 5-day co-culture and overnight tritiated thymidine incorporation to measure the ability of Treg subsets to suppress the proliferation of Tconvs.

Figure 3.15 shows a summary of the previously reported Treg subsets which we chose to compare using the Treg micro-suppression assay; naïve $CD31^+$ Tregs (RTEs), naïve $CXCR5^+CD31^+$ Tregs, and the memory T helper-like Treg subsets Th1, Th2, Th9, Th17, Th17.1, and Th22-like Tregs. Figure 3.16 shows the strategy used to sort B cells, Tconvs, and bulk Tregs during FACS sorting. From here, figure 3.17 shows the strategy used to FACS sort the previously reported Treg subsets from bulk Tregs during the suppression assay setup.

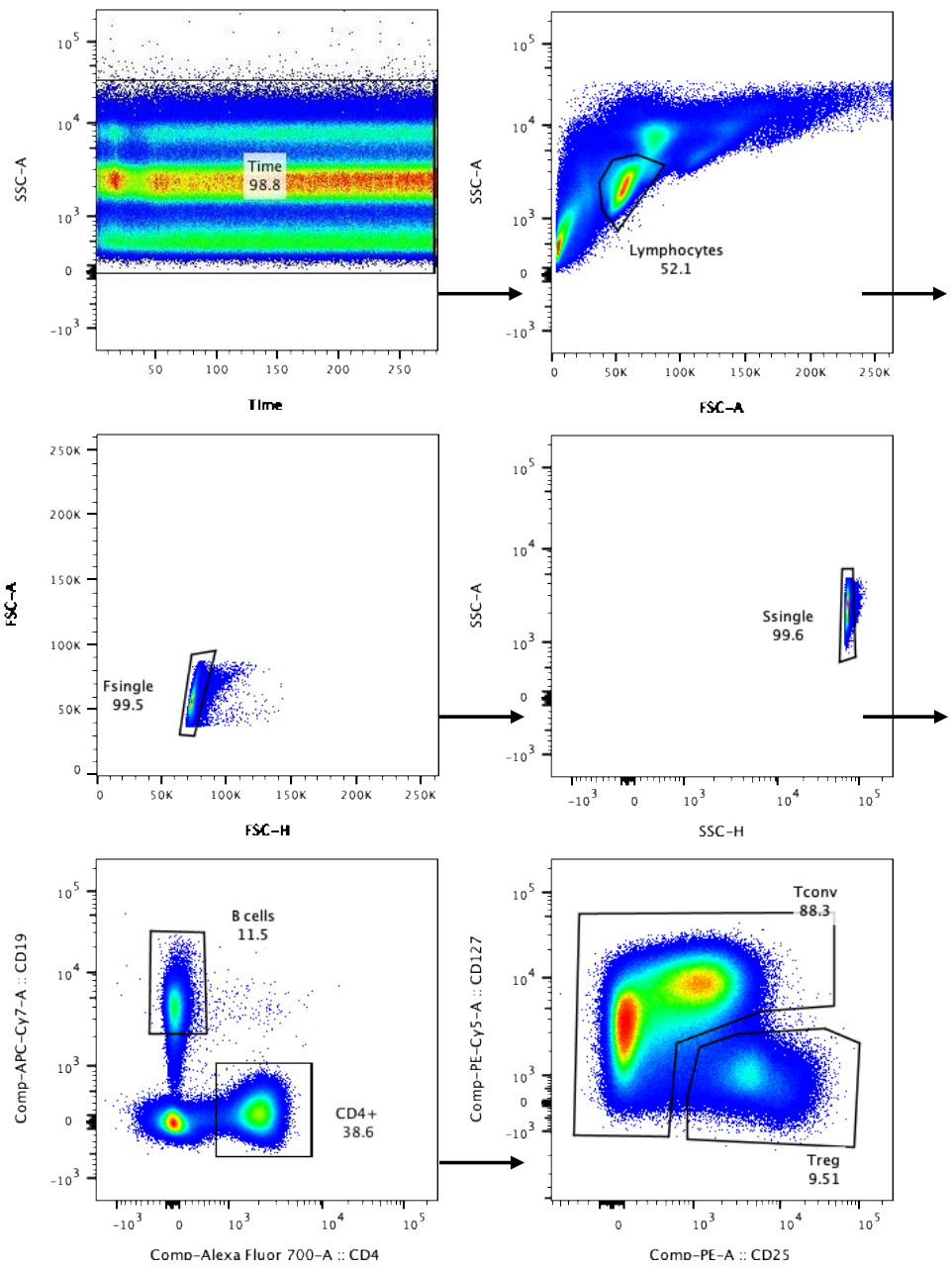

Figure 3.16: Tconv and B cell sorting strategy. Representative plots showing the FACS sorting strategy of B cells and Tconv cells used for the Treg micro-suppression assay.

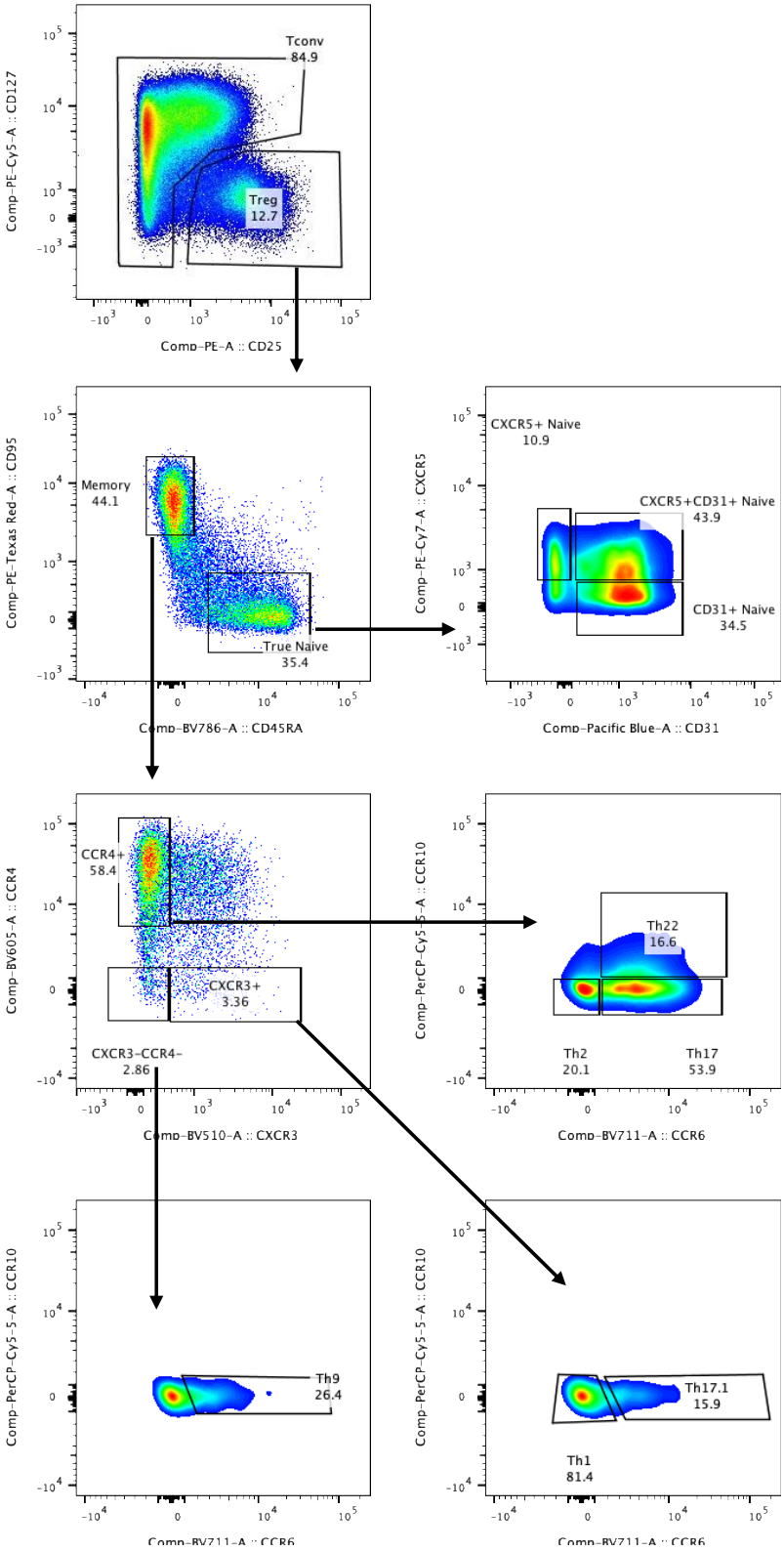

Figure 3.17: Treg subset sorting strategy. Representative plots showing the FACS sorting strategy used for simultaneous cell sorting of previously reported Treg subsets used for the Treg micro-suppression assay.

Figure 3.18 A shows the raw counts per minute recorded from co-cultures containing each Treg subset, Tconvs, and B cells, or Tconvs and B cells only (No Treg) for each donor. Percentage suppression was then calculated using the formular described in 3.2.4. Percentage suppression data is shown in figure 3.18 B and 3.18 C tabulates the significant differences in this data as shown by p values. As shown here a number of significant changes were detected between Treg subset groups. Firstly, the only subset to achieve a significantly increased percentage suppression compared to bulk Tregs was the naïve $CD31^+$ Tregs (figure 3.18 B, and D). This subset and the naïve $CD31^+CXCR5^+$ Tregs were also significantly better suppressors than bulk memory Tregs and Th17 (naïve $CD31^+$ only), Th2, Th22, Th1, and Th9-like memory Tregs (figure 3.18 B). There was a borderline significant increase in suppressive capacity between the naïve $CD31^+$ subsets compared to bulk naïve Tregs, and bulk naïve compared to bulk memory Tregs. Bulk naïve Tregs were also significantly more potent suppressors than the Th22, Th1, and Th9 memory subsets. The only subset which performed significantly worse in this suppression assay than bulk Tregs were the Th22 -like memory Treg subsets. There were no significant differences in suppression between the memory helper-like Treg subsets. In order to eliminate inter-donor variation in the suppressive capacity of bulk Tregs, percentage suppression could be normalised. When the data were normalised to make bulk suppression 100%, the same significant increase in naïve $CD31^+$ Treg suppression and significant decrease in Th22-like Tregs was observed (figure 3.18 E). In summary, the naïve $CD31^+$ Tregs performed significantly better in our Treg micro-suppression assay than bulk Tregs and several memory helper-like Treg subsets.

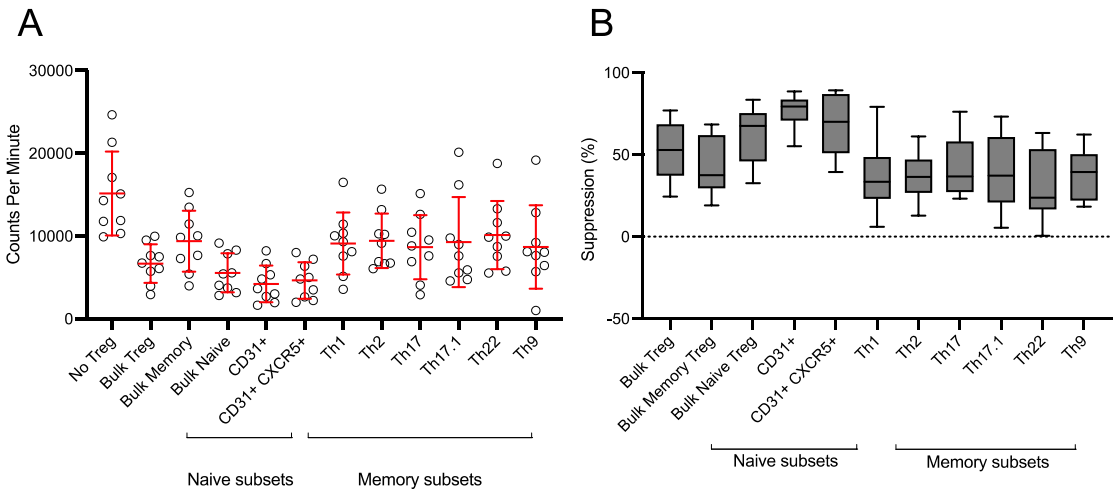

C

Tukey's multiple comparisons test	Summary	P Value
Bulk Treg vs. CD31⁺	*	0.0227
Bulk Memory Treg vs. CD31⁺	**	0.0088
Bulk Memory Treg vs. CD31⁺CXCR5⁺	*	0.0387
Th17 vs. CD31⁺	*	0.0285
Th2 vs. CD31⁺	**	0.0013
Th2 vs. CD31⁺CXCR5⁺	*	0.0143
Th22 vs. CD31⁺	**	0.0056
Th22 vs. CD31⁺CXCR5⁺	**	0.0043
Th1 vs. CD31⁺	**	0.0025
Th1 vs. CD31⁺CXCR5⁺	*	0.0426
Th9 vs. CD31⁺	**	0.0097
Th9 vs. CD31⁺CXCR5⁺	*	0.0297
Bulk Naive Treg vs. CD31⁺	*	0.0446
Bulk Memory Treg vs. Bulk Naive Treg	*	0.049
Bulk Naive Treg vs. Th22	*	0.011
Bulk Naive Treg vs. Th1	*	0.0252
Bulk Naive Treg vs. Th9	*	0.0386
Bulk Treg vs. Th22	*	0.0338

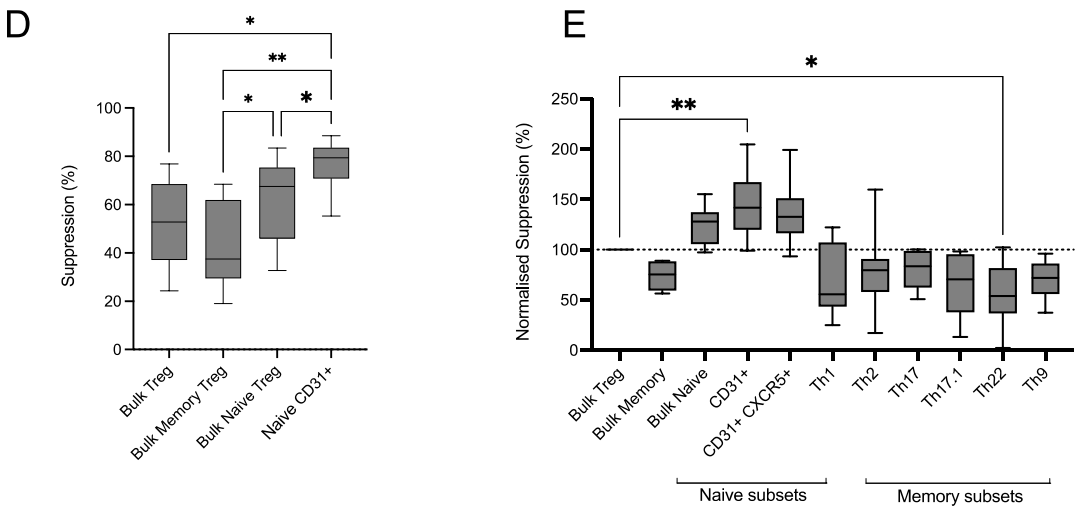

Figure 3.18: Healthy donor naïve CD31⁺ Tregs were the most suppressive subset as analysed by the Treg micro-suppression. Individual Treg subsets were co-cultured with Tconvs and B cells in the presence of PHA for 6 days and per-well proliferation was assessed by tritiated-thymidine incorporation for the final 18 hours of culture. Percentage suppression was calculated using the number of counts per minute in wells not containing Tregs and

counts per minute within Treg-containing wells and using the formula described in the methods section. (A) Comparative counts per minute recorded in co-cultures of different Treg subsets. (B) Percentage suppression calculated per Treg subset group. (C) Significant differences in percentage suppression between Treg subsets. (D) Percentage suppression per bulk groups and naïve CD31+ Tregs. (E) Percentage suppression normalised to make the Bulk Treg suppression 100% suppression. Significance was calculated by two-way ANOVA with Dunnet's post hoc test or Turkey's multiple comparisons test (*= $p < 0.05$; **= $p < 0.01$) (n=9).

3.3.5 Preliminary data showing suppression of cytokines by Treg subsets

At day-5 of the micro-suppression assay described above, half the culture supernatants were replaced with media containing tritiated thymidine. This presented an opportunity to store and later analyse these supernatants for cytokines secreted during co-cultures of B cells, Tconvs, and Treg subsets. The data described in the following figures are from 2 independent donors only and should therefore be treated as preliminary.

Using the LegendPlex multiplex assay, it was possible to analyse multiple cytokines in the culture media simultaneously. Figure 3.19 A shows the mean concentrations of type 1 cytokines in the culture supernatants of co-cultures containing B cells and Tconvs alone (no Tregs) and B cells and Tconvs in co-culture with bulk Treg, bulk memory Tregs, bulk naïve Tregs, and naïve $CD31^+$ Tregs.

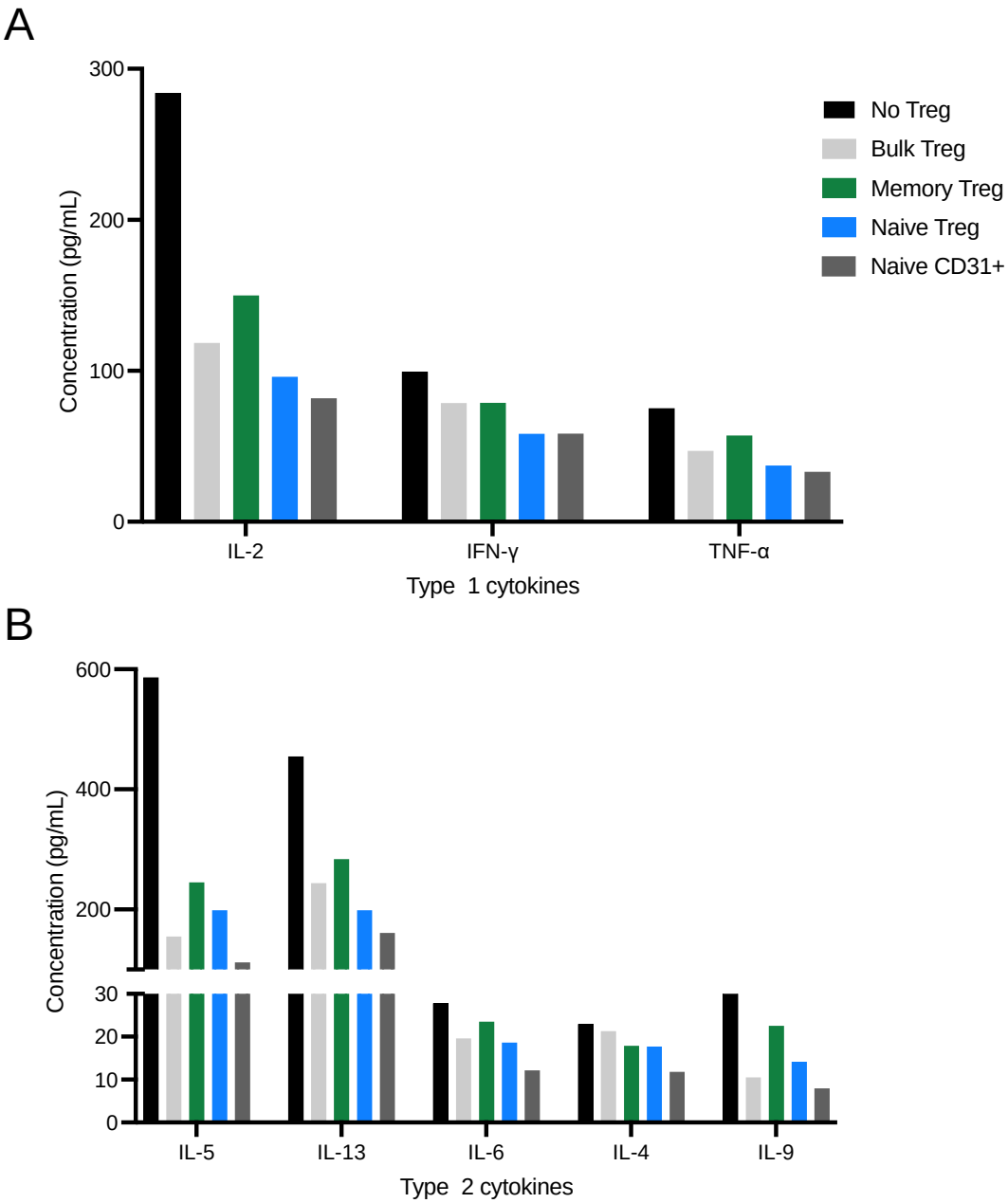

Figure 3.19: Type 1 and type 2 cytokines were present at lowest concentrations in naïve Treg subset culture supernatants. Cytokines in culture supernatants were collected at day 5 of the micro-suppression assay and stored at -80. Concentrations of cytokines within the culture supernatants were assessed using the LEDENDPlex 13-plex cytokine array kit (n=2).

As outlined in chapter 1.5.1, suppression of IL-2 secretion by Tconvs is thought to be a main mechanism of suppression utilised by Tregs during suppression assays which limits Tconv proliferation (Oberle et al., 2007) and Tregs intrinsically cannot produce IL-2 themselves. The concentration of IL-2 in the culture supernatants drastically reduced in the presence of Tregs compared to no Treg wells (figure 3.19 A). However, in support of our suppression assay results, the suppression of IL-2 production during co-cultures of Treg subsets followed a similar trend to our proliferation data. Namely, there was a trend towards a higher concentration of IL-2 found in memory Treg-containing supernatants, followed by bulk Tregs, naïve Tregs, and naïve $CD31^+$ Treg co-cultures contained the lowest concentration of IL-2. A similar trend in concentration of TNF-α was observed within the culture supernatants. Furthermore, supernatants from bulk Tregs and memory Treg-containing wells contained equal concentrations of IFN-γ, as did supernatants from naïve Treg and naïve $CD31^+$ containing wells which was reduced compared to bulk and memory Tregs. A very similar trend to IL-2 concentrations was observed when assessing the concentrations of type 2 cytokines IL-5, IL-13, IL-6, IL-4, and IL-9, with the highest concentrations of these cytokines always being found in wells containing memory Tregs, and the lowest in those containing naïve $CD31^+$ Tregs (figure 3.19 B). In the case of IL-5 and IL-13, the concentrations of these cytokines in the culture supernatants halved in the presence of any Treg subsets.

Figure 3.20 shows the mean concentrations of cytokines within the culture supernatants of each Treg subset co-culture. Notably, Th1-like and Th17.1 Treg subsets contained the highest concentrations of IFN-γ, higher than that of the no Treg wells. Similarly, wells containing Th2-like Tregs had the highest concentrations of IL-4, IL-6, and IL-13 which are considered classical type 2 cytokines. Naïve $CD31^+$ and naïve $CD31^+CXCR5^+$ Treg co-cultured consistently contained the lowest concentrations of these cytokines. In summary, trends towards differences in IL-2 concentrations were observed in co-cultures containing different subsets of Tregs, and type 1 and type 2 cytokines were enriched in wells containing Th1 or Th17.1, and Th2 Treg subsets, respectively.

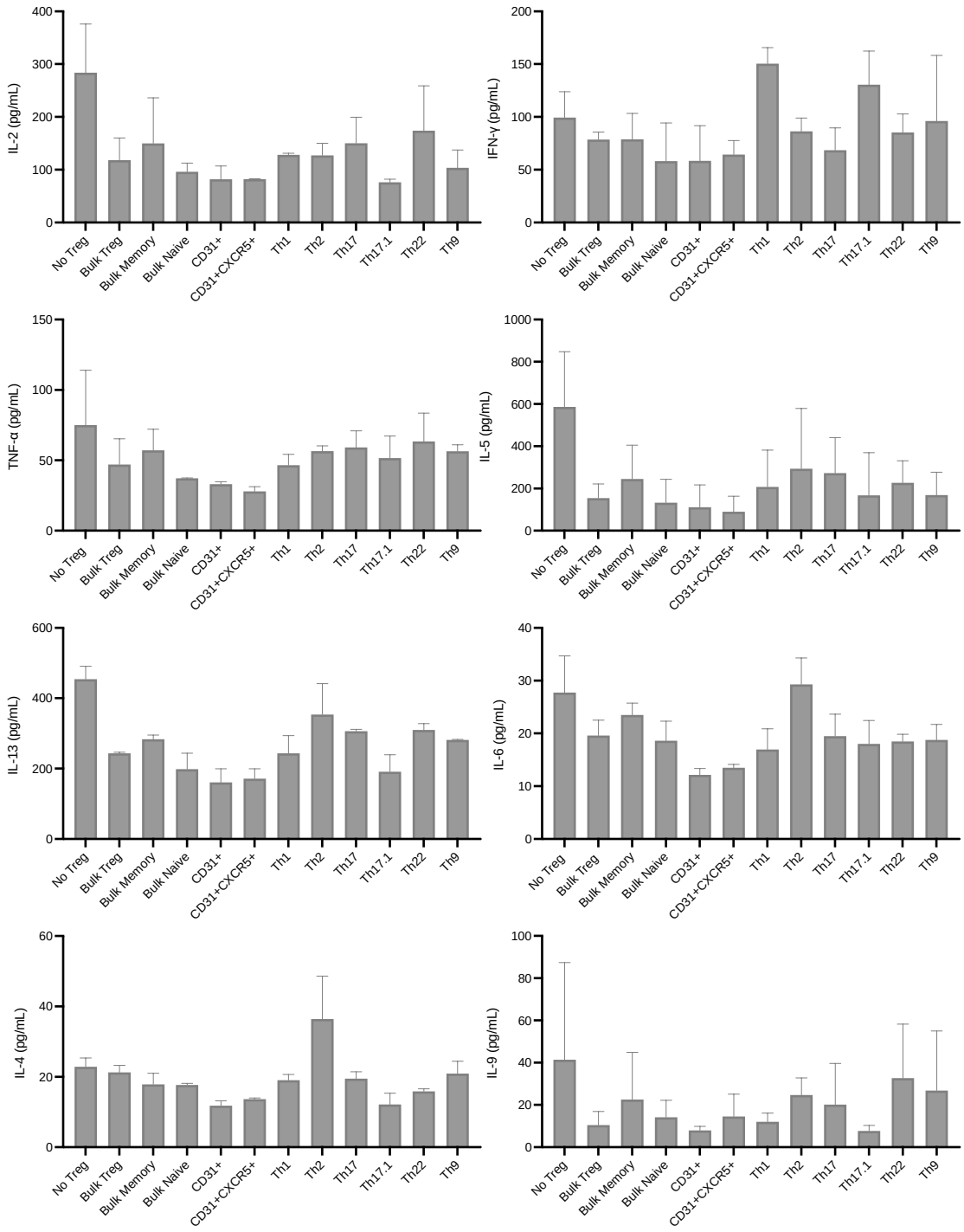

Figure 3.20: Relative cytokine production by Treg subsets. Cytokines in culture supernatants were collected at day 5 of the micro-suppression assay and stored at -80 . Concentrations of cytokines within the culture supernatants were assessed using the LEDENDPlex 13-plex cytokine array kit (n=2).

3.4 Discussion

In this chapter, we have characterised the surface phenotype of Treg subsets in healthy donors using our Treg surface marker panel, and we observed a wide variety in potential Treg surface phenotypes. Our data shows that the most diverse surface phenotypes in healthy donors were found within the memory compartment which could express any of the surface markers apart from CD45RA (figures 3.2-3.3). This is to be expected as many of the chemokine receptors in our panel, such as CCR4, CXCR3, CCR6, and CCR10, and other effector molecules such as ICOS and CD95 are known to be expressed predominantly by memory T cells (Eksteen et al., 2006; Huehn et al., 2004; Ito et al., 2008; Sather et al., 2007; Weiss et al., 2011). Naïve Tregs were limited to expression of CD31, CXCR5, CD49d, and CD73. Expression of some markers were more influenced by inter-donor variation than with memory/naïve status such as CD73 and CD49d (figure 3.3). This finding is also supported by the results of Schuler et al. (2014) which showed that the frequency of $CD4^+CD73^+$ cells could vary by up to 18% in different healthy donors. Höllbacher et al. (2020) also showed a wide variation in CD73 expression by RNA-sequencing in healthy donors. An initial study by Kleinewietfeld et al. (2009) argued that *bona fide* Tregs do not express CD49d on their surface, and $CD49d^+$ cells should be depleted from Treg suspensions to ensure purity. Contrary to this, our data has shown that both memory and naïve Tregs are able to express CD49d (figure 3.3), however analysis of the suppressive function and the methylation status of the TSDR in these cells would be needed to determine Treg functionality in these cells.

We observed naïve Treg subsets which could express CD31 and CXCR5 (figure 3.2-3.4), which as indicated in chapter 1 have been widely reported in previous studies. For example, a decreased frequency of $CD31^+$ naïve Tregs has been reported in several human pathologies such as MS, coronary heart disease, and IPF (Haas et al., 2007c; Hou et al., 2017; Huang et al., 2017). Additionally, these naïve RTE Tregs have been used to demonstrate an increase in thymic output in response to low-dose IL-2 therapy as an increased frequency of these cells has been observed in peripheral blood in human trials to treat GvHD (Whangbo, Kim, Mirkovic, et al., 2019; Whangbo, Kim, Nikiforow, et al., 2019). In our healthy donors, the majority of naïve Tregs expressed CD31 (figure 3.6) and around 15% of naïve Tregs co-expressed CXCR5 and CD31. A study by Kimmig et al. (2002) showed that T cells co-expressing CD45RA and CD31 had a TREC content which was 8 times higher than $CD45RA^+CD31^-$ T cells, suggesting that naïve $CD31^+$ thymically-derived T cells are of a more naïve phenotype than CD45RA-single positive cells. This also suggests that Tregs expressing CD31 may be thymically-derived or 'natural' Tregs rather than peripherally-induced.

CXCR5 expression by naïve Tconvs was found in a much rarer population of cells than in Tregs, in agreement with Fonseca et al. (2017) which showed that Tfr cells are found mostly in the $CD45R0^-$ naïve fraction in peripheral blood, however Tconv Tfh cells are mostly $CD45R0^+$, and Tfr $CD45R0^+$ were enriched in lymphoid tissues. In this paper, as in our data in figures 3.3-3.4, the authors did also demonstrate that $CXCR5^+$ Tregs could co-express CD31 in the blood, however $CXCR5^+$ Tregs were not found in the thymus or in cord blood, suggesting that CXCR5 expression is acquired upon entering the periphery, and that this subset

represents a transient, immature precursor to the CD45R0^{+} Tfr cells found in lymphoid tissues.

Our data in figure 3.6 showed that the memory helper-like subsets Th1, Th2, Th9, Th17.1, Th17, Th22 could be reproducibly identified in healthy donor peripheral blood in both the Tconv and Treg compartments. The frequencies of Th1 and Th17.1-like Tregs were much lower on average than their Tconv counterparts, largely owing to the significant reduction in CXCR3-expressing Tregs compared to Tconvs (figure 3.7). Previous studies have suggested that CXCR3^{+} Tregs are enriched in tissues e.g. within the pancreas, at mucosal interphases, or in tumours (Höllbacher et al., 2020; Koch et al., 2009; Tan, Mathis, & Benoist, 2016). Although Th1, Th2, Th17, Th17.1 and Th22-like Tregs have previously been described in studies such as Duhen et al. (2012) and Halim et al. (2017), Th9-like Tregs have not been as frequently reported. IL-9-producing Tregs have been reported as drivers of disease in the context of lung cancer (Heim et al., 2022) and protective in mouse models of nephrotoxic serum nephritis (Eller et al., 2011), and IL-9 has been shown to support Treg suppressive function *in vitro* and in EAE models *in vivo* (Elyaman et al., 2009). In addition, the frequency of Tregs expressing PU.1, a Th9-transcription factor, has been shown to be reduced in allergic rhinitis patients in response to allergen immunotherapy treatment (Qiao et al., 2022). To our knowledge, no publications to date have characterised Th9-like Tregs according to the surface chemokine receptor profile which mirrors that of Th9-Tconvs as used in publications such as (Zhong et al., 2017), however we detected these cells at a low frequency in Tregs (figure 3.6). Our data in figure 3.5 shows that these cells did express levels of FoxP3 comparable to naïve Tregs

and were the Treg subset with the highest frequency of Helios^{+} cells. In addition, our comparative data from the *in vitro* micro-suppression assay shown in figure 3.18 showed that these cells did have the capacity to suppress Tconv proliferation. As shown in figure 3.5, we found a potential for higher Tconv contamination in the Treg helper-like memory subsets compared to naïve subsets. It's possible that this contamination may have influenced our results when comparing the *in vitro* suppressive capacity of Treg subsets via the Treg micro-suppression assay (discussed in more detail below).

As well as taking a literature-based approach using previously reported Treg subsets for our analysis, we also valued the use of clustering tools to generate unbiased populations of Tregs based on their surface phenotype. Given the number of markers being simultaneously analysed, it would not have been possible to use Boolean gating to characterise every possible subset. We saw similarities between some of the unbiased populations identified in our data in figures 3.10-3.12 and those identified by Mason et al. (2015), and found that some of the unbiased populations overlapped with our manually gated populations described above. Firstly, although our analysis generated 26 Treg clusters compared to 22 clusters in the aforementioned study, our Treg dataset consisted of data from 10 healthy donors compared to 4. Therefore, the increased number of donors would be expected to increase the variation within the dataset. Using unbiased clustering, Mason et al., (2015) also identified a distinct cluster of CD45RA^{+} naïve Tregs expressing CD31. Additionally, as in our data, ICOS and CD49d were expressed at different levels in most of the 22 clusters identified in this study. However, CD73 was expressed only in two distinct clusters with no

variation in expression levels within different clusters, which is what we found in relation to this marker as only cluster 14 shown in figure 3.10 expressed high levels of CD73. These overlapping findings gave us confidence that our unbiased analysis was identifying clusters which represent true Treg biology and not random variations in surface phenotype.

Despite this, as shown in figure 3.13, we found several clusters which co-expressed low levels of CD45RA and CD95. Of note, CD95 was not used in Mason et al., (2015) and therefore these populations did not arise in their analysis. We hypothesised that these clusters were in the process of differentiating from a naïve to a memory phenotype and therefore would not be stable clusters which could be reproducibly found in several donors, rather these cells represented a ‘snapshot’ of transitional Treg phenotypes. This proved to be the case when we analysed the Treg clusters in individual donors and found that many of the novel clusters identified in the concatenated dataset were noticeably different from donor to donor (figure 3.13). It is possible that this is the reason why isolation of live cells with complex surface phenotypes identified through unbiased clustering of flow cytometry data is rarely seen in the literature. A recent study by Luo et al. (2021) used single cell transcriptomics to identify clusters of Tregs, and following this, a selection of surface markers were selected as candidates to represent each subset. Each of these subsets were then FACS sorted for functional analyses on the basis of positive or negative expression of a maximum of 4 Treg surface markers. Moreover, a study by Kordasti et al. (2016) used unbiased surface staining analyses to identify two Treg subsets which were FACS sorted for functional analyses. However, these two subsets differed only

on expression of CD45RA, CCR4, and CD95, which when compared to our data in figure 3.10 means these two populations were simply memory and naïve Tregs making them simple to gate on during FACS sorting. It is possible that a panel of 12 Treg surface markers as seen in our data, with many of these markers having a range of expression levels, allows for too much nuance between subsets. For example, clusters 7 and 13 in our data shown in figures 3.12 and 3.13 are low for CCR10 and CXCR3, respectively in comparison to other clusters. However as shown in figure 3.13, this 'low' expression was variable between donors and could make it difficult to accurately set gates during FACS sorting to ensure these populations are being sorted correctly. Therefore a more binary approach as seen in Luo et al. (2021) would make isolation of unbiased clusters of Tregs more feasible in future work.

Given these observations in our unbiased analysis of Treg subsets, we chose to focus on the previously reported Treg subsets which we had reproducibly detected in several donors (figures 3.4-3.6) for our comparison of Treg subset *in vitro* suppressive function. In our hands, using our Treg micro-suppression assay, our data showed that naïve $CD31^+$ Tregs were the only subset with a significantly increased capacity to suppress Tconv proliferation compared to bulk $CD4^+CD25^{hi}CD127^{low}$ Tregs and several memory Treg subsets such as Th2, Th17, Th1, Th22, and Th9 subsets (figure 3.18). We also found that naïve $CD31^+CXCR5^+$ Tregs were significantly more potent suppressors of Tconv proliferation than several memory subsets. Although the naïve $CD31^+$ and $CD31^+CXCR5^+$ Treg subsets have been reported previously in the literature, we believe that this is the first report in which these naïve subsets have been directly

compared to bulk Tregs and memory Treg subsets. And finally, we saw a borderline significant increase in the suppressive capacity of naïve CD31^{+} Tregs compared to bulk naïve Tregs.

Taken together, these results suggest an enhanced suppressive phenotype of not only naïve Tregs, but of those naïve Tregs which express CD31 (RTE Tregs). One interpretation of these results could be that Tregs with an extremely naïve phenotype respond better upon stimulation during *in vitro* suppression assays than memory Tregs. However, CD31 itself has intrinsic immune regulatory properties through homophylic interactions with other CD31 molecules and can be expressed by many immune cell types and endothelial cells (reviewed by Marelli-Berg, Clement, Mauro, & Caligiuri, 2013). This intrinsic immune regulatory capacity of CD31 is seemingly under-reported, especially in the case of Tregs. For example, CD31-deficient mice have been shown to have an increased acceleration and severity of disease phenotypes in EAE and collagen-induced arthritis (CIA) mice (Graesser et al., 2002; Wong, Hayball, Hogarth, & Jackson, 2005). Furthermore, a T cell inhibitory role has been suggested for this molecule as co-engagement of CD31 and TCR/CD3 on the same cell has been shown to attenuate downstream TCR signalling through disruption of calcium and protein-kinase-c signalling (Newton-Nash & Newman, 1999) and through inhibition of ZaP-70 phosphorylation (Ma et al., 2010).

As CD31 is expressed by T cells and B cells, it could be hypothesised that Tregs could use homophylic CD31 interactions to dampen TCR and BCR signalling in Tconvs and B cells during our Treg micro-suppression assay. Indeed a study by

Wilkinson et al. (2002) showed that CD31$^{-/-}$ mice have a hyper-activated B cell response with increased numbers of circulating B cells, autoantibodies, and SLE-like disease (Wilkinson et al., 2002) and CD31 has been shown to inhibit B cell receptor signalling (Henshall, Jones, Wilkinson, & Jackson, 2001).

Ma et al. (2010) showed that Tregs from CD31$^{-/-}$ mice had a reduced suppressive capacity in a three-cell *in vitro* suppression assay. However, Tconvs from CD31$^{-/-}$ mice were still susceptible to Treg-induced suppression of proliferation, strengthening the hypothesis that CD31^{+} Tregs could be acting on B cells in our assays. We observed that approximately 50% of bulk naïve Tregs expressed CD31 (figure 3.6) and therefore the potential benefits of CD31 in T/B cell inhibition could also be relevant to bulk naïve Tregs, which may explain why only a borderline significant difference in suppression was observed between these subsets. Future work should aim to compare memory CD31^{+} Tregs, which exist at a lower frequency than in the naïve compartment (figure 3.3), and naïve CD31^{+} Tregs to ascertain whether CD31 alone renders a suppressive advantage. We believe that in light of this evidence, the suppressive properties and potential therapeutic properties of naïve CD31^{+} Tregs should be further investigated.

We are aware that our finding that naïve Treg subsets were more potent suppressors of Tconv proliferation than memory Treg subsets is contrary to many previous reports which have compared the *in vitro* suppressive function of naïve and memory Tregs, and so we were keen to investigate why our results differed. Some of the earliest papers reporting on human Treg *in vitro* function using tritiated thymidine incorporation reported memory CD45R0^{+}CD25^{hi} Tregs as

being more suppressive than $CD45RA^{+}CD25^{+}$ Tregs (Baecher-Allan et al., 2001; Jonuleit et al., 2001; Taams et al., 2002). However as this was before CD127 was used as a negative Treg marker, it's possible the $CD45RA^{+}$ Tregs which express lower CD25 and FoxP3 than memory Tregs (figures 3.2-3.5) were highly contaminated by activated Tconvs which would proliferate strongly in response to stimulation. A seminal paper by Miyara et al. (2009) characterised the three fractions of Tregs which are the most commonly reported Treg subsets (described in chapter 1.7.2). In this study, they showed in data from one donor that in co-culture with $CD45RA^{-}$ memory Tregs 26.1% of Tconv responder cells proliferated, and in $CD45RA^{+}$ naïve Treg co-cultures, 42.9% proliferated. Additionally, the authors noted that during their dye-dilution suppression assay, naïve Tregs took on a memory phenotype and were highly proliferative, however memory Tregs did not proliferate and underwent apoptosis.

Although we have seen minimal proliferation of non-Tconv cells during our micro-suppression assay (chapter 6), we acknowledge that if Treg subsets have different proliferative capacities during this assay that this may affect our interpretation of the results as our use of thymidine incorporation relies on Tconv proliferation as a read-out and does not allow us to track the phenotype of dividing cells as is possible in dye-dilution suppression assays. Therefore, this can be considered a limitation of using thymidine incorporation to compare the suppressive capacities of different Treg subsets. However with this in mind, if the proliferation of naïve Tregs following PHA stimulation was skewing our results, we would expect to see the opposite effect to our results in figure 3.18 whereby wells containing highly proliferative naïve Tregs would have an increased number

of counts per minute and therefore a lower percentage suppression would be observed in these subsets.

As discussed in chapter 1, the set-up of the Treg micro-suppression assay may have a large effect on the outcome of the results e.g. it is possible that naïve Tregs have a large suppressive effect on APCs which would be missed when using a two-cell assay. In our micro-suppression assay, Tregs were co-cultured with Tconvs and B cells for 6 days with proliferation being measured during the last 18 hours of culture, however Miyara et al. (2009) co-cultured Tregs with naïve Tconvs for a period of 3.5 days. It could be hypothesised that the longer period of co-culture used in our assay gave a longer window for naïve Tregs to express proteins with effector functions such as cytokines or APC-modulating molecules which in turn suppressed Tconv proliferation. In addition, as the authors used only naïve Tconvs as responder cells, these cells may have been less receptive to suppression by naïve Tregs than memory Tconvs of total Tconvs as used in our assay.

Despite these differences between our Treg subset suppression results compared to the aforementioned studies, several other studies have indicated no significant difference in the suppressive capacities of naïve and memory Tregs or better suppression by naïve Tregs (Baecher-Allan et al., 2006a; Booth et al., 2010; Hou et al., 2017; Miyara et al., 2015; Seddiki et al., 2006; Valmori et al., 2005). It should also be noted that although results were preliminary, we saw the lowest concentration of IL-2 in supernatants from naïve Treg co-cultures compared to memory and bulk Treg co-cultures (figure 3.19). As suppression of

IL-2 production from Tconvs is considered one of the key mechanisms of suppression observed in *in vitro* suppression assays (Thornton & Shevach, 1998), it was encouraging to us that we saw a similar trend in suppression of IL-2 as was seen in the suppression of Tconv proliferation results. As Tregs inherently cannot produce IL-2, we can be sure that any reductions in IL-2 concentration compared to no-Treg wells shown in figure 3.19 were not due to differences in Treg IL-2 secretion. Despite this, as show in figure 3.5, we suspect that sorted memory T helper-like Treg populations may have had a higher contamination of Tconv cells than naïve Tregs. If so it is possible that these contaminating Tconvs could have secreted more IL-2 and this could also have affected the results of the Treg micro-suppression assay shown in figure 3.18. In future experiments, use of a dye-dilution style suppression assay in select Treg subsets could help to shed light on whether some of the limitations described above were truly affecting out data such as differential proliferation of Treg subsets and contamination of $CD4^{+}CD25^{hi}FoxP3^{low}$ Tconvs during FACS sorting of memory Tregs. However it should be noted that as far more cells are needed for dye-dilution suppression assays, it would not be possible to carry out an investigation into multiple Treg subsets simultaneously from a single donor which is the benefit of using our micro-suppression assay.

During the comparative Treg subset micro-suppression assay, we saw no significant differences in suppressive capacity between T helper-like memory Treg subsets or indeed compared to bulk memory Tregs (figure 3.18). This finding supports the notion suggested by previous studies that chemokine receptors do not play a role in Treg suppression or targeting specific responder cells, rather

these receptors can grant Tregs access to certain tissues in order to carry out regulatory functions. Studies by Feuerer et al. (2010) and Höllbacher et al. (2020) suggested using transcriptomic data that although Tregs could express different chemokine receptors at their surface, the gene expression profiles of different T helper-like Treg subsets were largely overlapping and less diverse than their Tconv counterparts. Additionally, although several *in vivo* mouse studies have suggested that T helper-like Tregs could have evolved to specifically target their Tconv helper counterparts (Kluger et al., 2016; Nosko et al., 2017), a study by Halim et al. (2017) showed that these human Treg subsets suppress Tconv helper subset proliferation without preference *in vitro.* We originally hypothesised that by analysing whether the concentration of type 2 cytokines was reduced in the culture supernatants of Th2-like Treg/Tconv/B cell co-cultures, this may help to support these previous findings that T helper subsets could preferentially suppress their Tconv helper counterparts. However, on the contrary we found that IL-6, IL-4 and IL-13 were present at the highest concentrations in Th2-like Treg co-culture supernatants (figure 3.20) implying that these cells were themselves secreting these cytokines. The same was observed in the case of Th1 and Th17.1 Tregs and IFNγ (figure 3.20).

In this chapter we show that significant heterogeneity in cell surface marker expression is observed within the Treg pool and that the surface phenotype of subsets of Tregs does not perfectly mirror that of Tconvs. We observed that unbiased clustering tools offer a powerful insight into the deep complexity of the Treg pool when using large flow cytometry panels, however panels of this size mean that the inter-donor variation within Treg clusters is sometimes high. When

directly comparing the *in vitro* suppressive capacity of Treg subsets, naïve Tregs proved to be the most suppressive, especially those expressing CD31. We believe that this warrants further exploration of the *in vitro* function of this Treg subset.

4 Chapter 4. Analysis of the changing phenotype of expanded Treg subsets

4.1 Introduction

Cellular therapies have been described as a 'third revolution' of biomedicine, following the unprecedented success of biologics such as antibodies and soluble receptors, and that of small-molecule drugs (Fischbach, Bluestone, & Lim, 2013). Cells have several advantages over biologics and small molecules as therapies including being able to sense and react to their surroundings, having multiple mechanisms of action allowing them to interact with and manipulate diverse cell types, and an ability to migrate towards specific tissues and signalling gradients. Chimeric antigen receptor (CAR) T cell therapies with an engineered specificity towards CD19 were the first success story in the field of cellular immunotherapies as this treatment was shown to be efficacious in treating B cell precursor acute lymphoblastic leukaemia (Maude et al., 2018). Adoptive T cell therapies are now being considered for the treatment of autoimmune diseases and induction of transplant tolerance.

Tregs are being widely tested in clinical trials as cellular therapies for the treatment of conditions such as GvHD and T1D (Bluestone et al., 2015b; Brunstein et al., 2011). Trials to date have shown that infusion of *ex vivo* expanded autologous Tregs is safe and can be completed under fully good manufacturing practice (GMP)-compliant conditions (Marek-Trzonkowska et al., 2014). One recent trial in kidney transplant patients has shown that this therapy is as effective as standard generalised immunosuppressive therapy when given

in combination with a reduced course of immunosuppressants, which could reduce the risks associated with long-term use of potent immunosuppressants such as malignancy and chronic infections (Sawitzki et al., 2020). Tregs also have the advantage of bystander suppressive mechanisms, meaning that therapeutic Tregs specific to tissue-related antigens could be directed to exert their suppressive effects at specific inflammatory sites without the need to recognise disease-specific antigens.

Pre-clinical studies first demonstrated that adoptively transferred Tregs can alleviate inflammation and autoimmune symptoms. The first experiments characterising $CD4^+$ Tregs by Sakaguchi *et al.* (1995) demonstrated that adoptive transfer of Tregs into athymic nude mice which were pre-inoculated with CD25-depleted T cell suspensions could prevent autoimmune disease development in a dose-dependent manner. Adoptive transfer of Tregs can delay diabetes onset in NOD mice (Salomon et al., 2000) and can prevent development of EAE (Kohm, Carpentier, Anger, & Miller, 2002). Moreover, a single dose of transferred Tregs was able to slow disease progression of collagen-induced arthritis (CIA) in mice and Tregs were observed infiltrating the inflamed synovium suggesting a localised response (Morgan et al., 2005).

However, despite the promising pre-clinical evidence and good safety profiles of Treg therapies in phase I/II studies (Sawitzki et al., 2020), there are a number of significant challenges associated with the process of manufacturing GMP-compliant human Tregs. Firstly, due to the low frequency of Tregs in peripheral blood and the large number of Tregs needed for Treg therapies (between 0.5-

$10x10^6$ cells per kg of bodyweight), Tregs must be expanded *ex vivo* prior to infusion. Despite being highly proliferative *in vivo*, Tregs are anergic *in vitro* (Levings et al., 2001). However Tregs can be stimulated to expand *in vitro* by culturing the cells in the presence of high doses of IL-2 and a source of TCR/co-stimulation such as anti-CD3/CD28 beads or co-culturing with 'feeder' cells (Fraser et al., 2018; Levings et al., 2001; Reading et al., 2021). Secondly, as FACS sorting using monoclonal antibodies raised in non-human species is often not considered a GMP compliant process in the UK, Tregs are more commonly isolated for therapeutic uses through magnetic enrichment of $CD25^+$ cells meaning the potential for contamination with activated Tconvs is high (Hippen et al., 2011), and as Tconvs are highly responsive to IL-2, these cells can quickly outgrow Tregs during expansion. In addition, Tregs can lose FoxP3 expression and their suppressive function during repeated rounds of expansion (Marek et al., 2011).

To overcome these issues, Tregs can be expanded in the presence of rapamycin, which restricts the proliferation of Tconvs by inhibiting mTOR and inducing apoptosis (Strauss et al., 2007), promotes maintenance of FoxP3 expression and suppressive capacity during expansion (Scottà et al., 2013), and can be used within a GMP-compliant expansion protocol (Fraser et al., 2018). As described in chapter 1.3.2, signalling through the IL-2 receptor can induce signal transduction through the PI3K/Akt/mTOR pathway in Tconvs which promotes cell cycle progression, however signalling through this pathway is inhibited in Tregs by high expression of PTEN, making Tregs resistant to rapamycin-induced cell cycle arrest and apoptosis (Strauss et al., 2007; Valmori et al., 2006). Instead, IL-2

signalling predominantly induces STAT5 signalling in Tregs which promotes the expression of Treg signature genes (Zheng et al., 2010). The combination of IL-2 and rapamycin therefore favours Treg growth (Figure 4.1).

Many studies to date have shown that Treg sources enriched for naïve CD45RA$^+$ Tregs such as umbilical cord or paediatric thymic tissue, or indeed purified CD45RA$^+$ Tregs maintain a higher expression of FoxP3 and suppressive capacity during expansion than memory Tregs, meaning naïve Tregs may be a more optimal starting material for expansion, possibly due to lower contamination with Tconv cells (Bernaldo-de-Quirós et al., 2022; Brunstein et al., 2011; Hoffmann et al., 2006; Putnam et al., 2009; Seay et al., 2016). In conclusion, in order to generate an expanded Treg product which is suitable for infusion into patients, it is crucial to begin with Tregs which have the potential to yield high cell numbers from a limited number of starting cells and maintain good Treg phenotypic stability during this expansion process.

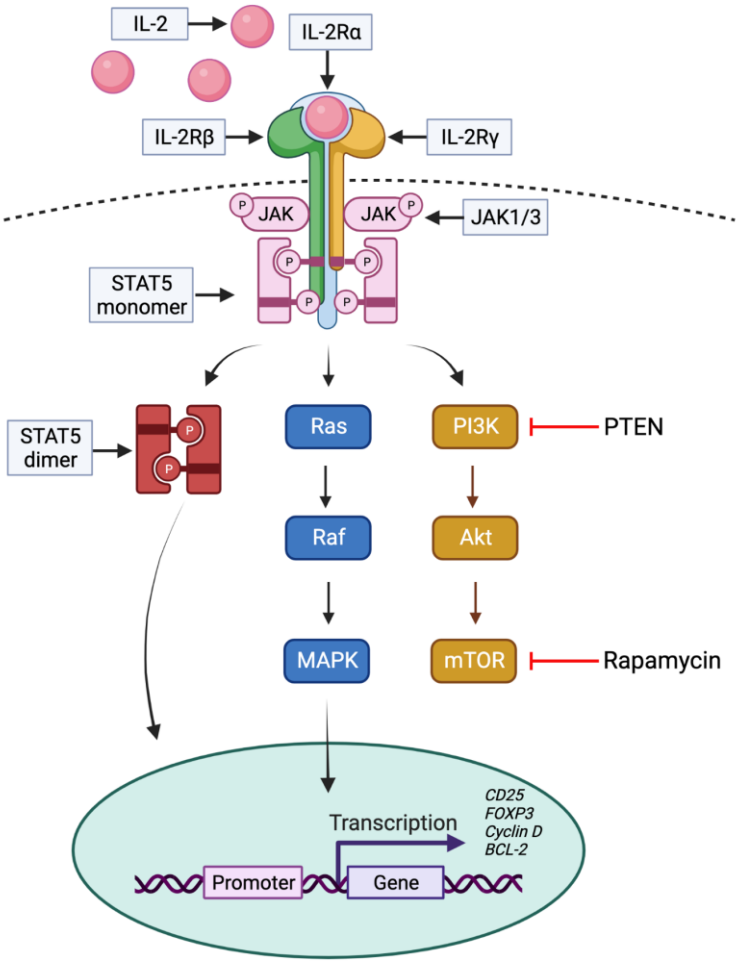

Figure 4.1: IL-2 signalling pathways and rapamycin. IL-2 binds its surface receptor which can be composed of 3 subunits; the IL-2 receptor α, β , and γ chains. Trimerisation of all 3 subunits forms the high affinity IL-2 receptor which is constitutively expressed by Tregs and transiently expressed by activated Tconvs. Ligand binding promotes recruitment of JAK1/3 non-receptor tyrosine kinase proteins which phosphorylate tyrosine residues on the IL-2 receptor-β chains. This can induce signal transduction through 3 signalling pathways in Tconvs; the STAT5, Ras/Raf/MAPK, and PI3K/Akt/mTOR pathways. Rapamycin targets the mTOR complex thus inhibiting cell cycle progression in Tconvs. In Tregs, signalling predominantly occurs through the STAT5 pathway and high expression of PTEN inhibits signalling through the PIK3/Akt/mTOR pathway, making Tregs resistant to rapamycin treatment. Created in BioRender.com

We have shown in chapter 3 that naïve $CD31^+$ Tregs have a high suppressive capacity in *in vitro* suppression assays which require the presence of APCs, and we also observed a trend suggesting that naïve subsets were better suppressors

of IL-2 during this suppression assay. Previous studies have shown that in many immune-mediated diseases, the balance of subsets of Tregs within the total Treg pool can be altered in peripheral blood in comparison to healthy controls (Hou et al., 2017; Huang et al., 2017; Steinborn et al., 2012; Verma et al., 2021). It is also of note that naïve T cells, including Tregs, are known to decrease in frequency with age due to thymic involution (Reviewed by Salam et al., 2013) which inversely correlates with incidences of autoimmune disease with advancing age. Therefore, it is plausible that if the suppressive capacity of Treg subsets differ and the frequencies of less suppressive subsets increases with age or in autoimmune disease patients, then the use of 'bulk' Tregs as an expansion product for cellular therapies could differ widely from person to person. It could therefore be hypothesised that selecting a single subset for expansion could yield more consistent results. In addition, there is evidence that the $CD45RA^+$ fraction of bulk Tregs have a better survival rate post-infusion in humans than memory Tregs (Bluestone et al., 2015b), thus emphasising the importance of understanding Treg subsets in designing successful Treg therapies.

As our data from chapter 3 suggests that naïve $CD31^+$ Tregs could represent the most suppressive Treg subset compared to bulk Tregs and previous reports suggest that tissue sources which are enriched for naïve Tregs make a superior expansion product to peripheral bulk Tregs, data in this chapter will investigate the following research questions:

1. Do naïve $CD31^+$ Tregs have a superior *ex vivo* expansion potential to bulk Tregs?

2. Can naïve $CD31^+$ Tregs maintain a more stable Treg phenotype during *ex vivo* expansion than bulk Tregs?
3. During a long expansion protocol, do naïve $CD31^+$ Tregs subsets maintain some features of their original surface phenotype or do all subsets take on a similar phenotype after multiple rounds of stimulation?

In addition to naïve $CD31^+$ Tregs, we chose to expand $CD45RA^-$ memory Tregs, $CD45RA^+$ naïve Tregs, and bulk Tregs as comparators. Conventionally, in generating expanded Tregs for therapeutic purposes, Tregs are expanded for between 14-36 days (Fraser et al., 2018; Putnam et al., 2009). We chose to extend our Treg expansion process to 42 days (3 phases with re-stimulation every 14 days) in order to monitor how extended expansion affects the phenotype of the cells and whether there are phenotypic indications that the expanded Treg subsets have exceeded the optimal duration of expansion by the end of the expansion period.

4.2 Materials and methods

Methods pertaining to cell culture media and buffers, PBMC isolation, $CD4^+$ magnetic enrichment, and cryopreservation were carried out as described in chapter 2.

4.2.1 Immunofluorescent staining

Thawed $CD4^+$ T cells were counted to calculate the necessary volumes of antibodies to add per $10x10^6$ cells. Cells were then transferred to FACS tubes which were centrifuged at 400xg for 5 minutes. An antibody mastermix was then added to the cells followed by a 30-minute incubation at 4°C. The master mix contained the following mouse anti-human antibodies: CD127 PE-Cy5, CD25 PE, CD4 AF700, CD19 APC-Cy7, CD45RA BV786, CD95 PE-CF594, CD31 BV421 (Table 4.1). Cells were then washed with 3ml of cold FACS buffer, centrifuged at 400xg for 5minutes, and resuspended in 3ml of FACS buffer (~$20x10^6$ cells/ml). Finally the cells were passed through a 35μm cell strainer into polypropylene FACS tubes prior to FACS sorting.

Table 4.1: Fluorochrome-conjugated antibodies used in cell surface staining prior to Treg FACS sorting and expansion

Fluorochrome	Marker	Clone	Supplier	μL/10x10^6 cells
PE-Cy5	CD127	A019D5	BioLegend	2.5
PE	CD25	2A3	BD Biosciences	5
PE	CD25	M-A251	BD Biosciences	5
AF700	CD4	OKT4	BioLegend	2
APC Cy7	CD19	9F10	BioLegend	2
BV786	CD45RA	HI100	BioLegend	0.5
PE-CF594	CD95	DX2	BD Horizon	1
BV421	CD31	WM59	BioLegend	2.5

4.2.2 Fluorescence-activated cell sorting

Sorting was carried out using a BD FACSAria IIu cell sorter. Bulk Tregs were identified as $CD19^-CD4^+CD25^{hi}CD127^{lo}$. Memory Tregs were isolated as $CD19^-CD4^+CD25^{hi}CD127^{lo}CD45RA^-CD95^+$, and naïve Tregs were $CD19^-CD4^+CD25^{hi}CD127^{lo}CD45RA^+CD95^-$. Naïve $CD31^+$ Tregs were $CD19^-CD4^+CD25^{hi}CD127^{lo}CD45RA^+CD95^-CD31^+$ (figure 4.4). Treg subsets were sorted into 2.5ml of cold XV15 media in polypropylene FACS tubes.

4.2.3 Treg activation

After sorting, the FACS tubes containing the isolated Treg subsets were centrifuged at 400xg for 5 minutes. Supernatants were discarded and Tregs were resuspended in the residual volume in the tubes (~70µL) and counted. Tregs were then incubated for 5 minutes at RT using a 1:1 ratio of cells to Gibco™ Dynabeads™ Human T-Activator CD3/CD28 for T Cell Expansion and Activation (Life Technologies). Cells were then vortexed and plated in 96-well round-bottom plates at a density of 10,000, 20,000, 30,000, or 50,000 cells per well in 100µL of VX15 media. 100µL of Treg feeding media was then added to each well giving working concentrations of 600U/ml of IL-2 and 125ng/ml rapamycin. Tregs were incubated at 37°C with 5% CO_2.

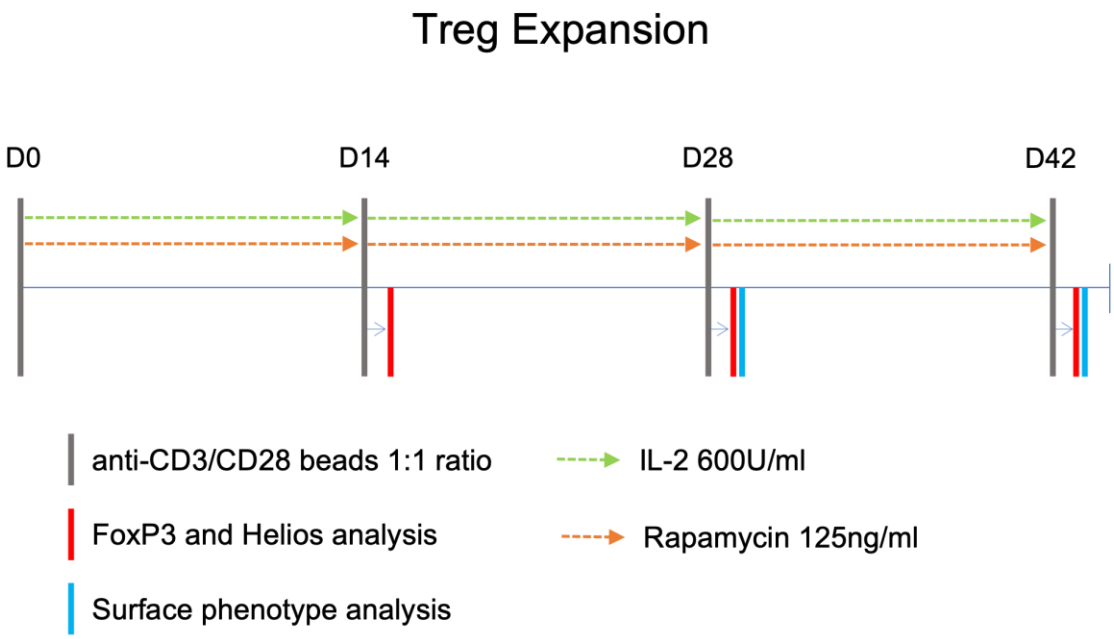

Figure 4.2: Expansion timeline for Treg subsets. For expansion, Tregs were stimulated on days 0, 14, and 28 with anti-CD3/CD28 beads. On these days, an aliquot of each Treg subset was cultured in media without IL-2 for 48 hours prior to FoxP3 and Helios, and surface phenotype analysis by flow cytometry. Media was supplemented with IL-2 and rapamycin throughout the expansion process and half the media was replenished every 48 hours.

4.2.4 Treg culture and expansion

A schematic of the Treg expansion timeline is shown in figure 4.2. Expanding Tregs were fed every 48 hours by replenishing half the culture media with Treg feeding media containing IL-2 and rapamycin. Cells were split upon reaching 90% confluency. After 14 days (phase 1 of expansion), the cells were harvested, beads removed, and cells were counted and restimulated with CD3/CD28 beads at a 1:1 ratio. Each Treg subset underwent 3 phases of expansion totalling 42 days; activated with CD3/CD28 beads at days 0, 14, and 28.

4.2.5 Phenotyping of expanded cells by flow cytometry

At the end of each phase of expansion, Tregs were stained to evaluate the percentage of cells expressing the Treg markers FoxP3 and Helios. A 50,000 cell aliquot of each expanded Treg subset was collected on the day of re-activation and placed in wells containing media without IL-2 for 48 hours prior to staining. Cells were then collected into FACS tubes and washed twice with 3ml of DPBS. Cells were stained with Live/Dead Fixable Near-IR Dead Cell Stain Kit (Invitrogen) for 15 minutes at RT to determine viability. After washing twice with FACS buffer, the cells were resuspended and stained for surface antigens at 4°C for 30 minutes: CD127 BV421, CD25 PE, CD4 FITC (Table 4.2). After washing with FACS buffer, fixation and permeabilization was carried out for 40 minutes at RT using 1ml of fixation/permeabilisation buffer from the eBioscience™ Foxp3/Transcription Factor Staining Buffer Set. Cells were washed twice with diluted permeabilisation buffer, then incubated with antibodies specific to the intracellular transcription factors at RT for 40 minutes: FoxP3 AF647, Helios PE-Cy7. Cells stained with the AF647 Isotype control antibody AF647 [MOPC-21]

were used to help determine the correct position of the FoxP3^{+} gate. Finally, cells were washed again with permeabilisation buffer, and resuspended in FACS buffer for analysis.

Table 4.2: Fluorochrome-conjugated antibodies used in intracellular staining for FoxP3 and Helios assessment.

Fluorochrome	Marker	Clone	Supplier	µL/10x10^{6} cells
Master Mix 1				
BV421	CD127	A019D5	BioLegend	2.5
PE	CD25	2A3	BD Biosciences	5
FITC	CD4	SK4	BioLegend	2
Master Mix 2				
AF647	FoxP3	259D	BioLegend	5
PE-Cy7	Helios	22F6	BioLegend	2.5
AF647	Isotype	MOPC-21	BioLegend	5

As well as intracellular staining, at the end of phase II and phase III of expansion the surface phenotype of Tregs was also assessed using the Treg surface phenotyping panel described in chapter 3. A schematic diagram showing the total expansion protocol is shown in figure 4.3 A separate 50,000 cell aliquot of each expanded Treg subset was IL-2-starved for 48 hours prior to staining as with the intracellular staining panel. Surface and intracellular staining was divided into 2 separate panels as it was observed during optimisation steps that some fluorochrome-conjugated antibodies specific to chemokine receptors gave dim staining after fixation/permeabilisation. Staining was carried out using a surface staining antibody panel described in Table 4.3. Briefly, cells were collected into FACS tubes and washed twice with plain DPBS and centrifuged at 400xg for 5

minutes. After the second wash, pellets were resuspended in 500μL of plain DPBS, 500μL of a working solution of 1μL/mL of Live/Dead fixable near infrared dead cell (ThermoFisher) stain was added, and tubes were incubated at RT for 15 minutes. 2ml of FACS buffer was then added and tubes were centrifuged at 400xg for 5 minutes. This wash was repeated, then a master mix consisting of the following antibodies was added and cells were incubated at 37°C; CCR6 BV711, ICOS BV650, CCR4 BV605, CXCR3 BV510, CXCR5 PE-Cy7, CCR10 BUV395, and CD73 FITC. A second staining mastermix was then added and a 30-minute incubation at 4°C was carried out. Antibodies in the second master mix were CD45RA BV786, CD31 BV421, CD127 PE-Cy5, CD95 PE-CF594, CD25 PE, CD4-AF700, and CD49d BUV737. Cells were then washed with 2ml of FACS buffer and centrifuged at 400xg for 5 minutes. Cells were resuspended in 200μL of FACS buffer and stored on ice prior to acquisition. Data were acquired using a BD LSR Fortessa analyser.

Table 4.3: Fluorochrome-conjugated antibodies used for surface marker staining of expanded Treg subsets.

Fluorochrome	Marker	Clone	Supplier	µL/10x10^6 cells
Master Mix 1				
BV711	CCR6	G034E3	BioLegend	2
BV650	ICOS	DX29	BD Biosciences	5
BV605	CCR4	L291H4	BioLegend	2
BV510	CXCR3	G025H7	BioLegend	2
PE-Cy7	CXCR5	J252D4	BioLegend	2
BUV395	CCR10	1B5	BD Biosciences	1
FITC	CD73	AD2	BioLegend	5
Master Mix 2				
BV786	CD45RA	HI100	BioLegend	0.5
BV421	CD31	WM59	BioLegend	2.5
PE-Cy5	CD127	A019D5	BioLegend	2.5
PE-CF594	CD95	DX2	BD Horizon	1
PE	CD25	2A3	BD Biosciences	5
PE	CD25	M-A251	BD Biosciences	5
AF700	CD4	OKT4	BioLegend	2
BUV737	CD49d	9F10	BioLegend	5

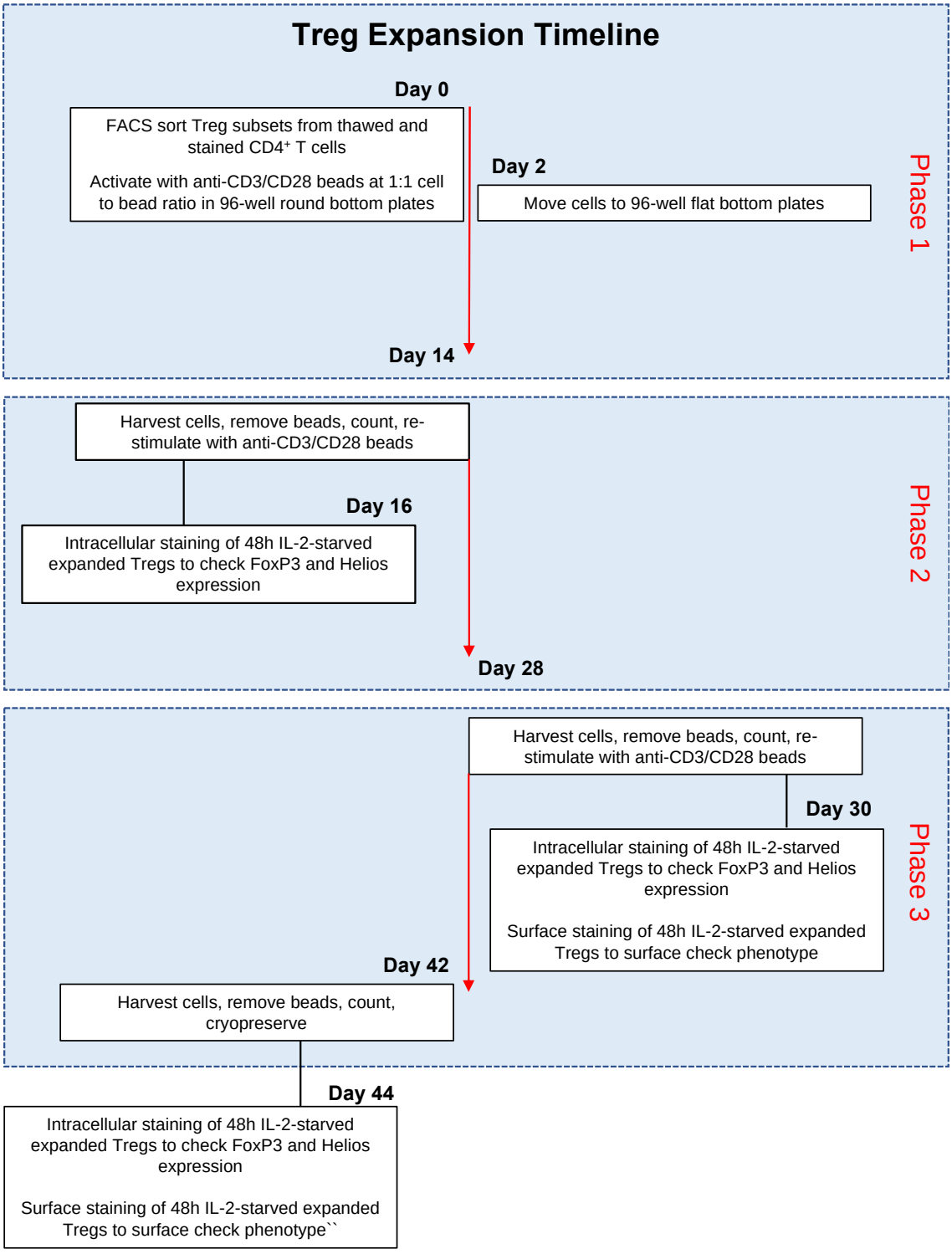

Figure 4.3. Schematic diagram of Treg expansion timeline. Cryopreserved CD4+ T cells were thawed and stained with a flow cytometry panel to identify Treg subsets prior to FACS sorting of subsets. Cells were then activated using a 1:1 bead to cell ratio of anti-CD3/CD28 beads and plated in 96-well round bottom plates. Cells were cultured throughout the expansion process in media supplemented with 600IU/ml of IL-2 and 125ng/ml of rapamycin and fed every other day. At day 2, cells were transferred to flat-bottomed plates. At the end of phase I (day 14) cells were harvested, and beads were removed by placing tubes in a

magnet. Cells from each Treg subset were counted and re-stimulated with anti-CD3/CD28 beads. 50,000 cell aliquots from each Treg subset were plated separately without beads and IL-2 for 48 hours prior to intracellular staining and flow cytometry. At day 28, this process was repeated with the addition of an additional aliquot of IL-2 starved cells to monitor the surface phenotype of the expanded subsets. At day 42, this process was repeated and any remaining cells were cryopreserved.

4.2.6 Data analysis

Expansion kinetics (cell number and fold expansion) data were derived from cell numbers calculated by manually counting the cells with a haemocytometer and data were plotted using Prism 9 software.

Analysis of flow cytometry data was carried out in FlowJo and OMIQ software where indicated. Expanded Tregs were manually gated as singlets < Live cells < $CD4^+$ events for intracellular and surface phenotype analysis. Use of CD25 and CD127 was not reliable in expanded cells as Tconvs activated by anti-CD3/CD28 beads and IL-2 also display a $CD25^{hi}CD127^{lo}$ surface phenotype. Scatter plot graphs showing frequencies of positive cells and MFIs were generated using Graphpad Prism 9 software. Statistical significance was determined using one-way ANOVA with either a Turkey's or Šídák's post-hoc test where indicated.

4.3 Results

4.3.1 Optimisation of the Treg expansion protocol

As naïve Tregs represent a rare fraction of the total Treg pool and our research ethics stipulated a maximum of 90ml of blood was to be drawn per donor, we first aimed to optimise the lowest starting cell number per well in which Tregs would expand. Naïve, memory, and bulk Tregs were FACS sorted into FACS tubes using the gating strategy shown in figure 4.4. Bulk Tregs were sorted as $CD19^{-}CD4^{+}CD25^{hi}CD127^{low}$ representing 6.77% of $CD4^{+}$ T cells, memory Tregs were sorted as $CD4^{+}CD25^{hi}CD127^{low}CD95^{+}CD45RA^{-}$ (69.8% of Tregs), and naïve Tregs were sorted as $CD4^{+}CD25^{hi}CD127^{low}CD95^{-}CD45RA^{+}$ representing 12.3% of Tregs in this donor. An example of the sort purity of memory Tregs is shown in figure 4.5 whereby purity of this subset was 98%.

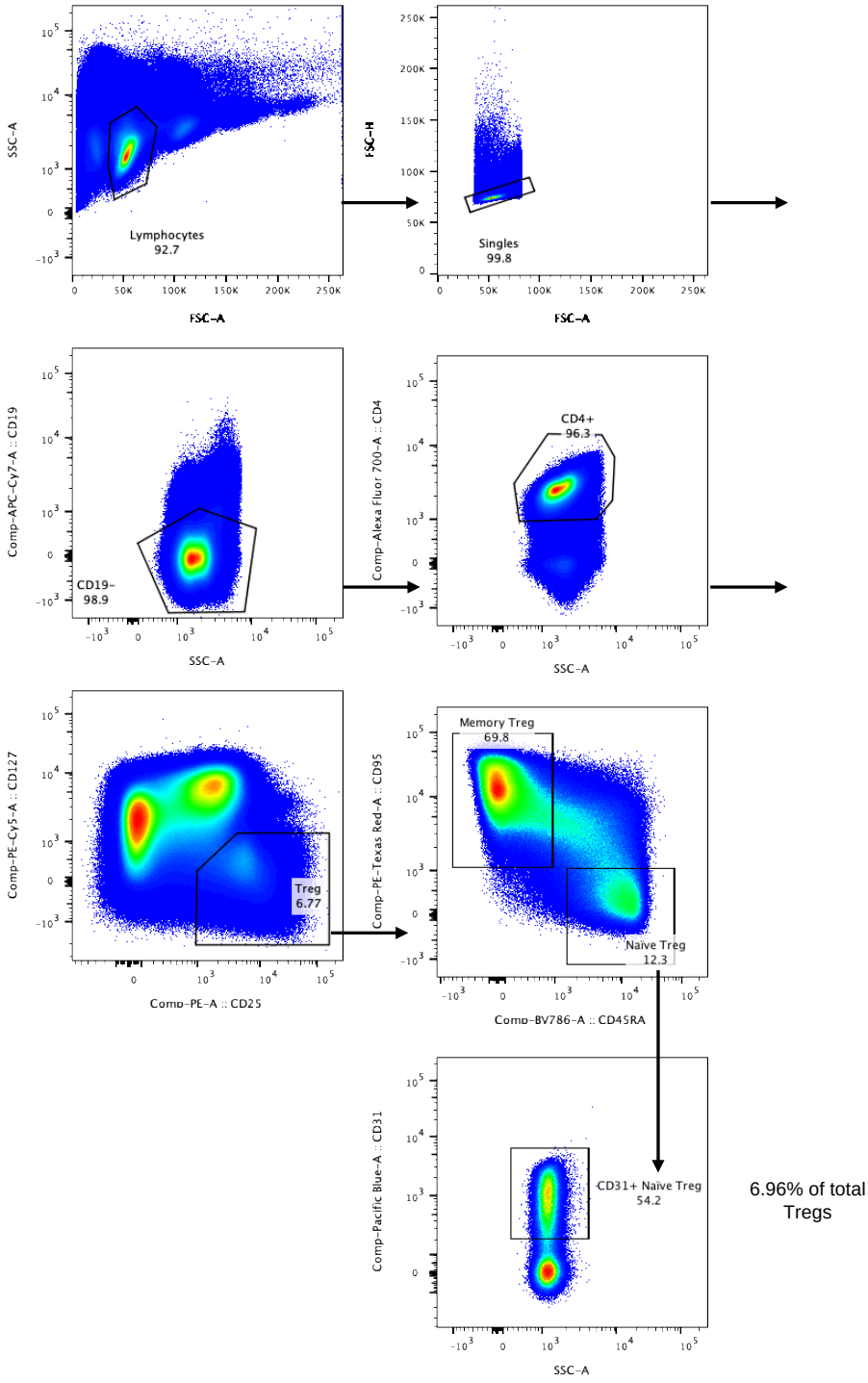

Figure 4.4: FACS sorting of Treg subsets. Enriched CD4$^+$ T cells were stained with a panel of fluorescently tagged monoclonal antibodies to identify Treg subsets and FACS sorted on a BD FACS Aria IIu cell sorter. Representative data from a single donor.

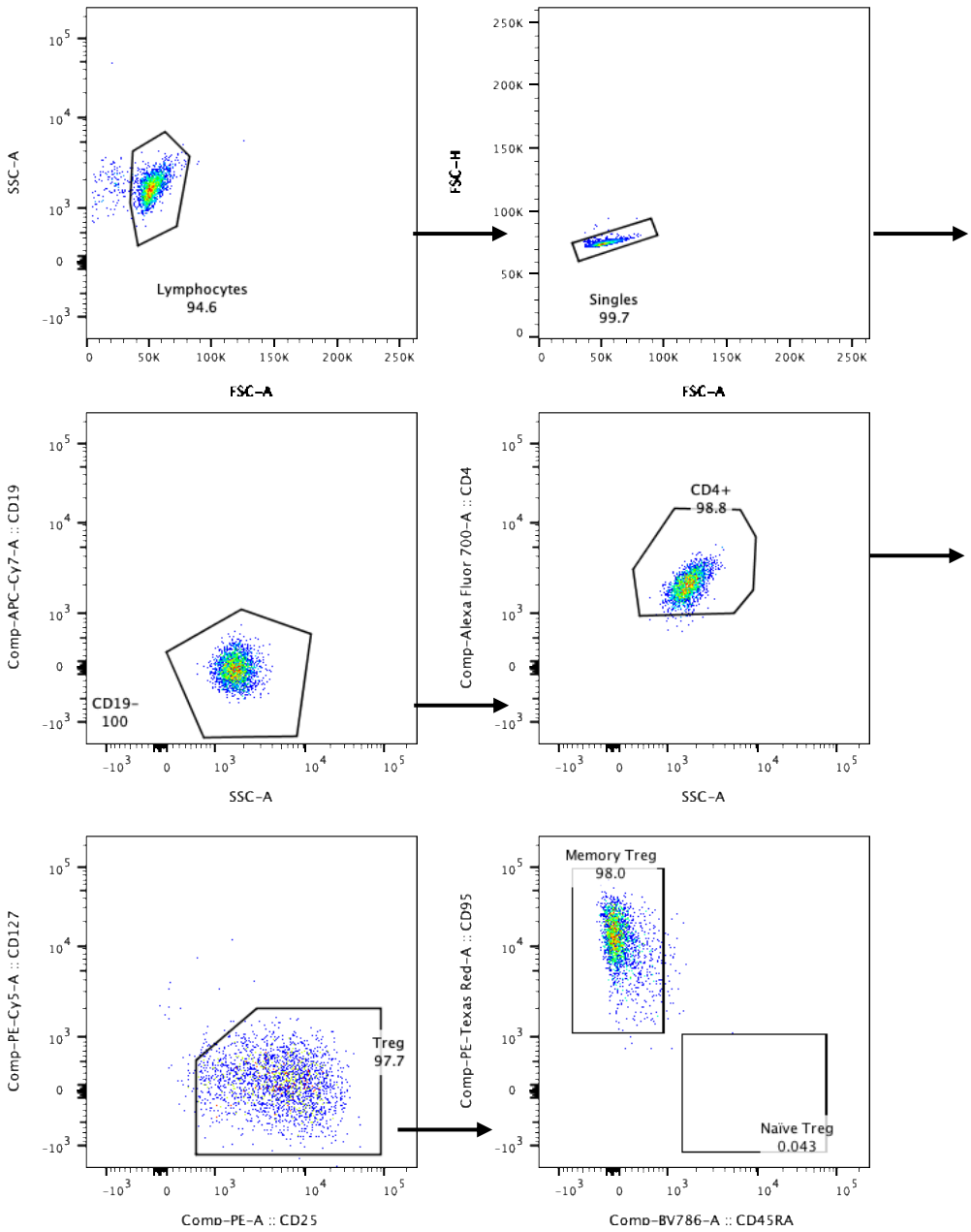

Figure 4.5: Purity of FACS sorted memory Tregs. Enriched CD4⁺ T cells were stained with a panel of fluorescently tagged monoclonal antibodies to identify Treg subsets and FACS sorted on a BD FACS Aria IIu cell sorter. An aliquot of memory Tregs were then re-acquired to analyse sort purity. Representative data from a single donor.

Cells were then counted and plated at a density of either 10,000, 20,000, or 50,000 cells per well and expanded for 26 days, with a restimulation with anti-CD3/CD28 beads at day 12 (2 phases). Figure 4.6 shows the cell counts and fold expansion of the Treg subsets plated at different densities at days 12 and 26 of expansion. In this donor, naïve Tregs had the highest expansion potential compared to bulk Tregs and memory Tregs. At 10,000 cells per well, naïve Tregs had a 16.65-fold expansion by day 12 and a 131.4-fold expansion by day 26. This was compared to a 4.34-fold and 12.75-fold expansion for bulk Tregs at days 12 and 26, respectively, a 2.64-fold and a 7-fold expansion for memory Tregs. At 20,000 cells per well, the fold expansion of naïve Tregs at day 12 was 19.51 and the fold expansion at day 26 increased to 280.85, showing a near exponential increase in expansion during the second phase (days 12-26) when the cell density doubled. For bulk Tregs and memory Tregs there was no increase in expansion potential at 20,000 cells per well. It was not possible to sort 50,000 cells per well of the naïve Tregs due to the rarity of this subset. However, bulk Tregs at day 26 had a 29-fold expansion; an increase in expansion potential compared to that at 10,000 and 20,000 cells per well. From this data from a single donor, we were able to see that a higher starting cell number per well yielded a greater cell number for bulk and naïve Tregs, therefore for future experiments it would be beneficial to sort at least 20,000 starting cells per subset prior to expansion.

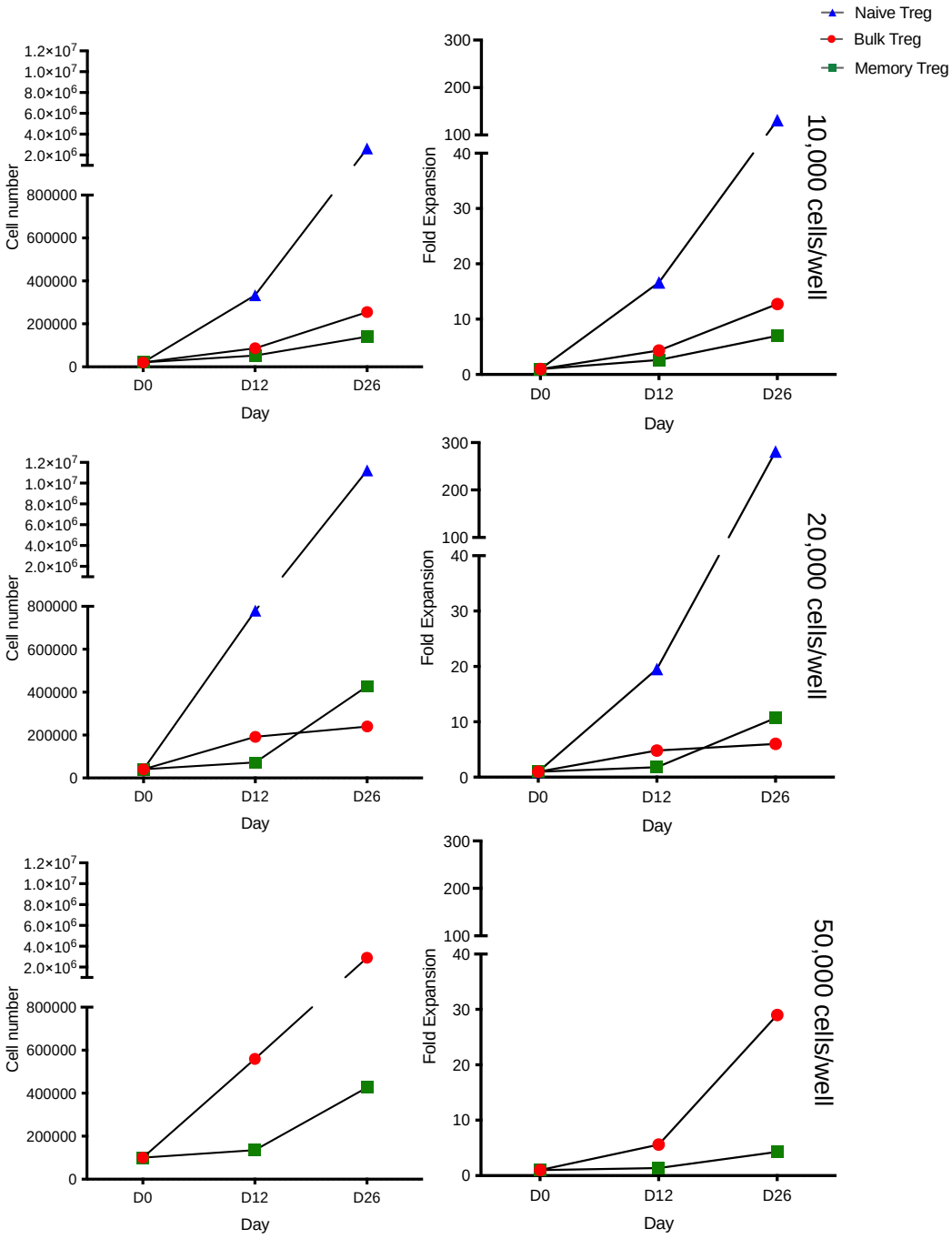

Figure 4.6: Treg subsets had higher rates of expansion when starting with a higher number of cells per well. FACS sorted Bulk (red), Memory (green), and Naïve (blue) Treg subsets were pre-stimulated at a 1:1 ratio of anti-CD3/CD28 beads to cells and plated in 96-well round-bottom plates at densities of 10,000 (top panel), 20,000 (middle panel), or 50,000 (bottom panel) cells per well. Cells were cultured throughout in media containing IL-2 and rapamycin. At Day 12 following cell harvesting and removal of beads, cells were counted and restimulated with anti-CD3/CD28 beads. Cells were then re-harvested and counted on day 26. Representative data from a single donor.

As described in 4.1, addition of rapamycin to culture media during Treg expansion is thought to suppress the outgrowth of any contaminating Tconvs and to maintain a regulatory phenotype in expanded Treg cultures. As an additional optimisation step, we expanded Tconvs and bulk Tregs for 14 days in the presence or absence of 125ng/ml of rapamycin. As shown in figure 4.7 A, in the absence of rapamycin, 14.3% of Tconvs were FoxP3^{+} and 0.032% of events were Helios^{+}. Only 45.3% of expanded Tregs were FoxP3^{+} and 9.68% were Helios^{+} in the absence of rapamycin, suggesting either a loss of FoxP3 expression or outgrowth of contaminating Tconvs. With the addition of rapamycin (figure 4.7 B) 28.4% of Tconvs were FoxP3^{+}, and 0.73% were Helios^{+}. Importantly, Tregs expanded in the presence of rapamycin were 97.5% FoxP3^{+} and 56.1% were Helios^{+}. These expanded Tregs also maintained a Treg surface phenotype of CD25^{hi}CD127^{low}, whereas in the absence of rapamycin, more events upregulated CD127. In conclusion, rapamycin was shown to support and maintain the surface and intracellular Treg phenotype during expansion. Moreover, some Tconvs did express FoxP3 during expansion, which increased in the presence of rapamycin, however the expression of Helios remained low in these expanded cells.

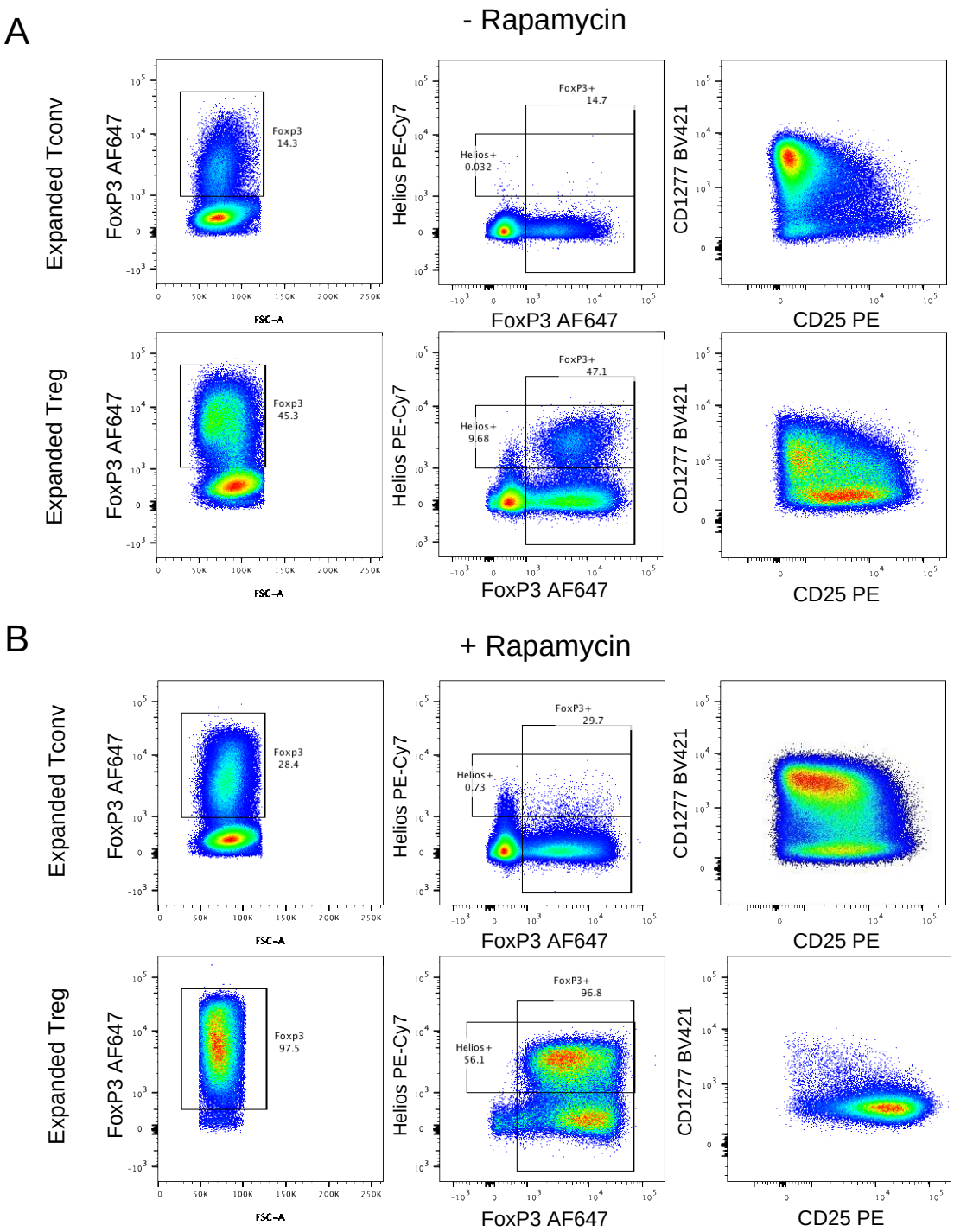

Figure 4.7: Rapamycin enhanced the expression of FoxP3 and Helios during 14 days of Treg expansion. Tregs and Tconvs were FACS sorted and stimulated to expand with anti-CD3/CD28 beads at a 1:1 bead to cell ratio in media supplemented with IL-2 and +/- rapamycin for 14 days. Cells were then collected, stained, and expression of Treg markers was analysed by flow cytometry. Data representative from a single donor. (A) FoxP3, Helios, and CD25 expression of Tregs and Tconvs expanded in the absence of rapamycin. (B) FoxP3, Helios, and CD25 expression of Tregs and Tconvs expanded in the presence of rapamycin.

4.3.2 Expansion potential of naïve CD31$^+$, naïve, memory, and bulk Tregs

Following optimisation of the expansion protocol, we then aimed to investigate the expansion potential of naïve CD31$^+$ Tregs, the most suppressive subset at baseline. We also expanded naïve Tregs to determine whether the CD31$^+$ phenotype renders an expansion advantage over simply a naïve phenotype, and memory Tregs, and bulk Tregs as comparators. Treg subsets were sorted using the strategy shown in figure 4.4 and expanded according to the methods described in 4.2.3. As shown in figure 4.8, in terms of expansion kinetics, there were no significant differences in expansion potential (fold-expansion) between subsets over the 6-week expansion period. Although there seemed to be a trend towards better expansion of naïve CD31$^+$ and naïve Tregs compared to memory Tregs at day 14 and day 42 of expansion, there was a large inter-donor variation in cell counts and therefore this trend did not reach significance (4.8 B+C).

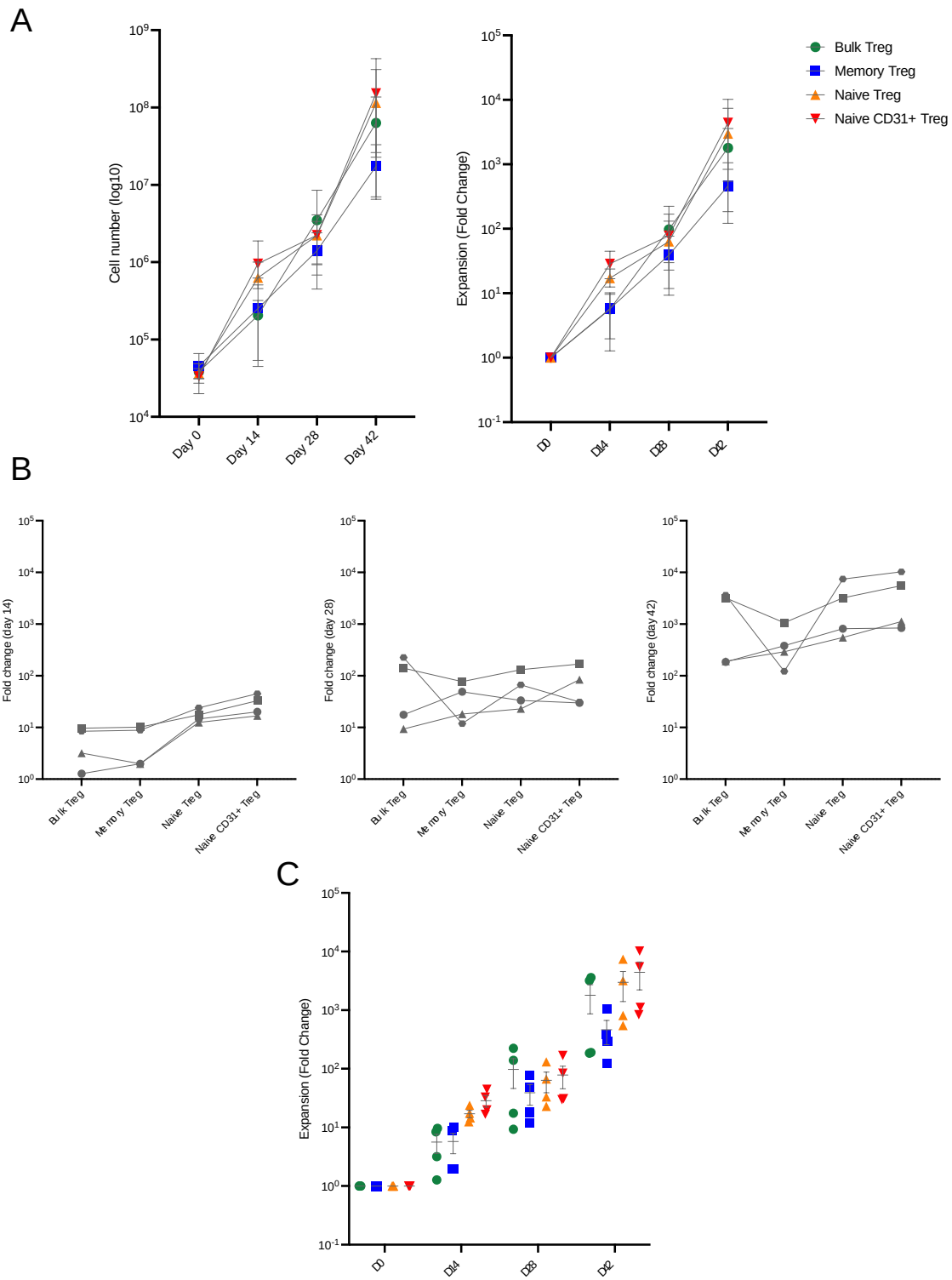

Figure 4.8: Different Treg subsets did not have significantly different expansion potentials at days 14, 28, or 42 of expansion. Bulk Tregs (green), memory Tregs (blue), naïve Tregs (yellow), and naïve CD31^{+} Tregs (red) and Tconvs were FACS sorted and stimulated to expand with anti-CD3/CD28 beads at a 1:1 bead to cell ratio in media supplemented with IL-2 and rapamycin for 42 days. (A) Cells were counted and re-stimulated with beads every 14 days and cell number and fold expansion were calculated. (B) Inter-donor variation in expansion at days 14, 28, and 42; individual donors are indicated by

symbols. (C) Inter-donor variation in expansion at days 14, 28, and 42. Statistical significance between groups at each timepoint was evaluated by one-way ANOVA with a Turkey's post-hoc test (no significant differences detected). Error bars show mean +/- SEM (n=4).

4.3.3 Treg phenotype stability of expanded Treg subsets

As described in 4.1, a common issue during *ex vivo* expansion of Tregs is loss of the Treg suppressive phenotype during multiple rounds of expansion, as indicated by a loss of FoxP3 expression. We therefore monitored the intracellular expression of FoxP3 and Helios during expansion. At days 14, 28, and 42, aliquots of expanded Treg subsets were IL-2-starved for 48 hours and subjected to analysis of intracellular FoxP3 and Helios by flow cytometry. At the end of phase I of expansion, it was not possible to measure FoxP3 and Helios expression in some donors due to low cell numbers. As shown in figure 4.9 A, we used isotype control antibodies for FoxP3 and Helios, and also expanded Tconvs to guide our gating analysis. Figure 4.9 B shows representative examples of flow cytometry data showing expression of FoxP3 and Helios in bulk Tregs, memory Tregs, naïve Tregs, and naïve $CD31^+$ Tregs at the end of phase I of expansion (14 days). As indicated in this donor, over 85% of events were $FoxP3^+$ in all expanded subsets, although the Helios expression was more variable.

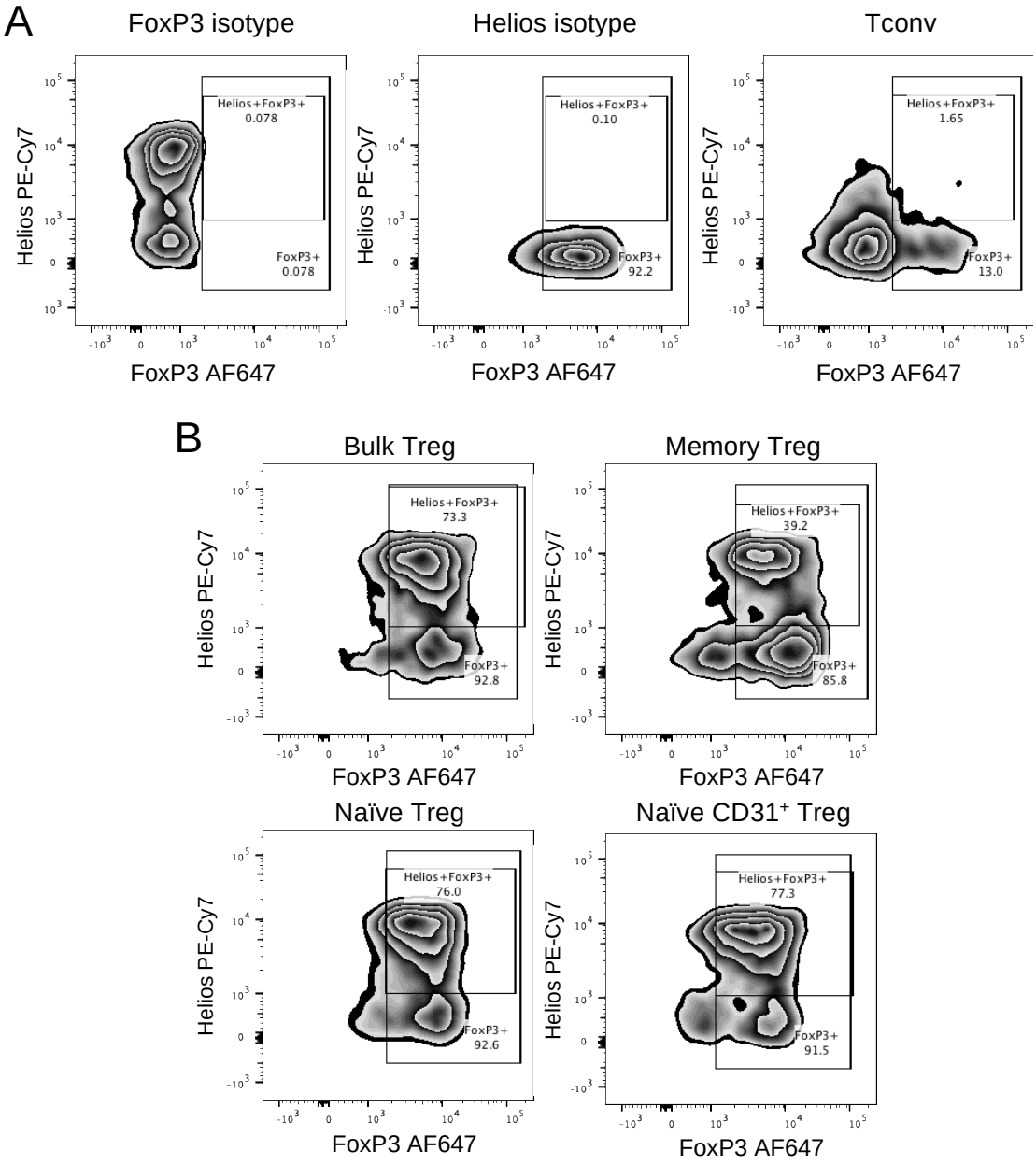

Figure 4.9: FoxP3 and Helios gating in expanded Treg subsets. Treg subsets were expanded by anti-CD3:CD28 bead stimulation in the presence of IL-2 and rapamycin for 14 days, then IL-2 starved for 48 hours prior to intracellular staining of FoxP3 and Helios. All gated on live $CD4^+$ events. (A) Isotype controls for FoxP3 and Helios, and also expanded Tconvs were used to guide gate placement. (B) Frequencies of FoxP3 and Helios positive cells in expanded Treg subsets from a single representative donor. Data acquired by flow cytometry using a BD LSR Fortessa analyser.

Figure 4.10 summarises the expression of FoxP3 and Helios in expanded subsets from 4 individual donors at the end of phases I, II, and III of expansion. The frequency of FoxP3 expressing cells in all donors remained at a minimum of 82% of evets throughout the 6 weeks of expansion. At the end of phase I, there were no significant differences in $FoxP3^+$ cells between bulk Tregs and any of the subsets. There was, however, a significantly higher frequency of $FoxP3^+$ cells in the naïve (mean 92.37%) and naïve $CD31^+$ (mean 94.07%) subsets compared to memory Tregs, although the mean expression of FoxP3 by memory Tregs was still 82.73%. By the end of phase II, the difference in FoxP3 expressing cells between naïve Tregs and memory Tregs lost significance, however there remained a significantly higher percentage of $FoxP3^+$ cells in the expanded naïve $CD31^+$ Tregs compared to memory Tregs. The mean frequencies of $FoxP3^+$ cells at the end of phase II of expansion were 83.75, 80.2, 90.71, and 91.98% for expanded bulk Tregs, memory Tregs, naïve Tregs, and naïve $CD31^+$ Tregs, respectively. At the end of phase III of expansion, the expression of FoxP3 by all subsets remained high and there were no significant differences in $FoxP3^+$ cell frequency between the subset groups. Figure 4.11 A shows that there were no significant differences in frequencies of $FoxP3^+$ cells when comparing the individual subsets at the end of phases I, II, and III of expansion.

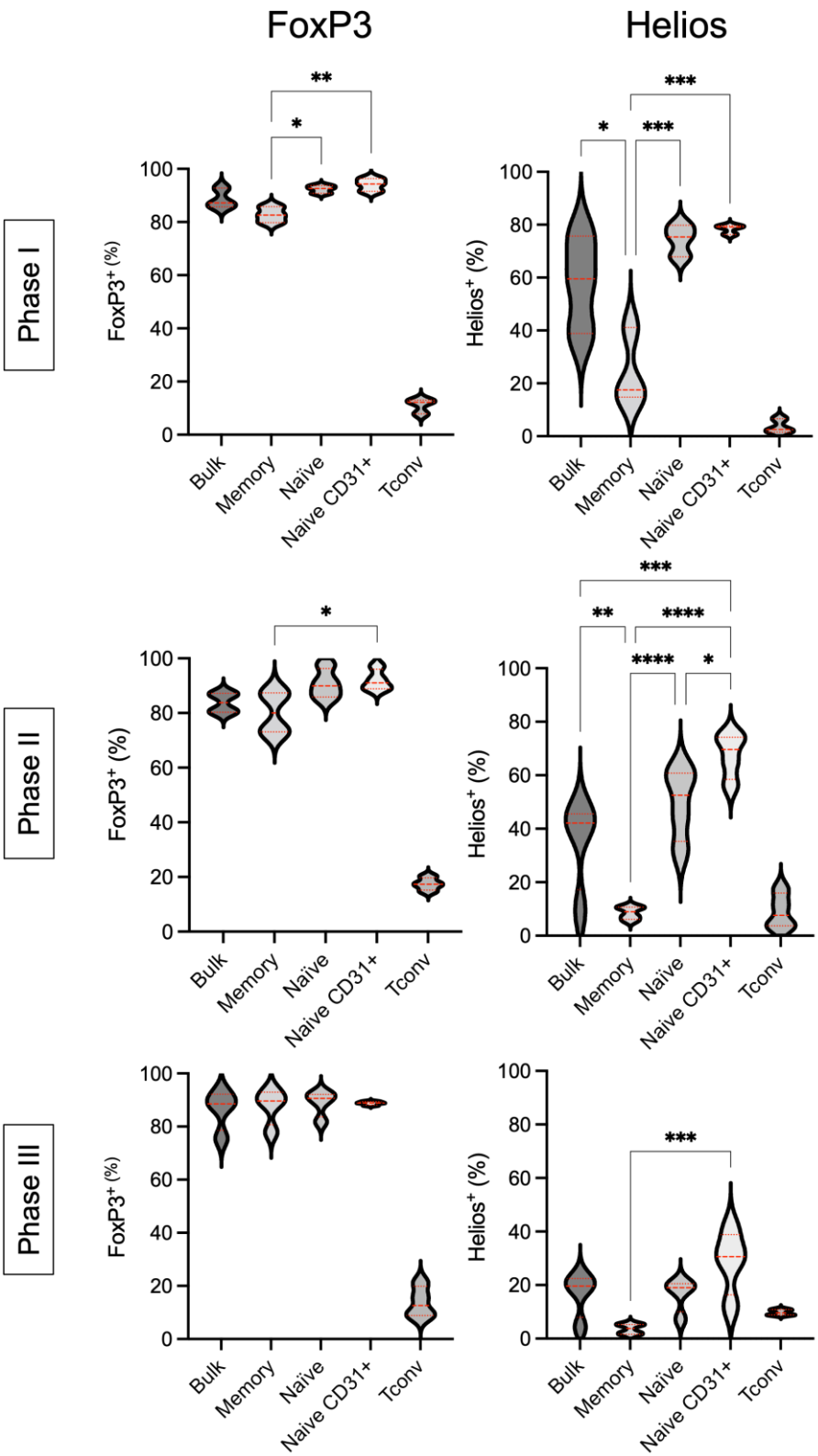

Figure 4.10: Naïve CD31$^+$ Tregs were the subset which maintained the highest expression of Helios at days 14, 28, and 42 of expansion, and the highest FoxP3 expression at days 14 and 28 of expansion. Treg subsets were expanded by anti-CD3:CD28 bead stimulation in the presence of IL-2 and rapamycin for 42 days. At days 14 (end of phase I, top panel), 28 (end of phase II, middle panel), and 42 (end of phase III,

bottom panel), an aliquot of each expanded subset was IL-2-starved for 48 hours prior to evaluation of FoxP3 (left) and Helios (right) expression. Data were acquired by flow cytometry using a BD LSR Fortessa analyser. Statistical significance between groups at each timepoint was evaluated by one-way ANOVA with a Turkey's post-hoc test. Lines show median and quartile values. (*= $p < 0.05$; **= $p < 0.01$, ***= $p < 0.005$, ****= $p < 0.0001$) (n=3 or n=4).

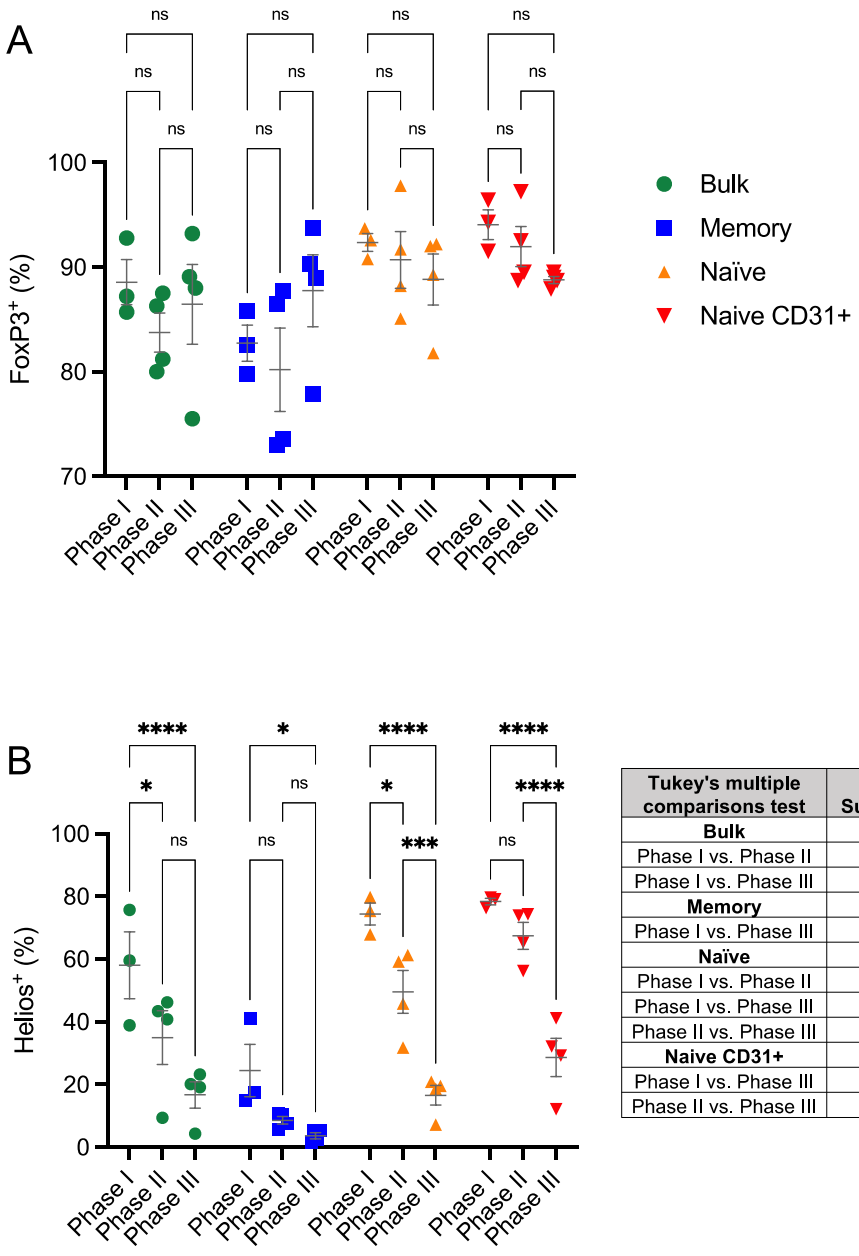

Tukey's multiple comparisons test	Summary	P Value
Bulk		
Phase I vs. Phase II	*	0.0211
Phase I vs. Phase III	****	<0.0001
Memory		
Phase I vs. Phase III	*	0.0400
Naïve		
Phase I vs. Phase II	*	0.0125
Phase I vs. Phase III	****	<0.0001
Phase II vs. Phase III	***	0.0004
Naive CD31+		
Phase I vs. Phase III	****	<0.0001
Phase II vs. Phase III	****	<0.0001

Figure 4.11: FoxP3 expression within subsets was unchanged at the end of phase I, phase II and phase III of expansion, while expression of Helios within Treg subsets was significantly reduced with expansion. Treg subsets were expanded by anti-CD3:CD28 bead stimulation in the presence of IL-2 and rapamycin for 42 days. At days 14 (end of phase I; n=3), 28 (end of phase II) (n=4), and 42 (end of phase III) (n=4), an aliquot of each expanded subset was IL-2-starved for 48 hours prior to evaluation of FoxP3 and Helios expression. Data were acquired by flow cytometry using a BD LSR Fortessa analyser. (A) Changes in FoxP3 expression within Treg subsets at different expansion timepoints. Bulk Treg = green, memory Treg = blue, naïve Treg = yellow, naïve CD31⁺ Treg = red. (B) Changes in Helios expression within Treg subsets at different expansion timepoints.

Statistical significance between groups at each timepoint was evaluated by one-way ANOVA with a Turkey's post-hoc test. No significant differences in FoxP3 expression were found. P values of Helios expression significant changes are shown in the table within panel B. Error bars show mean +/- SEM.

Helios expression was more variable between subsets during expansion. At the end of phase I, the naïve and naïve CD31$^+$ Tregs had a significantly higher frequency of Helios$^+$ cells than and memory Tregs (figure 4.10). There was no difference in Helios$^+$ cell frequency when comparing naïve Tregs and naïve CD31$^+$ Tregs with one another or with bulk Tregs, however memory Tregs had significantly fewer Helios$^+$ cells compared to bulk Tregs. The mean frequencies of Helios$^+$ cells at the end of phase I were 58.03, 24.47, 74.37, and 78.33% respectively for bulk Tregs, memory Tregs, naïve Tregs, and naïve CD31$^+$ Tregs. There was also large inter-donor variation in Helios positive cells within expanded bulk Tregs (SD= 18.44) which was smaller in the expanded subsets; memory SD= 14.47, naïve SD= 6.02, naïve CD31$^+$ SD= 1.78. By the end of phase II of expansion, the frequency of Helios$^+$ cells had fallen significantly compared to the end of phase I expansion in expanded bulk Tregs and naïve Tregs, but not in expanded memory and naïve CD31$^+$ Tregs (figure 4.11 B). At this stage, naïve CD31$^+$ Tregs had a significantly higher frequency of Helios$^+$ cells than all other subsets. Expanded memory Tregs also had a significantly lower frequency of Helios$^+$ events compared to bulk Tregs and naïve Tregs. By the end of phase III of expansion, however there was a significant reduction in Helios$^+$ events in every subset compared to the end of phase I, and in naïve and naïve CD31$^+$ Tregs the frequency of Helios$^+$ events at the end of phase III was significantly lower compared to those at the end of phase II of expansion (figure 4.11 B). The only significant difference remaining between Treg groups at this stage was a

significantly higher frequency of Helios$^+$ events in the naïve CD31$^+$ subset compared to the memory Treg subset. In summary, there was no significant change in the frequency of FoxP3$^+$ cells within any subset at different phases of expansion (figure 4.11 A). However the frequency of Helios$^+$ events fell significantly within every subset between the end of phase I and end of phase III of expansion (figure 4.11 B). Despite this, expanded naïve CD31$^+$ Tregs maintained a higher Helios$^+$ frequency than expanded memory Tregs throughout the expansion process and a higher frequency of FoxP3$^+$ cells at the end of the first and second phases of expansion.

4.3.4 Treg subset surface phenotype during expansion

Next, we explored how the surface phenotypes of the expanded Tregs changed over the course of 3 phases of expansion with a view to answer whether Tregs starting with a naïve phenotype yield a similar expansion product to memory Tregs. Expanded Treg subsets were stained using the Treg surface marker panel and analysed by flow cytometry at the end of phase II and phase III of expansion.

Figure 4.12 shows agglomerative hierarchal clustering of the MFI of individual marker expression on Treg subsets from two individual donors at the end of phase II of expansion (A) and phase III of expansion (B). As shown here, the expanded bulk Treg, memory Treg, naïve Treg, and naïve CD31$^+$ Treg subsets from 2 independent donors clustered together at the end of phase II of expansion.

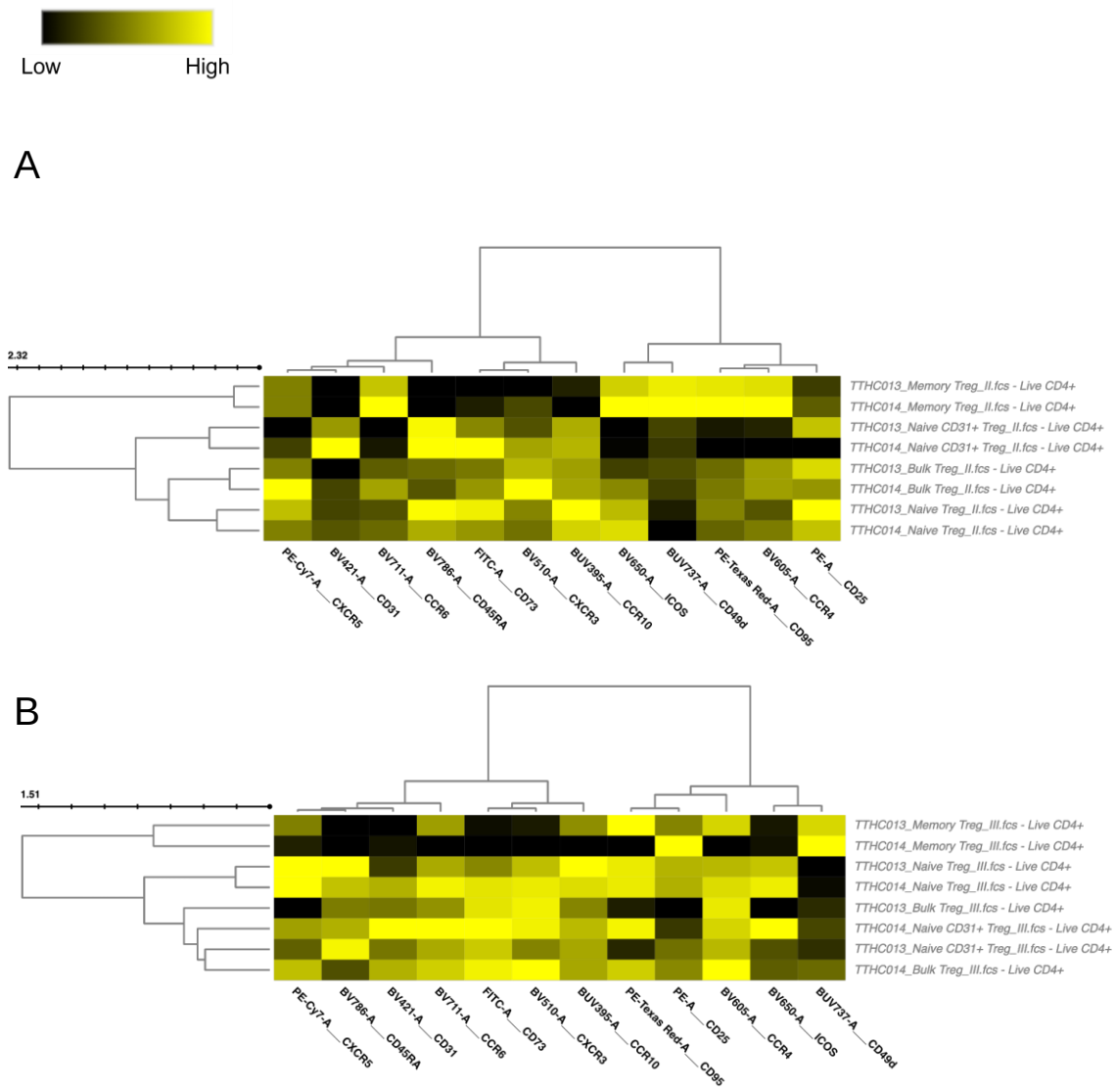

Figure 4.12: Individual Treg subsets cluster together based on surface phenotypes at days 28 and 42 of expansion. Bulk Treg, Memory Treg, Naïve Treg, and Naïve CD31^{+} Treg subsets were FACS sorted and expanded in culture for 42 days using anti-CD3/CD28 beads, IL-2, and rapamycin. At days (A) 28 and (B) 42, an aliquot of each subset was rested in media without IL-2 for 48 hours prior to immunofluorescent staining. Cells were then stained and data were acquired on a BD LSR Fortessa. Dendrograms on the left of the histograms show agglomerative hierarchal clustering of expanded Treg subsets. Scale shows low to high mean fluorescence intensities of markers.

This shows that the phenotype of the cells at the beginning of expansion has more of an impact on the surface phenotypes of the expanded cells at day 28 of expansion than the impact of donor variation. By the end of phase III memory, naïve, and naïve $CD31^+$ Treg still clustered together, however bulk Tregs from the two donors clustered separately. In addition, memory Tregs defined the first clade separated on the dendrogram meaning their surface phenotype was the least similar to all other expanded subsets.

The MFI was then individually analysed for each surface marker and statistically significant changes between Treg subsets at phase II and phase III, and also differences between phases within the same subset were calculated. Firstly, as shown in figure 4.13, the expression of CD49d was significantly altered between expanded subsets. Namely, at the end of phase II of expansion, expanded memory Tregs expressed significantly higher CD49d than all other subsets (figure 4.13 A). There was no significant difference in CD49d expression between bulk Tregs, naïve Tregs, or naïve $CD31^+$ Tregs. By the end of phase III of expansion, a slight increase in the MFI of CD49d in the expanded bulk Tregs meant that the significant difference in CD49d expression between bulk and memory Tregs was lost. When comparing the CD49d expression between phases, there were no significant changes in CD49d expression between phase II and phase III in any subsets. From this we may conclude that CD49d expression is stable within memory Tregs and is not upregulated by naïve or naïve $CD31^+$ Tregs in response to a third round of stimulation by anti-CD3/CD28 beads.

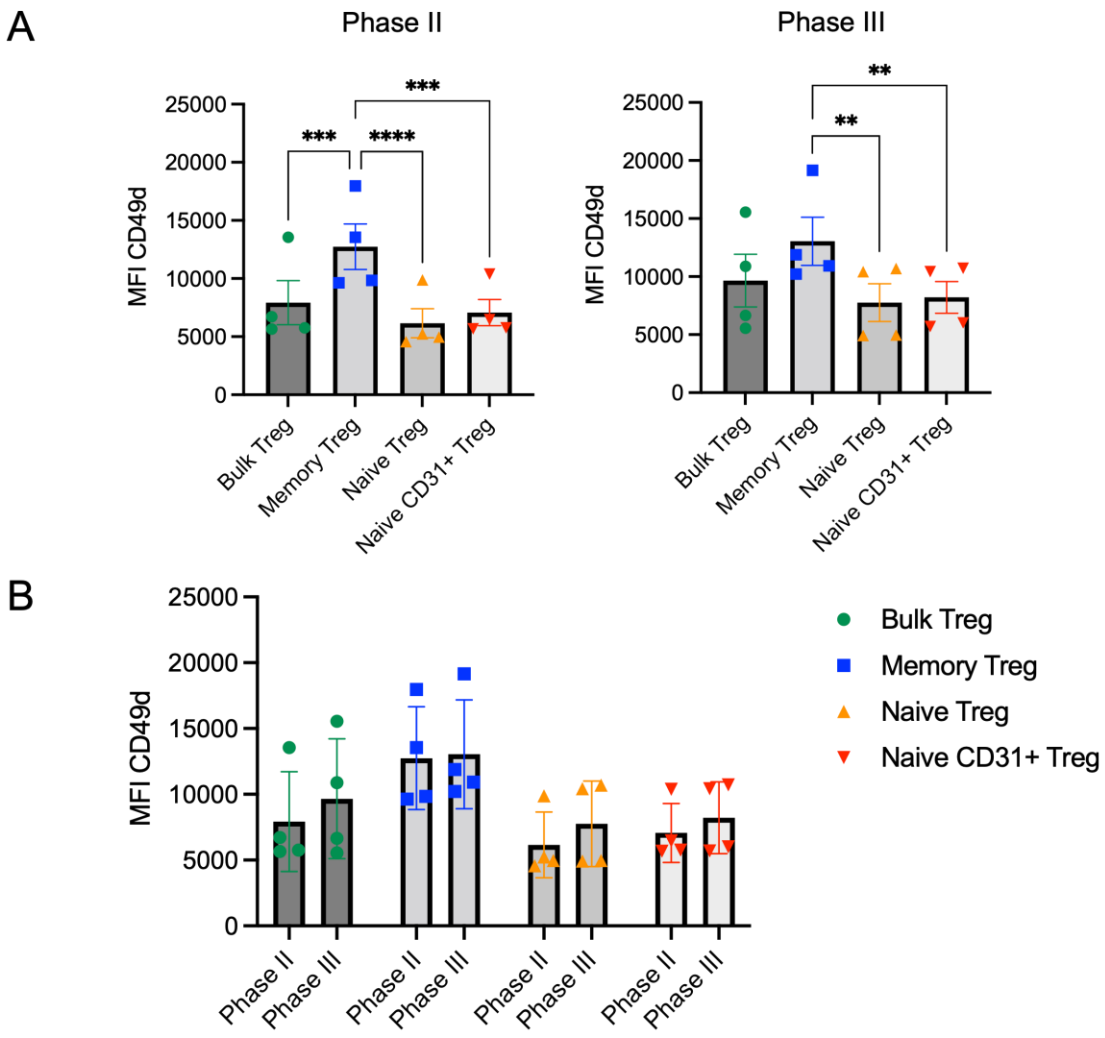

Figure 4.13: Expression of CD49d does not significantly change within subsets when analysed at days 28 and 42 of expansion. Bulk Treg, Memory Treg, Naïve Treg, and Naïve CD31^{+} Treg subsets were FACS sorted and expanded in culture for 42 days using anti-CD3/CD28 beads, IL-2, and rapamycin. At days 28 (end of phase II) and 42 (end of phase III), an aliquot of each subset was rested in media without IL-2 for 48 hours prior to immunofluorescent staining. Cells were then stained and data were acquired on a BD LSR Fortessa. Statistical significance between groups at each timepoint was evaluated by one-way ANOVA with a Turkey's post-hoc test (A) or Šídák's multiple comparisons test (B). Error bars show mean +/- SEM (*= $p < 0.05$; **= $p < 0.01$, ***= $p < 0.005$, ****= $p < 0.0001$) (n=4). MFI= mean fluorescence intensity.

As shown in figure 4.14, there was no significant difference in expression of ICOS between Treg groups at the end of phase II or III of expansion. There was however, a general trend towards an increase in ICOS expression from phase II to phase III in all expanded subsets, and this change reached significance in the case of the naïve $CD31^{+}$ Tregs (figure 4.14 B). Similarly, there were no significant changes in CD73 expression between subsets at the end of phase II or phase III, or between phases (figure 4.15 B). In terms of the surface chemokine receptors CCR10, CXCR3, CCR4, CCR6, and CXCR5, there were no significant changes in expression of these markers between phases or groups (figure 4.16).

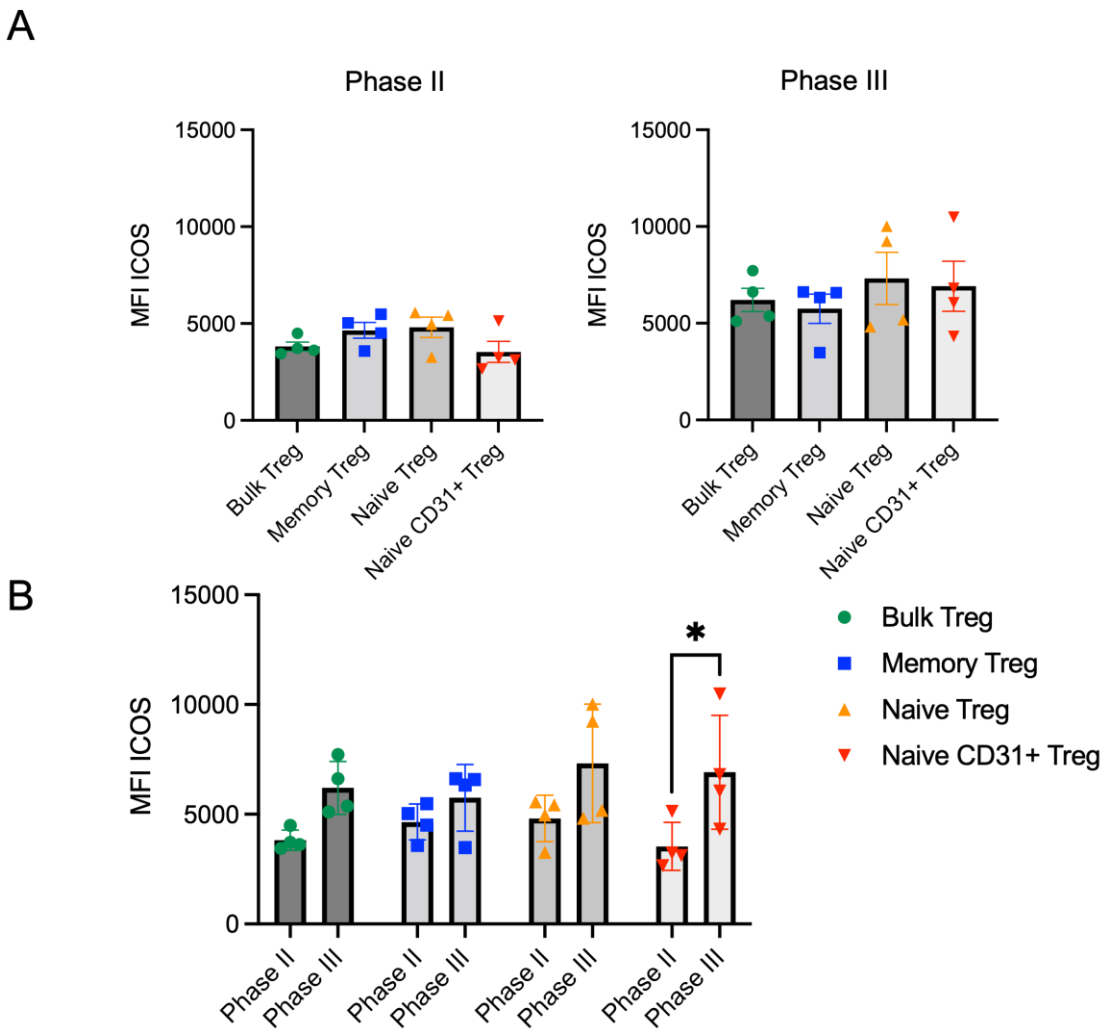

Figure 4.14: Expanded naïve CD31⁺ Tregs significantly upregulated ICOS at day 42 of expansion. Bulk Treg, Memory Treg, Naïve Treg, and Naïve CD31⁺ Treg subsets were FACS sorted and expanded in culture for 42 days using anti-CD3/CD28 beads, IL-2, and rapamycin. At days 28 (end of phase II) and 42 (end of phase III), an aliquot of each subset was rested in media without IL-2 for 48 hours prior to immunofluorescent staining. Cells were then stained and data were acquired on a BD LSR Fortessa. Statistical significance between groups at each timepoint was evaluated by one-way ANOVA with a Turkey's post-hoc test (A) or Šídák's multiple comparisons test (B). Error bars show mean +/- SEM (*= $p < 0.05$) (n=4). MFI= mean fluorescence intensity.

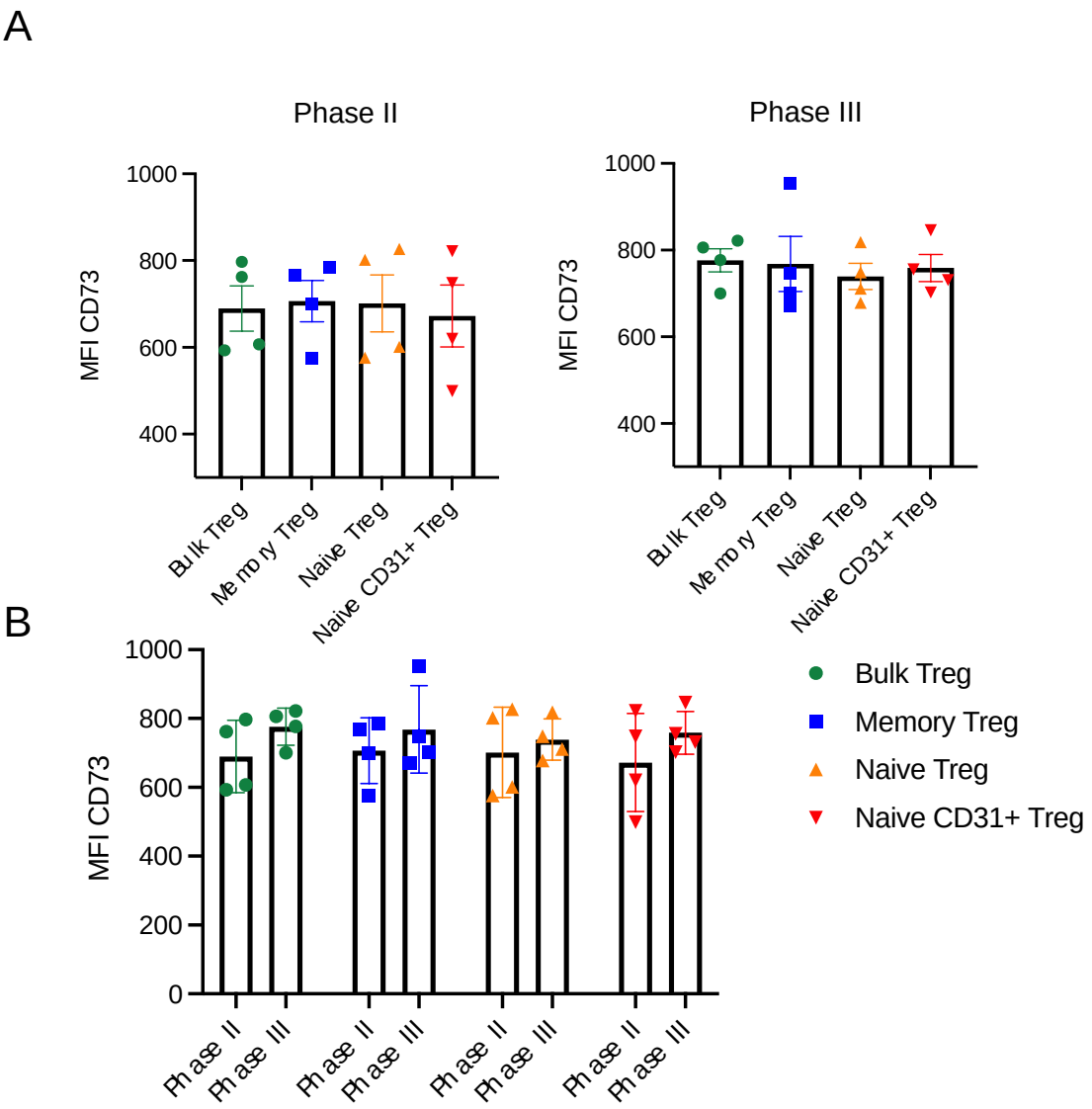

Figure 4.15: Level of CD73 expression was unchanged at days 28 and 42 of expansion of Treg subsets. Bulk Treg, Memory Treg, Naïve Treg, and Naïve CD31^{+} Treg subsets were FACS sorted and expanded in culture for 42 days using anti-CD3/CD28 beads, IL-2, and rapamycin. At days 28 (end of phase II) and 42 (end of phase III), an aliquot of each subset was rested in media without IL-2 for 48 hours prior to immunofluorescent staining. Cells were then stained and data were acquired on a BD LSR Fortessa. Statistical significance between groups at each timepoint was evaluated by one-way ANOVA with a Turkey's post-hoc test (A) or Šídák's multiple comparisons test (B) (no significant differences observed). Error bars show mean +/- SEM (n=4). MFI= mean fluorescence intensity.

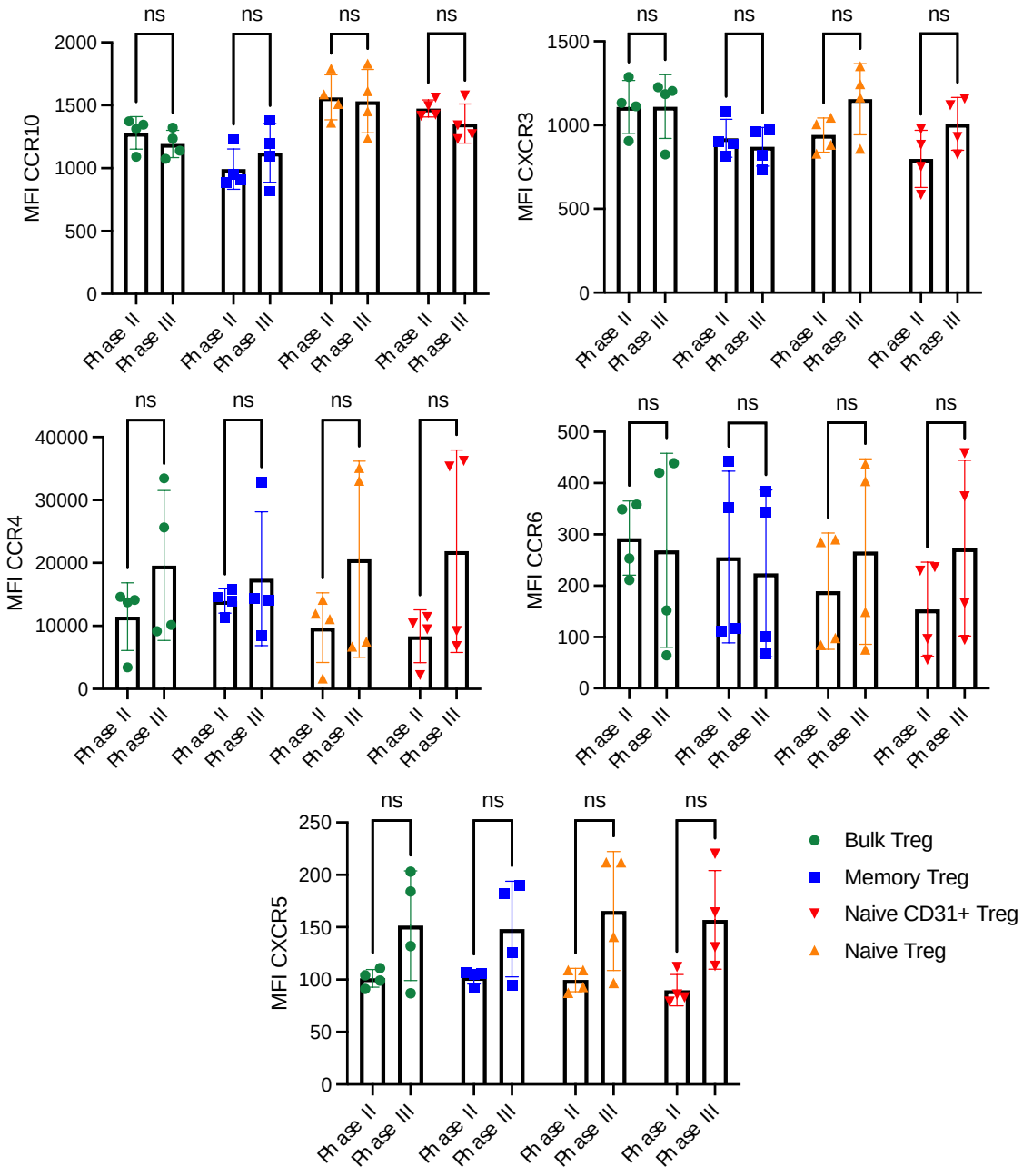

Figure 4.16: Level of CCR10, CXCR3, CCR4, CCR6, and CXCR5 expression was unchanged at days 28 and 42 of expansion of Treg subsets. Bulk Treg, Memory Treg, Naïve Treg, and Naïve CD31^{+} Treg subsets were FACS sorted and expanded in culture for 42 days using anti-CD3/CD28 beads, IL-2, and rapamycin. At days 28 (end of phase II) and 42 (end of phase III), an aliquot of each subset was rested in media without IL-2 for 48 hours prior to immunofluorescent staining. Cells were then stained and data were acquired on a BD LSR Fortessa. Statistical significance between groups at each timepoint was evaluated by oneway ANOVA with a Šídák's multiple comparisons test (no significant differences observed). Error bars show mean +/- SEM (n=4). MFI= mean fluorescence intensity.

We observed differences in expression of markers of naivety/memory even after cells had been expanded through three phases of expansion with anti-CD3/CD28 beads. As shown in figure 4.17, naïve and naïve CD31$^+$ Tregs continued to express significantly higher CD45RA than both bulk Tregs and memory Tregs at the end of phase II of expansion. There was no significant difference in CD45RA expression between naïve and naïve CD31$^+$ Tregs. Expanded bulk Tregs also expressed significantly higher CD45RA than expanded memory Tregs. At the end of phase III, all the significant differences described in CD45RA expression between Treg groups remained significant. As shown in figure 4.17, CD45RA expression fell significantly between the end of phase II to phase III expansion in the naïve and naïve CD31$^+$ Tregs. We then investigated whether naïve CD31$^+$ Tregs were able to maintain their phenotype during 3 phases of expansion.

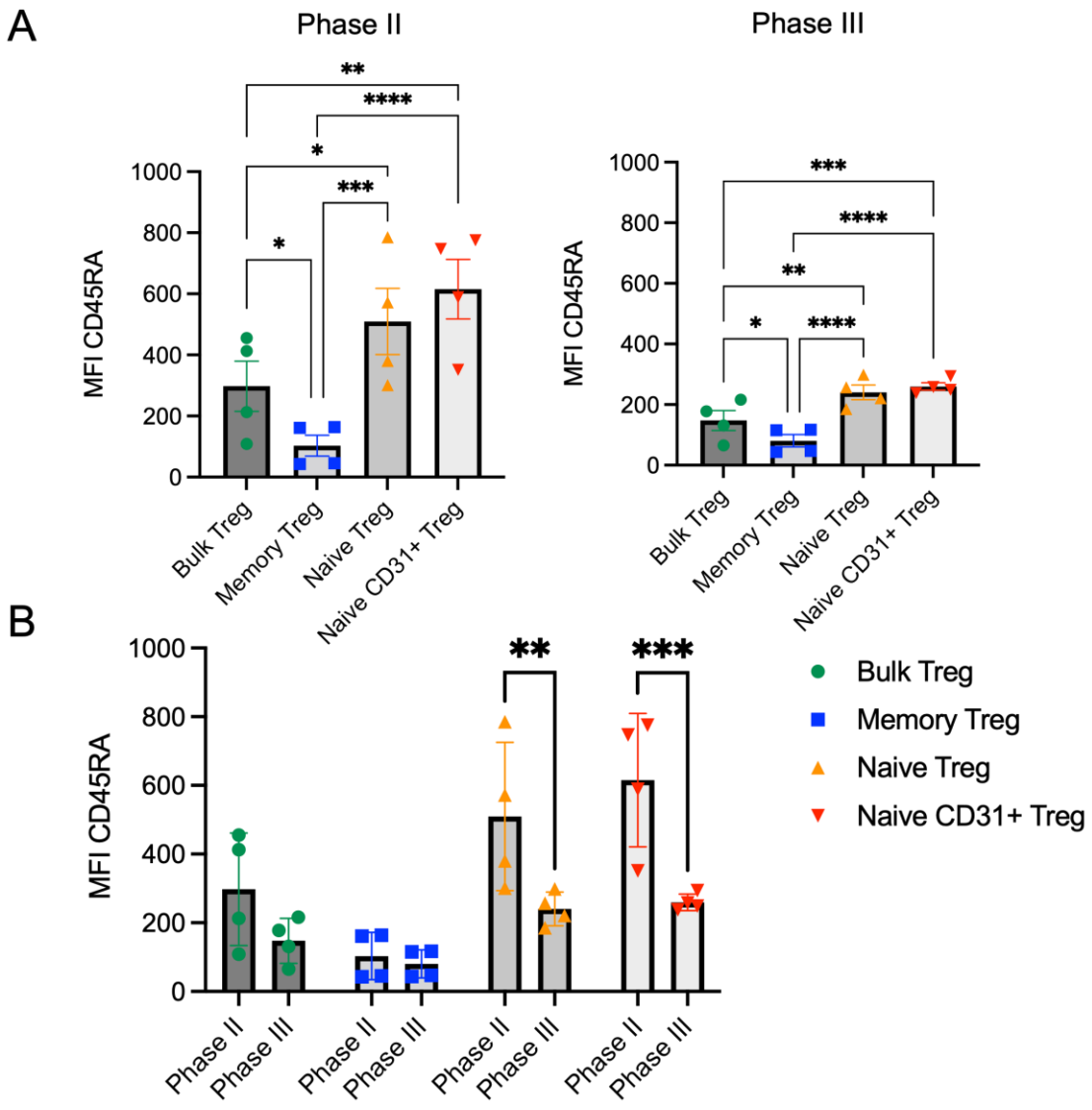

Figure 4.17: Expression of CD45RA remained highest in expanded naïve Treg subsets at days 28 and 42 of expansion but was significantly reduced within both naïve Treg subsets between these timepoints. Bulk Treg, Memory Treg, Naïve Treg, and Naïve CD31⁺ Treg subsets were FACS sorted and expanded in culture for 42 days using anti-CD3/CD28 beads, IL-2, and rapamycin. At days 28 (end of phase II) and 42 (end of phase III), an aliquot of each subset was rested in media without IL-2 for 48 hours prior to immunofluorescent staining. Cells were then stained and data were acquired on a BD LSR Fortessa. Statistical significance between groups at each timepoint was evaluated by one-way ANOVA with a Turkey's post-hoc test (A) or Šídák's multiple comparisons test (B). Error bars show mean +/- SEM (*= p < 0.05; **= p <0.01, ***= p <0.005, ****= p <0.0001) (n=4). MFI= mean fluorescence intensity.

As shown in figure 4.18 A, at the end of both phase II and phase III of expansion, naïve CD31$^+$ Tregs maintained the highest expression of CD31 compared to all other subsets including naïve Tregs, which represents the only significantly different surface feature between these two subsets during expansion. Expanded naïve Tregs also had a significantly higher expression of CD31 compared to both bulk Tregs and memory Tregs at the end of phase II, however these differences in expression had ceased by the end of phase III. As shown in figure 4.18 B, there was a significant decrease in expression of CD31 between phase II and phase III of expansion in both naïve subsets. The differences in CD45RA and CD31 expression between expanded Treg subsets is evident in figure 4.18 C which shows representative flow cytometry data from a single donor at the end of phase II of expansion. Finally, contrary to CD45RA expression, expanded memory Tregs expressed significantly higher levels of surface CD95 at the end of phase II of expansion compared to naïve and naïve CD31$^+$ Tregs (figure 4.19 A). Although there was a trend towards an increase in CD95 expression by naïve and naïve CD31$^+$ Tregs by the end of phase III which caused a loss in the significant differences seen in the phase II data, no Treg subsets experienced a significant change in CD95 expression between phases II and III of expansion (figure 4.19 B).

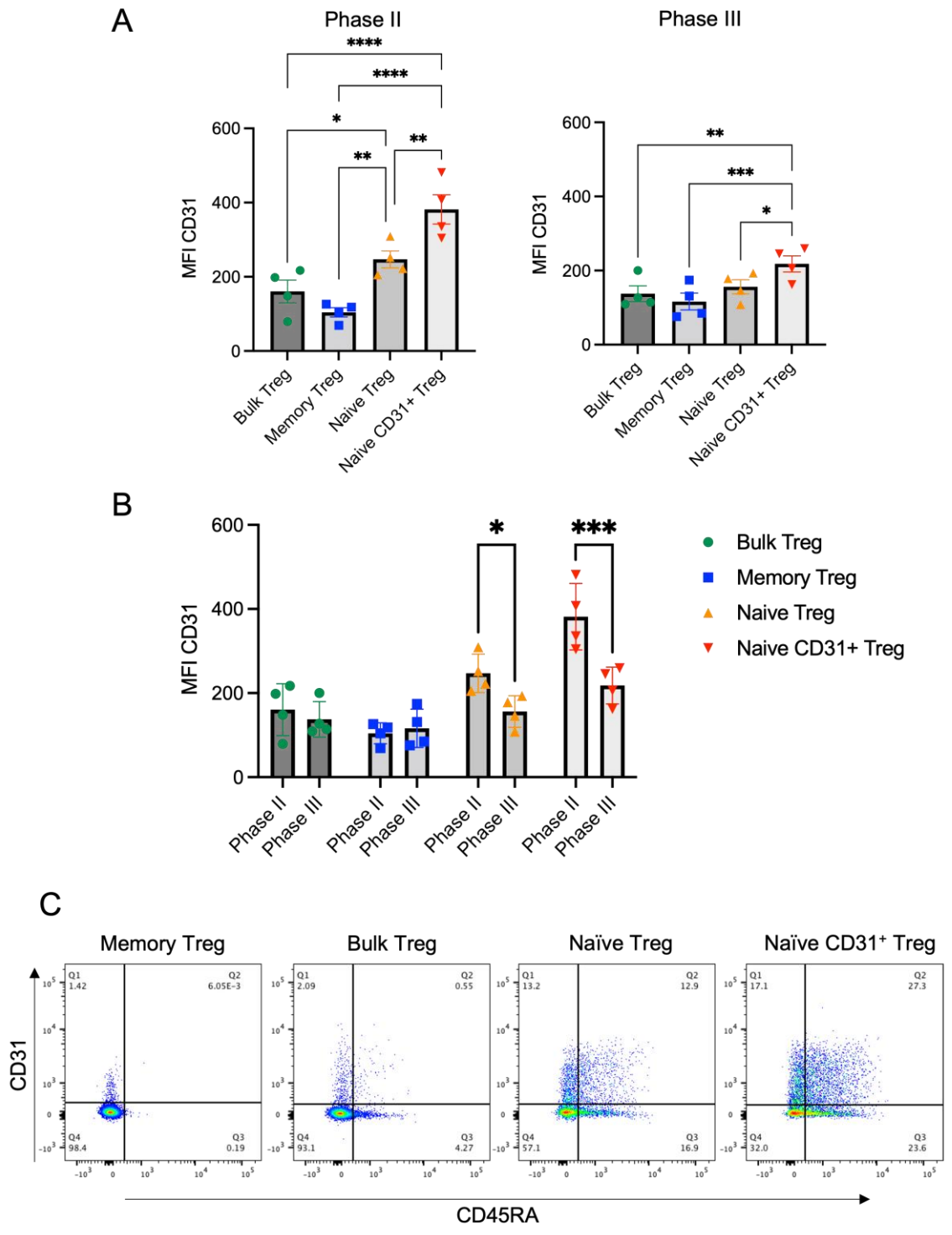

Figure 4.18: Expression of CD31 remained highest in the expanded naïve CD31 Treg subset at days 28 and 42 of expansion but was significantly reduced within both naïve Treg subsets between these timepoints. Bulk Treg, Memory Treg, Naïve Treg, and Naïve CD31⁺ Treg subsets were FACS sorted and expanded in culture for 42 days using anti-CD3/CD28 beads, IL-2, and rapamycin. At days 28 (end of phase II) and 42 (end of phase III), an aliquot of each subset was rested in media without IL-2 for 48 hours prior to immunofluorescent staining. Cells were then stained and data were acquired on a BD LSR

Fortessa. Statistical significance between groups at each timepoint was evaluated by one-way ANOVA with a Turkey's post-hoc test (A) or Šídák's multiple comparisons test (B). (C) Representative examples of flow cytometry data showing CD31 and CD45RA expression at the end of phase II of expansion. Error bars show mean +/- SEM (*= $p < 0.05$; **= $p < 0.01$, ***= $p < 0.005$, ****= $p < 0.0001$) (n=4). MFI= mean fluorescence intensity.

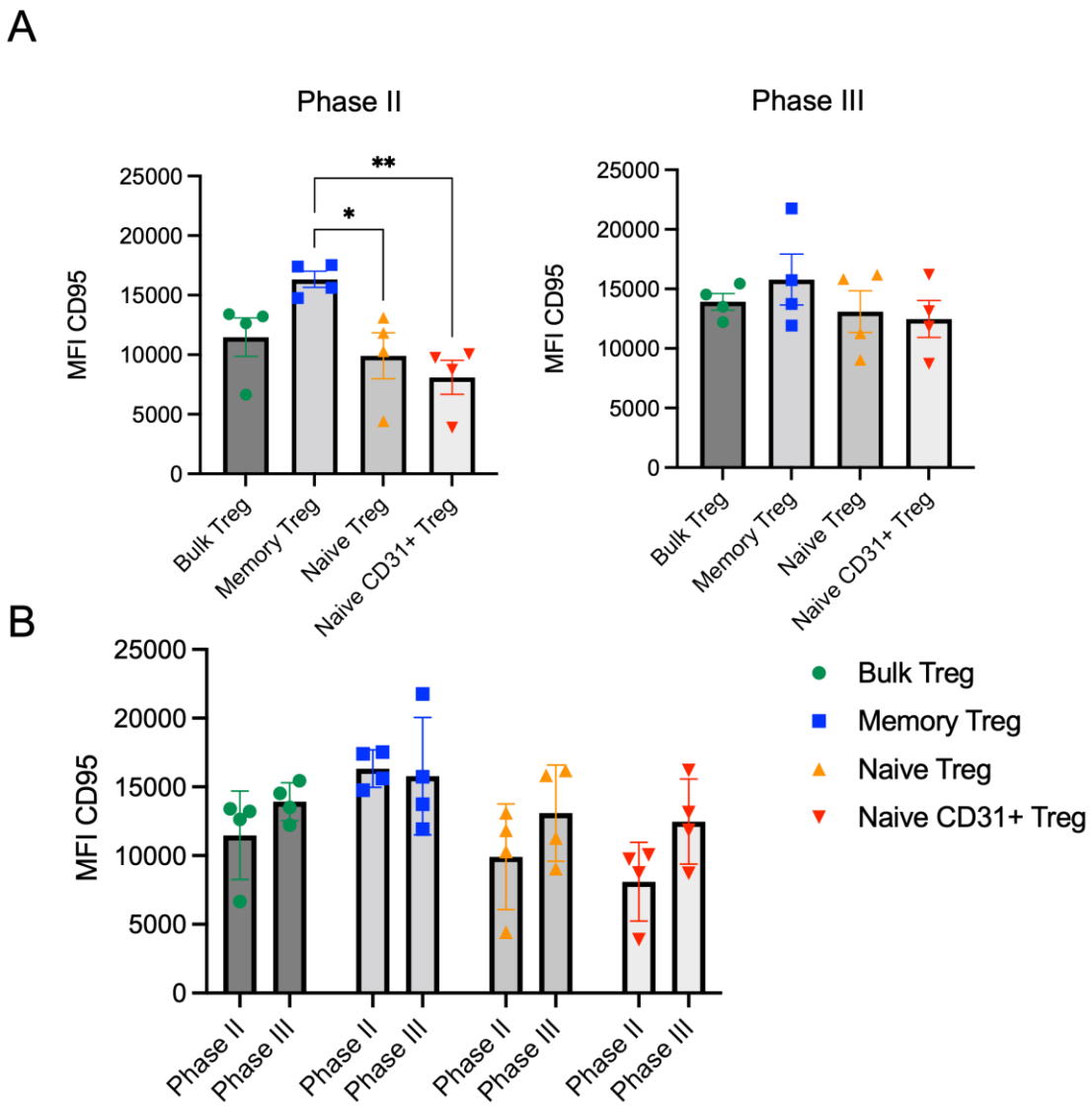

Figure 4.19: Level of CD95 was not significantly altered within subsets at days 28 and 42 of expansion of Treg subsets. Bulk Treg, Memory Treg, Naïve Treg, and Naïve CD31^{+} Treg subsets were FACS sorted and expanded in culture for 42 days using anti-CD3/CD28 beads, IL-2, and rapamycin. At days 28 (end of phase II) and 42 (end of phase III), an aliquot of each subset was rested in media without IL-2 for 48 hours prior to immunofluorescent staining. Cells were then stained and data were acquired on a BD LSR Fortessa. Statistical significance between groups at each timepoint was evaluated by one-way ANOVA with a Turkey's post-hoc test (A) or Šídák's multiple comparisons test (B). Error bars show mean +/- SEM (*= $p < 0.05$; **= $p < 0.01$) (n=4). MFI= mean fluorescence intensity.

As CD3/CD28 bead activation is a strong TCR stimulus, it could be expected that all naïve cells would have converted to memory status by the end of 3 phases of expansion. However, as shown in figure 4.17, some cells within the expanded naïve Treg subsets expressed high levels of CD45RA at the end of 6 weeks of culture, although the frequency of these cells was significantly reduced between the end of phase II and the end of phase III. We investigated this further by analysing the surface phenotype of the $CD45RA^{+}$ cells. Interestingly, as shown in figure 4.20 A, the $CD45RA^{+}$ cells were found co-expressing CD95, and no cells had a true naïve $CD45RA^{+}CD95^{-}$ surface phenotype. These $CD45RA^{+}CD95^{+}$ cells also co-expressed CCR4, a marker of antigen experience (B). As previously indicated, at the end of both phases II and III the $CD45RA^{+}CD95^{+}$ fraction was significantly higher in frequency in the naïve and naïve $CD31^{+}$ subsets compared to both memory and bulk Tregs, and bulk Tregs had a significantly higher frequency of these cells than memory Tregs (figure 4.20 C). However, of note, there was a significant decrease in frequency of these cells from the end of phase II to the end of phase III of expansion in the naïve and naïve CD31+ Tregs (D). In summary, expanded naïve Treg subsets had a prevailing fraction of cells which co-expressed markers of naivety and memory after 6 weeks of expansion, however this subset did appear to dilute in frequency by the end of the expansion process.

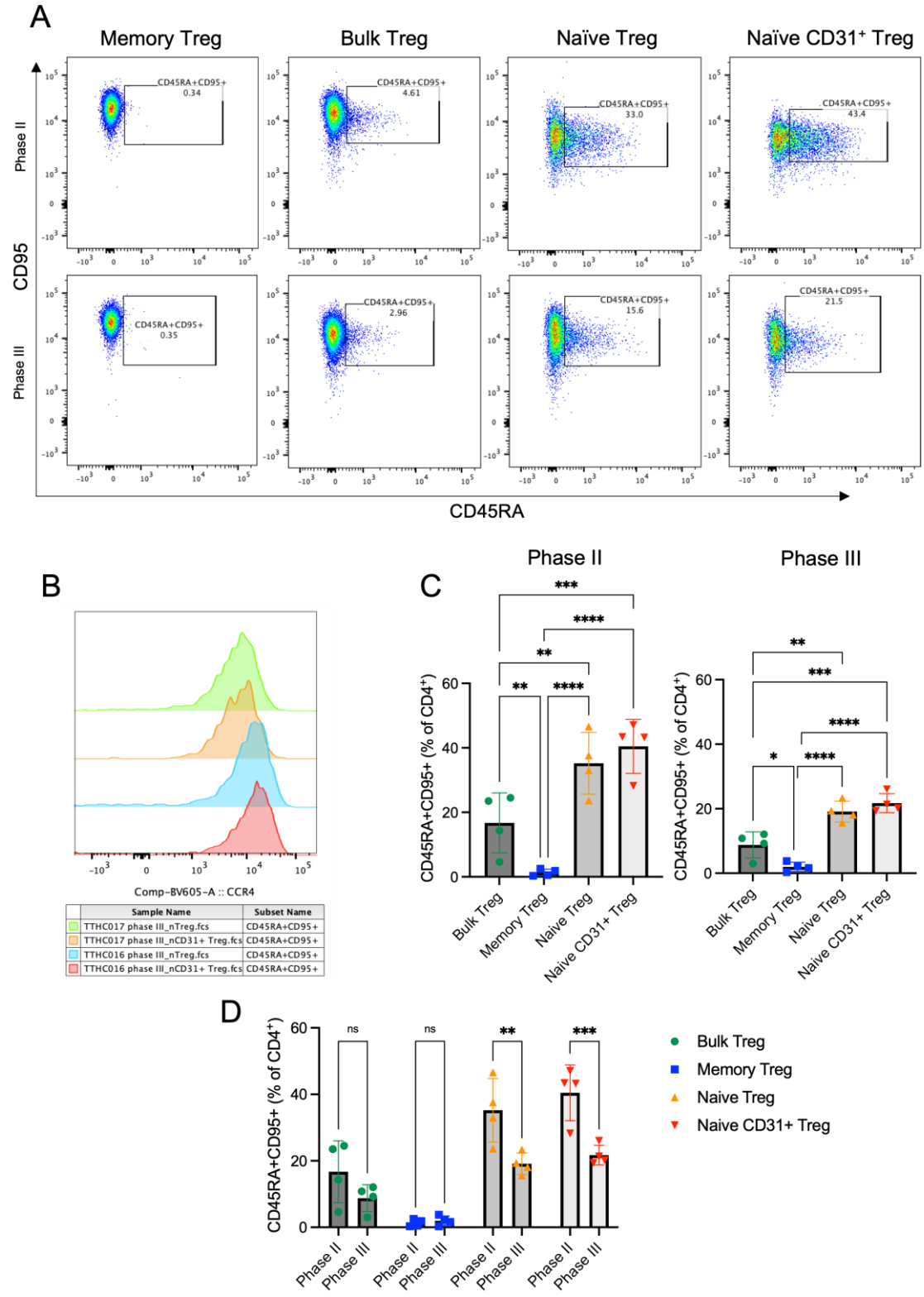

Figure 4.20: Expanded naïve and naïve CD31⁺ Tregs contained the highest frequency of CD45RA⁺CD95⁺ Tregs at days 28 and 42 of expansion of Treg subsets. Bulk Treg, Memory Treg, Naïve Treg, and Naïve CD31⁺ Treg subsets were FACS sorted and expanded in culture for 42 days using anti-CD3/CD28 beads, IL-2, and rapamycin. At days 28 (end of

phase II) and 42 (end of phase III), an aliquot of each subset was rested in media without IL-2 for 48 hours prior to immunofluorescent staining. Cells were then stained, and data were acquired on a BD LSR Fortessa. Statistical significance between groups at each timepoint was evaluated by one-way ANOVA with a Turkey's post-hoc test or Šídák's multiple comparisons test (A) representative data showing CD45RA and CD95 expression in expanded Treg subsets. (B) MFI of CCR4 in expanded naïve and naïve CD31+ Tregs from two donors. (C) Differences in the frequency of CD45RA+CD95+ cells between expanded subsets at phase II and phase III of expansion. (D) Differences in the frequency of CD45RA+CD95+ cells within expanded subsets at phase II and phase III of expansion. Error bars show mean +/- SEM (*= $p < 0.05$; **= $p < 0.01$, ***= $p < 0.005$, ****= $p < 0.0001$) (n=4). MFI= mean fluorescence intensity.

4.4 Discussion

Treg expansion is an essential step in preparing Tregs for therapeutic purposes and expansion protocols have been optimised to yield the greatest number of pure Tregs possible (Fraser et al., 2018; Sawitzki et al., 2020). In the previous chapter, we showed that naïve $CD31^+$ Tregs had superior *in vitro* suppressive capacities compared to bulk and memory Tregs. Previous reports have suggested that memory Tregs consisting of helper-like phenotypes are phenotypically unstable upon expansion and have a potential to convert into pathogenic Tconv cells (Canavan et al., 2016; Miyara et al., 2009). Previous studies have also shown that upon expansion, $CD45RA^+$ Tregs had better FoxP3 stability than memory $CD45RA^-$ Tregs (Canavan et al., 2016; Hoffmann et al., 2006). Therefore, in this chapter we aimed to investigate whether pure populations of naïve $CD31^+$ Tregs could represent an even better candidate for Treg therapies than naïve Tregs, memory Tregs, or indeed bulk Tregs which contain on average only ~24% naïve Tregs (figure 3.6) and have been the most commonly used for Treg therapeutic trials to date.

The frequency of naïve Tregs in peripheral blood is a limiting factor of potentially using naïve and naïve $CD31^+$ Tregs as autologous therapies which make up only around 7% of total Tregs (figure 4.4). As shown in figure 4.6, naïve Tregs appeared to expand better when a higher starting number of cells was sorted on day 0 of expansion, suggesting that a more dense culture of cells during early stages of activation promotes expansion. This could be aided in future *in vitro* experiments by using v-bottom plates at the beginning of expansion rather than round-bottom to maximise contact between the cells.

In some donors, it was not possible to FACS sort 50,000 cells each of bulk Tregs, memory Tregs and naïve Tregs before running out of sample (figure 4.6). However, in other donors we found we were able to FACS sort approximately 40,000 cells each of bulk Tregs, memory Tregs, naïve Tregs and naïve $CD31^+$ Tregs (figure 4.8). This was presumably due to (as shown in chapter 3) the frequency of naïve Tregs being highly variable from donor to donor and it is known that the frequency of naïve Tregs decreases with age (reviewed by Salam et al., 2013). This large variation in the frequency of naïve Tregs could make it difficult to predict the required volume of blood needed to isolate and expand naïve Tregs from patients. The dose of Tregs used to date has varied significantly between different clinical trials from approximately $90x10^6$ cells (NCT03654040) to escalations of up to $5000x10^6$ cells (NCT02145325). However in this latter trial, cells were obtained from patients by leukapheresis and cryopreserved prior to Treg expansion, giving the opportunity to obtain high cell numbers (Mathew et al., 2018). Alternatively, Tregs can also be cryopreserved post-expansion (Fraser et al., 2018), which would allow for multiple bleeds to be taken from a single

patient at different timepoints. Additionally, a recent study by MacDonald et al. (2019) which tested various GMP-compliant protocols showed that expanded Tregs cryopreserved shortly after restimulation were more viable and expressed higher FoxP3 upon thawing than those frozen at the end of a stimulation phase. These protocols could potentially overcome the issue of generating enough FoxP3^{hi} expanded cells from a rare starting subset of Tregs.

As shown in figure 4.7, addition of rapamycin to the Treg culture media helped to maintain a higher frequency of FoxP3^{+} Tregs with fewer CD127^{+} cells than without rapamycin over a 14-day expansion period. This stark difference in the frequency of cells with a Treg-like phenotype at the end of expansion perhaps explains why earlier studies in which Tregs were expanded without rapamycin suggested that Tregs could not be expanded for longer than two weeks without losing their phenotype (Marek et al., 2011). The preservation of Treg markers as seen in figure 4.7 could either mean that outgrowth of Tconvs was being suppressed or that rapamycin was inducing or maintaining a more Treg-like phenotype in the expansion product, or that both processes were happening simultaneously. A study by Valmori et al. (2006) showed that Tconvs expanded in the presence of rapamycin took on a phenotypic and functionally suppressive phenotype, rather than rapamycin selectively allowing for expansion of Tregs. However, although rapamycin seemed to induce a higher frequency of FoxP3^{+} and CD25^{hi}CD127^{low} cells in both the expanded Tconvs and Tregs, Helios expression was maintained to a much higher level in Tregs but was not highly induced in the expanded Tconvs. This suggests that contrary to the findings of Valmori et al. (2006), there were phenotypic differences between Tconvs and

Tregs cultured in the presence of rapamycin. The phenotype stability of Tregs at the terminal stage of *ex vivo* expansion is usually assessed via the frequency of $FoxP3^+$ cells and epigenetic analysis of Treg-specific demethylated regions (TSDR), however Helios is rarely used as a quality control marker (Bluestone et al., 2015a; Landwehr-Kenzel et al., 2018; Mathew et al., 2018). As we have shown that expanded Tconvs can display a $CD25^{hi}CD127^{low}FoxP3^+$ phenotype, *bona fide* Tregs which do not express Helios could be indistinguishable from these contaminating Tconvs. Therefore, the frequency of $FoxP3^+Helios^+$ cells could be a better estimate of pure Treg populations within expanded cultures, although this would exclude *bona fide* Tregs which are $Helios^-$, further limiting the number of passable expanded cells.

Our optimisation data from figure 4.6 suggested that naïve Tregs from this donor had a higher expansion potential than memory and bulk Tregs over a 26-day period. When expanding bulk Tregs, memory Tregs, naïve Tregs, and naïve $CD31^+$ Tregs, as shown in figure 4.8, although at day 14 and day 42 there was a trend towards naïve $CD31^+$ Tregs having the highest expansion potential, there were no significant differences in expansion potential between groups and all groups expanded well. Importantly, neither CD31 nor naïve status appeared to give an expansion advantage over other subsets. In a study by Scottà et al. (2013), a comparison was made between the expansion potentials of the 3 Treg subsets described by Miyara et al. (2009); $CD4^+CD25^+CD45RA^+$ naïve Tregs (fraction I), $CD4^+CD25^{hi}CD45RA^-$ memory Tregs (fraction II), and $CD4^+CD25^+CD45RA^-$ cytokine producing non-suppressive Tregs (fraction III). When expanded in the presence of rapamycin, the authors saw no expansion at

all in the memory fraction II Tregs, which is contrary to our results. One explanation for this could be that in this paper, the authors selected only the cells expressing the highest levels of CD25 when FACS sorting memory fraction II Tregs, which may have included more terminally differentiated and anergic cells. In our data shown in figure 4.8 C, there was a trend towards memory Tregs having less expansion potential than other subsets, however when FACS sorting memory and naïve subsets, we did not include CD25 expression to differentiate these subsets (figure 4.4). The authors showed that fraction I naïve Tregs and III $CD25^{+}CD45RA^{-}$ Tregs both expanded well, and therefore it is likely that our memory population consisted of a mixture of fraction II and fraction III memory Tregs. In support of this, a later study by the same group reported no difference in fold expansion between $CD4^{+}CD25^{hi}CD127^{lo}CD45RA^{+}$ naïve and $CD4^{+}CD25^{hi}CD127^{lo}CD45RA^{-}$ memory subsets after 12 days of expansion (Canavan et al., 2016), and similar results were found by Hoffmann et al. (2006) in the absence of rapamycin. Finally Scottà et al. (2013) also saw a significant expansion advantage of naïve Tregs compared to memory Tregs in the first 7 days of expansion, however this significant difference was lost after this period, and a similar trend was seen in our data (figure 4.8).

Although the surface phenotype of isolated Treg subsets does not appear to change the expansion potential of these subsets over several phases of expansion, previous literature is in agreement that expanded naïve Tregs maintain a higher frequency of $FoxP3^{hi}$ cells than memory Tregs (Canavan et al., 2016; Hoffmann et al., 2009, 2006). Our data in figures 4.10 and 4.11 therefore investigated whether the intracellular phenotype differed between naïve and

memory Tregs, and indeed whether naïve CD31$^+$ Tregs maintained an even better FoxP3$^+$ and Helios$^+$ phenotype during expansion. At the end of phase I we saw a significantly higher frequency of FoxP3$^+$ Tregs in both naïve and naïve CD31$^+$ Tregs compared to memory. This significant increase prevailed when comparing naïve CD31$^+$ and memory Tregs after the second phase of expansion, however by the end of phase III there was no difference in FoxP3$^+$ cell frequency between the groups. These results support the findings from previous studies that using only the naïve Treg fraction may yield a higher frequency of FoxP3^{hi} Tregs, however there seemed to be no particular advantage of selecting for naïve CD31$^+$ Tregs compared to naïve Tregs as no significant differences in FoxP3 were seen between these groups.

The percentage of FoxP3$^+$ cells also appeared to be stable throughout the expansion process with no significant differences occurring when comparing different expansion timepoints within subset groups (figure 4.11 A). Interestingly, when comparing the frequency of FoxP3$^+$ cells between expanded naïve and memory Tregs, Canavan et al., (2016) found that although the mean % of FoxP3$^+$ cells was similar, there were Tregs from more individual donors which lost FoxP3 expression in the memory Treg expansions. Our data in figure 4.11 seems to suggest that this also occurred in some donors in the expanded bulk Treg and memory populations, and to a lesser extent in the naïve Tregs although more replicates would be needed to confirm this. However, in the expanded naïve CD31$^+$ cells, all donors maintained high FoxP3 expression. Despite this promising data, it is clear from our optimisation data shown in figure 4.7 that Tconvs expanded in the presence of rapamycin can consist of ~30% FoxP3$^+$

cells, however it is unlikely that these cells would carry out suppressive functions *in vivo*. It is commonplace that the methylation status of the Treg TSDR is analysed in expanded Treg products and it has been shown that even when FoxP3 expression seems high, expanded memory Tregs can have a more methylated TSDR (Canavan et al., 2016; Hornero et al., 2017; Seay et al., 2016) Activated Tconvs expressing FoxP3 or Tregs with an unstable phenotype will not have a fully demethylated TSDR, meaning this is a more reliable indicator of a true Treg phenotype than frequency of FoxP3$^+$ cells (Baron et al., 2007; Hoffmann et al., 2009). Unfortunately, it was not possible to carry out TSDR analysis during the timeframe of this experimental chapter, however future work should aim to use both FoxP3 staining and TSDR methylation status to further elucidate whether naïve CD31$^+$ Tregs had a more stable Treg epigenetic status than other Treg subsets upon expansion. Also of note, this chapter would have benefited from a higher number of replicates throughout, however this was limited by a lack of access to human blood samples during the COVID pandemic, meaning previously banked PBMCs were relied upon for this work.

We showed in our data in figure 4.7 that despite an increase in FoxP3 expression, Helios expression was not substantially upregulated in Tconvs upon expansion with rapamycin. By the end of phase II of expansion, naïve CD31$^+$ Tregs had a significantly higher expression of Helios than all other subsets in which the frequency of Helios$^+$ cells had dropped significantly (figure 4.10 and figure 4.11B). This was the only parameter which was different in naïve CD31$^+$ Tregs compared to naïve Tregs. To explore this further, it is known that all thymically derived Tregs express Helios during development (Thornton et al., 2010) therefore it is to be

expected that naïve CD31^{+} RTE Tregs would express high levels of Helios at baseline, however it is encouraging to see that Helios expression does not drop significantly during the first two phases of expansion (figure 4.11). It is also known that Helios is expressed by a subset of Tregs which have superior TSDR demethylation, *in vitro* suppressive capacity, and *in vivo* FoxP3 stability than Helios^{-} Tregs, and gene expression analysis suggests that Helios^{-} Tregs are more similar to Tconvs (Thornton et al., 2019). Moreover, loss of Helios expression has been associated with full conversion to Tconvs under pro-inflammatory conditions (Nakagawa et al., 2016), which is especially concerning as enhanced systemic inflammation is observed in many autoimmune conditions which therapeutic Tregs aim to treat. This supports the notion discussed previously that FoxP3^{+}Helios^{+} Tregs in expanded populations may be a better indicator of stable Tregs.

Memory Tregs consistently had the lowest expression of Helios, which again suggests that this memory population may have a less stable Treg phenotype, therefore an interesting line of enquiry for future work would be to determine whether Helios expression correlates with Treg TSDR methylation in these subsets. The high FoxP3 expression but low Helios expression in memory Tregs may also denote a higher contamination of expanded Tconvs in this subset, as seen in chapter 3. Despite this, by the end of phase III of expansion, Helios expression had diminished significantly in all subsets (figure 4.11). In support of this, a recent study by Ou et al. (2021) showed that multiple rounds of TCR stimulation during Treg expansion lead to progressive methylation of the gene *IKZF2*, which encodes Helios. This may indicate that 3 phases of expansion may

be too long to keep a stable Treg phenotype in any of the subsets. Undoubtably, the data in this chapter would have been strengthened by a comparison of functional suppression by the Treg subsets at different stages of expansion as this would also have indicated the duration of expansion which gives the best suppressive phenotype, and future work should aim to explore this. In addition, analysis of inflammatory cytokines such as IFN-γ and IL-17 in the culture supernatant has been used by others as an indicator of potential loss of Treg suppressive stability and would be an informative line of enquiry for future work (Hoffmann et al., 2009; Scottà et al., 2013).

Finally, we saw significant differences in the expression of surface markers by the Treg subsets of interest during expansion, many of which were associated with a naïve/memory phenotype. This was surprising to us, as our original hypothesis was that by the end of 6 weeks of strong TCR stimulation and many rounds of division, all expanded subsets would have a fully-activated memory phenotype. Firstly, we saw that CD49d expression was higher in the expanded memory Tregs than the naïve subsets even after 6 weeks of expansion (figure 4.15). CD49d has been reported as denoting Tregs which produce inflammatory cytokines and have a poor suppressive capacity (Cuadrado et al., 2018; Kleinewietfeld et al., 2009). In light of our data in chapter 3, it is certainly true that CD49d can be highly expressed by T helper-like Treg subsets which have been shown to express activating cytokines (Duhen et al., 2012). However Cuadrado et al. (2018) also reported that CD49d and CCR4 expression are mutually exclusive in Tregs which was not seen in our data here or in chapter 3. Therefore, more research is needed to determine whether this marker has a functional role

in Tregs. A recent study by Jarvis et al. (2021) also showed that an increase in suppressive capacity post expansion was associated with a large increase in CD73 expression on the surface of Tregs compared to baseline. We saw no increase in CD73 expression between phase II and phase III, however acquiring Treg surface phenotype data from each donor at baseline may be informative in future experiments to address this.

Interestingly, we found that at the end of both phase II and phase III of expansion, naïve and naïve $CD31^+$ Tregs maintained higher expression of CD45RA than bulk Tregs or memory Tregs (figure 4.17) although the MFI of CD45RA did significantly decrease in both subsets between phase II and phase III. It is important to note that again there was no difference in the MFI of CD45RA between expanded naïve and naïve $CD31^+$ Tregs. As noted above, we anticipated that all subsets would take on a memory phenotype by the end of 6 weeks of expansion. Bluestone et al. (2015a) were able to track the phenotype of *ex vivo* expanded Tregs after infusion into patients by labelling the cells with deuterium allowing them to be distinguished from native Tregs. The authors observed that Tregs which were most frequent 91 days post-infusion were $CCR7^+CD45RA^+$ Tregs despite only a small number of Tregs being $CD45RA^+$ on the day of infusion. This could either suggest CD45RA re-expression or that the small number of naïve Tregs survived better *in vivo*, therefore it is encouraging that we saw a higher persistence of $CD45RA^+$ in the naïve subsets compared to bulk Tregs. Other studies have also demonstrated that expanded naïve Tregs can maintain expression of other markers associated with naivety such as CD62L and CCR7 (Canavan et al., 2016; Fraser et al., 2018; Hoffmann et al., 2006). As

well as maintaining a CD45RA$^+$ phenotype, naïve CD31$^+$ Tregs were also seen to maintain higher levels of CD31 during expansion than any other subset. As we suspect from our results in chapter 3 and other studies (Henshall et al., 2001; Ma et al., 2010) that CD31 may have its own intrinsic regulatory properties, persistence of CD31 through expansion may support Treg mediated suppression in the expanded product, however more research is needed to confirm this. We also saw a significant reduction in CD31 and Helios expression in this subset between phase II and III of expansion, and therefore future experiments could explore whether there is a correlation between these markers during expansion.

Finally, we observed that naïve Tregs had also upregulated CD95 during the course of expansion, and almost all cells which expressed CD45RA were found to be co-expressing CD95 (figure 4.20). These CD45RA$^+$CD95$^+$ cells were significantly more frequent in expanded naïve and naïve CD31$^+$ Tregs than in bulk and memory Tregs. As this phenotype had not previously been reported in expanded Tregs, we sought to understand what this phenotype could mean as our data in chapter 3 showed us that cells expressing high levels of CD45RA and CD95 are usually mutually exclusive. A brief search of current literature showed us that T cells co-expressing CD45RA and CD95 are found in the stem cell-like memory compartment in Tconvs (Gattinoni et al., 2011a), although this subset has not previously been reported in Tregs. From here we hypothesised that Tregs with a stem-cell like memory phenotype which can self-renew upon stimulation may be arising in our expanded Treg products. The data in the following results chapter investigated this further. It must be acknowledged that although the expression of CD45RA, CD95 and CD31 was higher in the naïve and naïve CD31

subsets, there was an evident drop in cells expressing this phenotype between phase II and phase III of expansion. This may be due to a residing population of naïve cells within these cultures remaining unstimulated during the course of expansion which were gradually activated during expansion. However, given the 6-week duration of expansion in constant contact with anti-CD3/CD28 beads, we feel that it is unlikely that ~20% of the cells would remain unstimulated by the end of phase III (figure 4.20 C). Another explanation could be that cells expressing this phenotype are less proliferative and were therefore gradually diluted out of the cultures when expanding cells were split and half of the cells were discarded. In future studies, analysis of TCR diversity within the expanded cell populations may also be informative. Using naïve and naïve $CD31^+$ Tregs as a starting material could potentially have given rise to a greater TCR diversity in the polyclonally expanded cell product than in memory and bulk Tregs which may contribute to a greater *in vivo* survival advantage.

To conclude, in this chapter we have shown that naïve $CD31^+$ Tregs have no expansion advantage over bulk Tregs, memory Tregs, or naïve Tregs. We saw no significant advantage of naïve $CD31^+$ Tregs compared to naïve Tregs or bulk Tregs in terms of FoxP3 expression, however this subset did have a higher frequency of $FoxP3^+$ cells compared to memory Tregs at the end of phases I and II of expansion. However, naïve $CD31^+$ Tregs had a higher frequency of $Helios^+$ Tregs than any other subset at the end of phase II of expansion, and Helios is thought to correlate with good suppressive capacity and Treg epigenetic stability. Finally, we observed a curious population of $CD45RA^+CD95^+$ cells which was prevalent within the expanded naïve and naïve $CD31^+$ Treg cultures. These cells

co-expressing these markers which typically denote naivety and memory, respectively are explored further in the following chapter.

5 Chapter 5. Investigation of Tregs with a stem cell-like memory phenotype

5.1 Introduction

During the Treg expansion experiments described in Chapter 4, we observed that at the terminal stage of a long expansion period of 6 weeks, a proportion of Tregs expanded from naïve Treg and naïve CD31$^+$ Treg subsets continued to express CD45RA, while expanded memory Tregs did not. This result helped to answer one of our research questions for this chapter which was whether cells expanded from different Treg subsets take on the same phenotype after multiple rounds of expansion, or whether some cells within the expanded cell product retained some of their original phenotype. Some of these expanded naïve Tregs co-expressed CD95 and CD45RA at the end of expansion and co-expression of markers of naivety and memory is reminiscent of stem cell-like memory T cells (Tscm) which have been reported in the CD4$^+$ and CD8$^+$ Tconv compartment.

Similar to stem cells within organs, stem cell-like memory immune cells are a distinct subset of memory T cell which can repopulate the pool of terminally differentiated cells while undergoing self-renewal to maintain a stem-like niche with longevity *in vivo.* Before the discovery of Tscm cells, the T cell compartment in humans was conventionally divided into naïve (T naïve; CD45R0$^-$ CCR7$^+$CD62L$^+$), central memory (T_{CM}; CD45R0$^+$CCR7$^+$CD62L$^+$) and effector memory (T_{EM}; CD45R0$^+$CCR7$^-$CD62L$^-$) T cells. A murine study was then the first to report a population of memory CD8$^+$ T cells which co-expressed a classically

naïve phenotype such as $CD44^{lo}CD62L^{hi}$ and expressed high levels of stem cell antigen-1 (Sca-1) Bcl-2, and the IL-2 receptor-β (Zhang, Joe, Hexner, Zhu, & Emerson, 2005). These cells showed self-renewal capacity, the ability to generate T_{CM} and T_{EM} progeny, and transferred GvHD to into recipient mice.

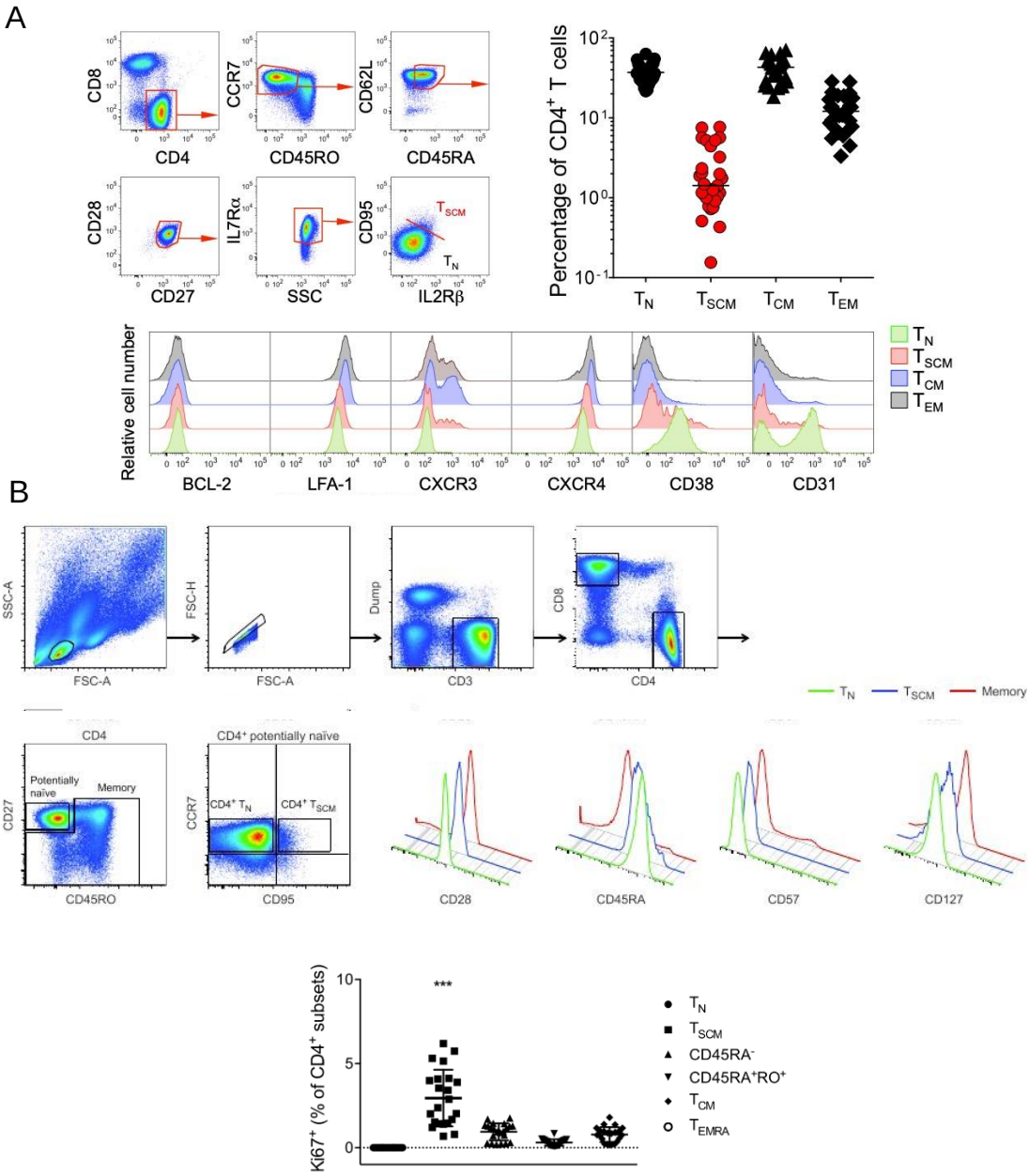

Figure 5.1: Stem cell-like memory CD4⁺ phenotype. (A) Flow cytometry data showing the phenotype of stem cell-like memory cells which have a self-renewing and rapid proliferative capacity, taken from Gattinoni et al. (2011). (B) Phenotype of stem cell-like memory CD4 T cells taken from Ahmed et al. (2016). These cells express a combination of naïve and memory markers on their cell surface but are negative for CD45R0 and are Ki67 positive when stained directly *ex vivo.*

A study by Gattinoni et al. (2011) then gave definitive evidence that Tscm cells also exist in the human T cell compartment. This study showed that both $CD4^+$ and $CD8^+$ T cells could be detected expressing a combination of naïve and memory markers such as CD45RA, CD62L, CD27, CCR7, CD95, CXCR3, CD28, but crucially did not express CD45R0, and this phenotype has been replicated in other studies such as (Ahmed et al., 2016) (figure 5.1). When measuring TCR rearrangement excision circles (TRECs) which are found at high levels in naïve T cells and diluted during expansion of memory cells, Tscm cells displayed significantly reduced TREC content compared to naïve T cells and showed proliferative capacity through Ki67 expression. Furthermore, unlike naïve T cells, these cells could rapidly secrete effector cytokines and proliferate upon stimulation with anti-CD3/CD28 beads or homeostatic cytokines. However, while generating memory cell progeny, some cells were able to renew and maintain their original Tscm phenotype (figure 5.2).

Subsequent studies have shown that yellow fever specific $CD8^+$ T cells phenotypically reminiscent of Tscm cells can be detected up to 25 years after yellow fever vaccination (Fuertes Marraco et al., 2015). Long-lived Tscm cells are also detectable in non-human primates and are induced during acute infection (Lugli, Dominguez, et al., 2013). Moreover, a study by Biasco et al. (2015) revealed that Tscm cells can persist for up to 12 years in immunodeficient patients after receiving haematopoietic stem cell transplants. Tscm cells may also play an important role in perpetuating autoimmune disease as the frequency of circulating Tscm cells which are reactive to autoantigens have been found to correlate with disease severity in RA (Cianciotti et al., 2020), aplastic anaemia,

autoimmune uveitis, and SLE (Hosokawa et al., 2016). Finally, a study by Scholz et al. (2016) has shown that $CD4^+$ Tscm cells can be induced *in vitro* by stimulating naïve cells with anti-CD3/CD28 beads in the presence of IL-2 and rapamycin, a method which is strikingly similar to the Treg expansion protocol used in chapter 3.

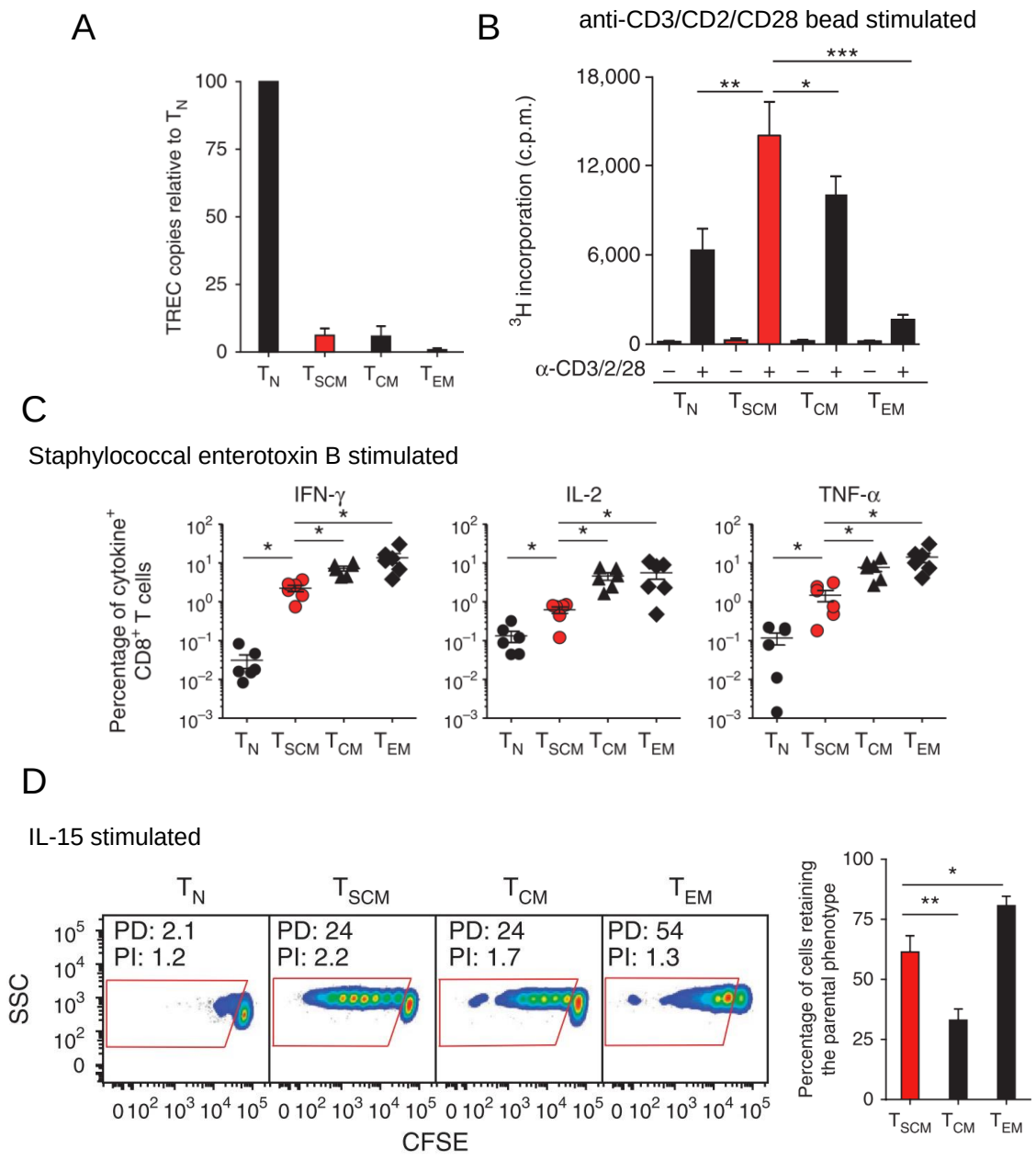

Figure 5.2: Stem cell-like memory T cell *in vitro* function. (A) Stem cell-like memory T cells (Tscm) which have a surface phenotype which is very similar to naïve T cells have significantly fewer TCR rearrangement excision circles (TRECs) than true naïve T cells. (B) Unlike naïve T cells, Tscm cells have a rapid *in vitro* proliferative capacity when stimulated with anti-CD3/CD2/CD28 beads. (C) Tscm cells stimulated with Staphylococcal enterotoxin B (SEB) can rapidly produce effector cytokines. (D) Homeostatic cytokines such as IL-15 cause a rapid proliferative response in Tscm compared to naïve T cells and these cells have a self-renewing capacity in that they maintained a $CCR7^+CD62L^+CD45RA^+CD45R0^-$ phenotype.

To date, Tscm cells have not been reported within the human Treg compartment. Given the extreme longevity of Tscm cells *in vivo* and their ability to produce functional progeny, it could be hypothesised that if cells akin to Tscm cells also occurred in the Treg compartment, these cells could make promising candidates for Treg cell therapies. This short, exploratory chapter of very preliminary results will therefore test the following hypotheses:

1. Cells with a stem cell-like memory phenotype can be found within the human Treg compartment.
2. Cells with a stem cell-like memory phenotype proliferate *in vitro* and can self-renew on expansion.

We aimed to optimise a flow cytometry panel which would identify Tscm cells expressing FoxP3 and Helios, and also to devise functional assays which could reveal stem cell-like memory properties in these cells.

5.2 Materials and methods

Buffers and media were prepared according to the methods described in Chapter 2. PBMC isolation, $CD4^+$ magnetic enrichment, cell cryopreservation and thawing were carried out according to the methods described in chapter 2.

5.2.1 Immunofluorescent staining for flow cytometry

For flow cytometry, up to $10x10^6$ PBMCs were transferred to 5ml FACS tubes and washed twice with DPBS. Pellets were resuspended and a 1μL/mL of solution of Live/Dead Aqua fixable cell stain (ThermoFisher) was added before incubating for 15 minutes at room temperature in the dark. Cells were then washed twice with FACS buffer and following pelleting by centrifugation at 400xg for 5 minutes, cells were resuspended and the first mastermix containing antibodies specific to chemokine receptors CCR7 BV711 and CXCR3 PE-Cy5 was added. Tubes were incubated at 37°C for 15 minutes. A second mastermix containing antibodies specific to other surface markers was then added and tubes were incubated for 30 minutes; CD8 BUV737, CD28 BUV563, CD45RA BUV395, CD127 BV786, CD45R0 BV650, CD27 BV605, CD95 PE-CF594, CD25 PE, CD4 AF700, CD62L APC-Cy7 (table 5.1). After centrifugation at 400xg for 5 minutes, cells were resuspended, and 1ml of fixation/permeabilisation buffer was added before incubating at room temperature for 40 minutes. Cells were washed twice with permeabilisation buffer, then a final mastermix containing antibodies specific to intracellular markers was incubated with the cells for 40 minutes at room temperature; FoxP3 AF647, Helios PE-Cy7, FITC Ki67. A final two washes in permeabilisation buffer were carried out, and cells were resuspended in FACS

buffer and kept on ice prior to acquisition. Data were acquired using a BD LSRFortessa analyser.

Table 5.1: Fluorochrome-conjugated monoclonal antibodies used to characterise stem cell-like memory T cells by flow cytometry

Fluorochrome	Marker	Clone	Supplier	μL/10x10^6 cells
Master Mix 1				
BV711	CCR7	G043H7	BioLegend	1
PE-Cy5	CXCR3	1C6/CXCR3	BD Biosciences	5
Master Mix 2				
BUV737	CD8	SK1	BD Biosciences	0.5
BUV563	CD28	L293	BD Biosciences	5
BUV395	CD45RA	HI100	BD Biosciences	0.5
BV786	CD127	HIL-7R-M21	BD Biosciences	2.5
BV650	CD45R0	UCHL1	BioLegend	2.5
BV605	CD27	L128	BD Biosciences	5
PE-CF594	CD95	DX2	BD Horizon	1
PE	CD25	2A3	BD Biosciences	5
PE	CD25	M-A251	BD Biosciences	5
AF700	CD4	OKT4	BioLegend	2
APC-Cy7	CD62L	DREG-56	BioLegend	5
Master Mix 3				
AF647	FoxP3	259D	Beckman Coulter	10
PE Cy7	Helios	22F6	BioLegend	2.5
FITC	Ki67	35/Ki-67	BD Biosciences	10

5.2.2 Fluorescence-activated cell sorting of T cell subsets

For cell sorting, cells were prepared similarly to the surface staining method described above. Briefly, thawed enriched $CD4^+$ T cells were washed twice with FACS buffer and pelleted by centrifugation. After resuspension, chemokine receptor-specific fluorescently-labelled monoclonal antibodies were incubated with the cells for 15 minutes at 37°C (Table 4.1). For this panel, this included CCR7 BV711 only. Following this, a second mastermix with the remaining surface antigen-specific antibodies was added and tubes were incubated at 4°C for 30 minutes. This mastermix consisted of CD45R0 BV650, CD27 BV605, CD127 PE-Cy5, PE-CF594 CD95, CD25 PE, and CD4 AF700. Finally, cells were washed twice in FACS buffer, and following centrifugation, cells were resuspended in FACS buffer and passed through a 35μm cell strainer cap into new polypropylene FACS tubes. Cells were stored on ice prior to FACS sorting on a BD FACSAria IIu cell sorter.

Table 5.2: Fluorochrome-conjugated monoclonal antibodies used in surface staining to FACS sort T cell subsets for proliferation and expansion experiments.

Fluorochrome	Marker	Clone	Supplier	μL/10x10^6 cells
Master Mix 1				
BV711	CCR7	G043H7	BioLegend	1
Master Mix 2				
BV650	CD45R0	UCHL1	BioLegend	2.5
BV605	CD27	L128	BD Biosciences	5
PE-Cy5	CD127	A019D5	BioLegend	2.5
PE-CF594	CD95	DX2	BD Horizon	1
PE	CD25	2A3	BD Biosciences	5
PE	CD25	M-A251	BD Biosciences	5
AF700	CD4	OKT4	BioLegend	2

5.2.3 Proliferation assays of T cell subsets

Enriched CD4$^+$ T cells were thawed and counted as described in chapter 2. Cells were collected into 50ml falcon tubes, washed twice with DPBS and centrifuged to pellet at 400xg for 5 minutes. Cells were then labelled with CellTrace violet (CTV) proliferation dye (Thermofisher) to measure proliferation by dye dilution. A 1μL/mL solution of CTV solution was prepared and incubated with the cells for 20 minutes at 37°C in a waterbath. Pre-warmed RPMI was then added and cells were pelleted by centrifugation at 400xg for 5 minutes. Cells were then resuspended in warm RPMI and tubes were incubated for a further 10 minutes in the waterbath to allow acetate hydrolysis to take place. At the end of this incubation, two washes were carried out using FACS buffer and cells were transferred to 5ml FACS tubes. Immunofluorescent staining of cell surface antigens was then divided into a 15-minute incubation at 37°C for CCR7 BV711,

and a 30-minute incubation with the remaining antibodies at 4°C; CD45R0 BV650, CD27 BV605, CD127 PE-Cy5, PE-CF594 CD95, CD25 PE, and CD4 AF700 (Table 5.2). Cells were then washed in FACS buffer and pelleted by centrifugation at 400xg for 5 minutes. Finally, cell pellets were resuspended in FACS buffer and passed through a 35μm cell strainer into polypropylene FACS tubes and kept on ice prior to cell sorting. FACS sorting was carried out on a BD FACSAria IIu cell sorter.

The following T cell subsets were subjected to FACS sorting; Tconvs: T_{CM}, T_{EM}, T naïve, Tscm; Tregs: T_{CM}, T_{EM}, T naïve, Tscm. 5000 cells per well of T cell subsets were sorted according to the sort strategy outlined in figure 5.7 directly in 96-well plates containing X-VIVO 15 culture media supplemented with 5% human AB serum. Cells were stimulated to proliferate with a 1:1 bead to cell ratio of anti-CD3/CD28 beads and cultured in X-VIVO 15 media containing 5% human AB serum and 100 U/ml of IL-2. Cells were then placed in an incubator and cultured for 5 days.

At day 5, cells from each T cell subset were harvested into individual FACS tubes. Following two washes in plain DPBS, viability staining was carried out by incubating the cells with a 1μL/mL solution of Live/Dead fixable near infrared cell stain for 15 minutes at room temperature in the dark. Surface staining using the same method as described for the first day of this assay was repeated. Data were then acquired using a BD LSRFortessa analyser.

5.2.4 Expansion of T cell subsets

For experiments testing the self-renewal capacity of Tscm cells, T cell subsets were expanded for 14 days to analyse whether a pool of cells FACS sorted on Day 0 as Tscm cells maintain their original phenotype. Following PBMC isolation and cryopreservation, thawed enriched $CD4^+$ T cells were washed twice in FACS buffer, and surface staining was carried out using the same method described in the above proliferation assay section (Table 5.2). Following surface staining, cells were washed twice with FACS buffer and pelleted by centrifugation. Finally, pellets were resuspended in FACS buffer, filtered through a 35μm cell strainer, and placed in polypropylene FACS tubes on ice before FACS sorting using a BD FACSAria IIu sorter.

Treg and Tconv T_{CM}, T_{EM}, T naïve, Tscm subsets were sorted using the gating strategy shown in figure 5.7. Up to 30,000 cells of each subset were sorted into FACS tubes containing culture media. Following sorting, tubes were centrifuged at 400xg for 5 minutes, and pellets were resuspended in the residual volume in the tubes after removing supernatants (~70μL) and counted using a Trypan blue counterstain and a haemocytometer. A 1:1 ratio of beads to cells was then added to tubes and a 5-minute pre-stimulation was carried out. Following this, each T cell subset was plated in a single well in 96-well round bottom plates and an equal volume of Treg feed media was added to each well. Half the media was replenished every 48 hours. As cells expanded, cells were transferred into 48, 24, and 12 well plates, then cells were split upon reaching 90% confluency.

At day 14, cells were harvested and washed twice with DPBS. Cells were then incubated with a 1μl/ml solution of Live/Dead fixable blue cell stain (ThermoFisher) for 15 minutes at room temperature in the dark. Two washing steps using FACS buffer were carried out before cells were subjected to cell surface staining. Firstly, the CCR7 BV711 antibody was added to tubes and a 15-minute incubation at 37°C followed. A mastermix containing the following antibodies was then added to each tube and cells were incubated at 4°C for 30 minutes; CD45RA BV786, CD45R0 BV650, CD27 BV605, CXCR3 BV510, CD127 PE-Cy5, CD95 PE-CF594, PE CD25, CD4 AF700, CD62L APC-Cy7 (Table 5.3). Cells were then washed twice in FACS buffer, pelleted by centrifugation, and fixed and permeabilised by incubating with 1ml of fixation/permeabilisation buffer for 40 minutes at room temperature. Following two washes in permeabilisation buffer and pelleting by centrifugation, pellets were then resuspended, and a third mastermix containing the following antibodies was incubated with the cells for 40 minutes at room temperature in the dark; FoxP3 AF647, Helios PE-Cy7, Ki67 FITC (Table 5.3). Finally, cells were washed twice in permeabilisation buffer, and cells were resuspended in FACS buffer prior to acquisition using a BD LSRFortessa.

Table 5.3: Fluorochrome-conjugated monoclonal antibodies used to analyse the phenotype of 14-day expanded T cell subsets

Fluorochrome	Marker	Clone	Supplier	µL/10x10^6 cells
Master Mix 1				
BV711	CCR7	G043H7	BioLegend	1
Master Mix 2				
BV786	CD45RA	HI100	BioLegend	0.5
BV650	CD45R0	UCHL1	BioLegend	2.5
BV605	CD27	L128	BD Biosciences	5
BV510	CXCR3	G025H7	BioLegend	2
PE-Cy5	CD127	A019D5	BioLegend	2.5
PE-CF594	CD95	DX2	BD Horizon	1
PE	CD25	2A3	BD Biosciences	5
PE	CD25	M-A251	BD Biosciences	5
AF700	CD4	OKT4	BioLegend	2
APC-Cy7	CD62L	DREG-56	BioLegend	5
Master Mix 3				
AF647	FoxP3	259D	Beckman Coulter	10
PE Cy7	Helios	22F6	BioLegend	2.5
FITC	Ki67	35/Ki-67	BD Biosciences	10

5.2.5 Data analysis

Flow cytometry data in this chapter was all preliminary and derived from a single donor per experiment, therefore no statistical analysis was carried out. Flow cytometry data were analysed using FlowJo 9 software. Flow cytometry data from day 14-expanded T cell subsets was analysed in OMIQ software.

5.3 Results

5.3.1 Cells with a stem cell-like memory phenotype exist in the Treg compartment

Firstly, we aimed to optimise a flow cytometry panel which would allow us to identify whether $CD4^+$ T cells with a phenotype akin to stem cell like memory cells described in publications such as Gattinoni et al. (2011) and Ahmed et al. (2016) also occurred in the Treg compartment. We first compiled a list of definitive Tscm markers from these two publications (table 5.3) and then designed a 16-colour flow cytometry panel including markers to identify Tregs such as CD25, CD127, FoxP3, and Helios (table 5.1).

Table 5.3: Markers used to define T stem cell-like memory cells by Gattinoni et al. (2011) and Ahmed et al. (2016).

Tscm marker	+ or – on Tscm	Used in Gattinoni *et al.* (2011)?	Used in Ahmed *et al.* (2011)?
CD4	+	✓	✓
CD8	+	✓	✓
CD45RA	+	✓	✓
CD45R0	-	✓	✓
CCR7	+	✓	✓
CD27	+	✓	✓
CD28	+	✓	✓
CD122	+	✓	
CD95	+	✓	✓
CD62L	+	✓	
CXCR3	+	✓	✓
Ki67	+		✓

We devised a gating strategy based on those used in the aforementioned publications which would allow us to identify stem cell-like memory $CD4^+$ T cells. These cells express a mixture of naïve and memory markers resulting in a $CD4^+CCR7^+CD45R0^-CD62L^+CD45RA^+CD27^+CD28^+CXCR3^+CD95^+$ phenotype, the most important factors being co-positivity for CD45RA and CD95 and being negative for CD45R0 expression. In the Gattinoni et al. (2011) paper, the authors gated on CD127 (IL-7-receptorα) positive cells, however we reasoned that we could not use the $CD127^+CD95^+$ fraction of cells to investigate Tscm Tregs as all Tregs should express low levels of CD127. Therefore, we instead gated on the $CXCR3^+CD95^+$ fraction, as Tscm were also described as being $CXCR3^+$ in this paper (shown in figure 5.1). As shown in figure 5.3, this gating strategy could be

used to identify T_{CM} and T_{EM} cells, which have a $CD45R0^{+}CCR7^{+}$ and $CD45R0^{+}CCR7^{-}$ phenotype, respectively. Cells which are potentially naïve or 'naïve-like' were $CCR7^{+}CD45R0^{-}$ and this gate was named as such as it could contain both true naïve T cells and Tscm cells. After further gating on the $CD45RA^{+}CD62L^{+}$ cells and $CD27^{+}CD28^{+}$ cells, Tscm cells could be distinguished from true naïve cells as they expressed CD95 and CXCR3.

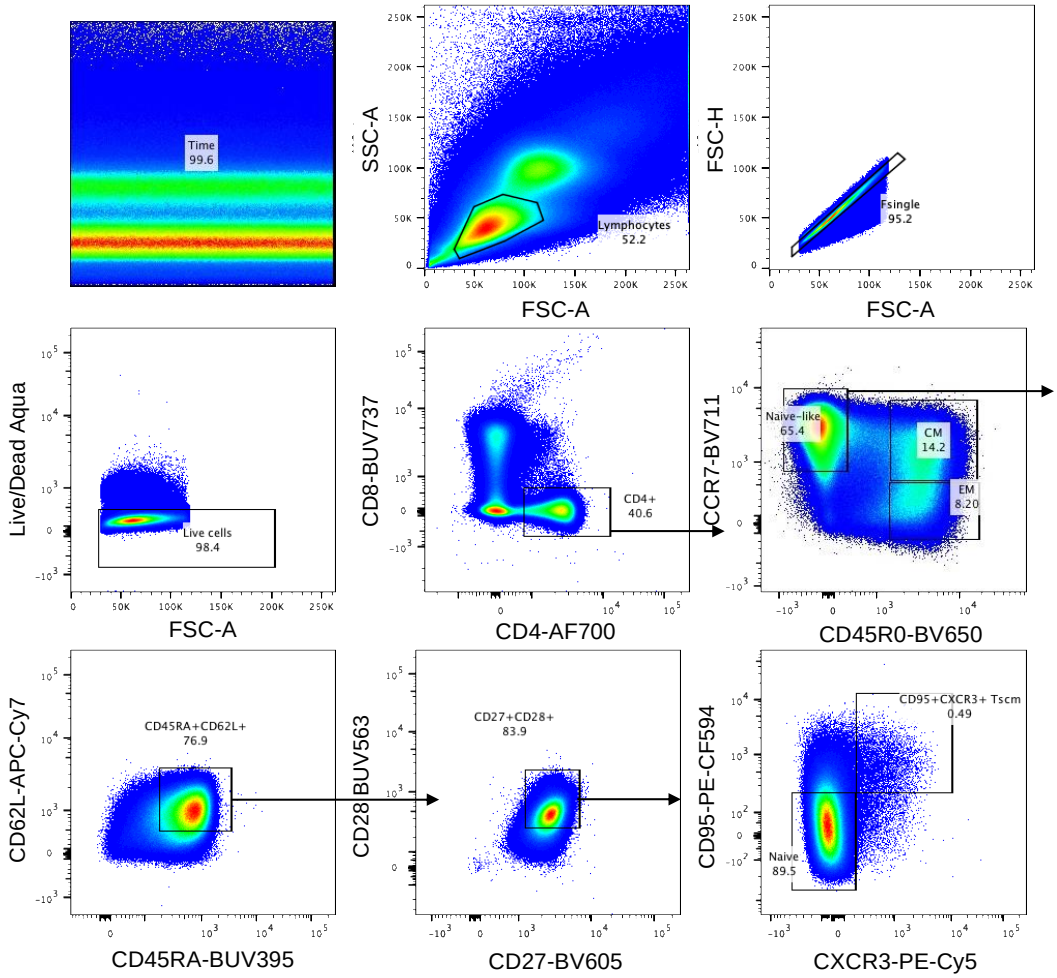

Figure 5.3: Initial gating strategy used to identify total CD4⁺ stem cell-like memory cells. Cryopreserved PBMCs from a healthy donor were stained with fluorochrome-conjugated antibodies and acquired for flow cytometric analysis using a BD LSRFortessa analyser. This gating strategy was designed using previously published literature and can be used to identify CD4⁺ central memory (CM), effector memory (EM), naïve, and stem cell-like memory (Tscm) cells.

From this total $CD4^+$ Tscm gate, we then looked for cells which had a Treg phenotype. As shown in figure 5.4 A, from within the $CD95^+CXCR3^+$ Tscm gate, we observed a population of cells which had a Treg phenotype. We trialled several common Treg gating methods such as $CD25^{hi}FoxP3^+$, $CD25^{hi}CD127^{low}$, and $FoxP3^+Helios^+$, although these cells occurred at a very low frequency of around 0.02% of total $CD4^+$ T cells in this donor. We could also identify Tscm cells by beginning with the $CD4^+CD25^{hi}FoxP3^+$ Treg gate (figure 5.4 B) which represented around 0.7% of Tregs in this same donor. This showed that Tregs with a Tscm-like surface phenotype existed in this donor.

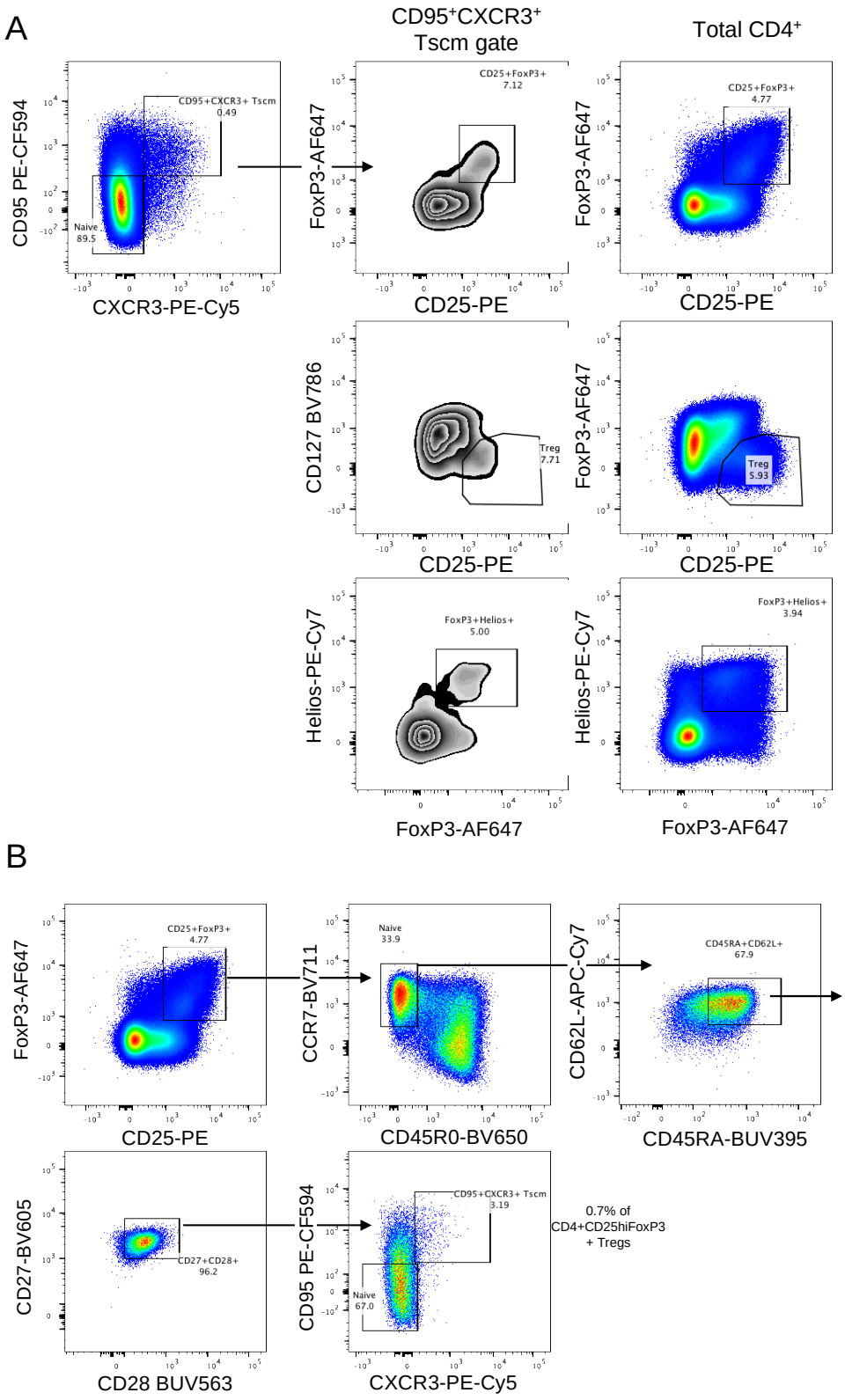

Figure 5.4: Initial gating strategy used to identify Tregs with a stem cell-like memory (Tscm) phenotype. Cryopreserved PBMCs from a healthy donor were stained with fluorochrome-conjugated antibodies and acquired for flow cytometric analysis using a BD LSRFortessa analyser. (A) Identifying Tregs from within the Tscm gate shown in figure 5.3. (B) Identifying Tscm-like cells from within the Treg $CD4^{+}CD25^{hi}FoxP3^{+}$ gate.

As Tscm cells are known to be proliferative *in vivo*, we also compared the frequency of Ki67$^+$ cells in T_{CM}, T_{EM}, T naïve, and Tscm cells within the Tconv and Treg compartments (figure 5.5). We found that *ex vivo* stained T_{EM} cells from both the Tconv at Treg compartment had the highest frequencies of Ki67$^+$ cells, followed by T_{CM} cells. In this donor, both T_{CM} and T_{EM} populations had a higher frequency of proliferating cells in the Treg compartment than in the Tconv compartment which aligns with previous reports showing that memory Tregs are highly proliferative *in vivo*, despite being anergic *in vitro*. As expected, the frequency of Ki67$^+$ cells within the naïve compartment was very low at 0.088% in Tconvs and 0.06% in Tregs. Interestingly, the frequency of Ki67$^+$ cells was higher in both the Tconv Tscm and Tregs with a Tscm-like phenotype compared to the naïve cells at 3.85% and 6% of Tscm-like cells, respectively. This suggests that although naïve and Tscm-like Tregs had a very similar surface phenotype, these cells may be functionally distinct *in vivo.* This phenotypic data points towards a stem cell-like memory phenotype within the Treg compartment, therefore next we aimed to investigate the *in vitro* function of these cells.

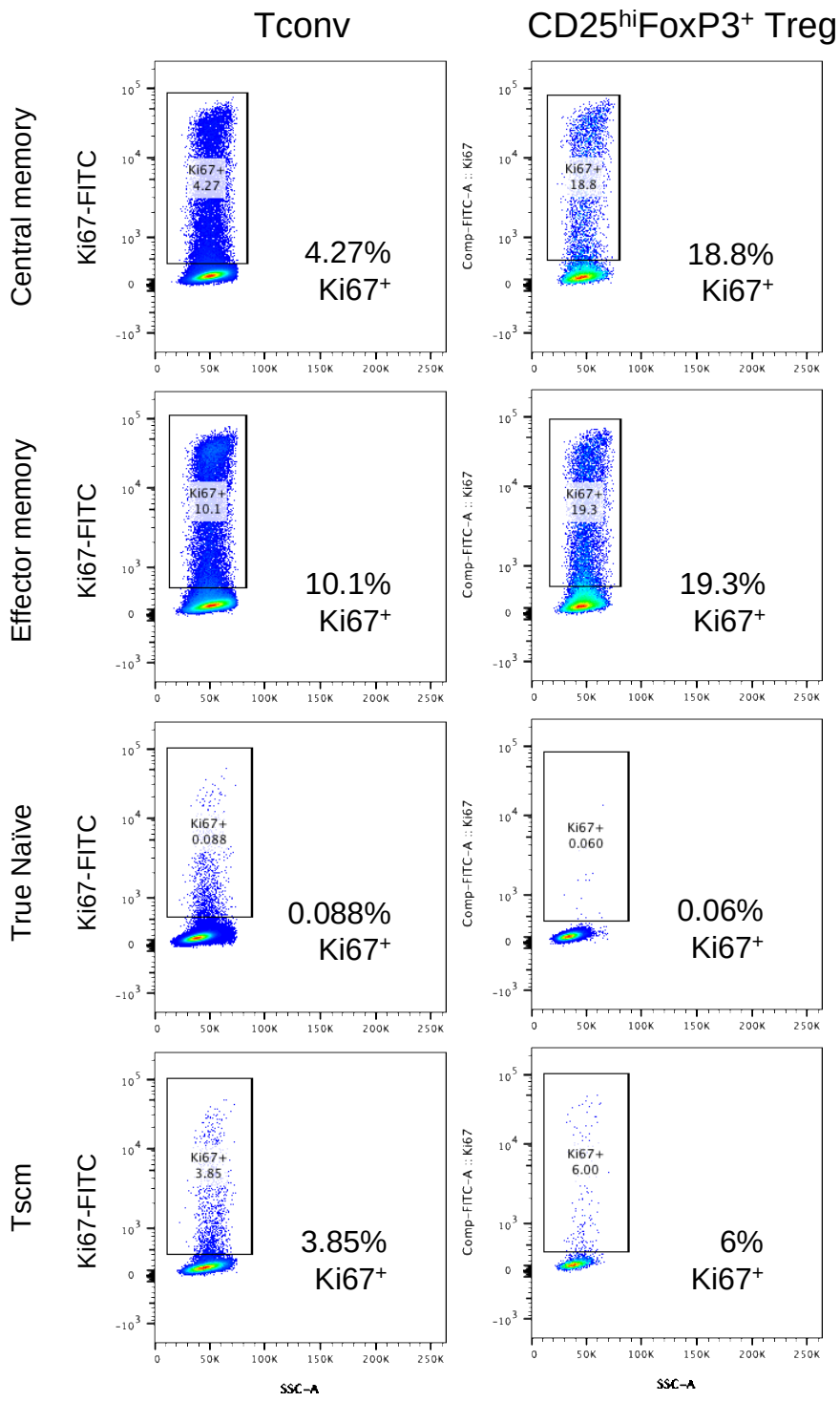

Figure 5.5: Ki67⁺ cells were more frequent in the gated stem cell-like memory (Tscm) Tconvs and FoxP3⁺ Tregs than in true naïve Tconvs and Tregs. Cryopreserved PBMCs from a healthy donor were stained with fluorochrome-conjugated antibodies and acquired for flow cytometric analysis using a BD LSRFortessa analyser. Ki67 staining was used to evaluate the percentage of proliferating cells within the central memory, effector memory, naïve, and T stem cell-like memory compartments of Tconvs (left panels) and Tregs (right panels).

5.3.2 Isolating stem cell-like memory Tregs for functional analysis

As described above, Tregs with a Tscm-like phenotype were identified using a 16-colour flow cytometry panel, however in order to isolate pure populations of T cell subsets by FACS sorting on a 4 laser BD FACS Aria-IIu, this would allow a maximum of 15 colours, however a maximum of 14 colours is recommended. Therefore, we investigated ways to reduce the number of markers in this original panel without affecting the purity of the T_{CM}, T_{EM}, T naïve, and Tscm populations. A methods paper by Lugli, Gattinoni, et al. (2013), from the same authors who published the first description of Tscm cells in humans (Gattinoni et al., 2011a), showed that a condensed flow cytometry panel could be used to identify and isolate Tscm cells to the same level of accuracy and with the same *in vitro* function as the larger original panel. Using this condensed panel, potential naïve cells gated as $CCR7^{+}CD45R0^{-}$ could be accurately divided into true naïve cells and Tscm cells using only either CD62L for fresh cells or CD27 for cryopreserved cells, and CD95. We applied this condensed gating strategy to our experiments (figure 5.6 A). From the naïve-like $CD27^{+}$ gate, Tscm cells could be identified by plotting CD95 against CCR7 as Tscm cells have slightly lower levels of expression of CCR7 than naïve T cells and observing CD95 vs CCR7 expression within total $CD4^{+}$ cells helped to set this gate accurately. From this Tscm gate using the condensed panel, cells with a Treg phenotype were again found (figure 5.6 B).

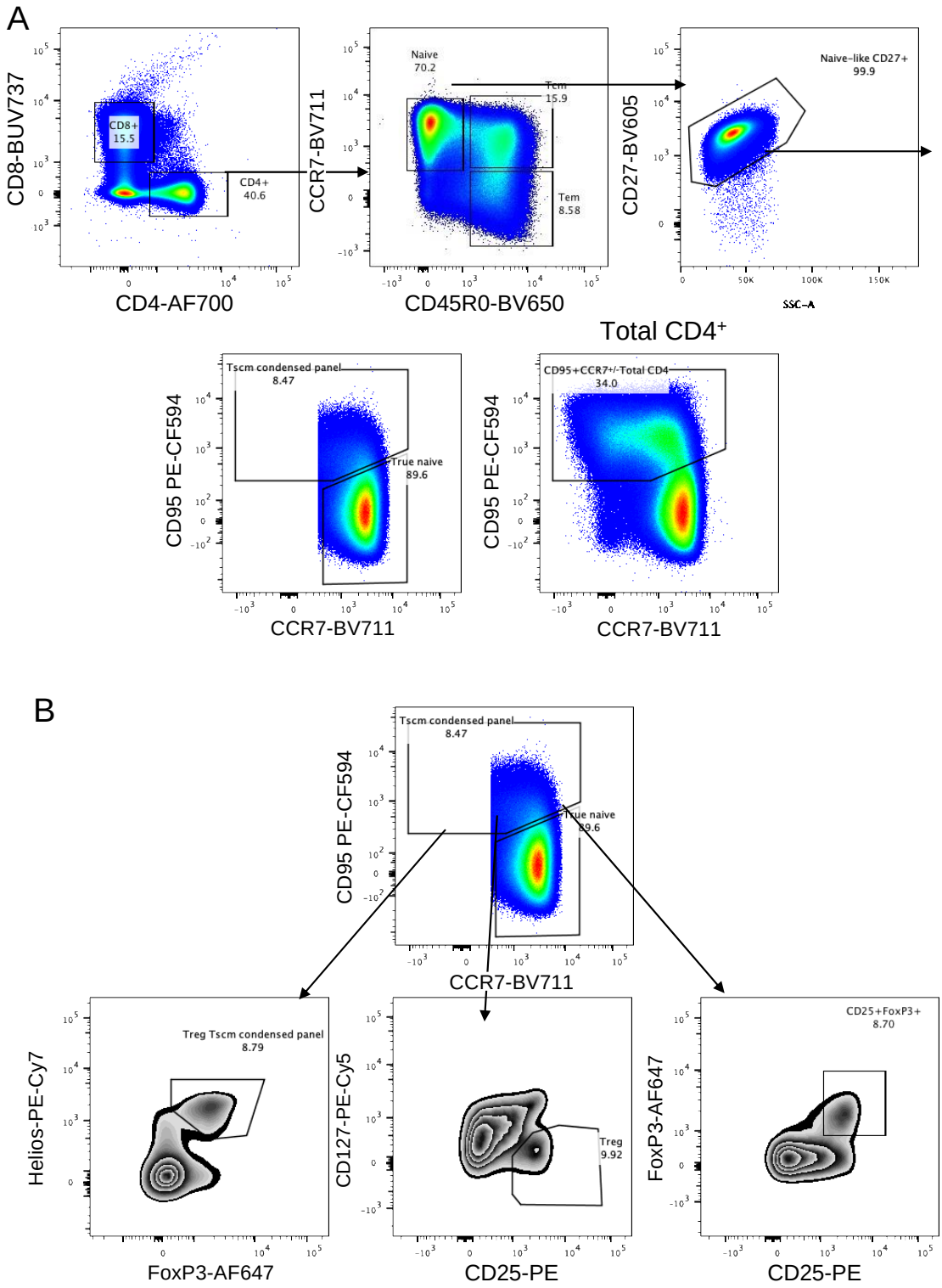

Figure 5.6: Tregs with a stem cell-like memory (Tscm) phenotype can be identified using a condensed stem cell-like memory gating strategy. Cryopreserved PBMCs from a healthy donor were stained with fluorochrome-conjugated antibodies and acquired for flow cytometric analysis using a BD LSRFortessa analyser. (A) This condensed gating scheme

shown is based on a revised gating strategy to isolate stem cell like memory cells published in Lugli, Gattinoni, et al. (2013). (B) Tscm cells can have a Treg phenotype.

Using this condensed panel, we then sought to isolate pure populations of these T cell subsets in order to compare their function *in vitro*. As shown in the work of Gattinoni et al. (2011) in figure 5.2, there are several *in vitro* functional properties which set Tscm cells apart from naïve cells including their ability to rapidly secrete effector cytokines and proliferate on stimulation, and their ability to preserve a niche of cells which maintain their original stem cell-like phenotype while generating memory progeny. As we aimed to elucidate the function of Tregs which had a phenotype akin to Tscm cells, measuring secretion of effector cytokines such as IL-2, IFN-γ, and TNF-α and proliferation in response to IL-7 and IL-15 as described in previous publications would not be appropriate as these functions are not characteristic of Tregs. Instead, we aimed to analyse the ability of Tregs with a Tscm-like phenotype to rapidly proliferate in response to anti-CD3/CD28 bead stimulation and also to analyse the ability of these cells to self-renew during expansion.

In order to compare the ability of T cell subsets to rapidly proliferate, cells were pre-labelled with CellTrace violet (CTV) proliferation dye to measure the proliferation of each cell population in response to 5 days of anti-CD3/CD28 bead stimulation and IL-2 as Tregs would not survive in culture without IL-2 supplementation. T_{CM}, T_{EM}, T naïve, and Tscm cells were FACS sorted from both the Tconv and Treg compartments of healthy donor PBMCs according to the gating strategy shown in figure 5.7. In this donor, using this gating strategy the cells with a Tscm-like phenotype were ten-fold more frequent in Tregs than in Tconvs.

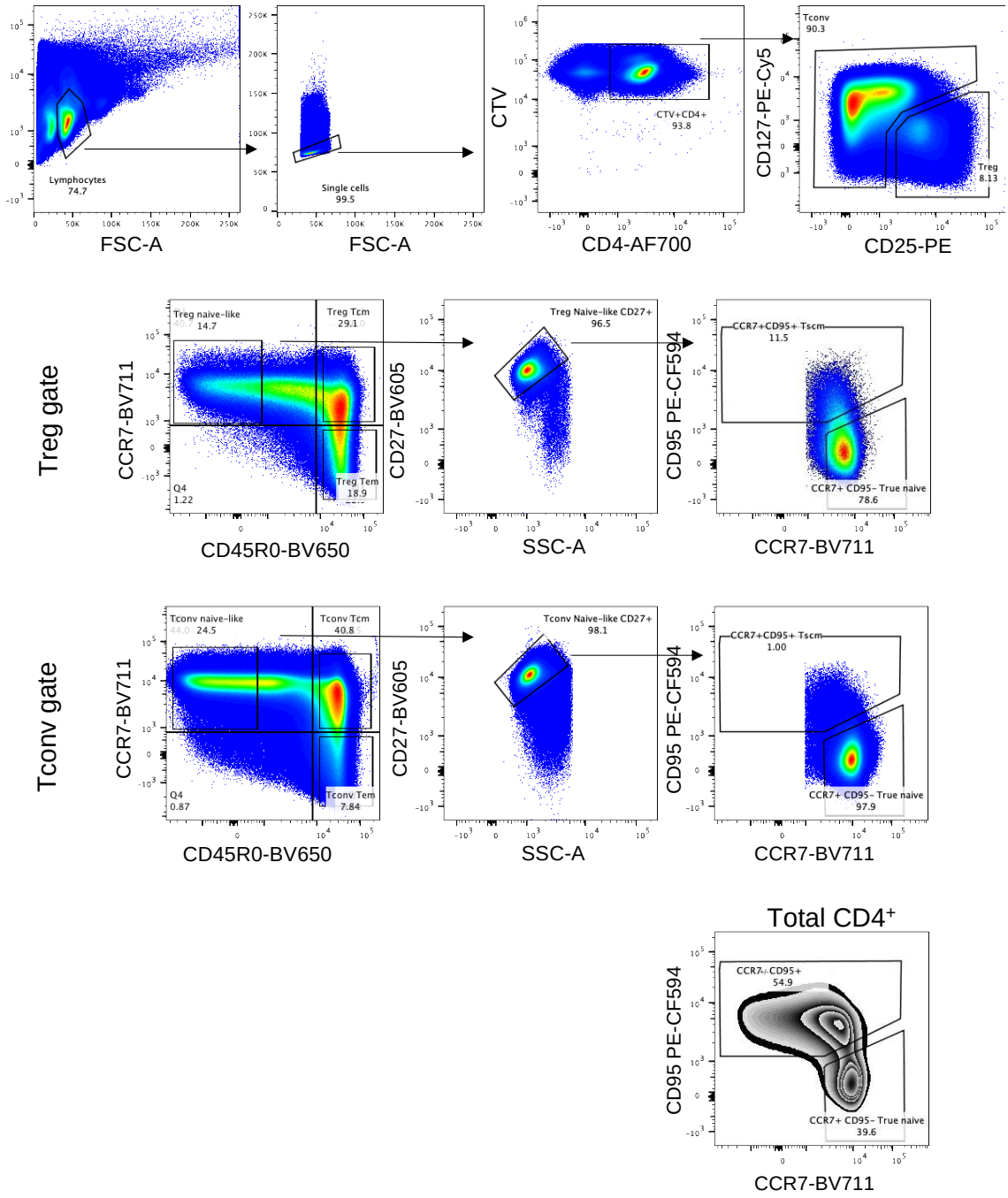

Figure 5.7: Tregs and Tconvs with a stem cell-like memory phenotype can be FACS sorted from cryopreserved PBMCs. Cryopreserved PBMCs from a healthy donor were labelled with cell trace violet (CTV) proliferation dye, stained with fluorochrome-conjugated antibodies, and FACS sorted using a BD FACS Aria-IIu cell sorter. Proliferation of the central memory (Tcm), effector memory (Tem), naïve, and stem cell-like memory T cells (Tscm) sorted from the Tconv and Treg compartments could then be monitored over the following 5 days by CTV dye dilution.

At day 5, cells were collected and analysed by flow cytometry. Figure 5.8 shows the proliferation profiles of T_{EM}, T_{CM}, T naïve, and cells with a Tscm-like phenotype in Tconvs and Tregs. Within Tconvs, all T cell subsets expanded over the 5-day period. In this single donor, the population with the higher percentage of cells divided (PD) was the True naïve Tconvs in which 95.1% of cells had divided compared to the unstimulated control. This was followed closely by the Tscm Tconvs of which 92.2% had divided. 86.9% of T_{CM} Tconvs underwent division compared to only 65.5% of T_{EM} Tconvs. All Tconv subsets underwent approximately 6 rounds of cell division, and the population with the highest frequency of cells in the latest round of cell division was the Tscm Tconvs, and this was reflected in the number of events within the live $CD4^+$ cell gate at 6220 events which was the highest number of any of the T cell subsets.

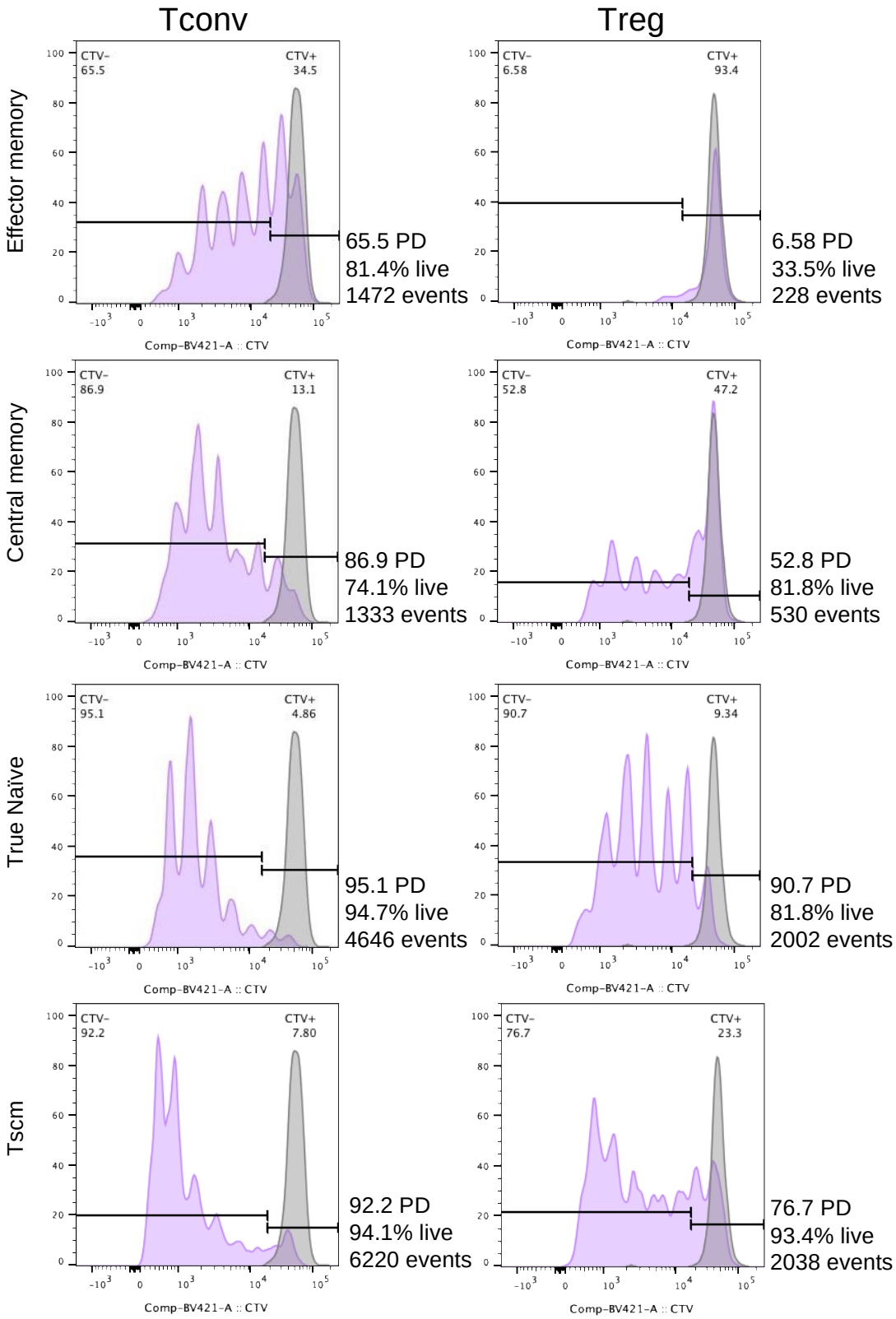

Figure 5.8: Naïve and stem cell-like memory (Tscm) cells from the Tconv and Treg compartments were more proliferative in culture than memory subsets. PBMCs were labelled with Cell Trace violet (CTV) and surface stained prior to FACS sorting of effector memory, central memory, true naïve, and cells with a stem cell-like memory phenotype (Tscm) from the Tconv and Treg pool. Cells were stimulated with anti-CD3/CD28 beads and

cultured with IL-2 for 5 days. Proliferation data on day 5 were acquired on a BD LSRFortessa and analysed via CTV dye dilution. PD= percentage divided

Within the Treg subsets, there was minimal proliferation in the T_{EM} subset with only 6.58% of cells divided more than the unstimulated control. T_{EM} Tregs also did not survive well in culture, with only 33.5% of events falling into the live $CD4^+$ T cell gate and only 228 events in total were recorded in this gate. T_{CM} Tregs did not proliferate as strongly as T_{CM} Tconvs as only 52.8% of cells had divided. The Treg subset which proliferated most in response to the stimulus was again the true naïve Tregs in which 90.7% of cells had divided. In the Treg Tscm population 76.7% of cells had divided, however again we observed that this subset had the highest frequency of cells in the latest stage of division. Although this data could imply that Tscm-like Tconvs and Tregs are less proliferative than naïve cells, it could also be hypothesised that as well as giving rise to memory progeny upon proliferation, a proportion of Tscm cells remained in a quiescent, self-renewing state meaning that the percentage of divided cells would be lower than those in the naïve pool. Therefore, we investigated the surface phenotype of the Tconv and Treg Tscm cells to analyse whether there was evidence of a population of cells maintaining their original phenotype upon stimulation.

Figure 5.9 shows flow cytometry data of cells with a Tscm-like surface phenotype which were isolated by FACS sorting from both the Treg and Tconv pools and cultured for 5 days using the stimulation method described in the previous figure. In both the Treg and Tconv Tscm-like cells, after 5 days of anti-CD3/CD28 stimulation most of the cells retained a $CCR7^+CD95^+$ phenotype, however the cells all upregulated CD45R0 with no evidence that a pool of self-renewing

CD45R0$^-$ cells remained which is integral to the Tscm phenotype. As shown below, cells which were isolated by FACS sorting using an identical gating scheme which were not stimulated with anti-CD3/CD28 beads did not upregulate CD45R0 although these cells did downregulate their expression of CCR7 which may have been a result of IL-2 stimulation which was required for survival of Tregs in culture. This suggests that the anti-CD3/CD28 bead stimulation converted all cells which began with a phenotype akin to Tscm cells into memory T cells.

Although we did not see any evidence of stem cell-like memory function in Tregs or Tconvs from these experiments, we were still keen to investigate how a CD45RA$^+$CD95$^+$ phenotype was maintained in some cells within the 6-week expanded naïve and naïve CD31$^+$ Tregs described in chapter 4. The main difference between the culture conditions used in chapter 4 compared to those used in the current chapter was the addition of rapamycin to the cell culture media throughout expansion in the former chapter. Intriguingly, a study by Scholz et al. (2016) showed that phenotypic and functional Tscm cells could be generated from naïve CD4$^+$ T cells *in vitro* through culture with rapamycin. This raises the hypothesis that the CD45RA$^+$CD95$^+$ phenotype observed in the expanded naïve Treg subsets may have been induced by rapamycin. To this end, we then investigated whether sorted Tconvs and Tregs with a Tscm-like phenotype expanded for 14 days in the presence of rapamycin maintained a pool of cells with a Tscm-like phenotype, or indeed whether cells with a Tscm-like phenotype could arise from naïve Tconv and Treg precursors.

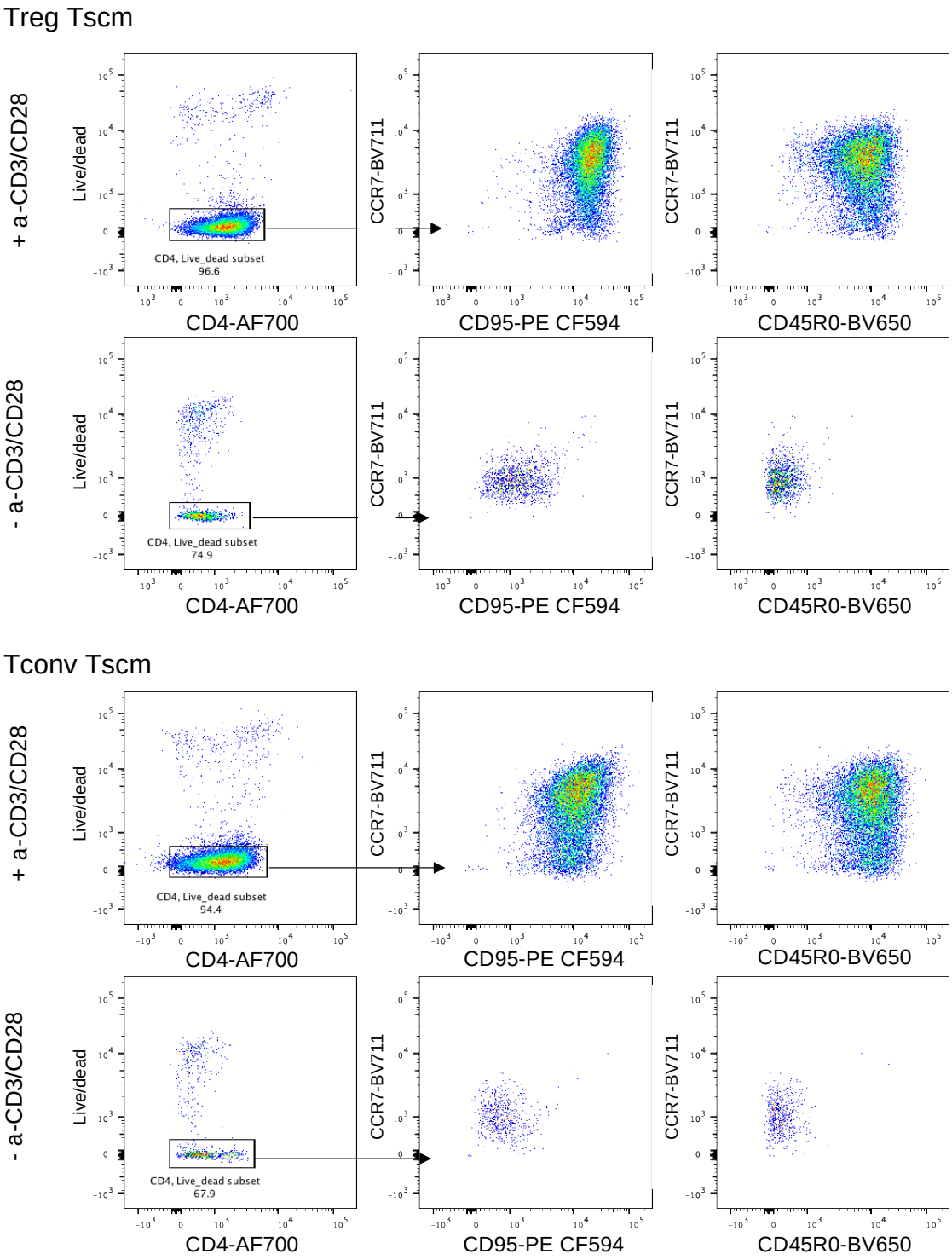

Figure 5.9: FACS sorted Tregs and Tconvs with a stem cell-like memory phenotype both upregulated CD45R0 over 5-days of stimulation. Cryopreserved PBMCs from a healthy donor were stained with fluorochrome-conjugated antibodies and FACS sorted using a BD FACS Aria-IIu cell sorter to isolate Tconv and Treg cells with a stem cell-like memory phenotype (Tscm). Cells were stimulated with anti-CD3/CD28 beads (+αCD3/CD28; or non-bead stimulated negative controls -αCD3/CD28) and cultured with IL-2 for 5 days. Cells were harvested and re-stained on day 5 and data were acquired on a BD LSRFortessa to analyse

the cell surface phenotypes. Top panels: end phenotype of isolated Tregs with a Tscm phenotype +/- 5 days of anti-CD3/CD28 bead stimulation. Bottom panels: end phenotype of isolated Tconvs with a Tscm phenotype +/- 5 days of anti-CD3/CD28 bead stimulation.

5.3.3 Rapamycin maintained expression of naïve markers on 14-day expanded naïve and Tscm-like Tregs but not Tconvs

T cells with a $T_{CM,}$ $T_{EM,}$ T naïve, and Tscm-like phenotype were isolated from the Tconv and Treg pools by FACS sorting according to the gating strategy shown in 5.7, however for the following experiments, cells were not labelled with CTV. Cells were then expanded for 14 days in the presence of anti-CD3/CD28 bead stimulation, IL-2 and rapamycin, to replicate the Treg expansion conditions used in chapter 4, and the phenotype of each subset was analysed on day 14.

As shown in figure 5.10, at the end of the 14 days of expansion, the expanded T cell subsets had differing levels of CD45R0 and CCR7 in this single donor. Within the expanded Tconv subsets, both T_{CM} and T_{EM} cells had mostly a $CD45R0^{+}CCR7^{-}$ phenotype. In the expanded naïve Tconv subset, 74.6% of cells maintained a $CD45R0^{-}$ phenotype and 43.3% of cells were $CD45R0^{-}CCR7^{+}$. A large proportion of the Tscm-like Tconvs upregulated CD45R0, with only 32.85% of cells being $CD45R0^{-}$ and only 3.85% maintained a $CD45R0^{-}CCR7^{+}$ phenotype, meaning very few cells could be described as having maintained their original phenotype.

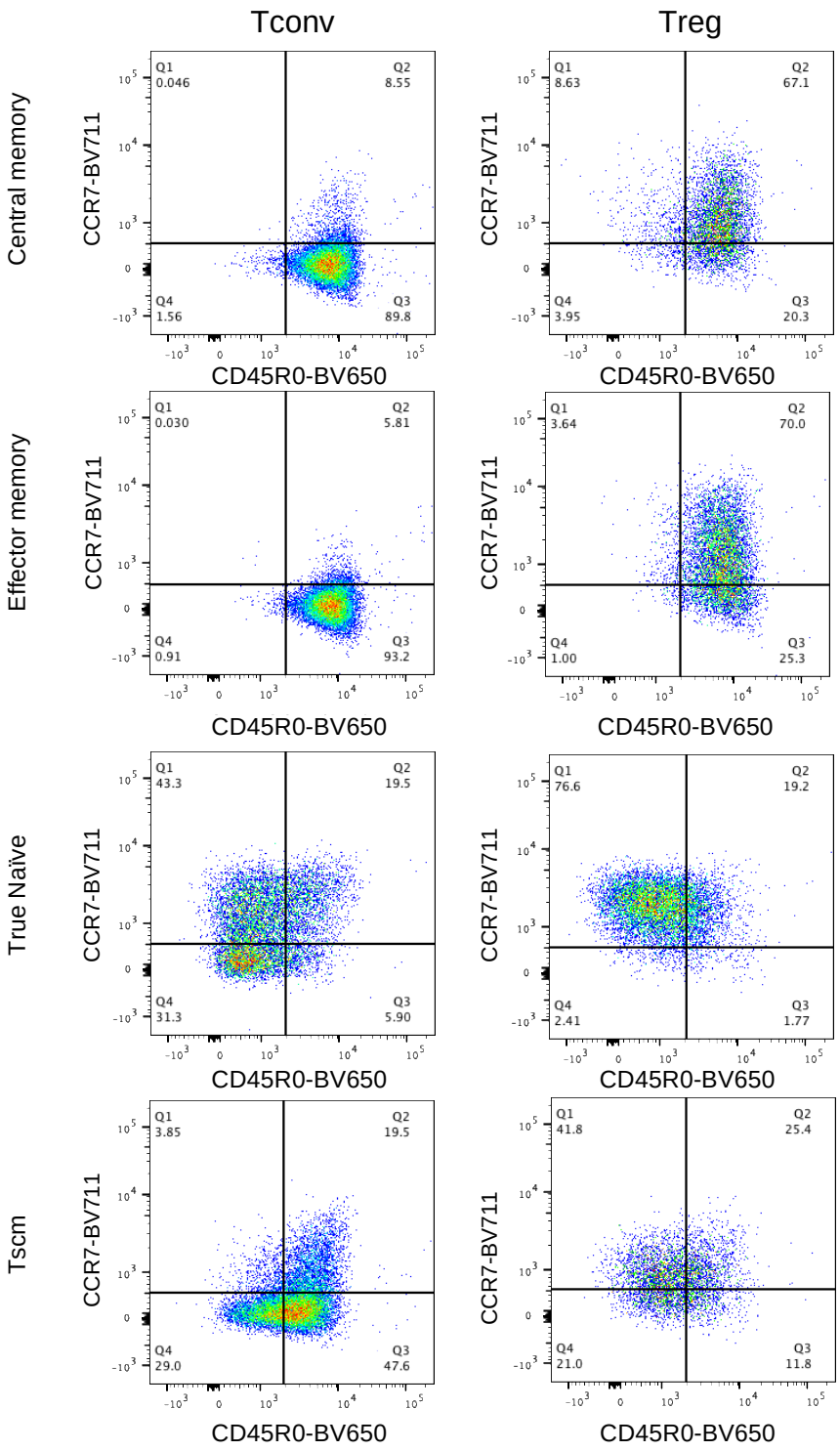

Figure 5.10: Rapamycin suppressed the upregulation of CD45R0 during expansion of naïve and Tscm Tregs but not Tconvs. Cryopreserved PBMCs from a healthy donor were stained with fluorochrome-conjugated antibodies and FACS sorted using a BD FACS Aria-IIu cell sorter to isolate Tconv and Treg cells with central memory, effector memory, true naïve, and stem cell-like memory phenotypes (Tscm). Cells were stimulated with anti-

CD3/CD28 beads and cultured with IL-2 and rapamycin for 14 days. Cells were re-stained and data were acquired on a BD LSRFortessa to analyse the cell surface phenotypes.

Within the Treg pool, again T_{CM} and T_{EM} populations were $CD45R0^+$ however a greater proportion of these expanded cells were $CD45R0^+CCR7^+$ compared to Tconvs at 67.1% and 70%, respectively. Within the cultured naïve Tregs 79.01% of cells were $CD45R0^-$ after culture which was comparable to the 74.9% in naïve Tconvs, however, the $CD45R0^-CCR7^+$ fraction was higher in the expanded naïve Tregs at 76.6% of cells compared to 43.3% in the naïve Tconvs. Finally, a higher frequency of $CD45R0^-$ cells was found in the cultured Tscm-like Tregs compared to the cultured Tscm-like Tconvs at 62.8% compared to 32.85%. Moreover, 41.8% of Tscm-like Tregs maintained a $CD45R0^-CCR7^+$ phenotype compared to just 3.85% in the expanded Tconvs. In summary, this data suggests that rapamycin can suppress the upregulation of memory markers on expanded naïve Tregs but not Tconvs, which is in agreement with data from chapter 4.

As well as CD45R0 and CCR7, expanded cells were also analysed for surface expression of CD45RA and CD95 (figure 5.11) and CD27 (figure 5.12), as Tscm-like cells should have a surface $CD45R0^-CCR7^+CD45RA^+CD95^+CD27^+$ phenotype. As shown in figure 5.11, as expected, expanded T_{CM} and T_{EM} subsets from both Tconvs and Tregs had a $CD95^+CD45RA^-$ memory phenotype. The expanded true naïve cells from both the Tconvs and Tregs maintained 51.5% and 53.2% of cells expressing a $CD45RA^+CD95^+$ phenotype, respectively. However, only 5.16% of expanded naïve Tregs were $CD45RA^-$ compared to 31.44% of expanded naïve Tconvs, again suggesting that naïve Tregs expanded in the presence of rapamycin had a better maintenance of naïve markers than in

Tconvs. When comparing the expression of CD45RA and CD95 in the expanded Tscm-like Tregs and Tconvs, 62.5% of Tscm-like Tregs had a $CD95^{+}CD45RA^{+}$ phenotype, while only 28.2% of Tscm-like Tconvs shared this phenotype. In addition, over 98% of Tscm-like Tregs were $CD95^{+}$ compared to only 86.8% in Tconvs. Finally, as shown in figure 5.12 true naïve and Tscm-like Tregs maintained a much higher expression of CD27 than all other subsets at the end of expansion with over 97% of evets being $CD27^{+}$ in both Treg subsets.

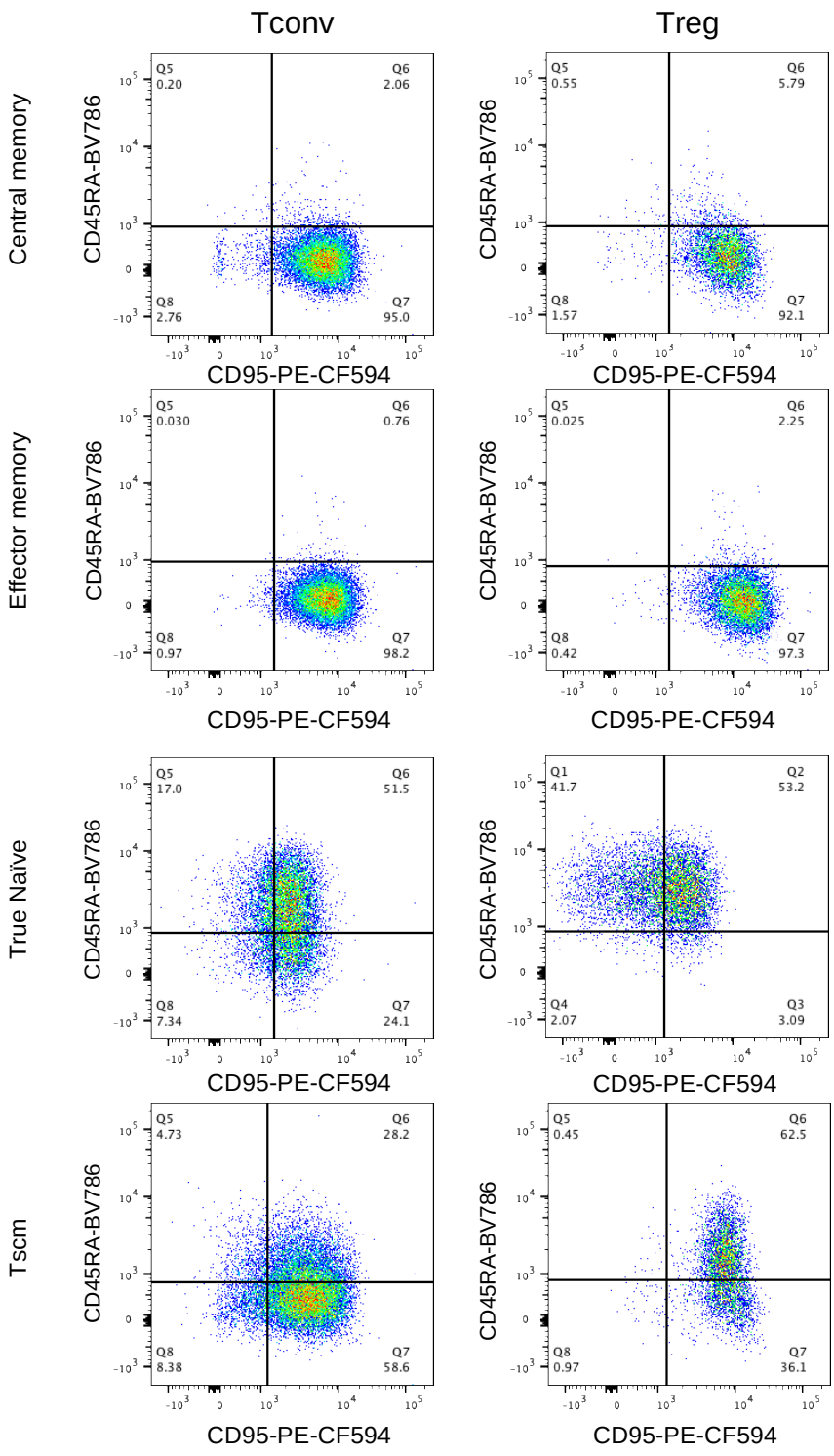

Figure 5.11: Rapamycin stimulated co-expression of CD95 and CD45RA during expansion of naïve and Tscm Tregs. Cryopreserved PBMCs from a healthy donor were stained with fluorochrome-conjugated antibodies and FACS sorted using a BD FACS Aria-IIu cell sorter to isolate Tconv and Treg cells with central memory, effector memory, true naïve, and stem cell-like memory phenotypes (Tscm). Cells were stimulated with anti-CD3/CD28 beads and cultured with IL-2 and rapamycin for 14 days. Cells were re-stained and data were acquired on a BD LSRFortessa to analyse the cell surface phenotypes.

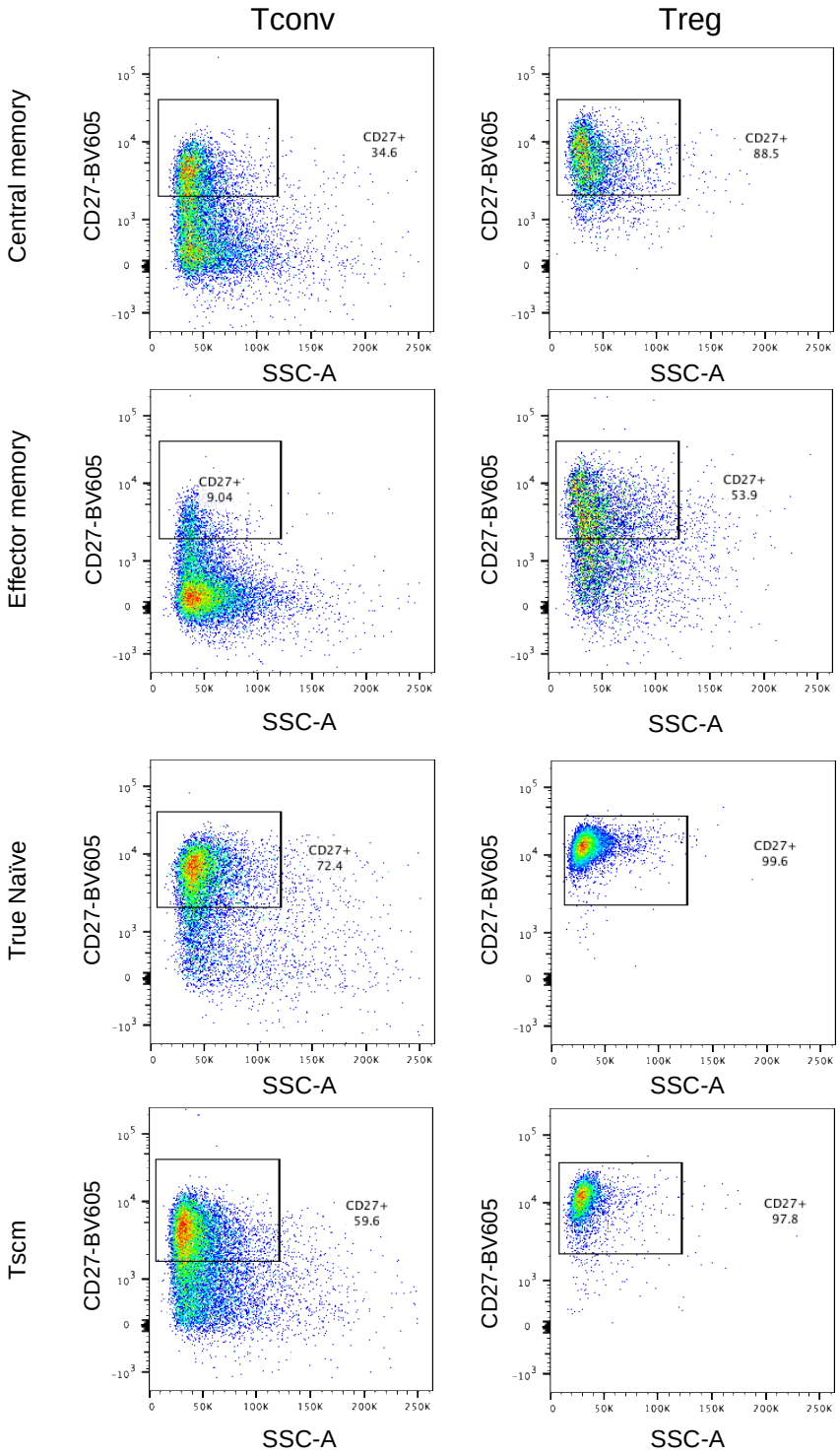

Figure 5.12: All naïve and Tscm Tregs expanded in the presence of rapamycin expressed CD27. Cryopreserved PBMCs from a healthy donor were stained with fluorochrome-conjugated antibodies and FACS sorted using a BD FACS Aria-IIu cell sorter to isolate Tconv and Treg cells with central memory, effector memory, true naïve, and stem cell-like memory phenotypes (Tscm). Cells were stimulated with anti-CD3/CD28 beads and cultured with IL-2 and rapamycin for 14 days. Cells were re-stained and data were acquired on a BD LSRFortessa to analyse the cell surface phenotypes.

As a general trend, all expanded Treg subsets had a higher proportion of $CD27^+$ cells than their Tconv counterparts. Expanded T_{CM} Tregs were 88.5% $CD27^+$ compared to 34.6% in T_{CM} Tconvs. T_{EM} Tregs were 53.9% $CD27^+$ compared to 9.04% of T_{EM} Tconvs. $CD27^+$ expanded naïve Tregs were at a frequency of 99.6% compared to 72.4% in Tconvs, and Tscm-like Tregs were 97.8% $CD27^+$ while Tscm Tconvs were 59.6% $CD27^+$. The frequency of cells which had a $CD45R0^-CCR7^+CD45RA^+CD95^+CD27^+$ surface phenotype at the end of 14 days of expansion is shown in table 5.4. As expected, there were very few cells (<1.7%) with a Tscm-like phenotype in the expanded T_{CM} and T_{EM} subsets in Tconvs and Tregs. The T cell subset with the highest frequency of cells with a Tscm-like phenotype was the expanded true naïve Tregs, followed by Tscm-like Tregs. Within the Tconv compartment, 13.3% of expanded naïve cells and only 1.1% of expanded Tscm-like cells displayed this phenotype. From this we can conclude that in this donor, when cells were expanded in the presence of rapamycin, cells with a Tscm-like phenotype arose most frequently in the expanded naïve Tregs over the course of 14 days of expansion, followed by Tscm-like Tregs. This data appears to shed light on a previously unknown effect of rapamycin specifically on Tregs, as Tregs with a naïve-like phenotype prior to strong TCR stimulation maintain expression of these naïve markers and suppress upregulation of memory markers such as CD45R0.

Table 5.4: Frequency of cells with a stem cell-like memory phenotype within 14-day expanded T cell subsets.

T cell subset	% of cells with CD45R0$^-$ CCR7$^+$CD45RA$^+$CD95$^+$CD27$^+$ phenotype post-expansion
Tconv T_{CM}	0.00
Tconv T_{EM}	0.00
Tconv true naïve	13.3
Tconv Tscm-like	1.10
Treg T_{CM}	1.70
Treg T_{EM}	0.1
Treg true naïve	39.6
Treg Tscm-like	29.3

Dimensionality reduction of the concatenated data from expanded T_{CM}, T_{EM}, T naïve and Tscm-like cells from Tconvs and Tregs helped to provide a possible explanation for why more expanded naïve Tregs had a Tscm-like phenotype than expanded Tscm-like Tregs. As shown in figure 5.13 A and B, expanded Tconv T_{CM} and T_{EM} cells had low MFIs for CD45RA, CCR7, CD27, and FoxP3, and high MFIs for memory markers such as CD45R0 and CD95.

Naïve Tregs and Tconvs mostly occupied distinct regions within the optSNE plot which had a low CD45R0 MFI and high MFIs for naïve markers such as CD45RA. Naïve cells also occupied regions which were relatively low in CD95 expression which may be expected when comparing to the MFI of memory populations. Meanwhile, the Tscm-like Tregs had regions of high cell density in CD45R0^{low} CD45RA^{hi} CD95^{hi} MFIs, however there was also a diffuse spread of events into regions with a high CD45R0 MFI which may be expected in the case of a self-renewing population which was generating memory progeny. The relatively high

expression of CD27 by naïve and Tscm-like Treg populations can also be seen here as in the previous figures. Cells within the CD45R0^{low} CD45RA^{hi} CD95^{hi} MFI regions in expanded Treg Tscm-like cells also had a low MFI for the proliferation marker Ki67 suggesting quiescence, a high MFI for CD27 and CD62L, and some expressed CXCR3 which suggests a Tscm-like phenotype. However, the same could not be said for Tconv Tscm-like expanded cells as nearly all events fell within CD45R0-high regions suggesting very few of these cells had self-renewal capacity under these expansion conditions. In conclusion, this data provides compelling evidence that Treg Tscm-like cells expanded in the presence of rapamycin retain co-expression of naïve markers and CD95 while generating memory progeny, which is not seen in the Tconv pool. The expanded naïve Tregs expressed several naïve markers but some also expressed low levels of CD95 suggesting a possible induction of a Tscm-like phenotype in the presence of rapamycin. To conclude this chapter, this data provides minimal evidence that expanded Tscm-like Tconvs had a self-renewing capacity, however within the Treg naïve and Tscm compartments there was evidence for a self-renewing pool of cells. Moreover naïve and Tscm Tregs expanded in the presence of rapamycin for 14 days suppressed the upregulation of CD45R0, however in the absence of rapamycin, these cells became CD45R0^{+} within 5 days of expansion.

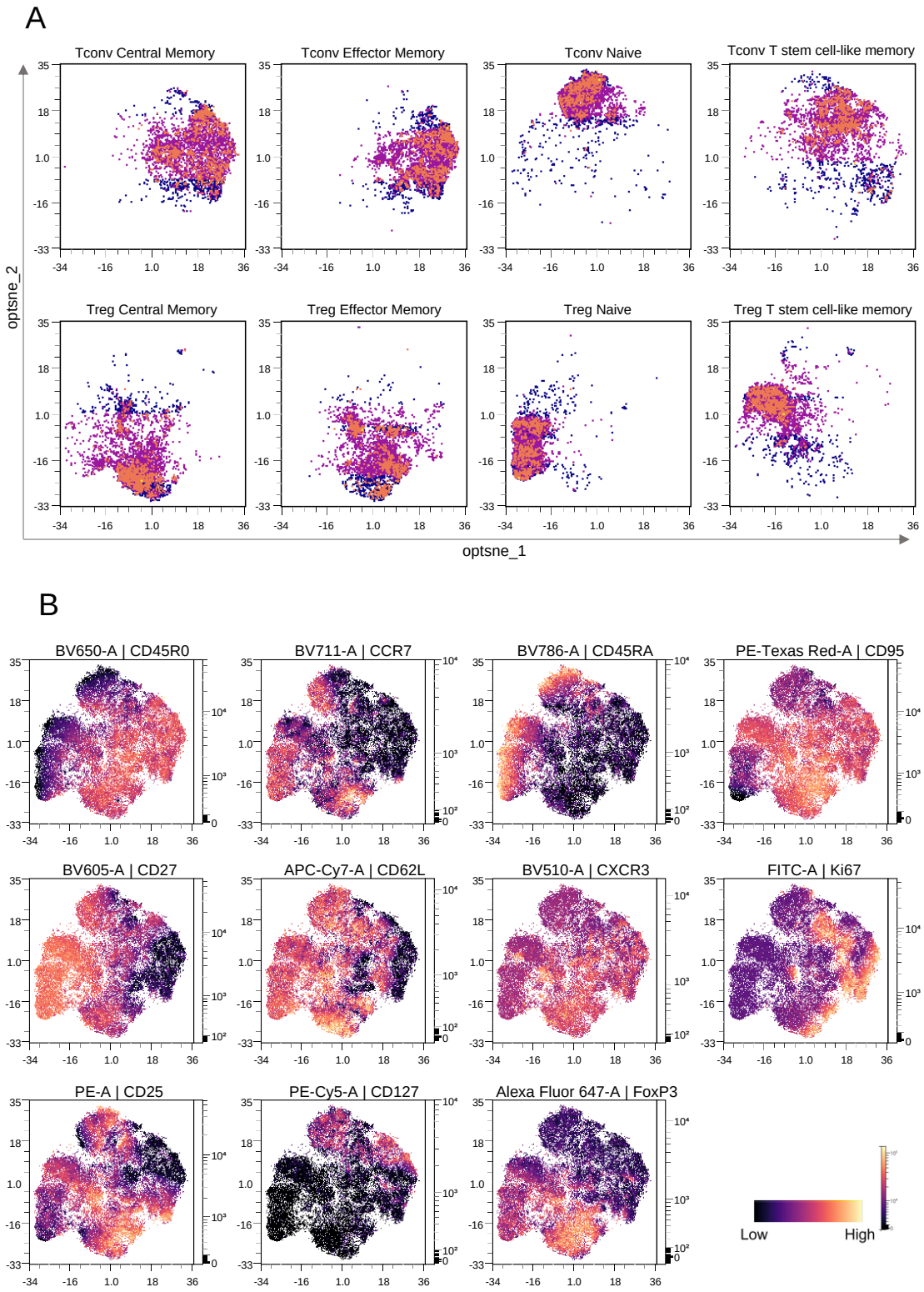

Figure 5.13: Rapamycin induced a stem cell-like memory phenotype in 14-day expanded naïve Tregs. PBMCs were stained and FACS sorting was used to isolate Tconv and Treg cells with central memory, effector memory, true naïve, and stem cell-like memory phenotypes (Tscm). Cells were stimulated with anti-CD3/CD28 beads and cultured with IL-2 and rapamycin for 14 days. Cells were re-stained and data were acquired on a BD LSRFortessa to analyse the cell surface phenotypes. Dimensionality reduction was carried

out using the opt-SNE algorithm in OMIQ software. Dimensionality reduction is shown by subset (A) and concatenated (B). Scales indicate low to high MFIs of each marker.

5.4 Discussion

Data in this experimental chapter was intended as an open-ended, preliminary investigation into the potential stem cell-like memory properties of a population of $CD45RA^{+}CD95^{+}$ Tregs which was prominent within 6-week expanded naïve Tregs in chapter 3. The findings of Gattinoni et al. (2011b) demonstrated a phenotypic and functional ability for cells in the human Tconv compartment to simultaneously encompass properties of naïve and memory cells, thus named stem cell-like memory cells owing to their ability to proliferate while preserving a niche of self-renewing cells. Other $CD4^{+}$ T cell subsets are known to co-express markers of naivety and memory, such as effector memory re-expressing CD45RA cells (TEMRA), which exhibit a $CCR7^{-}CD45RA^{+}CD27^{-}CD28^{-}$ phenotype and expression of cytolytic molecules, however these cells do not display stem cell-like properties (Tian et al., 2017). Cells akin to Tscm cells are yet to be reported in the Treg compartment.

Using a panel of surface and intracellular markers, we identified cells with a phenotype matching Tconv Tscm cells within the Treg compartment (figure 5.3-5.4). These cells expressed markers of naivety such as $CD45RA^{+}CCR7^{+}CD62L^{+}$, were double positive for CD28 and CD27, and also expressed the characteristic memory marker CD95, and were positive for FoxP3 and Helios (figure 5.3-5.4). Due to restrictions on our ability to draw blood from healthy donors during the COVID pandemic, results in this experimental chapter (and in chapter 4) were from one donor only and therefore future work would require several more

replicates to confirm these results. In this donor, the Tregs within the Tscm-like gate represented a similar proportion to Tregs present in total $CD4^+$ cells (~7%). We felt that these cells were distinct from Treg subsets identified by unbiased clustering methods in chapter 3 which had a 'transitioning' phenotype as these subsets expressed CD45RA and CD95 at a low level, whereas Tregs with a Tscm-like phenotype were distinctly $CD45RA^+CD95^+$. When compared to naïve Tregs, a higher proportion of these cells expressed the proliferation marker Ki67 when analysed directly *ex vivo* (figure 5.5) which suggests that these Treg subsets played distinct roles *in vivo*.

In order to isolate these cells to carry out functional analyses, we were required to condense this original panel guided by methods in the publication by Lugli, Gattinoni, et al. (2013) which claimed that a utilising 3 markers rather than 7 to identify naïve-like cells had a minimal impact on the proportion of Tscm cells ($CD95^+$ naïve-like) recorded in the $CD4^+$ and $CD8^+$ compartments. This 3-marker strategy to identify naïve cells was based on findings of a previous publication which showed that a minimum of 3 naïve markers was needed to minimise contamination of the naïve pool with functional memory T cells with cytokine-producing properties and low TCR diversity (De Rosa, Herzenberg, Herzenberg, & Roederer, 2001). It is clear from our data that a higher frequency of Tregs was observed in the final gate of our 3 naïve-marker panel (figure 5.6 B) than in the 7 naïve-marker panel (figure 5.4 A) within the same donor. As most peripheral Tregs have a memory phenotype, the higher frequency of Tregs when using a less stringent panel may indicate a higher contamination of memory cells using the 3-naïve marker panel. It is known that during isoform switching from CD45RA

to CD45R0, acquisition of CD45R0 on the cell surface occurs before CD45RA is fully shed resulting in a temporary double positive population which may not be possible to exclude when using only one of these markers (Courville & Lawrence, 2021). Therefore in future work, it may be of use to include more naïve-like markers such as CD62L and CD45RA in sort strategies where possible to limit memory cell contamination. However, the lower frequency of Tregs in the larger panel could also be explained by the fact that CXCR3 was used as a positive marker for Tscm-like cells in this panel as suggested in the Gattinoni et al. (2011b) paper, and it is known from our data in the previous chapters that CXCR3 expression in Tregs is limited compared to Tconvs.

When isolating Tscm-like Tconvs and Tregs, it was also evident that Tregs contained a much higher proportion of events in the $CCR7^{+}CD95^{+}$ Tscm-like gate than Tconvs which seemed to be driven by a higher frequency of $CD95^{+}$ cells. This was despite there being nearly double the frequency of $CD45R0^{-}CCR7^{-}$ naïve-like cells in Tconvs compared to Tregs. Although several publications have reported that total Tregs express higher levels of CD95 than Tconvs, it is likely that this is due to a higher prevalence of memory Tregs compared to Tconvs within the total Treg/Tconv pool (Banz, Pontoux, & Papiernik, 2002; Fritzsching et al., 2005, 2006). To our knowledge, this is the first study to report this high expression of CD95 within a naïve Treg pool validated by at least 3 naïve markers.

In addition to this promising phenotypic evidence of Tscm Tregs, we found some evidence of Tscm function in isolated Tscm-like Tregs compared to true naïve

cells. As shown in figure 5.8, in a 5-day proliferation assay, naïve Tregs and Tconvs had the highest percentage of divided cells followed by Tscm cells. However, this could indicate that expanded Tscm Tconvs and Tregs maintained a pool of quiescent, undivided cells which would indicate stem-like properties. We saw minimal proliferation of T_{CM} and T_{EM} Tregs in culture compared to naïve-like Treg subsets and T_{CM} and T_{EM} Tconvs. This is in agreement with findings by Miyara et al. (2009) which showed that naïve Tregs expand and proliferate upon expansion while memory subsets do not. This further supports our data from the comparative Treg subset micro-suppression assay in chapter 3 as this shows that in spite of minimal proliferation of memory Tregs and some proliferation of naïve Tregs, there were still fewer counts per minute recorded in wells containing naïve Tregs meaning these subsets were better suppressors of Tconv proliferation. In addition, this data suggests that 100U/ml of IL-2, as used in this experiment, was not sufficient to break quiescence of memory Treg subsets, while 600U/ml used in chapter 4 caused significant expansion of memory Tregs.

This data does, however, lie in contrast to previous reports by Gattinoni et al. (2011b) and Lugli, Gattinoni, et al. (2013) which showed that Tconv Tscm cells proliferated significantly more rapidly than naïve Tconvs in response to TCR/co-stimulation in culture (figure 5.2). It may be of significance that our stimulation protocol during this experiment differed to the protocol in these publications by the addition of IL-2 to the culture media as initial optimisation experiments showed us that none of the Treg subsets survived in culture without IL-2 supplementation (data not shown). Therefore, it is possible that true naïve Tregs are more responsive to anti-CD3/CD28 stimulation in the presence of IL-2, which

may present a further limitation of investigating Tscm function in Tregs. As mentioned above, proliferation in response to IL-7 and the rapid secretion of inflammatory cytokines was also demonstrated as a unique property of Tscm Tconvs in these publications, however this function in Tregs would typically denote Tregs with an unstable phenotype making it difficult to measure equivalent Tscm function in the Treg compartment. However, future work should aim to measure proliferation of Tconv Tscm cells in response to IL-7 and IL-15 as carried out in previous studies to evaluate whether these results can be reproduced in our hands. In addition, although we did observe a higher frequency of cells having undergone the most recent round of proliferation in Tscm-like Tconvs and Tregs which may have denoted rapid production of memory progeny (most diluted CTV staining figure 5.8), we also observed full upregulation of CD45R0 in activated Tscm Tregs and Tconvs (figure 5.9), while Gattinoni et al. (2011b) were able to detect 15% of stimulated cells which preserved their $CCR7^{+}CD45RA^{+}CD95^{+}CD45R0^{-}$ phenotype over a similar activation period. This negated any evidence for self-renewal within either the Tscm Tconvs or Tregs, meaning that under these experimental conditions we did not see any functional stem cell-like memory behaviour in Tregs and we found that this data did not replicate the findings from previous studies in the Tconv pool.

We found evidence in the literature that addition of rapamycin to the culture media during the expansion of naïve Treg subsets described in chapter 4 may have been inducing a $CD45RA^{+}CD95^{+}$ phenotype after repeated rounds of TCR stimulation (Scholz et al., 2016). Studies by Canavan et al. (2016) and Fraser et al. (2018) also found that rapamycin promoted expression of naïve markers, such

as CD62L, CD27, and CCR7, and markers of antigen experience such as CCR4 which was not seen within expanded total $CD4^+$ T cells or cultures expanded without rapamycin. This suggests that rapamycin may have a Treg-specific effect of promoting expansion of Tregs which maintain expression of naïve markers. Therefore, we next sought to identify whether our Treg expansion protocol led to either an induction of a Tscm phenotype from naïve Tconv or Treg precursors, or preserved a Tscm-like pool within expanded Tscm-like Tconvs and Tregs.

When analysing the surface phenotypes of expanded T_{CM}, T_{EM}, naïve, and Tscm-like T cells from both the Treg and Tconv pools, we observed distinct differences in the surface phenotypes of these expanded subsets between Tconvs and Tregs. For example, we observed a much lower conversion of Tscm-like Tregs to a $CD45R0^+$ phenotype during the 14-day expansion in the presence of rapamycin (figure 5.10) compared to 5-day expanded Tscm-like Tregs in the absence of rapamycin (figure 5.9) and this was accompanied by expression of CCR7 in a large proportion of the cells which suggests that these cells were not taking on a TEMRA-like phenotype. Cells within expanded Tconv subsets were mostly $CCR7^-$. However, CCR7 expression was markedly increased in all expanded Treg subsets compared to Tconvs, suggesting that this promotion of naïve markers in the presence of rapamycin was a Treg-specific effect. CCR7 is an important lymphoid tissue homing molecule expressed to a high level by naïve and T_{CM} cells in both Tconvs and Tregs and does not infer intrinsic suppressive properties (Zhang et al., 2009). However, several studies have reported an increase in CCR7 expression in Tregs during expansion in the presence of rapamycin (Battaglia et al., 2006; Strauss, Czystowska, Szajnik, Mandapathil, &

Whiteside, 2009; Strauss et al., 2007; Veerapathran, Pidala, Beato, Yu, & Anasetti, 2011). Importantly, we also saw an upregulation of CCR7 in the expanded T_{EM} Treg subset which characteristically do not express CCR7 and was not observed in Tconvs or in T_{EM} Tregs at baseline (figure 5.7), however this subset did also upregulate CD45R0. Therefore, it is possible that this upregulation of CCR7 in all Treg subsets was skewing the frequency of cells with a Tscm-like phenotype in the expanded naïve and Tscm-like Tregs.

In a similar vein, we saw much higher expression of CD27 in all Treg subsets compared to equivalent subsets in Tconvs, however expanded naïve and expanded Tscm-like Tregs were almost entirely $CD27^+$ (figure 5.12). CD27 is expressed by naïve T cells and can be transiently upregulated in activated memory cells such as T_{CM} cells (Nolte, Van Olffen, Van Gisbergen, & Van Lier, 2009). This co-stimulatory marker can also be expressed by both Tconvs and Tregs, and although $CD27^+$ Tconvs are non-suppressive (Duggleby, Shaw, Jarvis, Kaur, & Hill Gaston, 2007), $CD27^+$ Tregs represent a subset with potent suppressive capacity (Arroyo Hornero et al., 2020; Coenen, Koenen, Van Rijssen, Hilbrands, & Joosten, 2006; Ruprecht et al., 2005). Furthermore, several studies have also described an enrichment of $CD27^+$ Tregs when expanded in either the presence or absence of rapamycin (Arroyo Hornero et al., 2020; Coenen et al., 2006; Fraser et al., 2018; Koenen, Fasse, & Joosten, 2005).

As this strong expression of CD27 was not observed to the same extent in the expanded Tconv subsets, and it is known that Tregs can upregulate CD27 upon expansion with or without rapamycin, this again made it difficult to assess whether

CD27 was a marker of enhanced Tscm potential in the expanded naïve and Tscm-like Tregs or simply an intrinsic marker of recently activated Tregs. Despite this, the expanded naïve subsets from Tregs appeared to be particularly adept at taking on a Tscm-like phenotype. Aside from CCR7 and CD27 which were increased in all Treg subsets upon expansion, more $CD45RA^{+}CD95^{+}$ cells were found in expanded naïve Tregs and Tscm-like Tregs than in Tconvs, leading to 39.6% and 29.5% of cells baring a Tscm-like phenotype at the end of expansion, respectively (table 5.4). In addition, the higher prevalence of cells with a Tscm-like phenotype in the expanded naïve Treg subset compared to Tscm-like Tregs could be explained by rapid production of memory progeny by Tscm-like Tregs while a Tscm-like phenotype was being induced in naïve Tregs (figure 5.13). However, we saw minimal evidence of this same pattern occurring in the Tconv pool which should have served as a control for induction of Tscm-like behaviour.

There are several limitations to this T cell subset expansion experiment, the first being a lack of a negative control showing expansion of each subset in the absence of rapamycin, therefore it cannot be conclusively shown that the $CD45RA^{+}CD95^{+}$ cells seen to arise from expanded naïve Treg subsets are induced by rapamycin. Future experiments should aim to include this condition, although this would require a lower number of starting cells per subset in order to duplicate the experimental conditions, and this would also carry a risk of outgrowth of Tconv cells and loss of Treg phenotype in the expanded Tregs.

A further factor which complicates the interpretation and comparison of data from Tconv and Treg subsets is that Tconvs proliferate more rapidly in culture than

Tregs. For this reason, it could be hypothesised that the reason that we observed a higher expression of CD45RA and lower CD45R0 in the 14-day expanded naïve and Tscm-like Treg subsets compared to those in the Tconv pool (figure 5.10 + 5.11) are simply due to a slower kinetic shedding of CD45RA from the cell surface of Treg subsets, therefore flow cytometry data alone could be unreliable. However, contrary to this hypothesis, a rapid upregulation of CD45R0 was observed in Tscm-like cells over a 5 day expansion period in the absence of rapamycin (figure 5.9). Future experiments could adopt a longer set of time-course experiments with CTV labelling to measure proliferation where the changing phenotype of naïve Treg subsets is observed over several time points. Alternatively, analysis of gene expression profiles of each subset in response to rapid stimulation would give a clear indication of how T_{CM}, T_{EM}, T naïve, and Tscm-like T cells respond in the early stages of activation. Use of 10x analysis would be a powerful tool to simultaneously analyse both the surface and gene expression profiles of these subsets in future experiments.

In summary, in this experimental chapter we showed that in a single donor, cells with a stem cell-like memory surface phenotype which appeared to be proliferative were detected in the Treg compartment in peripheral blood. We did not observe conclusive evidence of stem cell-like memory function in Tscm-like cells from either the Tconv or Treg pool in the absence of rapamycin as these cells upregulated CD45R0 in culture. However, addition of rapamycin to culture media during expansion appeared to select for a large population of cells which had a Tscm-like phenotype in expanded naïve Tregs, which was driven my maintenance of naïve markers. Given that this effect appeared to be Treg-

specific, future work should aim to further investigate whether this ability of rapamycin to induce a persistent naïve phenotype in expanded Tregs plays a role in enhancing Treg suppressive function.

6 Chapter 6. Comparative phenotype and function of peripheral human Tregs in pregnancy-related disorders

6.1 Introduction

6.1.1 Immune dysregulation in pre-eclampsia and GDM

Tregs are instrumental in regulating the maternal immune response throughout pregnancy in order to protect the developing foetus expressing paternal antigens from being recognised as foreign, which can lead to pregnancy failure (Mjösberg et al., 2007). As outlined in chapter 1, several studies have reported that maternal Tregs become increasingly abundant during healthy pregnancies (Somerset, Zheng, Kilby, Sansom, & Drayson, 2004b) and play a vital role in establishing not only a state of tolerance towards foetal antigens but also in the development of the placental architecture (Care et al., 2018).

Failure of foetal-maternal tolerance induction and adaptation to new metabolic requirements during early pregnancy can result in pregnancy related disorders; some of the most common being pre-eclampsia and gestational diabetes mellitus (GDM) which both have an immune/inflammatory aetiology. Pre-eclampsia affects 4-10% of pregnancies and presents as new onset hypertension which can develop into multi-organ dysfunction and mortality in some patients (Collier, Smith, & Karumanchi, 2021). Hypertension can be managed through use of conventional β-blocker drugs such as labetalol, although the only curative treatment is delivery of the infant. Although this disease manifests as systemic

vascular dysfunction, several lines of evidence suggest that the underlying causes of pre-eclampsia are immunologically driven. For example, risk factors include nulliparity, *in vitro* fertilisation (IVF) using donor eggs, short co-habitation prior to pregnancy, and a change in sexual partner from previous pregnancies which all point towards a lack of tolerance of the maternal immune system towards foreign/paternal antigens (Mekie, Mekonnen, & Assegid, 2020).

Several immune components are known to be altered in pre-eclampsia including deposition of complement cascade proteins in the placenta and decidual tissue (Buurma et al., 2012), skewed differentiation of naïve $CD4^+$ T cells towards Th17 Tconvs rather than pTregs due to heightened inflammatory cytokines such as IL-1β and IL-6 (Santner-Nanan et al., 2009; Toldi, Rigó, Stenczer, Vásárhelyi, & Molvarec, 2011), and several studies have reported a reduced frequency of Tregs in the blood and decidua, with some also reporting reduced suppressive capacity in pre-eclampsia patients (Green et al., 2021; Hsu et al., 2012; Sasaki et al., 2007; Toldi et al., 2012, 2008; Zare, Namavar Jahromi, & Gharesi-Fard, 2019). A study by Tsuda et al. (2018) showed that there is clonal expansion of decidual effector Tregs in the third trimester of normal pregnancy but not in pre-eclampsia suggesting that peripherally induced male-antigen specific Tregs may be lacking in these patients. Others have suggested that pTreg generation is impaired in pre-eclampsia, however their use of Helios as a tTreg marker may be unreliable as pTregs can also express Helios (Hsu et al., 2012).

GDM arises in ~5-12% of pregnancies globally (Zhu & Zhang, 2016) and manifests as new onset glucose intolerance which can occur with no previous

history of type 1 or type 2 diabetes, and is driven by a failure to meet increased insulin demands due to increased insulin resistance during pregnancy (Reviewed by Harlev & Wiznitzer, 2010). GDM increases the long-term risk of type 2 diabetes in the mother and of foetal/ birth complications such as macrosomia, shoulder dystocia, and traumatic birth requiring caesarean section (Reviewed by Lekva, Norwitz, Aukrust, & Ueland, 2016).

There is evidence that low-level systemic inflammation is present from early in GDM pregnancies as evidenced by increased neutrophil counts in the first trimester (Sun et al., 2020) and increased levels of inflammatory cytokines such as IL-6 and TNF-α (Atègbo et al., 2006). A higher frequency of highly activated and a lower frequency of CTLA-4^+ $CD4^+$ T cells has been observed in GDM patients (Pendeloski et al., 2015). In addition, a study by Yang et al. (2018) showed a reduction in Treg frequencies and capacity to suppress Tconv cytokine production in GDM patients compared to at-risk controls who did not develop GDM. A recent study showed a reduced frequency of Tregs in peripheral, cord, and retroplacental blood in GDM and pre-eclampsia patients compared to normal pregnancy (Zhao et al., 2020). Conversely, other studies have shown no difference in overall Treg frequency in GDM compared to healthy pregnant women (Lobo et al., 2018; Schober et al., 2014). These differences may be due to differential use of CD25, CD127, and FoxP3 in gating on Tregs, however further studies are needed to clarify the frequency and function of Tregs in this disease.

Another study found a significant increase in Th17 and Th17.1 Tconv frequency in GDM compared to healthy controls which resulted in an increased Th17:Treg ratio which diminished post-partum (Sheu et al., 2018). Collectively, these studies suggest a state of general immune dysregulation driven by an inflammatory milieu in GDM patients.

The first line of intervention for GDM is diet alteration, and if no improvements are seen, drugs such as metformin and insulin are administered. Although these drugs have obvious effects on dysglycaemia, it is increasingly evident that immune cells can also be targets of these drugs. For example, insulin can suppress the production of pro-inflammatory markers such as c-reactive protein, IL-1β, and TNFα in T1D patients (Dandona et al., 2013). Metformin acts as an mTOR inhibitor, which as discussed in chapter 1, can inhibit the proliferation of Tconvs and promote a suppressive phenotype and selective Treg survival (Schuiveling, Vazirpanah, Radstake, Zimmermann, & Broen, 2018).

6.1.2 Treg subsets in pregnancy-related disorders

Several studies have reported differences in both peripheral blood and decidual Treg subsets during pregnancy related disorders. A study by Kisielewicz et al. (2010) showed that the mean expression of HLA-DR and suppressive capacity of Tregs was significantly reduced in preterm labour patients compared with healthy controls. Later work by the same group showed that during the second trimester in normal pregnancy, the proportion of CD45RA^{+} naïve Tregs increases while the proportion of CD45RA^{-}HLA-DR$^{+/intermediate}$ Tregs decreases in peripheral blood, possibly due to memory Treg migration to the foetal-maternal interface,

however this proportional increase in naïve Tregs fails in preterm birth and pre-eclampsia patients (Steinborn et al., 2012). Conversely, in GDM there is a significantly decreased proportion of circulating $CD45RA^+$ naïve Tregs and an increased proportion of activated $CD45RA^-HLADR^+$ Tregs which was accompanied by reduced suppressive capacity compared to healthy pregnancy (Schober et al., 2014). Irrespective of age, women who respond to IVF therapy had a higher frequency of naïve $CD45RA^+$ Tregs immediately before embryo transfer than those who did not become pregnant, and the suppressive capacity of these naïve Tregs was higher than those in the non-pregnancy women (Schlossberger et al., 2013).

The Steinborn group have shown that $CD31^+CD45RA^+$ RTE Tregs develop into $CD45RA^-CD31^-$ memory Tregs in the periphery in normal pregnancies, however in pre-eclampsia there is a significant reduction in circulating RTE Tregs and an increase in $CD45RA^-CD31^+$ memory Tregs suggesting an impairment in full Treg differentiation (Wagner et al., 2016; Wagner et al., 2015). CCR4 expression on T cells is known to aid migration to the foetal-maternal interface which expresses high levels of the CCR4 ligand CCL17 (Tsuda et al., 2002). A study by Boij et al. (2015) showed that $CCR4^+$ memory Tregs were higher in frequency in blood of pre-eclampsia patients compared with healthy pregnant women and the authors suggested that this could be evidence of impaired Treg migration to the decidua. Zhao et al. (2020) also showed that PD-1 expression on both peripheral and placental Tregs was reduced in pre-eclampsia patients. Finally, the expression of serum IL-35, mainly produced by Tregs, is significantly lower in GDM and pre-eclampsia patients than in normal pregnancy controls (Cao et al., 2018).

Together evidence shows that alterations in Treg phenotypes are prevalent in pregnancy-related disorders which provides a strong rationale for studying how the Treg phenotype affects suppressive function in pregnancy-related disorders.

We have shown in chapter 3 that the surface phenotype of Treg subsets can give rise to differing *in vitro* suppressive capacities of these subsets. Previous studies, each using small flow cytometry panels focusing on individual surface markers such as CD45RA, HLA-DR, CD31, or ICOS (Schober et al., 2014; Steinborn et al., 2012; Wagner et al., 2016; Wagner et al., 2015) have shown that Treg subset frequencies can be altered in pre-eclampsia and GDM, and that this can be accompanied by a reduction in *in vitro* suppressive capacity. However, the impact of different GDM therapeutic interventions on Treg subset frequencies and suppressive functions has not commonly been investigated. As described above, as many GDM patients are treated with potentially immune-modulating drugs, the impact of interventions such as metformin on Treg phenotype and function may have been under-appreciated in previous research. In this study, we therefore chose to stratify our GDM patient cohort into 3 distinct experimental groups; GDM on diet intervention, GDM on metformin, and GDM on metformin and insulin.

In this chapter, we aimed to investigate the following aims:

1) To use the Treg surface marker panel described in chapter 3 to investigate the frequencies of Treg subsets in peripheral blood of pregnant women with GDM on 3 separate treatment interventions, pregnant women with pre-eclampsia, or in normal pregnancies. We aimed to analyse and

compare the frequencies of Treg subsets previously described in the literature and in chapter 3.

2) To use unbiased clustering algorithms to guide our analysis of differences in frequencies of Treg subsets with novel surface phenotypes between patient groups.
3) Finally, due to limits on the approved volume of blood which could be drawn for this study, it was not possible to analyse the *in vitro* suppressive capacities of subsets of Tregs. Therefore, we aimed to compare the suppressive capacities of bulk Tregs between experimental groups and to correlate suppressive capacity to any significant changes to Treg subset frequencies.

6.2 Materials and methods

Preparation of buffers and culture media was carried out as described in chapter 2. Ethical approval for this project was granted by King's College Hospital Research Ethics Committee and informed consent was given by participants prior to blood draw. All patients were age matched to healthy pregnant controls (table 6.1). Age matching between patient groups was determined by one-way ANOVA with a Turkey's post-hoc test and no significant differences were recorded between any groups. Ethnicity was varied between groups as determined by the % of Caucasian participants. The BMI of the GDM on insulin and metformin group was significantly higher than the healthy control group, as determined by one-way ANOVA with a Turkey's post-hoc test. This is unsurprising as a significant risk of GDM occurrence is high BMI, and this patient group represents the patient

group requiring the most clinical intervention. Whole blood was collected from all participants during the third trimester at 36 weeks of gestation.

Table 6.1: Demographic data of pregnancy study participants. Age matching was determined by one way ANOVA with a Turkey's post-hoc test (no significant differences between groups)**.** BMI of GDM on metformin and insulin group was significantly higher than healthy pregnant women.

Group	Mean age (+/- SD)	Ethnicity (% Caucasian)	BMI
Healthy pregnant	35.3 (4.735)	90.000	28.35
GDM on diet	33.05 (4.018)	61.905	30.35
GDM on metformin	34.95 (4.695)	28.571	31.07
GDM on metformin and insulin	35.94 (5.879)	47.059	33.47 **
PIH/PET	32 (5.033)	80.000	28.57

For this study, we investigated the above aims while comparing 5 different experimental groups: 1) healthy pregnant (n=33), 2) GDM on altered diet (n=21), 3) GDM on metformin (n=21), 4) GDM on metformin and insulin (n=18), and 5) pregnant women with pregnancy-induced hypertension or pre-eclampsia (n=10). In this pilot study in which recruitment is still ongoing, it was not possible to recruit enough patients to ensure equal group sizes during the data collection timeframe of this experimental chapter. In addition, women with pregnancy-induced hypertension (PIH) and overt pre-eclampsia (PET) confirmed through positive proteinuria diagnosis were grouped together as progression to PET in PIH patients could not be ruled out until pregnancies came to full term. Patients with pre-existing hypertension were excluded. The 36-week timepoint of blood collection was chosen as pre-eclampsia diagnoses made after 34 weeks are

defined as early onset pre-eclampsia and are often associated with underlying co-morbidities such as impaired renal function, or other immune-mediated pregnancy complications such as antiphospholipid syndrome (Lindheimer & Chesley, 1987; Tanaka et al., 2015).

6.2.1 PBMC isolation

A total of 18ml of whole blood was collected into EDTA tubes. PBMCs were isolated and stored according to the published protocol outlined in Efthymiou et al. (2022) using SepMate PBMC isolation tubes (Stem Cell Technologies). After donation, whole blood was collected into 50ml falcon tubes and diluted 1:1 in PBS containing EDTA and 2% FBS (FACS buffer) and inverted to mix. Ficoll-Paque PLUS (GE Healthcare Pharmacia) density gradient separation media was pipetted into the bottom chamber of SepMate tubes through the insert. Diluted blood was then added to the tubes above the SepMate insert. PBMCs were then separated from whole blood by centrifuging tubes at 1200xg for 20 minutes at room temperature without the break. The majority of the plasma was then removed from the tubes and the layer containing PBMCs was poured into new 50ml falcon tubes. The tubes were topped up to 50ml with warm RPMI media and carefully inverted. Cells were then pelleted by centrifugation at 300xg for 8 minutes. After removing the supernatants and resuspending cell pellets, this wash step was then repeated using FACS buffer.

6.2.2 PBMC cryopreservation and thawing

PBMCs were counted, pelleted, and resuspended in cell freezing medium-DMSO (Sigma) and aliquoted into pre-cooled cryovials which were then transferred to

CoolCell cryogenic containers and placed in a -80°C freezer. The following day, cryovials were transferred to liquid nitrogen tanks for storage.

On the day of assay setup, cells were thawed according to the method described in chapter 2. Briefly, cryovials were placed in a 37°C waterbath until a small amount of ice remained within the samples. Vials were then moved to cell culture hoods and a Pasteur pipette was used to add pre-warmed thaw media to each vial. Samples were then transferred dropwise into 15ml falcon tubes containing warm RPMI and pelleted by centrifugation for 5 minutes at 400xg. Cells were then counted using a Trypan blue counterstain and a haemocytometer. All samples were rested at room temperature for 1 hour and then passed through a 35μm cell strainer to remove any dead cells. Up to $5x10^6$ PBMCs were then transferred to 5ml FACS tubes for suppression assay setup, while the remaining cells (~$10x10^6$) were then transferred to separate FACS tubes for immunofluorescent staining and flow cytometry analysis (figure 1).

Data collection from micro-suppression assays and Treg phenotyping were carried out across 6 experimental batches with approximately 20 samples processed per batch. Experimental groups were well mixed on each experimental day to minimise batch effects and blinding to experimental groups was carried out during assay setup and gating via flow cytometry analysis.

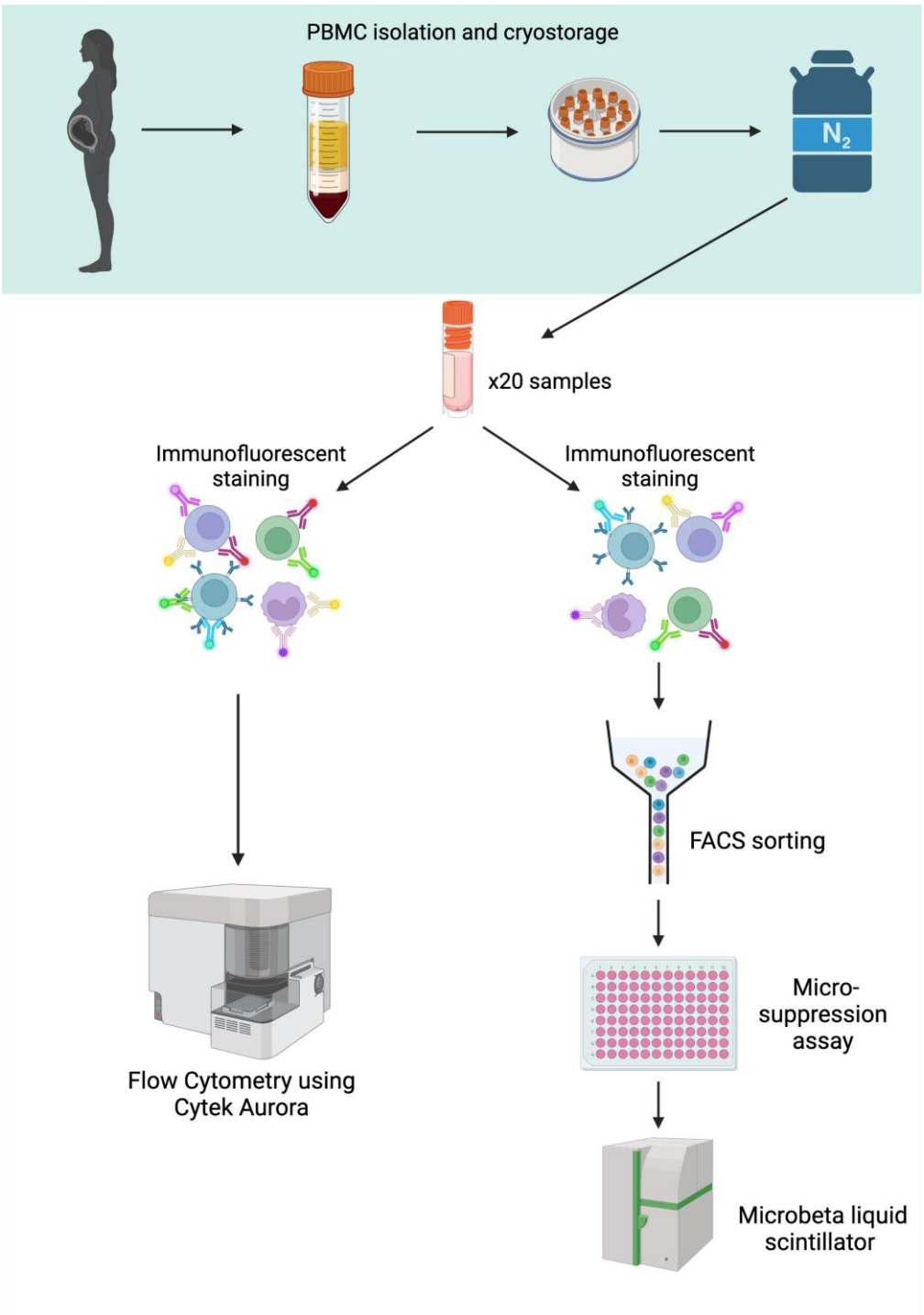

Figure 6.1: Experimental setup of Tregs in pregnancy study. PBMCs were isolated from pregnant women and cryopreserved prior to experimental setup. On each experimental day, ~20 samples were thawed per batch and each sample was divided in two to carry out a Treg micro-suppression functional assay and Treg phenotyping via spectral flow cytometry. Created using BioRender.com.

6.2.3 Bulk Treg micro-suppression assay

Following the PBMC thawing protocol described above, PBMCs from each donor were washed twice with FACS buffer (DPBS containing 2mM EDTA and 1% human AB serum) and pelleted by centrifugation at 400xg for 5 minutes. Cells were then resuspended in the residual volume remaining in the tube after removal of supernatants (~100uL) and stained with a mastermix of antibodies specific to cell surface antigens to identify B cells, Tconvs, and Tregs; CD4 AF700, CD19 APC-Cy7, CD127 PE-Cy5, CD25 PE (Table 6.2). Cells were incubated with the mastermix for 30 minutes at 4°C.

Table 6.2: Fluorochrome-conjugated monoclonal antibodies used to stain surface antigens prior to FACS sorting during the Treg micro-suppression assay.

Fluorochrome	Marker	Clone	Supplier	μL/10x10^6 cells
Master Mix				
AF700	CD4	OKT4	BioLegend	2
APC-Cy7	CD19	HIB19	BioLegend	2
PE-Cy5	CD127	A019D5	BioLegend	2.5
PE	CD25	2A3	BD Biosciences	5
PE	CD25	M-A251	BD Biosciences	5

Two washes using FACS buffer were then carried out, and finally cells were passed through a 35μm cell strainer into new polypropylene FACS tubes immediately before FACS sorting using a BD FACSAria IIu.

Cells from each donor were then FACS sorted into 96-well v-bottom plates containing culture media supplemented with 4μg/ml of phytohaemagglutinin (PHA). B cells, Tconvs, and Tregs were sorted directly into wells at a 2:1:1 (1000 B cells, 500 Tconvs, 500 Tregs) or a 4:2:1 (1000 B cells, 500 Tconvs, 250 Tregs) ratio. Wells containing B cells and Tconvs, and B cells and Tregs only were also included as controls (figure 6.2). 5 replicate wells were carried out per condition. After FACS sorting, plates were centrifuged at 400xg for 4 minutes, and cell pellets in each well were observed under a microscope. Plates were then placed in a tissue culture incubator to co-culture for 5 days.

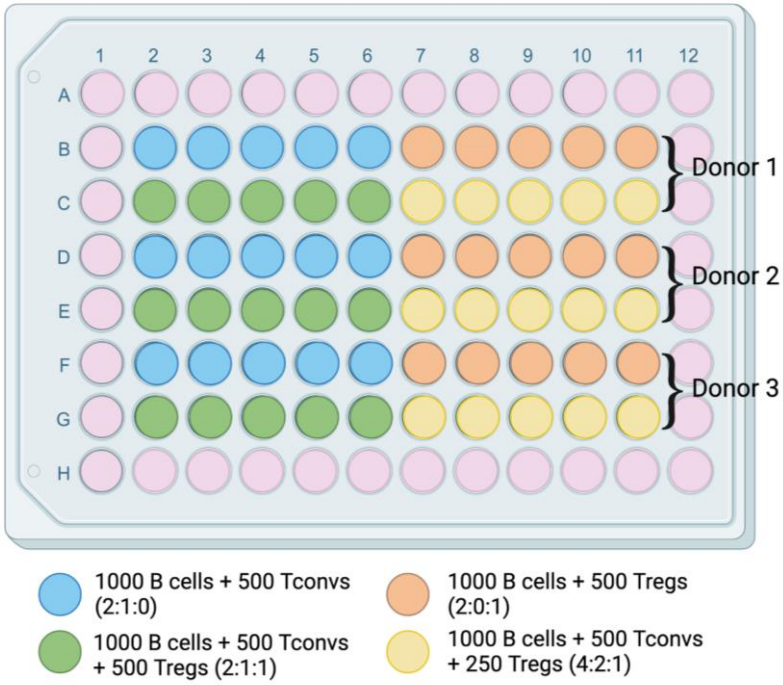

Figure 6.2: Plate layout for Treg micro-suppression assay in pregnant donors. B cells, Tconvs, and Tregs were FACS sorted directly into 96-well plates containing PHA-supplemented culture media. According to the plate layout shown above, 3 donors could be analysed per plate.

On day 5, half of the culture supernatant was removed and replaced with pre-warmed culture media containing 0.5μCi/well of tritiated thymidine (Perkin Elmer)

to measure thymidine incorporation, and co-culture was continued for a further 18 hours. The following day, the contents of each well was harvested onto glassfibre filter papers (Perkin Elmer) using a Packard Filtermat cell harvester and microwaved to dry. Dried filter papers were then placed in plastic bags, 5ml of BetaPlate Scint (Perkin Elmer) was added, and bags were sealed. The number of radioactive counts per minute in each well was then measured using a Wallac Trilux 1450 Microbeta plate reader (Wallac).

During data analysis, a pre-specified set of data quality control measures were followed: any wells in which the number of counts were more than double or less than half any of the other replicate values were counted as outliers and excluded. Any donors in which the control wells containing only B cells and Tconvs had fewer than 3000 counts per minute were excluded as non-proliferators (none recorded in this study). B cell and Treg only wells were included to evaluate any proliferation of these cells in response to PHA, and these gave <350 counts per minute in every donor meaning minimal proliferation took place. The mean counts per minutes were calculated per condition and the following formula was used to calculate percentage suppression:

$$Percentage\ Suppression = 100 - \left[\left(\frac{Sum\ of\ counts\ from\ wells\ containing\ Tregs}{Sum\ of\ counts\ from\ wells\ containing\ no\ Tregs}\right) \times 100\right]$$

6.2.4 Immunofluorescent staining for flow cytometry analysis

After resting for 1 hour after thawing and removing ~5x10^6 cells for the micro-suppression assay, PBMCs were prepared for flow cytometry analysis using the

method described below. Firstly, PBMCs were washed twice in DPBS and pelleted by centrifugation before undergoing viability staining using a 1μL/mL of Live/Dead fixable Blue cell stain (ThermoFisher) for 15 minutes at room temperature in the dark. Cells were then washed twice in FACS buffer and pelleted, and cell pellets were then resuspended in the residual volume in the FACS tubes after removing the supernatant. A mastermix of surface antibodies was then added to the cells to be incubated at 37°C for 15 minutes. This mastermix contained CXCR5 BV750, ICOS BV650, CCR4 BV605, CCR10 PerCP-Cy5.5, CD73 FITC, CXCR3 PE-Cy5, CCR6 PE-Dazzle 594 (Table 6.3). Following this incubation, a second mastermix containing further antibodies specific to surface antigens was added and incubated with the cells at 4°C for 30 minutes; CD3 BUV805, CD49d BUV737, CD45R0 BUV395, CD127 BV786, CD31 BV421, CD25 PE, CD45RA APC-Cy7, CD4 AF700, CD95 APC/Fire 810. At the end of this incubation, the cells were washed with FACS buffer, pelleted by centrifugation, and resuspended thoroughly before being fixed and permeabilised by adding 1ml of fixation/permeabilisation buffer for 40 minutes at room temperature. Cells were then washed twice with permeabilisation buffer, pelleted by centrifugation, and resuspended in the residual volume before a third mastermix containing antibodies specific to intracellular markers was added; FoxP3 AF647 and Helios PE-Cy7. Finally, cells were washed with permeabilisation buffer, pelleted, and resuspended in FACS buffer. Immediately before acquisition using a Cytek Aurora spectral analyser, cells were filtered through a 35μm cell strainer.

Table 6.3: Fluorochrome-conjugated monoclonal antibodies used to stain surface and intracellular antigens prior to flow cytometry analysis in the Tregs in pregnancy study cohort.

Fluorochrome	Marker	Clone	Supplier	µL/10x10^6 cells
Master Mix 1				
BV750	CXCR5	RF8B2	BD Biosciences	2
BV650	ICOS	DX29	BD Biosciences	5
BV605	CCR4	L291H4	BioLegend	2
PerCP-Cy5.5	CCR10	1B5	BD Biosciences	5
FITC	CD73	AD2	BioLegend	5
PE-Cy5	CXCR3	1C6/CXCR3	BD Biosciences	8
PE-Dazzle 594	CCR6	G034E3	BioLegend	2
Master Mix 2				
BUV805	CD3	UCHT1	BD Biosciences	0.3
BUV737	CD49d	9F10	BD Biosciences	2.5
BUV395	CD45R0	UCHL1	BD Biosciences	1
BV786	CD127	HIL-7R-M21	BD Biosciences	2.5
BV421	CD31	WM59	BioLegend	2.5
PE	CD25	2A3	BD Biosciences	5
PE	CD25	M-A25	BD Biosciences	5
APC-Cy7	CD45RA	HI100	BioLegend	0.3
AF700	CD4	OKT	BioLegend	2
APC/Fire 810	CD95	DX2	BioLegend	2
Master Mix 3				
AF647	FoxP3	259D	BioLegend	5
AF647	FoxP3	206D	BioLegend	5
PE-Cy7	Helios	22F6	BioLegend	2.5

6.2.5 Data analysis

Manual gating of previously reported Treg subsets was carried out using FlowJo software. Scatterplots showing frequencies of Treg subsets and bulk Treg suppression data were generated using Graphpad Prism 9 software. Statistical significance between groups in the micro-suppression assay and Treg subset frequencies was determined by one-way ANOVA with a Turkey's multiple comparisons test.

Unbiased analysis of flow cytometry data was carried out using OMIQ software. $CD4^{+}CD127^{lo}CD25^{hi}FoxP3^{+}$ Tregs were manually gated in FlowJo and imported into OMIQ. Treg events were then downsampled to 2000 events per donor before dimensionality reduction analysis. Opt-SNE was selected as the most optimal dimensionality reduction algorithm due to its ability to generate the most spatially resolved map and its ability to preserve local and global differences. Opt-SNE was carried out using the following parameters; CD45RA APC-Cy7, CD95 APC/Fire 801, FoxP3 AF647, CD45R0 BUV395, CD49d BUV737, CD31 BV421, CCR4 BV605, ICOS BV650, CXCR5 BV750, CD73 FITC, CD25 PE, CXCR3 PE-Cy5, Helios PE-Cy7, CCR6 PE-Dazzle 594, CCR10 PerCP-Cy5.5. FlowSOM clustering was then carried out using the same parameters plus opt-SNE 1 and opt-SNE 2. As described in Chapter 3, FlowSOM analysis requires the analyser to determine the number of appropriate clusters for the dataset (Cossarizza et al., 2019; Van Gassen et al., 2015). Therefore, based on our results in chapter 3 using a similar panel, FlowSOM analysis was run several times with a range of between 24-34 clusters, and clusters were analysed on an individual marker basis to determine whether the correct number of clusters has been reached. As

shown in figure 6.3, histogram overlays for each marker within each cluster could be used to determine whether under- or over- clustering had occurred. 6.3 A is an example of under-clustering as events within this cluster are not homogenous for CCR4 and CD73 expression. When FlowSOM was instructed to find 24 clusters, many clusters appeared under-clustered and therefore the FlowSOM algorithm was run again with instructions to find more clusters. The number of clusters was gradually increased until over-clustering had started to occur. Figure 6.3 B is an example of over-clustering whereby two separate clusters (31 and 32) had been identified with an almost-identical phenotype. Subtle differences in the MFI of markers such as CD45RA and CD31 were observed in these two clusters, however both clusters were clearly positive for these markers (compared to e.g. cluster 1 which was negative), therefore clusters such as these were merged. Newly merged clusters were renamed as FlowSOM 1-26 in the final figures. Heatmaps showing unbiased hierarchal clustering and EdgeR analysis were carried out using OMIQ software. Scatterplots showing the differences in abundances of each FlowSOM cluster were generated by exporting abundance data from OMIQ software and plotted in GraphPad Prism 9 software. Differences in abundances between experimental groups were determined by one-way ANOVA with a Turkey's post-hoc test.

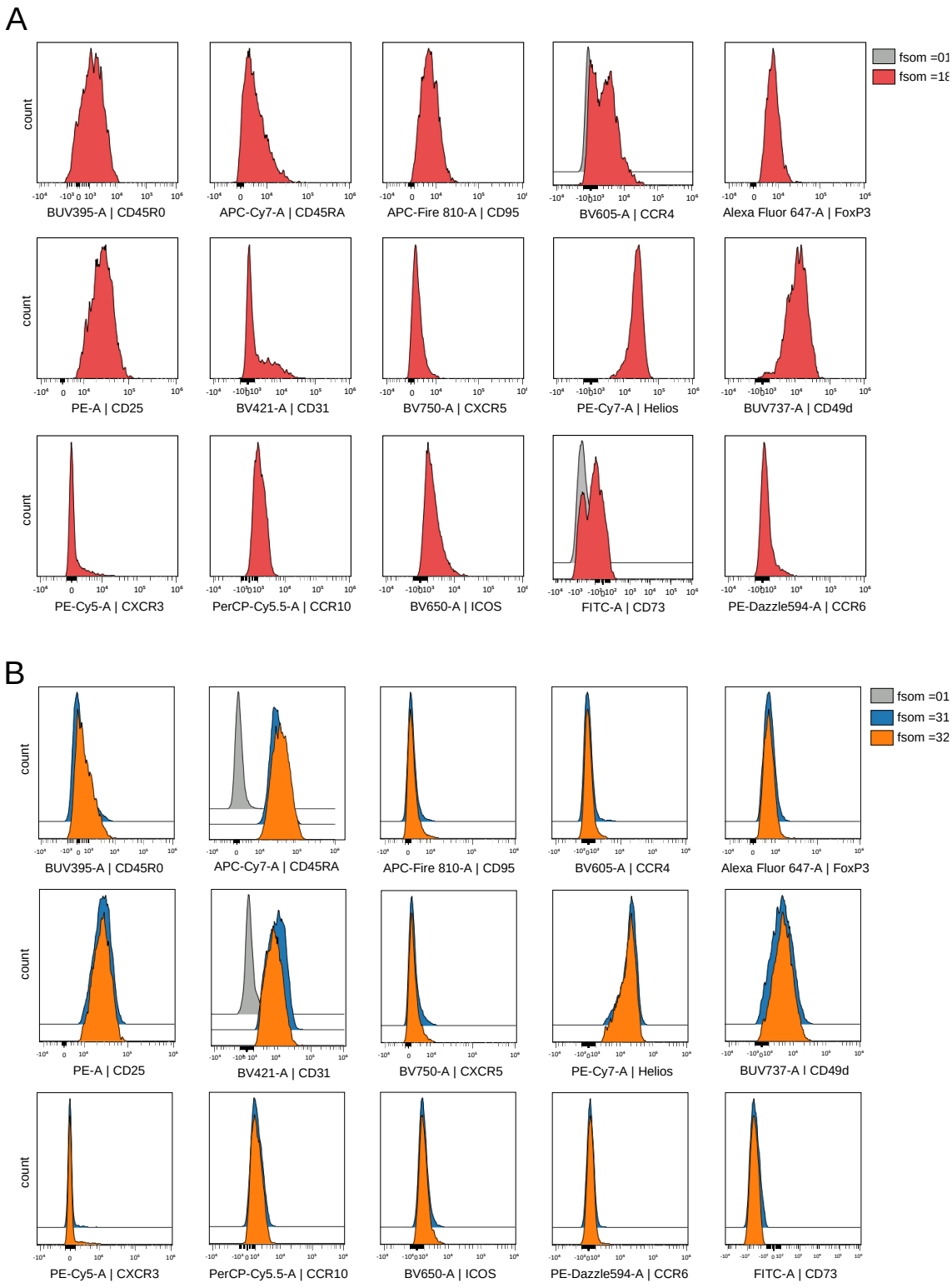

Figure 6.3: Representative histograms showing merged FlowSOM clusters. PBMCs (n=103) were stained and data acquisition carried out on a Cytek Aurora analyser. Gated bulk Tregs ($CD4^{+}CD25^{hi}CD127^{lo}FoxP3^{+}$) were down sampled to 2,000 events per donor and subjected to optSNE dimensionality reduction. FlowSOM was then used to find unbiased clusters of Treg events. K numbers of 24, 26, 28, 30, 32, and 34 clusters were trialled and

histogram overlays were used to compare clusters. (A) Representative example of under-clustering whereby cells within cluster 18 had a non-homogenous phenotype. (B) Representative example of over-clustering whereby cells within clusters 31 and 32 have the same phenotype so were merged. Analysed using OMIQ software.

6.3 Results

6.3.1 Tregs from pregnant women with GDM and pre-eclampsia have altered frequencies of previously reported Treg subsets compared to healthy pregnant women

PBMCs from healthy pregnant women, pregnant women with GDM on diet intervention, metformin, or insulin, and pregnant women with PIH/PET were isolated at 36 weeks of gestation, cryopreserved, and then analysed by flow cytometry to evaluate differences in the surface and intracellular phenotypes of Tregs between our experimental groups.

Figure 6.4 shows the gating strategy used to identify previously reported Treg subsets. This strategy identifies the same previously reported subset as shown in chapter 3, with the addition of FoxP3 gating on Tregs. As shown in figure 6.5, when gated as $CD4^{+}CD25^{hi}CD127^{low}FoxP3^{+}$ events, we observed no difference in the frequencies of total Tregs as a percentage of $CD4^{+}$ T cells between experimental groups.

When analysing the frequencies of Tregs with a memory phenotype, defined as $CD95^{+}CD45RA^{-}$ as per our gating strategy, we observed significant increases in the frequencies of these cells when comparing all GDM groups to the healthy pregnant controls. This increase was most significant when comparing the

healthy control group to the GDM patients on metformin and insulin, while the degree of significance between healthy controls versus GDM on diet, and healthy controls versus GDM on metformin was the same. There were no significant differences in the frequency of these subsets when comparing the GDM groups with different treatment interventions to one another, or when comparing the PIH/PET group patients to any other group.

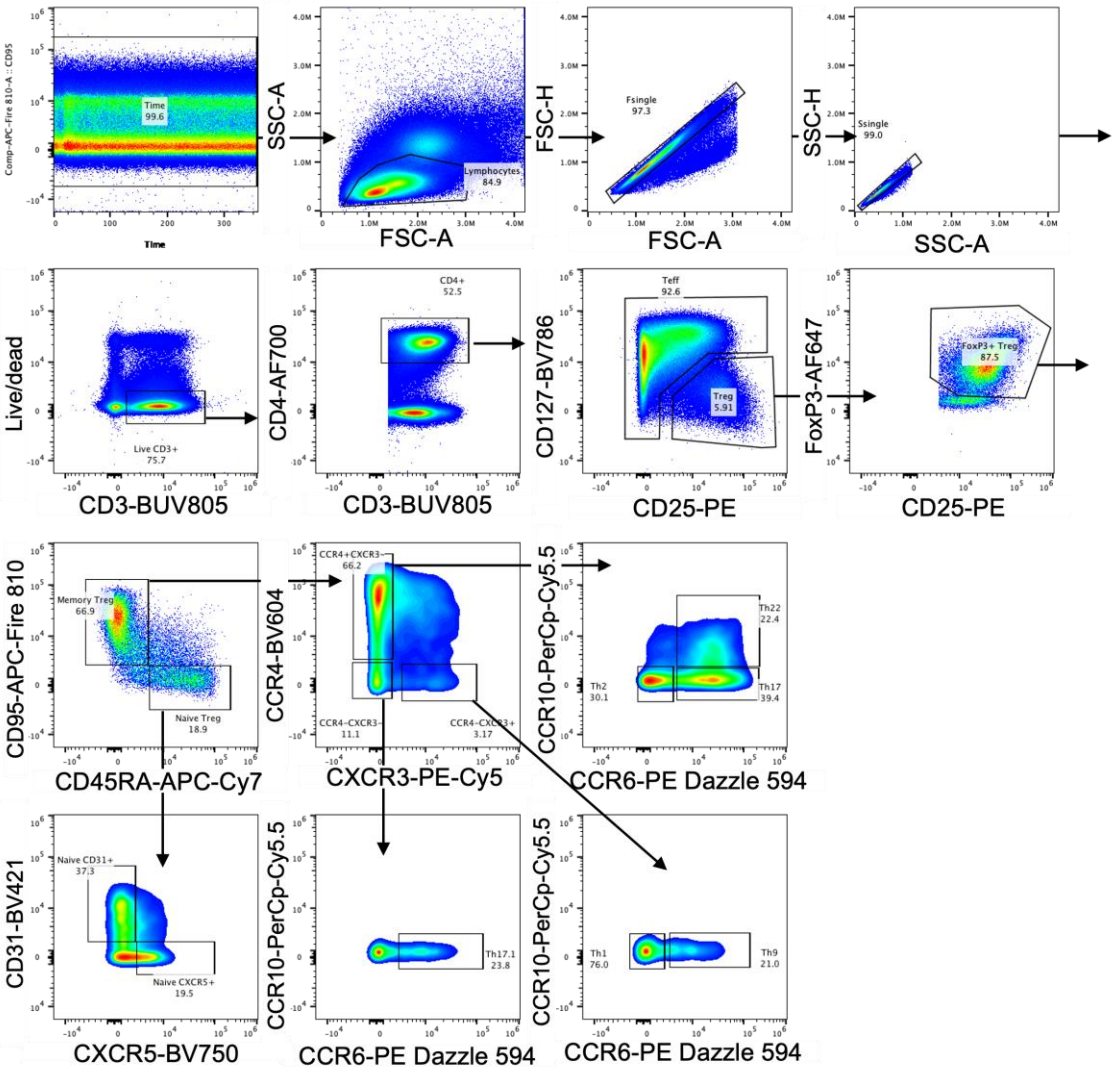

Figure 6.4: Gating strategy showing that recent thymic emigrant Tregs and T helper-like FoxP3^{+} Treg subsets could be identified by flow cytometry using surface expression of CD31 and of the chemokine receptors CCR4, CXCR3, CCR6 and CCR10. PBMCs from pregnant women at 36 weeks of gestation were stained and analysed by flow cytometry using a Cytek Aurora spectral analyser.

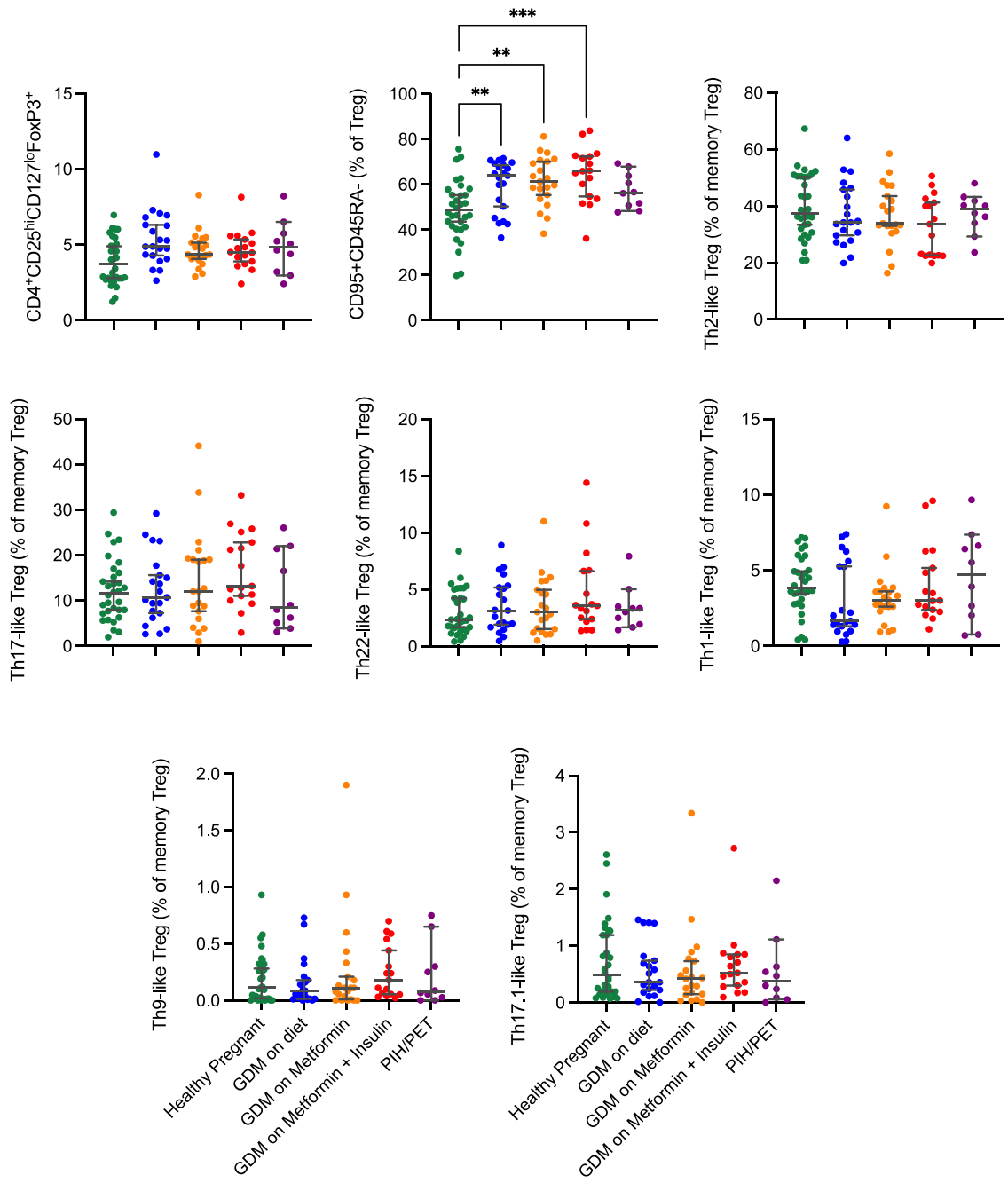

Figure 6.5: Tregs with a memory phenotype were enriched in pregnant women with gestational diabetes mellitus (GDM) on diet intervention, metformin, or metformin and insulin compared to healthy pregnant women. Cryopreserved PBMCs from pregnant donors were stained and surface markers were analysed by flow cytometry using a Cytek aurora analyser. Subsets of Tregs were gated from total $CD4^{+}CD25^{hi}CD127^{lo}FoxP3^{+}$ Tregs or from $CD4^{+}CD25^{hi}CD127^{lo}FoxP3^{+}CD45RA^{-}CD95^{+}$ memory Tregs where indicated. Significant differences between groups were determined by one-way ANOVA with a Turkey's post-hoc test. Error bars show mean +/- SEM (*= p < 0.05; **= p <0.01, ***= p <0.005). Healthy pregnant (green; n=33), GDM on diet (blue; n=21), GDM on metformin (yellow; n=21), GDM on metformin and insulin (red; n=18), PIH/PET (purple; n=10).

Within the $CD95^{+}CD45RA^{-}$ memory Treg gate, we then analysed the frequencies of Th2, Th17, Th22, Th1, Th9, and Th17.1-like Tregs in the different treatment groups. We found no significant differences in the frequencies of any of these helper-like memory Treg subsets between our treatment groups (figure 6.5). We then analysed the frequencies of the equivalent helper subsets within the Tconv pool. Firstly, there were no significant differences in the frequencies of total memory $CD95^{+}CD45RA^{-}$ cells within the Tconvs pool, showing that the significant increase in memory Tregs in the GDM groups compared the healthy controls was a Treg-specific effect (figure 6.6). In addition, in contrast to the Treg pool, there were some significant differences in the frequencies of helper subsets within Tconvs. Firstly, there was a general trend towards a decrease in the frequency of Th2 cells in all disease groups compared to healthy pregnant women, and the GDM on metformin group had a significantly lower frequency than the healthy group. Additionally, there was a trend towards an increase in Th17 Tconvs in the disease groups compared to the healthy pregnancy group, and this reached significance in the GDM on metformin and insulin group. There were no significant differences between any groups regarding the frequencies of Th22, Th1, Th9, and Th17.1 Tconvs.

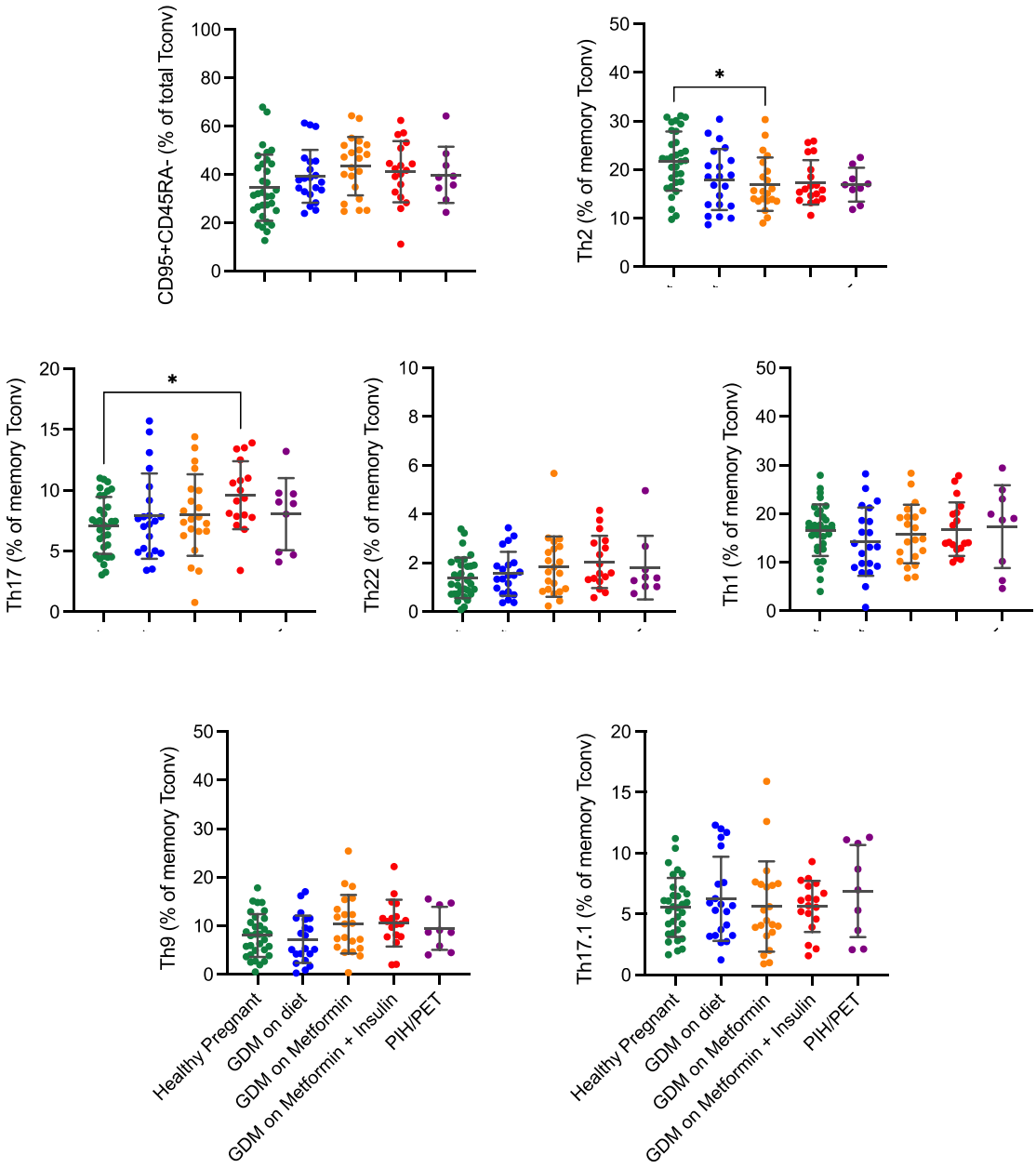

Figure 6.6: Th2 and Th17 Tconvs were enriched in pregnant women with gestational diabetes mellitus (GDM) being treated with metformin and with metformin and insulin, respectively. Cryopreserved PBMCs from pregnant donors were stained and surface markers were analysed by flow cytometry using a Cytek aurora analyser. Total Tconvs were gated as non-$CD25^{hi}CD127^{lo}$ $CD4^{+}$ events. Significant differences between groups were determined by one-way ANOVA with a Turkey's post-hoc test. Error bars show mean +/- SEM (*= $p < 0.05$; **= $p < 0.01$, ***= $p < 0.005$). Healthy pregnant (green; n=33), GDM on diet (blue; n=21), GDM on metformin (yellow; n=21), GDM on metformin and insulin (red; n=18), PIH/PET (purple; n=10).

We then investigated the frequencies of the previously reported naïve subsets within the different experimental groups (figure 6.7). Within the Treg pool, in correspondence with the increase in memory Treg subsets, we observed a trend towards a decrease in the frequencies of naïve Tregs ($CD95^{-}CD45RA^{+}$) within all disease groups compared to healthy controls, however the only significant differences recorded were between the healthy controls and GDM patients on metformin, and between healthy controls and GDM patients on metformin and insulin. Contrary to the significant difference in the frequency of memory $CD95^{+}CD45RA^{-}$ Tregs in the GDM on diet group compared to healthy controls (figure 6.5), there was no significant difference in naïve $CD95^{-}CD45RA^{+}$ Treg frequency compared to controls. In the case of Tconvs, the frequencies of naïve $CD95^{-}CD45RA^{+}$ cells between groups were unchanged. There was a significant increase in the frequency of naïve $CD31^{+}$ Tregs in the GDM on diet group compared to healthy controls, and there was no corresponding change within the Tconv pool. Finally, there was a trend towards a decrease in the frequency of naïve $CXCR5^{+}$ Tregs in the disease groups compared the healthy controls, and this difference reached statistical significance when comparing the healthy control group to the GDM on diet group. No such differences were observed in the Tconv pool, and the frequency of this subset in all groups was lower in Tconvs than in Tregs. In summary, the onset of GDM appears have an impact on the frequencies of naïve and memory Tregs which is not observed in the PIH/PET groups, and these differences in naïve and memory frequencies do not translate to the Tconv pool, although some independent differences in Tconv helper subset frequencies are observed here.

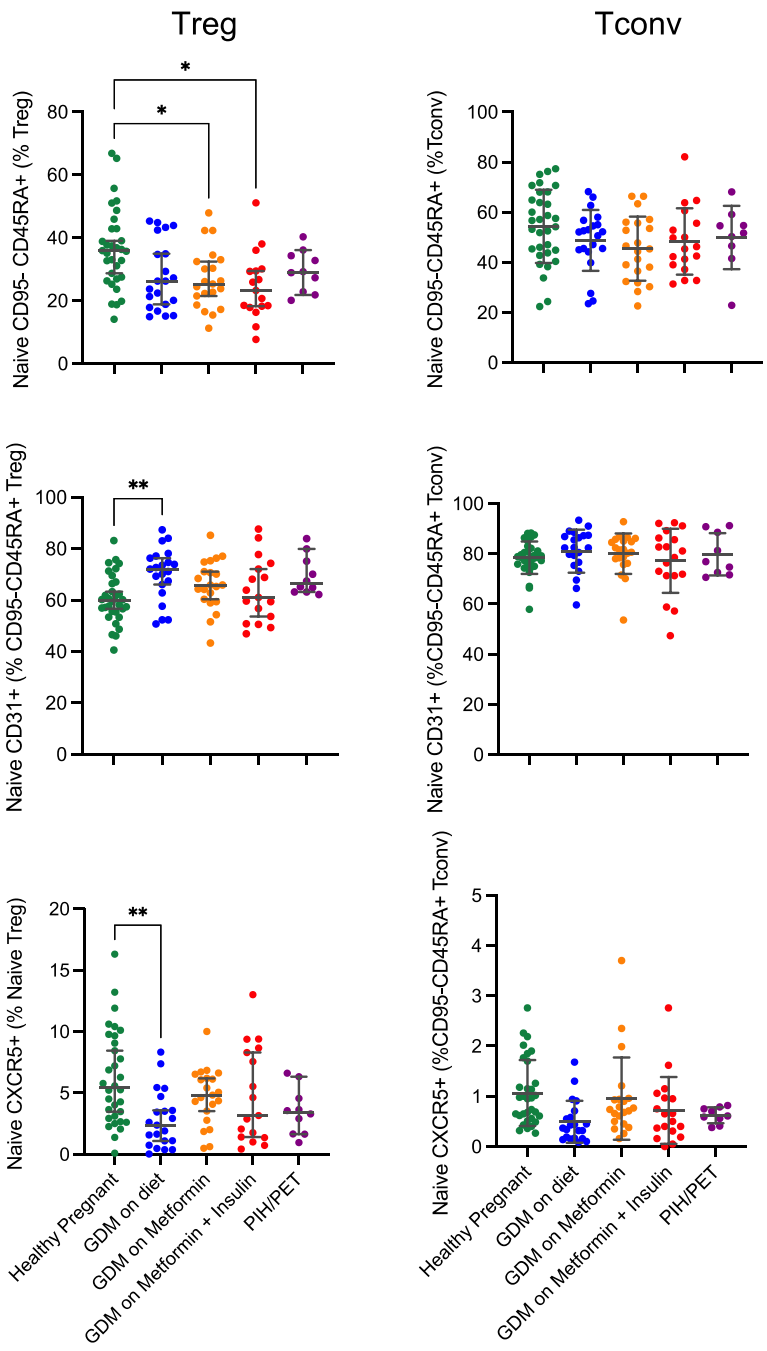

Figure 6.7: Naïve Tregs were significantly less frequent in pregnant women with gestational diabetes mellitus (GDM) on metformin, and on metformin and insulin, compared to healthy pregnant women. Cryopreserved PBMCs from pregnant donors were stained and surface markers were analysed by flow cytometry using a Cytek aurora analyser. Subsets of Tregs were gated from total $CD4^{+}CD25^{hi}CD127^{lo}FoxP3^{+}$ Tregs or from $CD4^{+}CD25^{hi}CD127^{lo}FoxP3^{+}CD45RA^{+}CD95^{-}$ naïve Tregs where indicated. Significant differences between groups were determined by one-way ANOVA with a Turkey's post-hoc test. Error bars show mean +/- SEM (*= $p < 0.05$; **= $p < 0.01$, ***= $p < 0.005$). Healthy pregnant (green; n=33), GDM on diet (blue; n=21), GDM on metformin (yellow; n=21), GDM on metformin and insulin (red; n=18), PIH/PET (purple; n=10).

6.3.2 Tregs from pregnant women with GDM and pre-eclampsia have altered frequencies of individual Treg surface markers

In order to elucidate how the expression of individual surface markers influenced the changes in previously reported Treg subsets described above, we investigated how the frequencies of cells differed on an individual marker basis between experimental groups.

As shown in figure 6.8, in addition to the increase in memory Tregs observed in the GDM groups compared to healthy controls on the basis of a $CD95^{+}CD45RA^{-}$ phenotype (figure 6.5), there was a significant increase in the expression of the memory marker CD45R0 when comparing healthy controls to all three GDM groups. The increase in $CD45R0^{+}$ Tregs was greater when comparing the GDM on metformin and GDM on metformin and insulin groups to healthy controls than when comparing the GDM on diet group to healthy controls. Again, we observed no significant differences in $CD45R0^{+}$ Tregs when comparing the GDM groups to one another, and there were no differences in the frequencies of these memory Tregs in the PIH/PET group compared to any other groups. We also observed the same differences between groups when comparing the frequencies of $CD95^{+}$ cells and the reverse was observed when analysing the frequencies of $CD45RA^{+}$ cells; healthy pregnant women had a significantly higher frequency of naïve Tregs compared to all GDM groups, and the magnitude of significance was greatest when comparing the GDM on metformin and GDM on metformin and insulin groups to healthy pregnant women. Tregs expressing CCR4, which is a marker exclusively expressed by T cells with antigen experience, were also significantly

increased in all GDM groups compared to healthy controls. The group with the most significantly increased $CCR4^+$ Tregs compared to healthy pregnant women was the GDM on metformin group, although there were no significant differences in CCR4-expressing Tregs between the different GDM intervention groups.

In addition to markers denoting memory/naïve status, Tregs expressing CCR6 were significantly more frequent in the GDM on metformin and insulin group compared to healthy controls (figure 6.8). $CXCR5^+$ Tregs, a marker for T follicular regulatory cells (Tfr), were also significantly reduced in all GDM groups compared to healthy controls. We also observed a significant increase in Tregs expressing ICOS in the GDM on metformin and GDM on metformin and insulin groups compared to healthy controls. This may again be linked to the increase in memory Tregs within these groups as our data from chapter 3 shows that ICOS expression is higher on memory Tregs than naïve Tregs. Finally, we observed an unexpected significant increase in the frequencies of $Helios^+$ Tregs in the GDM on diet, GDM on metformin, and PIH/PET groups compared to healthy controls. This was the only significant difference observed in the phenotype of the PIH/PET Tregs compared to Tregs in any other group. This confounded previous expectations as our data from chapter 4 showed that Helios expression in expanded Tregs was enriched in naïve Tregs, although the data from the current chapter show unstimulated Tregs.

We also analysed the frequencies of Tconvs expressing the individual markers described above to determine whether these changes were Treg-specific or occurred in all $CD4^+$ T cells. As shown in figure 6.9, none of the significant

changes in frequencies of Tregs expressing individual markers between experimental groups were observed in Tconvs. We saw no significant differences in markers of naivety/memory such as CD45R0, CD95, CD45RA, or CCR4 in the Tconv pool.

There were no significant differences between experimental groups in the frequencies of $CCR6^+$, $CXCR5^+$, $ICOS^+$ or $Helios^+$ Tconvs. Finally, as shown in figure 6.10, there were no significant differences in the frequencies of Tregs (A) expressing the surface markers CCR10, CD31, CXCR3, CD49d, or CD73 on an individual basis between experimental groups. In Tconvs (B), there were no significant differences in the frequencies of $CCR10^+$, $CD31^+$, or $CD73^+$ Tconvs between experimental groups. There was however a significant increase in $CXCR3^+$ Tconvs in the GDM on metformin and insulin group compared to healthy pregnant women, although there was a trend towards an increase in $CXCR3^+$ frequency which did not reach significance in the remaining two GDM groups compared to healthy controls. In addition, the frequency of $CD49d^+$ Tconvs was significantly reduced in the GDM on metformin group compared to healthy controls.

To conclude, many significant increases in the frequencies of individual markers associated with a memory status were observed in GDM groups compared to healthy controls, and also a reduced frequency of the Tfr marker CXCR5 was observed in GDM Tregs. These changes were not observed in the equivalent Tconv populations.

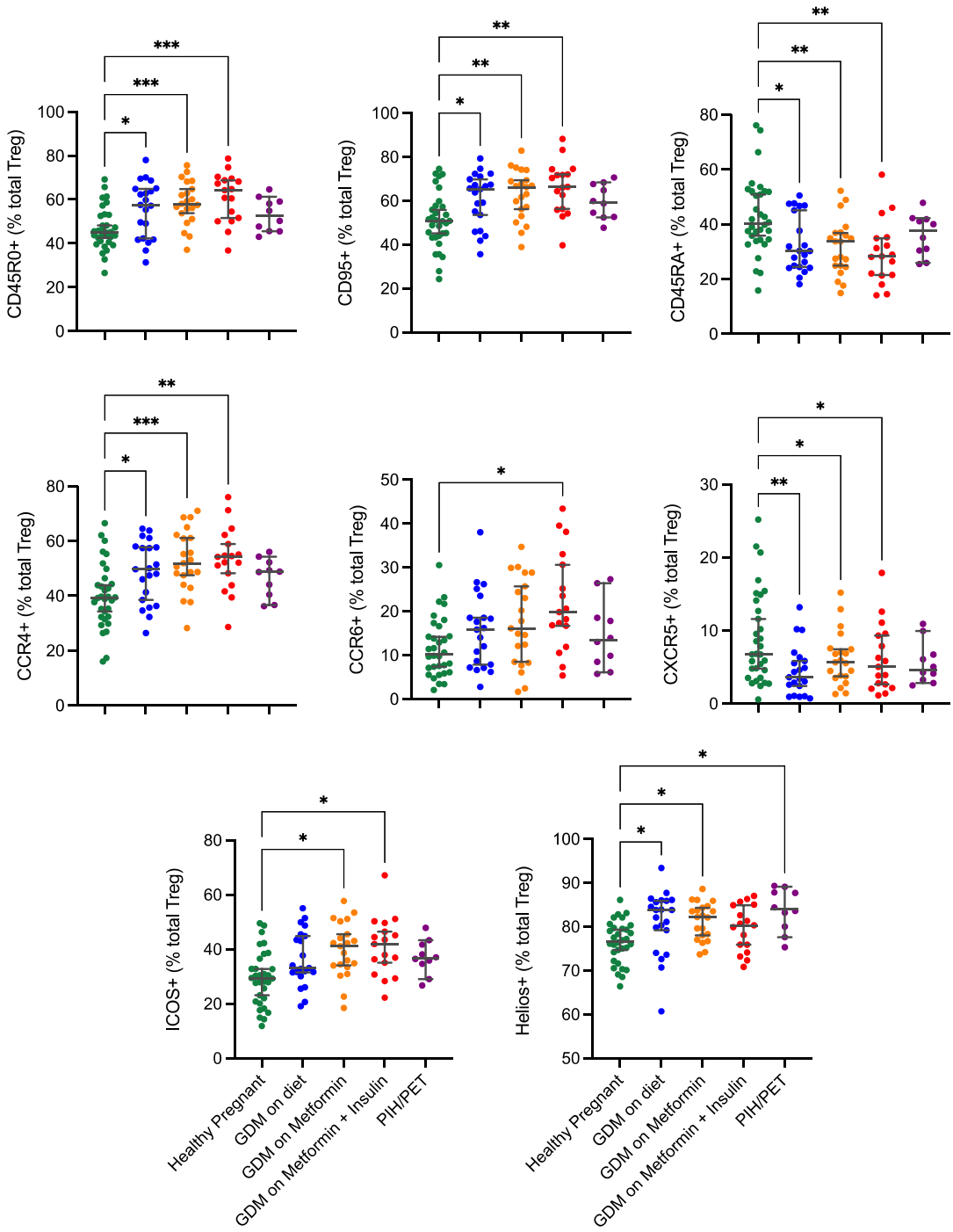

Figure 6.8: Tregs expressing individual markers of memory status were enriched in pregnant women with gestational diabetes mellitus (GDM) on diet intervention, metformin, or metformin and insulin compared to healthy pregnant women. Cryopreserved PBMCs from pregnant donors were stained and surface markers were analysed by flow cytometry using a Cytek aurora analyser. Subsets of Tregs were gated from total $CD4^{+}CD25^{hi}CD127^{lo}FoxP3^{+}$ Tregs or from $CD4^{+}CD25^{hi}CD127^{lo}FoxP3^{+}CD45RA^{-}CD95^{+}$ memory Tregs where indicated. Significant differences between groups were determined by one-way ANOVA with a Turkey's post-hoc test. Error bars show mean +/- SEM (*= $p < 0.05$; **= $p < 0.01$, ***= $p < 0.005$). Healthy pregnant (green; n=33), GDM on diet (blue; n=21), GDM

on metformin (yellow; n=21), GDM on metformin and insulin (red; n=18), PIH/PET (purple; n=10).

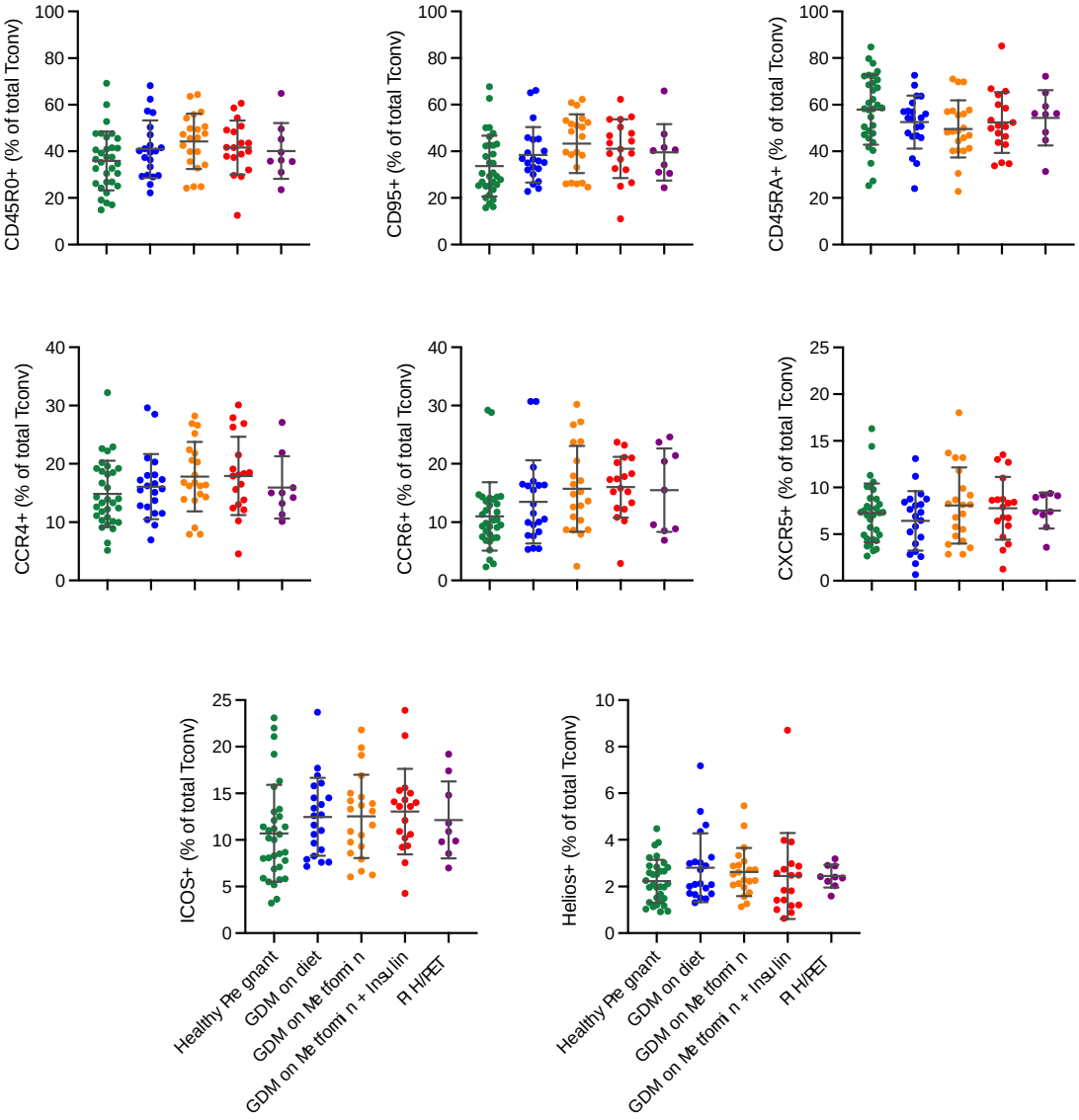

Figure 6.9: Frequencies of Tconvs expressing individual markers of memory status were unchanged in pregnant women with gestational diabetes mellitus (GDM) compared to healthy pregnant women. Cryopreserved PBMCs from pregnant donors were stained and surface markers were analysed by flow cytometry using a Cytek aurora analyser. Total Tconvs were gated as non-$CD25^{hi}CD127^{lo}$ $CD4^{+}$ events. Significant differences between groups were determined by one-way ANOVA with a Turkey's post-hoc test. Error bars show mean +/- SEM (*= p < 0.05; **= p <0.01, ***= p <0.005). Healthy pregnant (green; n=33), GDM on diet (blue; n=21), GDM on metformin (yellow; n=21), GDM on metformin and insulin (red; n=18), PIH/PET (purple; n=10).

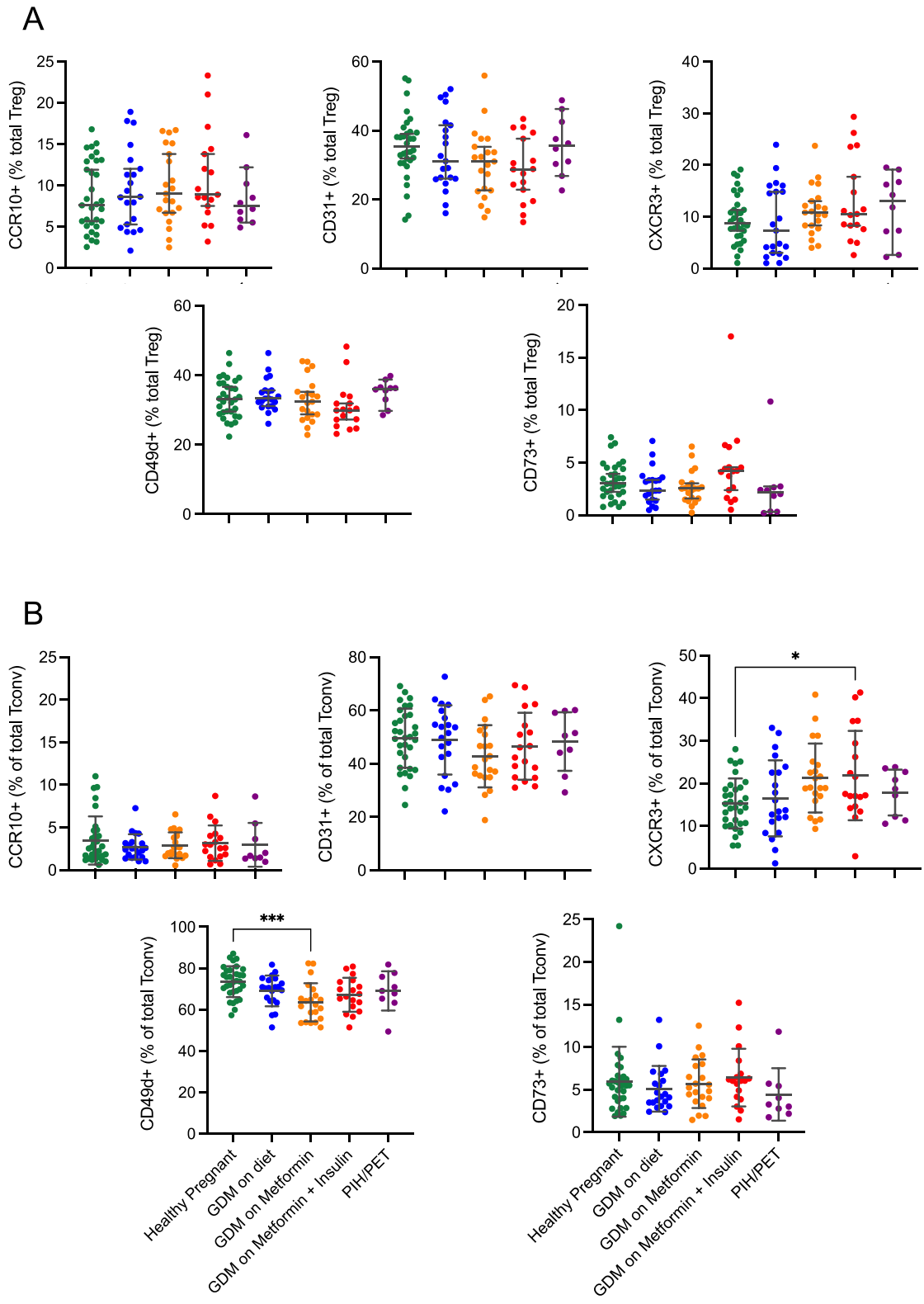

Figure 6.10: Frequencies of Tregs (A) and Tconvs (B) expressing non-significantly different individual markers in healthy pregnant women, pregnant women with GDM on diet intervention, metformin, or metformin and insulin, and pregnant women with PIH/PET. PBMCs were stained and surface markers were analysed by flow cytometry using a Cytek aurora analyser. Significant differences between groups were determined by one-

way ANOVA with a Turkey's post-hoc test. Error bars show mean +/- SEM (*= $p < 0.05$; **= $p < 0.01$, ***= $p < 0.005$). Healthy pregnant (green; n=33), GDM on diet (blue; n=21), GDM on metformin (yellow; n=21), GDM on metformin and insulin (red; n=18), PIH/PET (purple; n=10).

6.3.3 A comparison of unbiased clusters of Tregs from healthy pregnant women, pregnant women with GDM on diet intervention, metformin, or metformin and insulin treatment, and pregnant women with PIH/PET

In addition to the above Treg phenotype analysis which investigated the frequencies of known Treg subsets between experimental groups, we also used unbiased clustering tools which would help to elucidate the phenotypic differences in Tregs between groups in an unsupervised manner.

Firstly, manually gated Treg events ($CD4^+CD25^{hi}CD127^{lo}FoxP3^+$) from 103 donors from our different experimental groups were concatenated and optSNE was selected as a dimensionality reduction algorithm. As shown in figure 6.11, optSNE was successful in spatially segregating Treg events on the basis of memory/naïve markers as naïve events expressing CD45RA largely did not co-localise with CCR4, CD95, or CD45R0. $CD31^+$ events could be found in both memory and naïve regions, and as expected FoxP3 and CD25 expression was highest in memory regions. Helios positive and negative Treg events were spatially distinct on the optSNE map and a $Helios^-$ status seemed to be the driver of separation of the smaller clade seen towards the top left of the optSNE map. Expression of the chemokine receptor CXCR5, and CD73 and CD49d occurred in clusters of cells within the memory and naïve regions, whereas CCR10, CCR6, and CXCR3-expressing cells largely occurred in memory regions.

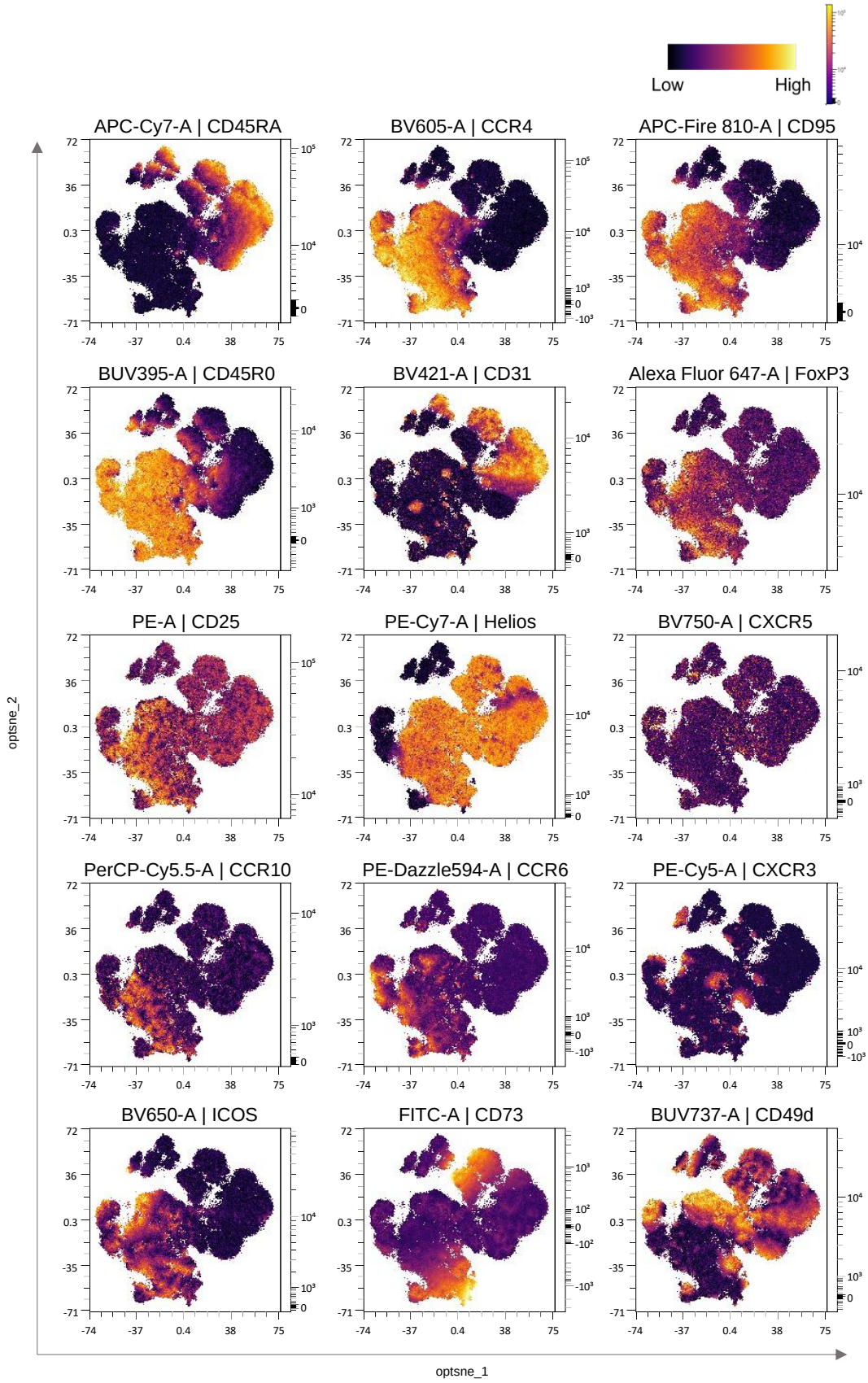

Figure 6.11: optSNE colour-axis overlays of Treg surface marker expression within the total pregnancy cohort. PBMCs from pregnant donors (n=103) were stained and data acquisition carried out on a Cytek Aurora analyser. Gated bulk Tregs

($CD4^+CD25^{hi}CD127^{lo}FoxP3^+$) were down sampled to 2,000 events per donor and the optSNE algorithm was used for dimensionality reduction analysis of the concatenated Treg dataset. Analysed using OMIQ software. Scales indicate low to high MFIs of each marker.

Next, unbiased clustering was carried out using the clustering algorithm FlowSOM. A detailed description of the methods used to identify the correct number of clusters can be found in 6.2.5 and figure 6.3. This process resulted in a total of 26 Treg clusters within this dataset, as shown in figure 6.12 which shows each FlowSOM cluster overlaid on the optSNE plot. The agglomerative hierarchal clustering of these 26 clusters are shown in the heatmap in figure 6.13 A. Once again, in agreement with the data in chapter 3 and in 6.11, markers expressed highly by memory Tregs such as CD25, CCR4, CD45R0, CCR10, FoxP3, ICOS, and CD95 clustered together on the marker dendrogram, and FlowSOM clusters with an activated memory status clustered together towards the bottom half of the heatmap. Naïve clusters expressing CD45RA and CD31 tended to cluster towards the top of the heatmap. As also seen in chapter 3, there appeared to be some 'transitioning' subsets which co-expressed markers of naivety such as CD45RA, and memory such as CD45R0 e.g. clusters 7, 9, 10, 11, and 22.

.

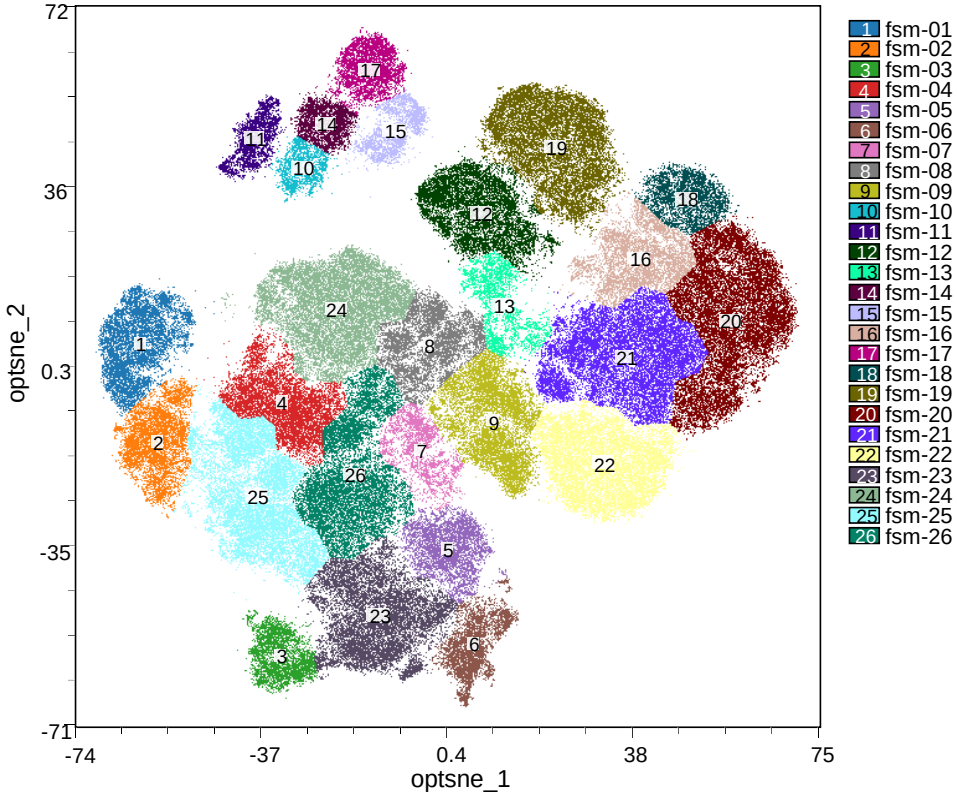

Figure 6.12: FlowSOM clustering identified 26 unbiased clusters of Tregs within the pregnancy study cohort. PBMCs from pregnant donors (n=103) were stained and data acquisition carried out on a Cytek Aurora analyser. Following $CD4^{+}CD25^{hi}CD127^{lo}FoxP3^{+}$ Treg gating, down sampling, and dimensionality reduction using the optSNE algorithm, the FlowSOM clustering algorithm was used to identify unbiased subsets of Tregs. Treg FlowSOM clusters were overlaid on the optSNE dimensionality reduction plot for visualisation.

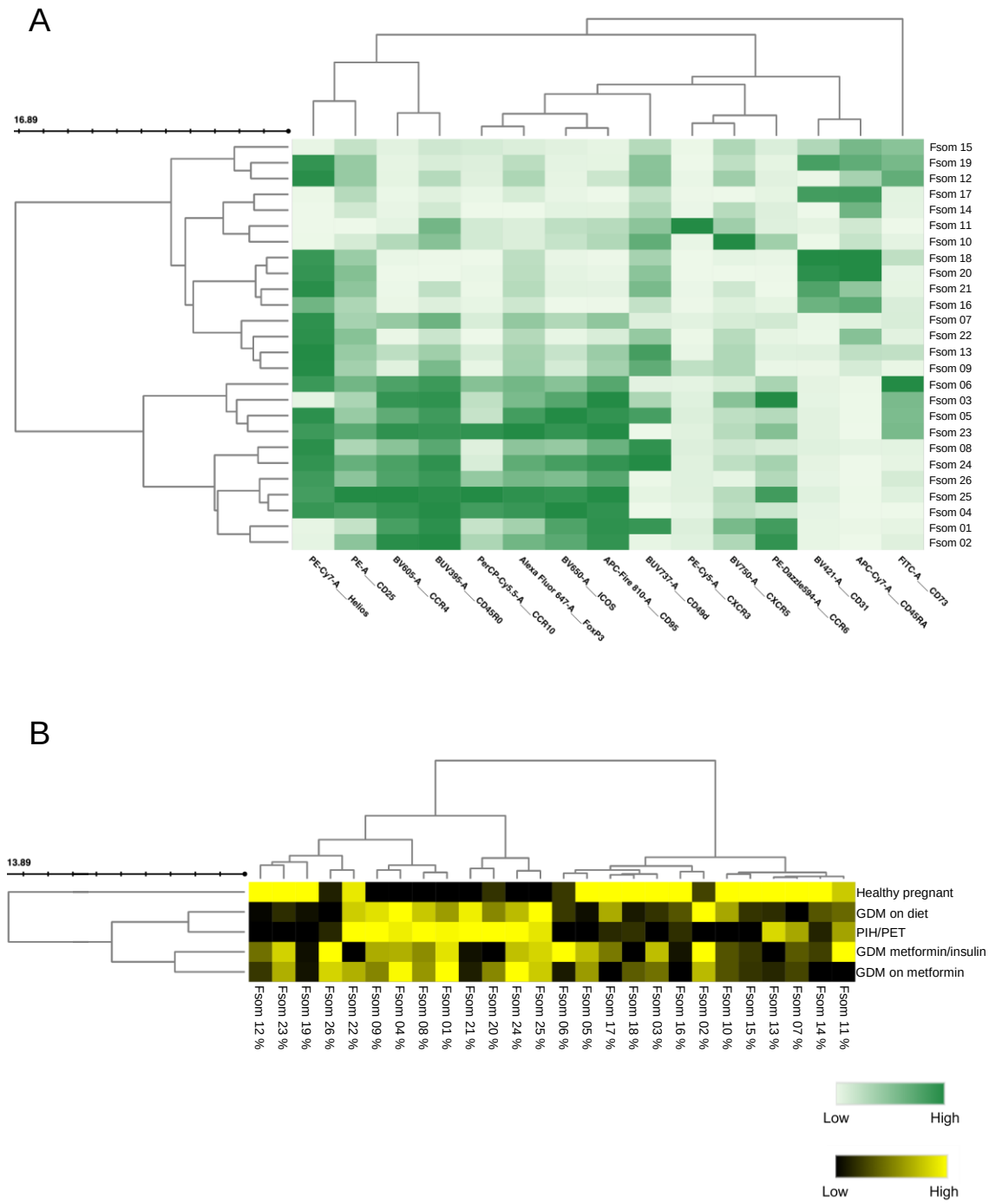

Figure 6.13: Healthy pregnant women had differing abundances of FlowSOM clusters to women with pregnancy-related disease. PBMCs from pregnant donors (n=103) were stained and data acquisition carried out on a Cytek Aurora analyser. Following $CD4^{+}CD25^{hi}CD127^{lo}FoxP3^{+}$ Treg gating, down sampling, and dimensionality reduction using the optSNE algorithm, the flowSOM clustering algorithm was used to identify unbiased subsets of Tregs. (A) Relative expression of each marker within each FlowSOM Treg cluster. (B) Relative abundance of each FlowSOM cluster, expressed as percentage of total Tregs, within each experimental patient group.

The heatmap in figure 6.13 B shows the relative abundances of each FlowSOM cluster within the different experimental groups. As shown by the experimental group agglomerative hierarchal clustering dendrogram on the left, according to the relative abundance of FlowSOM subsets within the concatenated donors from each experimental group, healthy pregnant women clustered separately to all other disease groups and the GDM on metformin group was the most spatially segregated from healthy pregnant women. Many of the naïve clusters which feature towards the top of heatmap 6.13 B, including 15, 19, 12, 17, 14 are the most abundant clusters in the healthy pregnant women relative to the other experimental groups. This finding aligns with our analysis above of manually gated Treg populations which showed that memory Tregs were more frequent in the GDM patient groups than in healthy pregnant women.

We then sought to investigate the differences in the abundances of each cluster between experimental groups in more detail. To do this, we first carried out edgeR analysis in each pregnancy-related disease group compared with healthy pregnant women. This analysis identified which Treg FlowSOM clusters were significantly altered in each disease group vs healthy pregnant women and results were visualised on the volcano plots shown in figure 6.14. Interestingly, largely the same FlowSOM clusters were identified as being significantly altered in the different disease groups compared to healthy pregnant women. FlowSOM clusters which were reproducibly and significantly increased in abundance in the healthy pregnant women compared to every disease group were clusters 12, 14, 15, 16, 18, and 19. Clusters 5, 3, and 23 were also significantly increased in healthy vs the GDM on diet group, and also healthy vs PIH/PET group. Clusters

3, 10, 13, 11, and 17 were also identified as significantly increased in abundance in the healthy vs GDM on metformin analysis. Finally, the frequencies of 17 and 10 were also identified as being significantly increased in the healthy group compared to the PIH/PET group.

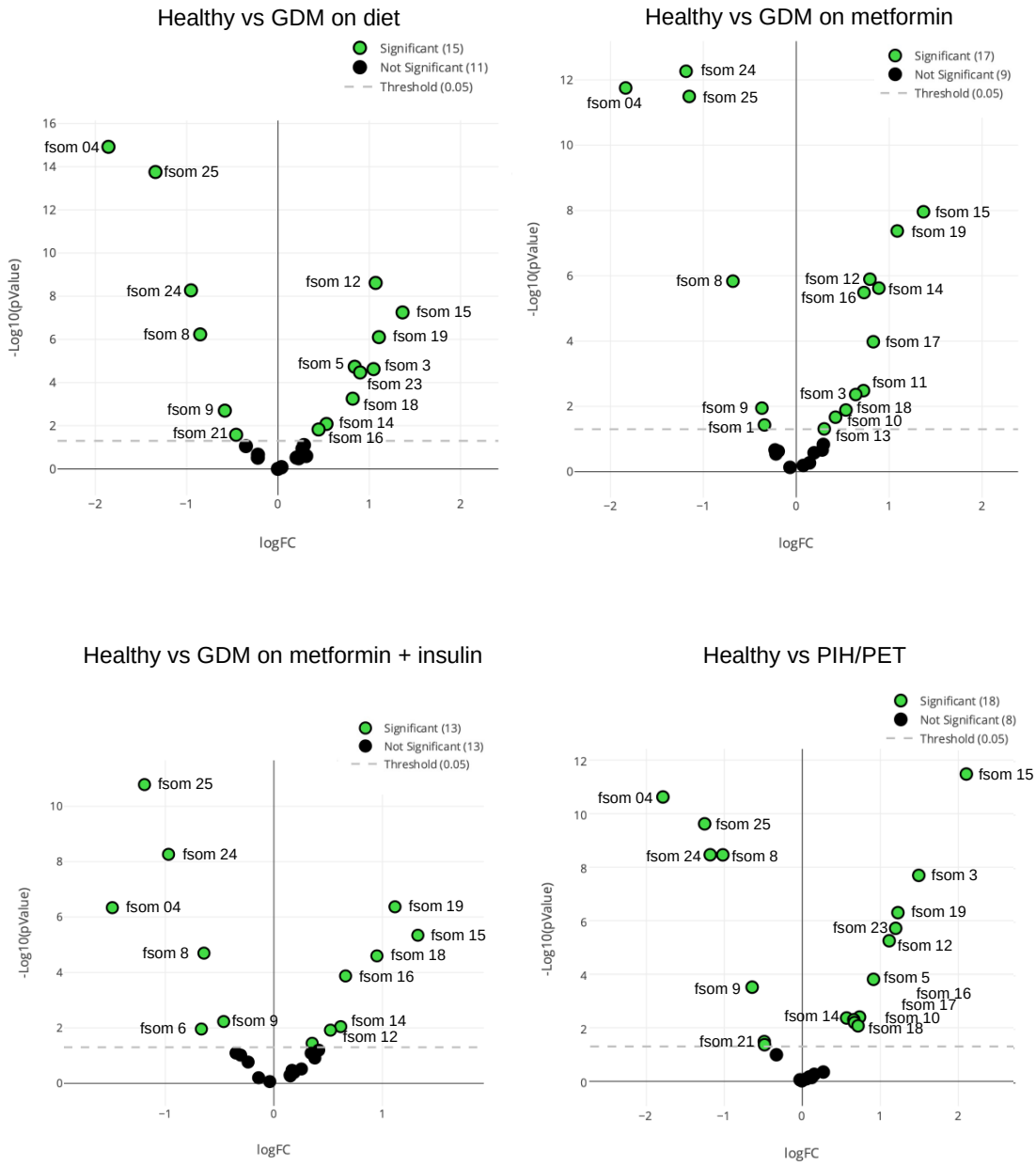

Figure 6.14: EdgeR analysis showing the differential abundances of Treg FlowSOM clusters in each disease group compared to healthy pregnant women. PBMCs from pregnant donors (n=103) were stained and data acquisition carried out on a Cytek Aurora analyser. Following $CD4^{+}CD25^{hi}CD127^{lo}FoxP3^{+}$ Treg gating, down sampling, and dimensionality reduction using the optSNE algorithm, the FlowSOM clustering algorithm was used to identify unbiased subsets of Tregs. Differences in abundance of FlowSOM clusters between healthy pregnant women and each individual disease group were identified by edgeR analysis. Degree of significance is shown by the –Log10(pvalue) on the left axis. Analysis carried out using OMIQ software.

In terms of clusters which were significantly decreased in abundance in the healthy group compared to each disease group, clusters 4, 8, 9, 24, and 25 appeared in every edgeR analysis of healthy vs each disease group (figure 6.14). Clusters 21, 1, and 6 also appeared as borderline-significantly decreased in some of the disease groups.

In total, according to the edgeR analysis, the PIH/PET groups had the most significantly altered clusters (18) compared to healthy controls, followed by 17, 15, and 13 respectively for the GDM on metformin, GDM on diet, and GDM on metformin and insulin groups. This is interesting as the above analysis which focussed on frequencies of previously reported Treg subsets and on Tregs expressing individual markers identified only one significantly altered parameter in the PIH/PET group compared to healthy controls which was frequency of Helios^{+} cells (figure 6.8). This emphasises the importance of taking an unbiased clustering approach to guide analysis of high dimensional flow cytometry data.

After identifying potential subsets of interest using edgeR analysis, we sought to explore the phenotypes of these clusters further and to confirm the differences in abundances of each cluster between groups as it was only possible to compare two groups at a time using edgeR analysis. The relative frequencies of each FlowSOM cluster (as a % of total Treg events within each donor) were analysed this time by one-way ANOVA to determine significant differences in the abundances of each cluster between all the experimental groups.

Figure 6.15 shows all the clusters which were identified as being significantly higher in abundance in the healthy pregnant group compared to other disease groups during edgeR analysis. In agreement with the edgeR analysis, clusters 12, 14, 15, 16, and 19 were significantly less frequent in all disease groups compared to healthy pregnant women. During edgeR analysis, cluster 18 was also identified as being significantly higher in frequency in healthy pregnant women compared to all other disease groups, however only GDM on diet and GDM on metformin and insulin groups had a significantly reduced frequency of this cluster compared to healthy controls in this analysis. Furthermore, cluster 17 was significantly reduced only in the GDM on metformin group compared to healthy pregnant women. The phenotypes of each of these FlowSOM clusters are shown in table 6.4. As identified here, clusters 12, 14, 15, 16, 17, 18, and 19 are all of a naïve phenotype expressing CD45RA and no CD45R0. Many of these naïve clusters also expressed CD73 such as clusters 12, 15, 18, and 19 which were some of the most differentially increased in healthy pregnant women compared to disease in the edgeR analysis. Clusters 3, 5, and 23 were also shown to be significantly decreased in GDM and PIH/PET groups compared to healthy controls. As shown in table 6.4, these 3 subsets had a memory phenotype ($CD45RA^{-}CD45R0^{+}CCR4^{+}CD95^{+}ICOS^{+}$). Interestingly, these 3 memory Treg clusters also all expressed CD73. There were no significant differences in the abundances of clusters 10 or 11 between experimental groups using this analysis. There were no significant differences observed in the abundances of any of the above clusters when comparing the different GDM or PIH/PET groups with one another.

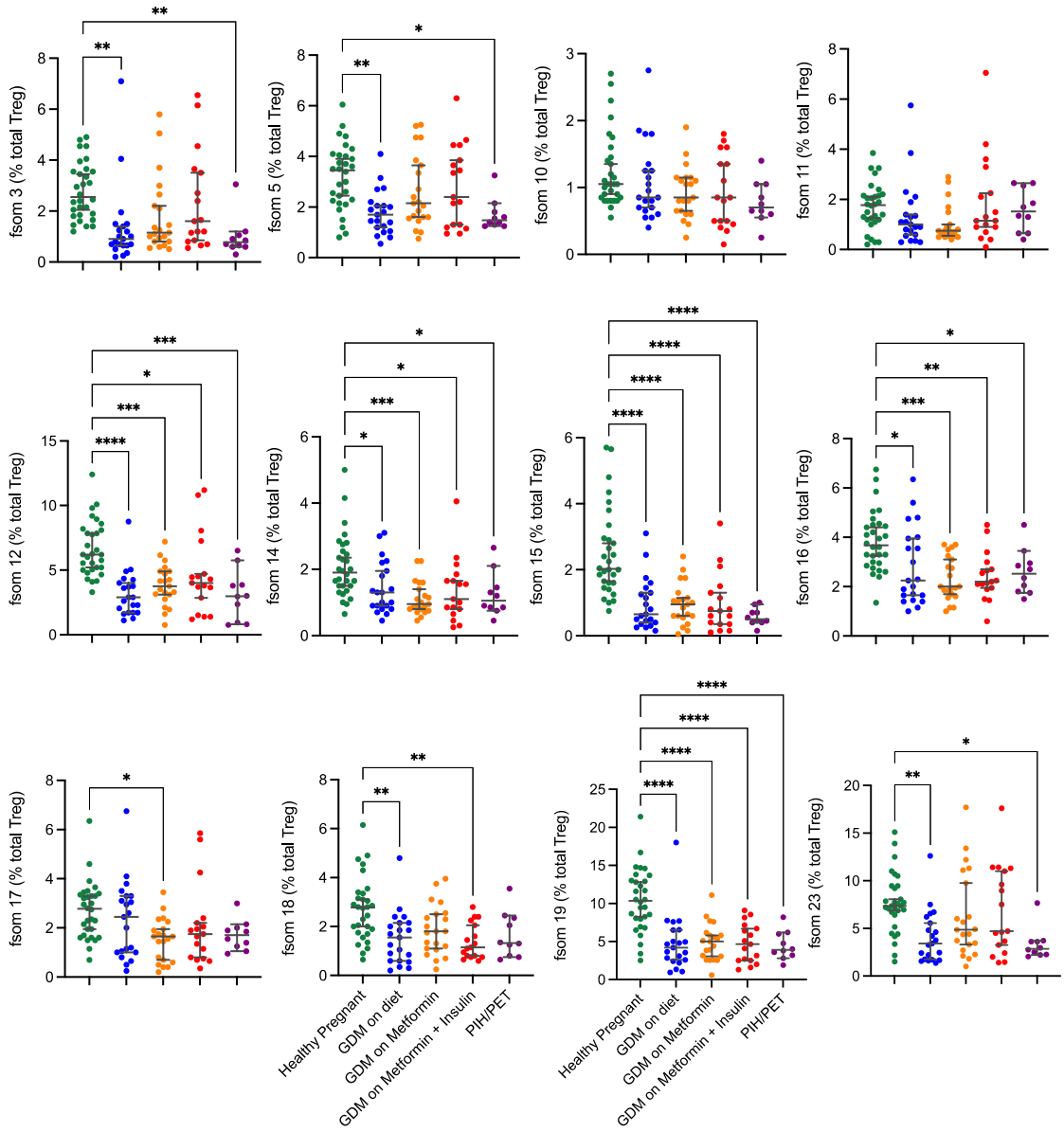

Figure 6.15: FlowSOM Treg clusters which were increased in abundance in healthy pregnant women compared to disease groups. PBMCs from pregnant donors (n=103) were stained and data acquisition carried out on a Cytek Aurora analyser. $CD4^{+}CD25^{hi}CD127^{lo}FoxP3^{+}$ Treg events were analysed by down sampling, dimensionality reduction using the optSNE algorithm, and flowSOM clustering. Following this, significant differences in the abundances of each cluster were compared between each experimental group by one-way ANOVA with a Turkey's post-hoc test. Error bars show mean +/- SEM (*= $p < 0.05$; **= $p < 0.01$, ***= $p < 0.005$, ****= $p < 0.001$). Healthy pregnant (green; n=33), GDM on diet (blue; n=21), GDM on metformin (yellow; n=21), GDM on metformin and insulin (red; n=18), PIH/PET (purple; n=10).

Table 6.4: Phenotypes of significantly altered FlowSOM Treg clusters.

FlowSOM cluster	Helios	CD25	CCR4	CD45R0	CCR10	FoxP3	ICOS	CD95	CD49d	CXCR3	CXCR5	CCR6	CD31	CD45RA	CD73	Frequency in healthy relative to disease groups	Naïve or Memory
3	-	+	+	+	-	+	+	+	-	-	+	+	-	-	+	Increased	Memory
4	+	+	+	+	+	+	+	+	-	-	-	-	-	-	-	Decreased	Memory
5	+	+	+	+	-	+	+	+	+	-	-	-	-	-	+	Increased	Memory
8	+	+	+	+	-	+	+	+	+	-	-	-	-	-	-	Decreased	Memory
12	+	+	-	-	-	+	-	-	+	-	+	-	-	+	+	Increased	Naïve
14	-	+	-	-	-	+	-	-	+	-	+	-	-	+	-	Increased	Naïve
15	-	+	-	-	-	+	-	-	+	-	+	-	+	+	+	Increased	Naïve
16	+	+	-	-	-	+	-	-	-	-	-	-	+	+	-	Increased	Naïve
17	-	+	-	-	-	+	-	-	-	-	-	-	+	+	-	Increased	Naïve
18	+	+	-	-	-	+	-	-	+	-	-	-	+	+	+	Increased	Naïve
19	+	+	-	-	-	+	-	-	+	-	+	-	+	+	+	Increased	Naïve
23	+	+	+	+	+	+	+	+	-	-	+	+	-	-	+	Increased	Memory
24	+	+	+	+	-	+	+	+	+	-	+	+	-	-	-	Decreased	Memory
25	+	+	+	+	+	+	+	+	-	-	+	+	-	-	-	Decreased	Memory

Figure 6.16 shows the relative abundances of clusters identified by edgeR which were significantly decreased in healthy pregnant women compared to the disease groups. Clusters 4, 8, 24, and 25 were all significantly increased in every disease group compared to healthy pregnant women. As shown in table 6.4, these clusters all shared a highly activated memory phenotype, expressing high levels of Helios, CD25, CCR4, CD45R0, FoxP3, and ICOS. These subsets may account for the unexpected increase in Helios single-positive Tregs seen in the GDM on diet, GDM on metformin, and PIH/PET groups compared to healthy controls (figure 6.8). Additionally, in contrast to the clusters which were relatively increased in healthy compared to disease groups, none of these clusters expressed CD73. FlowSOM clusters 1, 6, 9, and 21 which were identified as borderline significantly altered in edgeR analysis showed no differences in abundance using this analysis. Again, there were no significant differences when comparing the different GDM and PIH/PET disease groups to one another. Figure 6.17 also shows the abundance data for the remaining clusters in which no significant differences were recorded between experimental groups.

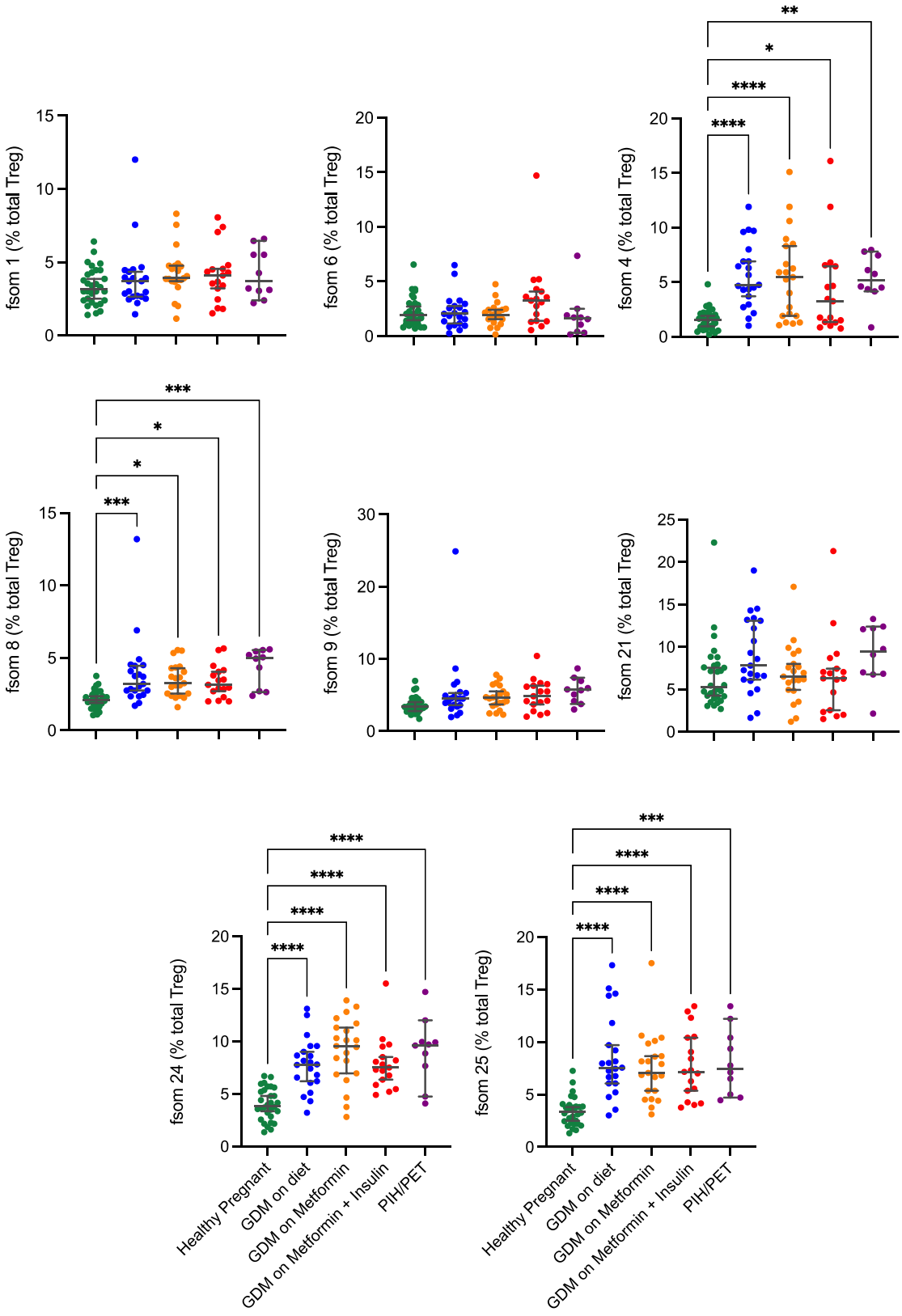

Figure 6.16: FlowSOM Treg clusters which had lower abundances in healthy pregnant women compared to disease groups. PBMCs from pregnant donors (n=103) were stained and data acquisition carried out on a Cytek Aurora analyser. $CD4^{+}CD25^{hi}CD127^{lo}FoxP3^{+}$ Treg events were analysed by down sampling, dimensionality reduction using the optSNE

algorithm, and flowSOM clustering. Following this, significant differences in the abundances of each cluster were compared between each experimental group by one-way ANOVA with a Turkey's post-hoc test. Error bars show mean +/- SEM (*= $p < 0.05$; **= $p < 0.01$, ***= $p < 0.005$, ****= $p < 0.001$). Healthy pregnant (green; n=33), GDM on diet (blue; n=21), GDM on metformin (yellow; n=21), GDM on metformin and insulin (red; n=18), PIH/PET (purple; n=10).

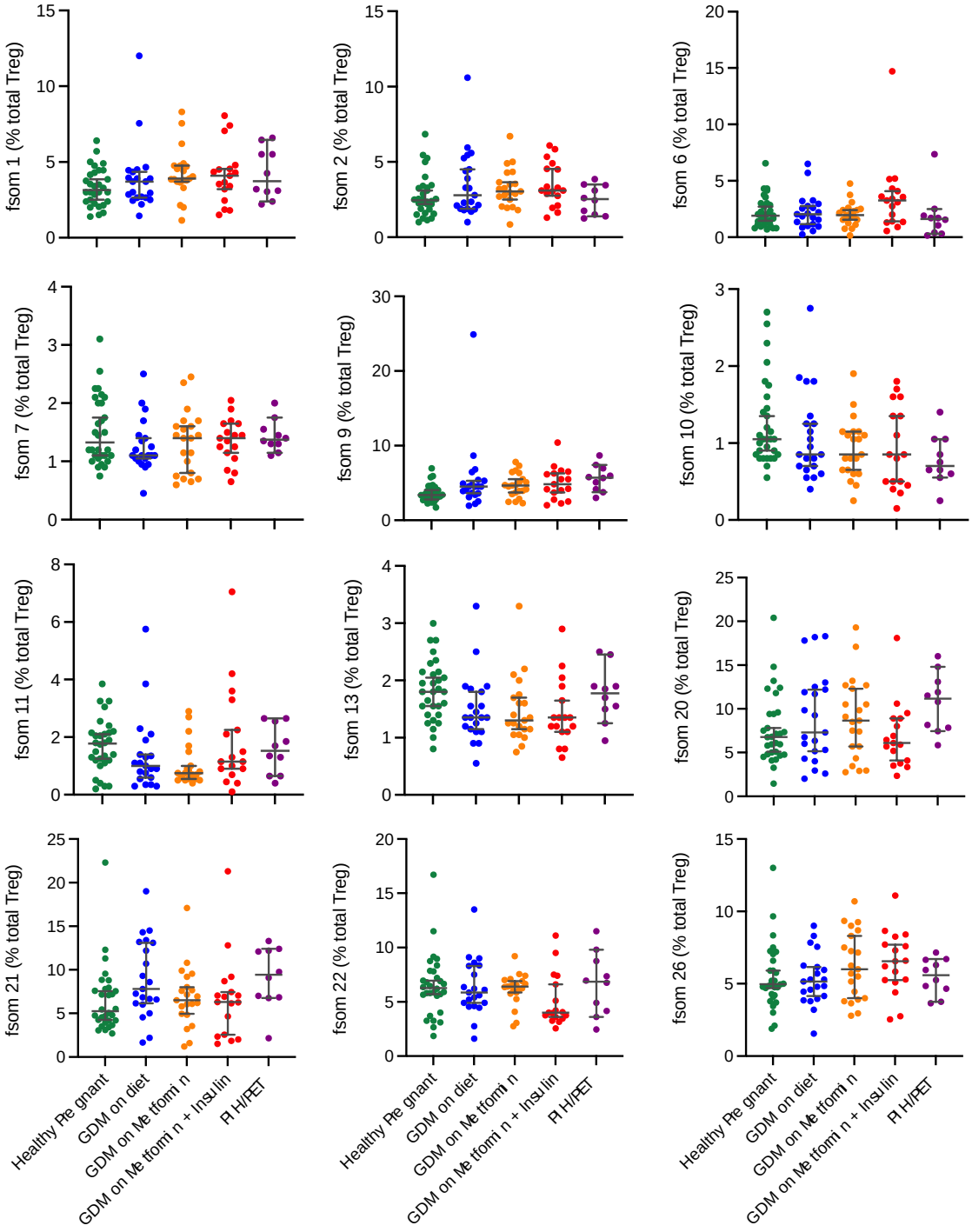

Figure 6.17: FlowSOM Treg clusters which were unchanged in abundance in healthy pregnant women compared to disease groups. PBMCs from pregnant donors (n=103) were stained and data acquisition carried out on a Cytek Aurora analyser. $CD4^{+}CD25^{hi}CD127^{lo}FoxP3^{+}$ Treg events were analysed by down sampling, dimensionality reduction using the optSNE algorithm, and flowSOM clustering. Following this, significant differences in the abundances of each cluster were compared between each experimental group by one-way ANOVA with a Turkey's post-hoc test. Error bars show mean +/- SEM (*=

p < 0.05; **= p <0.01, ***= p <0.005, ****= p <0.001). Healthy pregnant (green; n=33), GDM on diet (blue; n=21), GDM on metformin (yellow; n=21), GDM on metformin and insulin (red; n=18), PIH/PET (purple; n=10).

Collectively this data shows that by using unbiased clustering tools, most of the clusters which were significantly more abundant in healthy pregnant women compared to disease groups were of a naïve phenotype (7/10 clusters) which supports the previous data showing that memory Tregs were more frequent in disease groups than in the healthy pregnant women. Additionally, those subsets which were significantly more frequent in healthy pregnant women all expressed CD73, which interestingly was not identified as a single positive marker which was significantly altered in disease groups compared to healthy controls. These phenotypic differences may have consequences for the *in vitro* suppressive capacities of Tregs within the different experimental groups.

6.3.4 Tregs from pregnant women with GDM and pre-eclampsia have a reduced *in vitro* suppressive capacity compared to healthy women

The data above show clearly that Tregs from GDM patients are skewed towards a memory phenotype which is not observed within the Tconv pool. As described above, due to the limitations on the volume of blood it was possible to draw from each patient as stipulated by our research ethics, it was not possible to investigate the *in vitro* suppressive capacity of individual Treg subsets in this study. Instead, we then aimed to investigate whether this change in the frequencies of Tregs subsets within GDM patients had an impact on the *in vitro* suppressive capacity of the bulk Tregs from these patients.

The Treg *in vitro* micro-suppression assay was carried out according to the methods described in 6.2 (figure 6.1; figure 6.2). As shown in figure 6.18 A, counts per minute (CPM) values of wells containing only B cells and Tconvs with no Tregs show there were no significant differences in the ability of Tconvs to proliferate during the 5-day co-culture between experimental groups. Figure 6.18 B shows the CPM values in control wells containing only B cells and Tregs with no Tconvs. This shows that B cells and Tregs alone did not proliferate in response to PHA stimulation (all CPM values <350), suggesting any proliferation recorded in test wells is largely derived from Tconvs. As anticipated, the highest CPM values were recorded in the wells containing B cells and Tconvs with no Tregs (1:0 Tconv to Treg ratio), followed by a significant decrease in CPM values in wells containing B cells and Tconvs and Tregs at a 2:1 ratio, and finally the significantly lowest counts per minute were recorded in wells containing B cells and a 1:1 ratio of Tconvs to Tregs. As expected, this shows that a higher number of Tregs per well suppresses the amount of proliferation recorded.

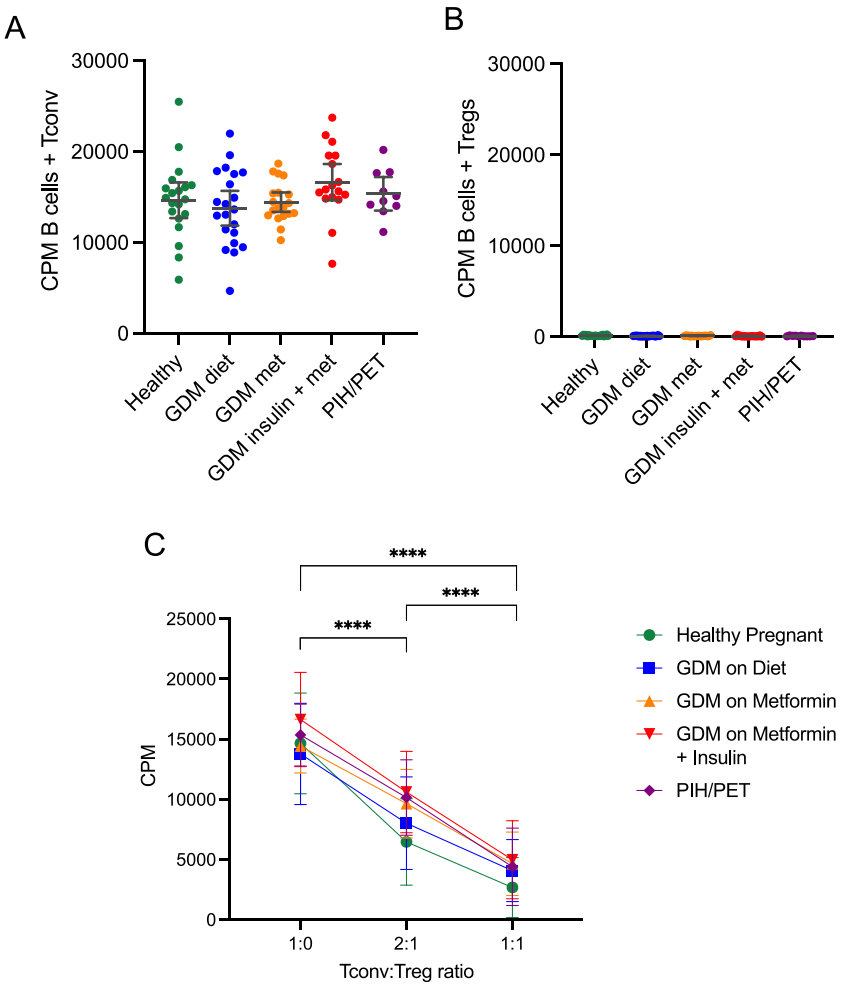

Figure 6.18: Tconvs from healthy pregnant donors and from pregnancy-related disease group patients had the same proliferative capacity *in vitro*. B cells, Tconvs, and bulk Tregs were sorted into 96-well plates and stimulated with PHA, and their suppression of Tconv proliferation was evaluated. (A) Counts per minute (CPM) in wells containing no Tregs within the different experimental groups. (B) CPM in wells containing no Tconvs within the different experimental groups. (C) CPM in wells containing 1000 B cells and 500 Tconvs only (1:0 Tconv to Treg ratio); 1000 B cells, 500 Tconvs and 250 Tregs (2:1 Tconv to Treg ratio); and 1000 B cells, 500 Tconvs and 500 Tregs (1:1 Tconv to Treg ratio). Significance between groups was determined by one-way ANOVA with a Turkey's post-hoc test. Error bars show mean +/- SEM (****= p <0.0001). Healthy pregnant (n=20), GDM on diet (n=21), GDM on metformin (n=19), GDM on metformin and insulin (n=18), PIH/PET (n=10).

The percentage suppression of bulk Tregs for each donor was then calculated from the raw CPM values using the method described in 6.2.3. As shown in figure 6:19 A, the only significant difference in bulk Treg suppressive capacity between experimental groups at a 1:1 Tconv to Treg ratio was a significant reduction in the GDM on metformin group compared to the healthy pregnant group. However, the 2:1 Tconv to Treg ratio allowed us to observe more variation between groups (figure 6.19 B). At this ratio, there was a significant decrease in the bulk Treg suppressive capacities of the GDM on diet, GDM on insulin, GDM on metformin, and PIH/PET groups compared to healthy controls. The most significant change was between the GDM on metformin group and the healthy control group, which was the only group to show a significant difference in suppression at a 1:1 Tconv to Treg ratio. There were no significant differences recorded in the bulk Treg suppressive capacity between the different disease groups. Figure 6.19 C shows that there was no correlation between the percentage suppression values at a 2:1 ratio of Tconvs to Tregs and the CPM values in wells from each donor containing B cells and Tconvs only (1:0 Tconv to Treg ratio). This shows that the suppressive capacity of bulk Tregs was independent of ability of the Tconvs to proliferate within each donor, therefore the percentage suppression values were not determined by the independent proliferative capacity of their Tconvs.

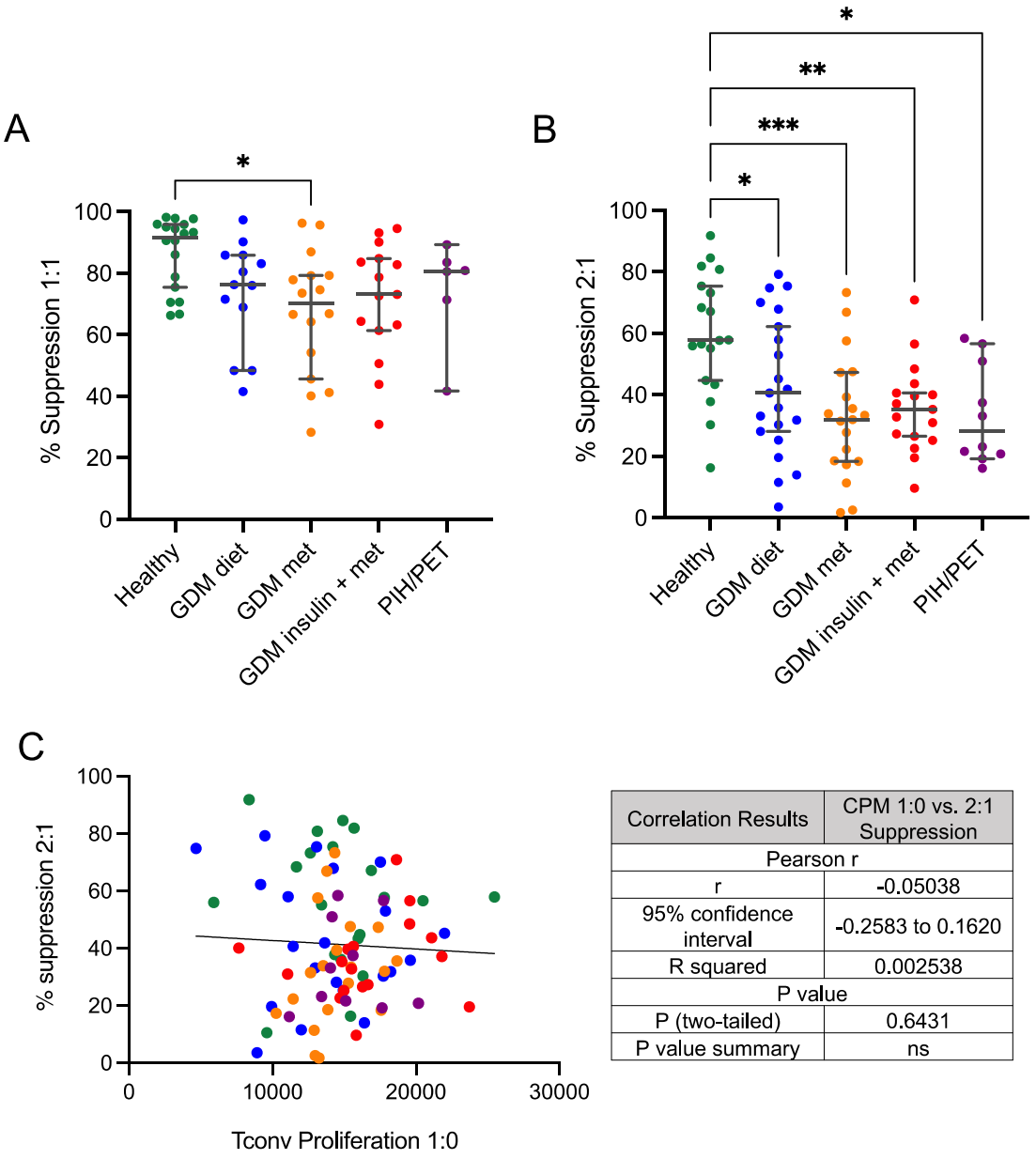

Correlation Results	CPM 1:0 vs. 2:1 Suppression
Pearson r	
r	-0.05038
95% confidence interval	-0.2583 to 0.1620
R squared	0.002538
P value	
P (two-tailed)	0.6431
P value summary	ns

Figure 6.19: Women with gestational diabetes mellitus and pregnancy-induced hypertension/pre-eclampsia had significantly reduced *in vitro* Treg suppression than healthy pregnant donors. B cells, Tconvs, and bulk Tregs were sorted into 96-well plates and stimulated with PHA, and their suppression of Tconv proliferation was evaluated. (A) Percentage suppression at a 1:1 Tconv to Treg ratio recorded per donor within the different experimental groups. (B) Percentage suppression at a 2:1 Tconv to Treg ratio recorded per donor within the different experimental groups. (C) Correlation results between percentage suppression at a 2:1 ratio and counts per minute (CPM) proliferation in B cell and Tconv only wells (1:0 Tconv to Treg ratio). Significance between groups was determined by one-way ANOVA with a Turkey's post-hoc test. Error bars show mean +/- SEM (*= $p < 0.05$; **= $p < 0.01$, ***= $p < 0.005$). 1:1 = Healthy pregnant (green; n=20), GDM on diet (blue; n=13), GDM

on metformin (yellow; n=16), GDM on metformin and insulin (red; n=15), PIH/PET (purple; n=6). 2:1 = Healthy pregnant (n=20), GDM on diet (n=21), GDM on metformin (n=19), GDM on metformin and insulin (n=18), PIH/PET (n=10).

Our phenotypic Treg data above showed us that the donors within the GDM groups had significantly higher frequencies of Tregs expressing a memory phenotype than healthy pregnant women. In addition, our data from chapter 3 demonstrated that memory Treg subsets performed significantly worse than naïve Tregs in our *in vitro* micro-suppression assay in healthy donors. We therefore hypothesised that the reduced suppressive capacity seen in the GDM groups may be driven by the increased frequency of memory Tregs within these donors. As shown in figure 6.20, there was a significant negative correlation between the frequency of $CD45R0^{+}$ memory Tregs, gated as a % of $CD4^{+}CD25^{hi}CD127^{low}FoxP3^{+}$ cells, and the percentage suppression values at a 2:1 Tconv to Treg ratio, showing that a higher frequency of memory Tregs has a significantly negative impact on the ability of bulk Tregs to suppress Tconvs proliferation.

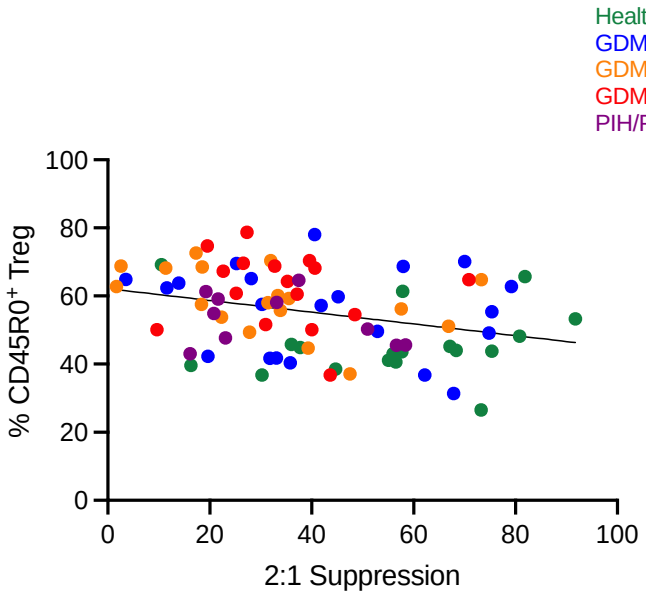

Correlation Results	2:1 Suppression vs. % CD45R0⁺ Treg
Pearson r	
r	-0.3220
95% confidence interval	-0.5028 to -0.1143
R squared	0.1037
P value	
P (two-tailed)	0.0030
P value summary	**

Figure 6.20: Positive correlation between Treg percentage suppression and frequency of memory Tregs. Correlation results between percentage suppression at a 2:1 ratio using the Treg micro-suppression assay and the % frequency of CD45R0⁺ Tregs within the total donor Treg pool. Correlation determined by Pearson's correlation test. Number of XY pairs=83.

6.4 Discussion

In this experimental chapter, we aimed to determine whether the phenotype and frequencies of Treg subsets investigated in the previous chapters could be altered in disease settings. Healthy pregnancies require spontaneous establishment of tolerance towards the semi-allogeneic foetus, and while this process requires an orchestrated response from several tolerogenic cell types and immune mediators, such as DCs, innate lymphoid cells (ILCs), cytokines, and progesterone, Tregs are recognised as key players in induction of foetal-maternal tolerance (reviewed by Tsuda, Nakashima, Shima, & Saito, 2019). Therefore, as Tregs take on a heightened tolerogenic role during pregnancy, a comparison of Tregs in healthy pregnancies and in pregnancy-related disorders

with immune-related aetiologies may be an opportunity to observe distinct differences in Treg subsets between these groups. Moreover, Treg dysfunction leading to sterile inflammation is increasingly implicated in common pregnancy related disorders, highlighting a need to further understand how Treg subsets play a role in these diseases (Boij et al., 2015; Green et al., 2021; Kisielewicz et al., 2010; Schober et al., 2014).

Several previous studies have reported a significant decrease in the frequency of Tregs in peripheral blood of pre-eclampsia and GDM patients compared to healthy pregnancies (Green et al., 2021; Lobo et al., 2018; Schober et al., 2014; Toldi et al., 2012, 2008; Yang et al., 2018; Zhao et al., 2020), although a near equal number of studies have not observed a change in Treg frequency (Boij et al., 2015; Hu et al., 2008; Paeschke et al., 2005; Schober et al., 2014; Steinborn et al., 2012). As shown in figure 6.5, using a stringent Treg gating method ($CD4^{+}CD25^{hi}CD127^{lo}FoxP3^{+}$) we observed no significant differences in the frequencies of total Tregs between any of our experimental groups. These discrepancies in Treg frequencies between different studies are likely to be caused by variation in the number of markers used to gate on Tregs. For example, studies such as Toldi et al. (2012) and Zhao et al. (2020) did not include CD127 and FoxP3 in their Treg gating strategies, respectively, meaning the potential for contaminating activated Tconvs falling into the Treg gates may have been higher. As systemic inflammation is known to be elevated in pre-eclampsia and GDM (reviewed by Collier et al., 2021; Lekva et al., 2016) it is possible that this could drive elevated levels of activated contaminating Tconvs.

In addition, the stage of pregnancy in which Treg frequencies were analysed may also be of significance as studies have demonstrated that *in vivo* Treg expansion is at its highest during the first trimester of healthy pregnancies, followed by a gradual decrease to normal levels at term (Sasaki et al., 2004; Somerset et al., 2004b). A study by Steinborn et al. (2012) demonstrated that the largest fluctuations in the composition of the Treg pool occur in the 10^{th}-20^{th} week of healthy pregnancies. When analysing the frequencies of Tregs during the early stages of pregnancy in recurrent unexplained miscarriage patients, both peripheral blood and decidual Tregs have been shown to be significantly reduced in frequency compared to healthy pregnancies (voluntary terminations) (Sasaki et al., 2004; Yang et al., 2008). It could therefore be hypothesised that analysing Treg frequencies during earlier stages of pregnancy when Tregs are most abundant may reveal greater differences between healthy and disease states. However, as both pre-eclampsia and GDM are most commonly diagnosed towards the end of the second trimester or later (reviewed by Green et al., 2021; Reddi Rani & Begum, 2016), in future studies it may be of value to study early fluctuations in Treg numbers in at-risk individuals, of whom an immodest proportion are likely to develop disease as seen in Yang et al. (2018).

Many publications to date have investigated the dynamics of the total Treg pool during pregnancy and pregnancy-related disorders, with the most studied being pre-eclampsia. However far fewer authors have investigated different subsets of Tregs. Despite no changes in the total Treg frequencies, we observed a significant increase in memory Tregs and a concurrent decrease in naïve Tregs in all GDM groups compared to healthy controls (figure 6.5 + 6.7 + 6.8). These

differences were observed when using combined CD45RA and CD95 phenotypes to define naïve and memory Tregs as per the gating strategy shown in figure 6.4 and in previous chapters, and also when using characteristic memory markers such as CD45R0, CD95, and CCR4, and CD45RA as a naïve marker on a single marker basis as a percentage of total Tregs (figure 6.8). Interestingly, we did not observe any significant differences in expression of these markers by Tconvs between the experimental groups (figure 6.6 + 6.7 + 6.9). From this we can be more confident in concluding that GDM is associated with a Treg-specific increase in the frequency of peripheral Tregs with a memory phenotype. Although care was taken to age-match GDM and pre-eclampsia patients to the participants in healthy pregnant group, the lack of changes in the memory Tconv pool serves as further confirmation that the increases in memory Tregs seen in GDM groups were not driven by advancing age. A study by Mahmoud, Abul, Omu, & Haines (2005) showed a significant increase in the frequency of $CD45R0^+$ and $HLA\text{-}DR^+$ cells, and a decrease in $CD45RA^+$ cells as a percentage of total $CD4^+$ T cells in GDM patients on insulin and on diet alteration compared to healthy pregnancies. However, the authors did not separate Tconvs from Tregs and in this study it appears that blood samples were drawn at different gestational ages between experimental groups. This was in agreement with another study by Pendeloski et al. (2015) which found that women with GDM had significantly higher $CD4^+$ T cells expressing CD69 and HLA-DR, pointing towards a more activated immune phenotype.

Furthermore, we saw no significant evidence suggesting that the different treatment interventions or indeed disease severity impacted on memory Treg

frequency in GDM patients (figure 6.5+ 6.7 + 6.8). Diet alteration is the first line of intervention in women diagnosed with GDM and up to 80% of women do not progress to requirement of drug interventions, representing a less severe form of disease (American Diabetes Association, 2017). Metformin and insulin are prescribed to patients with more severe dysglycaemia and approximately half of women initially prescribed metformin require addition of insulin (Rowan, Hague, Gao, Battin, & Moore, 2008). As there were no significant differences in the frequencies of Tregs expressing memory markers between GDM patients who had altered their diet alone and GDM patients being given the immune-modulatory drugs, we can deduce that this increase in memory Tregs in the GDM groups compared to healthy controls was a result of the disease process rather than drug interventions. However, there was a general trend towards an increase in memory markers such as CD45R0, CD95, and CCR4 on Tregs in the GDM on metformin and insulin group compared to GDM on diet group which may suggest a more pronounced phenotype in more severe disease, however this change was not significant. We also observed an increase in other markers which are known to be highly expressed on memory Tregs such as CCR6 and ICOS within the GDM groups on drug interventions (figure 6.8).

To our knowledge, only one other study has investigated subsets of Tregs in GDM patients stratified for diet and insulin intervention, and none has stratified for metformin intervention. In this study by Schober et al. (2014), the authors noted a significant decrease in $CD45RA^{+}$ Tregs in both GDM groups compared to healthy pregnant controls which is in agreement with our data. Additionally, a significant increase in Tregs expressing high levels of HLA-DR was observed in

the insulin-treated group compared to controls, again supporting the evidence for higher levels of activated Tregs in more severe disease. Building on these findings, our data shows that metformin treatment fails to rescue this activated memory Treg phenotype to levels seen in healthy controls. Previous *in vivo* studies have shown that metformin treatment increases the proportion of Tregs by inhibiting the differentiation of naïve $CD4^+$ T cells into Tconv helper subsets, which suggests a tolerogenic effect (Lee et al., 2015; Negrotto, Farez, & Correale, 2016; Sun et al., 2016). However, we saw no impact on the frequency or phenotype of total Tregs in the metformin-treated group compared to the GDM on diet intervention group.

Interestingly, we also observed a significant decrease in the expression of CXCR5 by Tregs within the GDM patient cohorts compared to healthy pregnant controls (figure 6.8). As previously discussed, this is a marker of Tfr cells, and to our knowledge this marker has not previously been investigated on Tregs in the context of pregnancy-related diseases. However, a number of studies to date have reported an increased frequency of circulating B cells and levels of IgA in GDM patients compared to healthy pregnant women and a positive correlation between B cell frequency and insulin resistance was found (Fagninou et al., 2020; Zhuang et al., 2019). This might imply a disrupted regulation of the germinal centre response and increased humoral immunity in GDM and the relationship between $CXCR5^+$ Tregs and B cells in GDM would be an interesting line of enquiry for future research.

Several previous studies have reported an imbalance in the frequencies of Tconv helper subsets in GDM patients, and it's possible that this is caused by a general increase in systemic inflammation in this disease. For example, studies by Atègbo et al. (2006) and Yang et al. (2018) have both shown an increase in serum concentrations of IL-6 and TNF-α in GDM mothers compared to healthy pregnant controls. Importantly, a body of evidence shows that IL-6 promotes the skewed differentiation of Th17 Tconvs over Tregs from naïve $CD4^+$ T cells (reviewed by Jones, Maerz, & Buckner, 2018). Our data showed no evidence of differences in the frequencies of memory helper-like Treg subsets in our GDM (or PIH/PET) patient cohorts (figure 6.5). However, we did observe a significant increase in Th17 Tconvs in some of our GDM cohorts which is in support of previous studies (Sheu et al., 2018; Sifnaios et al., 2019).

Contrary to these findings in the GDM cohort, we observed no differences in the frequencies of Treg or Tconv subsets expressing any of the individual surface markers analysed in the PIH/PET group compared to healthy pregnant women. However, as the PIH/PET group was the smallest, this group may have lacked statistical power. This is contrary to previous findings as many studies have demonstrated differences in the Treg pool and in the prevalence of helper Tconv subsets (Santner-Nanan et al., 2009; Toldi et al., 2011) driven by pre-eclampsia. For example, a study by Toldi et al. (2015) reported an increase in exhausted Tregs compared to healthy controls. Steinborn et al. (2012) reported a significant proportional increase in peripheral blood memory ($CD45RA^-$) Tregs and memory HLA-DR^+ Tregs in pre-eclampsia due to failure of an increase in naïve Tregs which is seen in healthy pregnancies, in agreement with (Shigeta et al., 2020). A

decrease in Tregs expressing other effector molecules such as PD-1 and GITR has also been reported in pre-eclampsia patients (Zhao et al., 2020). A further study by Boij et al. (2015) demonstrated a significant increase in $CCR4^+$ Tregs in pre-eclampsia compared to healthy pregnancy. As the CCR4 ligands are highly expressed at the foetal-maternal interface and $CCR4^+$ T cells and memory Tregs are found to be significantly increased in the decidua compared to in blood in healthy pregnancies (Tilburgs et al., 2008; Tsuda et al., 2002), from these previous studies it is possible to hypothesise that a failure of Treg trafficking to the decidua occurs during pre-eclampsia leading to a proportional increase in memory Tregs in the blood. In further support of this, a study by Tsuda et al. (2018) showed that clonal expansion of memory Tregs, possibly in response to paternal antigens, occurs in the decidua during normal pregnancies, however this is not observed in pre-eclampsia. Our results on an individual marker basis showed no indication that memory or activated Tregs were increased in peripheral blood in the PIH/PET group as these previous studies suggested (figures 6.5 + 6.7 + 6.8). Future work may also benefit from analysing expression of Treg homing ligands at the foetal-maternal interface in pre-eclampsia.

A study by Wagner et al. (2015) also observed a significant decrease in naïve $CD31^+$ Tregs in pre-eclampsia patients compared to normal pregnancy, however we observed no such differences in our data (figure 6.7). The only significant difference observed between our PIH/PET group compared to healthy controls was a significant increase in $Helios^+$ Tregs, which is contrary to a previous study which showed that $FoxP3^+Helios^+$ Tregs were unchanged in healthy pregnant compared to pre-eclampsia patients (Hsu et al., 2012). Due to limitations in our

recruitment of pre-eclampsia patients, in this study this group was possibly under-powered and required us to combine pregnant women with *bona fide* pre-eclampsia and those with PIH. In addition, for clinical reasons these women were being prescribed different drugs such as aspirin and labetalol. For this reason, this group may not have been a homogenous cohort which may explain why we did not see differences in this group compared to healthy controls. We plan to recruit more patients in the future and to only include patients who progress to pre-eclampsia in our analysis. In a similar vein, we were also not able to recruit enough GDM patients on insulin only and therefore in the future we hope to analyse these women as a separate cohort.

In addition to manually gating our Treg subsets of interest, we also took an unbiased clustering approach to identifying prevalent Treg subsets in our different experimental groups. To our knowledge, this is the first study using this approach when analysing Treg phenotypes in pregnancy cohorts. In agreement with our manual gating analysis, we observed that the majority of the Treg clusters which were significantly more frequent in healthy pregnant women compared to GDM and PIH/PET groups were of a naïve phenotype (figures 6.15 + 6.16). Moreover, all subsets which were significantly more frequent in GDM and PIH/PET patients compared to healthy controls were of a memory phenotype and this highlighted the importance of taking an unbiased clustering approach as no phenotypic differences were observed between the PIH/PET group and healthy controls when using manual gating. Interestingly, we found that many of the naïve clusters which were most increased in frequency in healthy compared to disease groups expressed CD73, and clusters 3 and 5 which were of a memory phenotype also

expressed CD73. This is the first study which has implicated several CD73-expressing Treg subsets as being reduced in GDM and PIH/PET patients compared to healthy pregnant women, accompanied by a skewed memory phenotype. This may indicate that Tregs in these patient groups are more activated due to an inflammatory environment, but fail to express some suppressive molecules. As outlined in chapter 1, catabolism of ATP to adenosine by CD73 and CD39 ectoenzymes is thought to be a key mechanism of Treg mediated suppression (Mandapathil et al., 2010). However, as well as its adenosine-producing regulatory properties, several studies have demonstrated an induction of CD73 surface expression on T cells following TCR stimulation (Borrione *et al.,* 1999; Massaia *et al.,* 1990). Therefore, together with our findings in this chapter, this could indicate that Tregs experience an abrogated level of TCR signalling in the periphery in pregnancy-related diseases. As it is known that continuous TCR signalling is essential to support Treg survival and function in the periphery (Seddon and Mason, 1999; Schmidt *et al.,* 2015), this provides further evidence of Treg dysfunction in GDM and PIH/PET.

Finally, we analysed the comparative *in vitro* suppressive capacities of bulk Tregs within our experimental groups using our Treg micro-suppression assay. At a 1:1 ratio of Tconvs to Tregs, we saw a significantly decreased percentage suppression in the GDM on metformin group compared to healthy controls. As reviewed by Shevach, (2018) a 1:1 ratio of Tconvs to Tregs can lead to strong suppression which limits inter-donor variation. However, at a 2:1 Tconv to Treg ratio, we saw a significantly decreased percentage suppression in each of the GDM intervention groups and PIH/PET group compared to healthy controls

(figure 6.19). This again seems to highlight that GDM drug interventions have little effect on improving Treg function as no differences were seen between these groups, and a significant drop in Treg suppressive activity was observed in the GDM group on altered diet alone. These findings support a number of previous studies which have found a reduced Treg suppressive capacity in GDM and pre-eclampsia (Schaier et al., 2012; Schober et al., 2014; Yang et al., 2018), however this is the first to stratify suppression by GDM treatment intervention showing altered diet, metformin, and insulin have no effect on improving Treg function. Finally, we showed that the percentage of memory Tregs within the whole patient cohort negatively correlated with the percentage suppression which further supports our finding that memory Tregs were more frequent in groups which performed worse in suppression assays, and also supports our data from chapter 3 showing that memory Tregs were less suppressive than naïve Tregs in our *in vitro* micro suppression assay.

To summarise this chapter, we found that an increase in the frequency of Tregs expressing memory markers in GDM patient cohorts correlated with a decreased *in vitro* suppressive capacity of bulk Tregs in these patients. We also observed a decreased suppressive capacity of PIH/PET patient Tregs compared to healthy controls despite seeing no differences in the surface phenotype of Tregs when using manual gating between these groups. However, unbiased clustering revealed several clusters of Tregs which had differential phenotypes between GDM and PIH/PET groups compared to healthy controls. Most of the Treg subsets which were differentially enriched in healthy pregnant women compared to disease groups had a naïve phenotype, supporting our manual gating findings,

and this unbiased clustering also highlighted that CD73 was expressed on several of the subsets enriched in healthy pregnant women. This finding opens an interesting line of questioning into whether CD73 function affects the overall Treg suppressive capacity in GDM and PIH/PET patients and future work should aim to investigate this. The increased prevalence of memory Tregs in the peripheral blood of GDM patients could be explained by two hypotheses; the first being an expansion of memory Tregs in the blood due to systemic inflammation, and the second being due to a disruption of trafficking of memory Tregs to the decidua which is observed in healthy pregnancies. Previous studies have failed to prove either hypothesis, however future work could benefit from analysing Treg subsets by frequency and also by absolute true counts in both the peripheral blood and the decidua. Finally, adopting tools such as 10x analysis could allow simultaneous analysis of the surface phenotypes and clonality of these Treg subsets to address these hypotheses.

7 Chapter 7. General discussion

7.1 Context of presented work

Since the discovery of Tregs, there has been an increasing understanding within the research field that maintaining unresponsiveness to self-antigens is a life-long process and that loss of tolerance at any stage of life could lead to inappropriate immune activation. Moreover, while the TCR repertoire of thymic Tregs may be determined early in life, it is now known that induction of tolerance towards non-virulent antigens, such as oral antigens or those expressed on the developing foetus, is a dynamic, adaptive process required throughout life to maintain a state of health, and induction of peripheral Tregs can help develop tolerance to novel immune challenges.

Research which has led to a deeper understanding of the mechanisms used by Tregs to regulate the immune response has also led to an increased knowledge of how these cells could be targeted in the tumour micro-environment. For this reason, an increasing number of pharmacological agents aiming to either enhance or attenuate Treg function in the context of inflammation and autoimmunity or malignancy are being investigated (reviewed by Eggenhuizen, Ng, & Ooi, 2020; Tanaka & Sakaguchi, 2019) as well as using live Tregs themselves as potential cellular therapies. Therefore, the need to understand the basic biology of Tregs and their subsets is greater than ever, and this thesis aimed to shed light on the phenotype and *in vitro* function of some of these subsets in healthy adult donors and during pregnancy. Understanding phenotypic and functional differences between Treg subsets, and indeed between Tregs and

Tconvs, will lead to a deeper understanding of how Tregs with the most potent properties of immune regulation, stability, and longevity could be harnessed for the best therapeutic outcomes or could be used as biomarkers for therapeutic success. The clinical trial NCT00525889 is a pertinent example where it was assumed that a change in Treg phenotype in response to rapamycin and low-dose IL-2 therapy in T1D patients would enhance Treg function, when in fact all participants experienced a loss of β-cell function. Therefore, although clinical trials routinely monitor the phenotype and expansion of Tregs in response to therapies, this data serves no functional purpose without an understanding of how these phenotypes relate to the suppressive function of the Tregs.

7.2 Main findings, limitations, and future perspectives

It is now known that rather than being a homogenous population of cells, Tregs are highly heterogeneous at their cell surface giving rise to subsets of cells which are diverse with regard to their suppressive mechanisms, target cells, and ability to migrate to different tissues. In the first experimental chapter, we investigated the phenotypic diversity of healthy donor Tregs at the cell surface using a panel of 14 surface markers which could also be used for FACS sorting of live cells for functional analyses. The key findings from this first chapter were firstly that by using manual gating of previously reported Treg subsets, we found that these subsets could be reproducibly found in 10 individual donors and that the frequency of these subsets differed in the Treg and Tconv pools. Unbiased analyses then confirmed the presence of many of these subsets but also identified novel clusters which had not previously been reported. However, we found that several of these novel clusters had substantial intra-cluster variation

making them difficult to reproducibly identify in different donors. This raises the question as to whether these clusters with complex surface phenotypes represent distinct and stable biological Treg subsets or if these clusters were momentary snapshots of Tregs with a changing phenotype at the time of data acquisition which featured in some donors but not all. Thus, although using unbiased analysis strategies such as these can highlight potential clusters of interest, this analysis method is unable to determine whether these clusters represent true biology and further investigations are required to confirm this. This is especially pertinent when analysing datasets from healthy donors consisting of a single cell type in which each cell has the potential to express every marker in the panel as many dimensionality reduction and clustering algorithms were trained on bone marrow tissue comprised of distinct lineages of cells which can be well separated during these analyses (Amir et al., 2013; Van Gassen et al., 2015). However, in chapter 6, it was encouraging to find the same clusters of interest being reproducibly and significantly more frequent in GDM patient groups compared to healthy controls using EdgeR analysis. Additionally, in chapters 3 and 5, the panel of markers used to analyse subsets of Tregs was limited by the number of channels on the FACS sorter available to us. However, this technology is ever-changing and the advent of spectral cell sorters may enable sorting and analysis of even more subsets within the same experiments. In hindsight, some additional markers which may have been of benefit to add to the panel in chapter 3 and also to the panel in chapter 6 when analysing the pregnancy cohort would have been CCR7, CD45R0, and CD27 which could have expanded our analysis of the phenotype and suppressive function of Tscm-like subsets (Lugli, Gattinoni, et al., 2013). In addition, HLA-DR, TIGIT, PD-1 are some of the markers which have

been shown to denote the most suppressive Tregs in previous studies and may warrant further investigation (Baecher-Allan et al., 2006a; Joller et al., 2014; Sage, Francisco, Carman, & Sharpe, 2013). Despite this, isolating more rare subsets of Tregs would require a higher volume of blood to be drawn from donors and this will always be a limitation in studies such as these. In addition it is not possible to use antibodies for cell sorting purposes which may interfere with the function of the target molecule during functional assays.

In chapter 3, we chose to focus on the previously reported Treg subsets for functional analyses. Using the Treg micro-suppression assay, we simultaneously analysed the suppressive capacity of 10 previously reported Treg subsets from healthy donors. This highlights the strength of using the micro-suppression assay which can give robust readouts of proliferation using >100x fewer cells than would be necessary for a dye dilution-type suppression assay. Our testing of this assay has previously showed that when using just 250 bulk Tregs per well, the CPM values fall within a tight range in the 6 replicates carried out per condition. However as discussed in chapter 3, a limitation of this technique is an inability to measure proliferation of each cell type present within the assay (i.e. Tconvs, B cells, and Tregs) whereas dye dilution assays allow the user to accurately track proliferation and analyse the phenotype of the proliferated cells and this may be more important when comparing different subsets of Tregs. Moreover, although we can see from our B cell and Treg only control wells that minimal proliferation occurs in the absence of Tconvs, it must be acknowledged that this is not a perfect control as these cells would not have been exposed to equal levels of IL-2 secreted by PHA-activated Tconvs as the test wells. We can expect from our

collective analysis in chapter 3 and the 5-day proliferation assay in chapter 5, and also evidence from previous studies (Miyara et al., 2009) that naïve Tregs are more proliferative than memory Tregs when stimulated *in vitro*, but despite this we still recorded fewer counts per minute and thus a higher suppressive capacity in the wells containing naïve Treg subsets. In addition, in designing these experiments, we felt that use of a three-cell assay with B cells as APCs would give the opportunity for more suppressive mechanisms to take place rather than mechanisms targeted to Tconvs alone, which may explain why our results pertaining to potent naïve Treg suppression differ from some reported in previous literature, as well as our use of PHA as a stimulus rather than anti-CD3 (Baecher-Allan et al., 2006a; Joller et al., 2014; Miyara et al., 2009). It should also be considered that in older studies where CD127 was not used to define Tregs, naïve Tregs and memory Tregs were often gated as $CD45RA^{+}CD25^{+}$ and $CD45R0^{+}CD25^{hi}$, respectively, and therefore naïve Tregs may have had more Tconv contamination.

We found that naïve Tregs, especially naïve Tregs expressing CD31 had the highest suppressive capacity using this assay, and to our knowledge, this is the first study to directly compare the function of these Tregs to memory subsets and bulk Tregs. This was also supported by our findings in chapter 6 which showed that a higher proportion of memory Tregs, which was observed in GDM patients compared to healthy pregnant controls, inversely correlated with the *in vitro* suppressive capacity of bulk Tregs. This was in agreement with previous studies which showed a higher frequency of activated $HLA\text{-}DR^{+}$ Tregs and a reduced suppressive capacity of Tregs from GDM patients compared to healthy pregnant

mothers (Schober et al., 2014). However, as with any *in vitro* assay, our use of a strong proliferation stimulus may not reflect how these cells behave *in vivo.* Indeed it is well documented that Tregs are highly proliferative *in vivo* but are anergic *in vitro* (Levings et al., 2001). However it has been shown that $CD31^{-/-}$ mice display B cell hyperproliferation and enhanced IgA secretion (Wilkinson et al., 2002), and Tregs from these mice have a reduced *in vitro* suppressive capacity (Ma et al., 2010) meaning this Treg subset may play an important *in vivo* role in B cell regulation. Although beyond the timing scope of this thesis, we believe that this result warrants further examination of the suppressive mechanisms used by this subset and whether this suppressive advantage is driven by CD31 itself which could be achieved by blocking this receptor in functional assays. This subset has also been shown to be increased in frequency in trials of low-dose IL-2 therapy, and therefore future work should aim to investigate whether these cells contribute to the efficacy of this drug. As culture supernatants were stored at day 5 of these assays, there is further scope for investigation of immunosuppressive cytokine secretion by these subsets. Furthermore, a comparative analysis of gene expression profiles of naïve $CD31^{+}$ Tregs at rest and after 5 days of activation could shed light on whether receptors targeting APCs are upregulated during this period. Finally, although the micro-suppression assay uses a relatively low number of Tregs per well (250 cells) it can be assumed that any FACS sorted population of Tregs will still encompass significant internal heterogeneity. For this reason, the future of suppression assays may lie in assays which could assess Treg function on a single cell basis.

The 4th and 5th experimental chapters both investigated the *ex vivo* phenotype and expansion properties of different subsets of Tregs including naïve $CD31^+$ Tregs and Tregs with a stem cell-like memory phenotype. Although initial phenotyping evidence suggested that cells with a Tscm phenotype may exist in the Treg compartment, we failed to show any convincing stem cell like functional properties of these cells. However, data from chapter 5 derived from a single donor only did suggest that a stem cell-like memory phenotype may have been induced in naïve Tregs and Tconvs with the addition of rapamycin. Data in this experimental chapter should obviously be treated as very preliminary as these experiments were carried out in a single donor only which was the main limitation of this chapter. To confirm these findings, future experiments should employ multiple rounds of expansion of cells from at least 4 donors and a negative rapamycin control to determine whether a self-renewing population with a Tscm phenotype prevails in these expanded naïve cells. Furthermore, as outlined in chapter 5, the use of single cell RNA sequencing of naïve Tregs, memory Treg populations, and Tregs with a Tscm-like phenotype after a very short period of <12 hours of activation may highlight whether the naïve and Tscm-like Tregs have a different rapid functional response under these conditions. Ultimately, if stem cell-like memory function were to be shown in the Treg compartment, it would be necessary to observe the ability of these cells to produce memory progeny while self-renewing *in vivo*, perhaps in the context of autoimmune disease models such as EAE or CIA mice.

As Treg expansion is an essential step in preparing autologous Treg therapies, it is crucial that a Treg subset suitable for therapeutic purposes would have good

expansion potential and good phenotypic stability. We found that naïve CD31$^+$ Tregs had an equal expansion potential to bulk, memory, or naïve Tregs and that this subset also expressed high levels of FoxP3 throughout expansion, and at day 28 of expansion this subset had a significantly higher proportion of Helios$^+$ cells than any other subset. However, this Helios expression did decrease significantly by day 42, which indicated that even in RTE Tregs with a very naïve phenotype, 6 weeks of expansion may lead to a loss of a stable Treg phenotype. One of the main limitations of this chapter was the lack of functional analysis of the suppressive capacity of each Treg subset at different stages during the expansion process. Although it was encouraging that we saw a higher expression of Helios in expanded naïve CD31$^+$ Tregs as the literature suggests that Helios is a marker of potently suppressive Tregs (Thornton et al., 2019), it is impossible to know whether this denoted good suppressive capacity in our expanded subsets without suppressive functional data to support this hypothesis. If in future experiments a positive correlation was found between intracellular Helios expression, a naïve CD31$^+$ surface phenotype, and good suppressive capacity in an expanded cell product then this surface phenotype could potentially be used as a surface biomarker for Helios expression which would be valuable when isolating live cells via FACS sorting as only surface markers can be used.

When considering the future of the field of Treg therapies, the optimal starting subset of Tregs may be of use in determining the stability of the expanded product, however attention in the research field is now focused on generating the optimal expanded Treg product by means of genetic engineering approaches. Engineering CAR Tregs with directed antigen specificity is at the forefront of Treg

therapy research as it is known that antigen specificity can help to direct Tregs towards certain target tissues in the context of organ transplantation, and due to bystander suppressive mechanisms, identification of disease causing antigens is not necessary (reviewed by Raffin, Vo, & Bluestone, 2019). Moreover, data have also suggested that the increased potency of antigen-specific Tregs leads to a reduced requirement for high cell numbers compare to polyclonal Tregs (Tang et al., 2004). As well as engineering antigen specificity, regulating the expression of other Treg-enhancing or disrupting genes by means of lentiviral transduction or gene silencing may also be achieved in therapeutic Tregs, such as *FOXP3, CTLA4, IL6R* (reviewed by Amini et al., 2020). Although these engineering approaches have been shown in animal models, key advances such as these using human cells are often pending patent protection and are therefore under-published. Furthermore, the need for large numbers of Tregs as a starting material may be completely overcome as a recent study has shown that ectopic co-expression of FoxP3 and Helios in Tconvs converts these cells into suppressive Tregs which delayed the onset of GvHD in rodents (Seng et al., 2020). Despite these advances, several commentators have expressed safety concerns regarding *in vitro* induced Tregs as some studies have shown that these cells are not as suppressive as native Tregs and that FoxP3 alone does not account for the whole Treg gene signature (Hill et al., 2007). Therefore, the rationale for determining the best endogenous Treg subsets for therapies continues, and it is possible that a ‘one size fits all’ approach is not optimal and that different disease backgrounds could respond better to different Treg subsets.

In chapter 6, we investigated the phenotype and frequency of Treg subsets in the peripheral blood of healthy pregnant women, GDM patients stratified for 3 different treatment interventions, and pre-eclampsia patients in the 36th week of pregnancy. Through manual gating we found that Tregs from GDM mothers under each treatment regimen were all skewed towards a memory phenotype, expressing surface markers such as CD45R0, CCR4, and CD95, and a significantly reduced frequency of CXCR5^{+} Tregs was observed. Using unbiased clustering tools, we also identified that the Treg subsets which were significantly more abundant in healthy pregnant women compared to all GDM groups and pre-eclampsia were predominantly of a naïve CD73^{+} phenotype. This finding lies in contrast to our data in chapter 3 in which CD73 was expressed at a minimal level in a small number of Treg clusters in healthy controls. This could be a reflection of true biology when comparing healthy non-pregnant to healthy pregnant controls, however it is also of note that data in the final experimental chapter were acquired on a spectral cytometer which may have improved the resolution of this marker which has a relatively low density at the cell surface. In future studies, it may be of value to include a healthy non-pregnant control group as this may shed light on markers which are induced in healthy pregnancy and may fail in pregnancy-related disorders. Moreover, as with any study analysing the phenotype of Tregs in peripheral blood in a disease affecting a specific organ, a limitation of this study may be that phenotypic differences in Tregs from GDM and pre-eclampsia patients compared to healthy controls in blood may not represent the phenotypes of these cells at the foetal-maternal interface. This could be addressed in future studies by analysing both peripheral blood and decidual Tregs from these patients.

Finally, results from our Treg micro-suppression assay showed that the capacity of bulk Tregs from GDM and pre-eclampsia mothers was significantly reduced compared to healthy pregnant controls, and that treatment intervention made no difference to suppressive capacity. Collectively this showed that the skewed memory phenotype of Tregs in the disease groups had a negative impact on Treg suppressive capacity, and an inverse correlation between the frequency of $CD45R0^{+}$ Tregs and suppressive capacity was found. Although our results in chapter 3 showed that naïve $CD31^{+}$ Tregs gave rise to the best suppression of Tconv proliferation, we found no evidence that the frequency of this subset was significantly altered between our healthy and disease groups, which supports the hypothesis that different disease mechanisms affecting Tregs will not benefit from a 'one size fits all' treatment regimen. To summarise, the data from this chapter showed an altered phenotype and function of Tregs in GDM patients which was not ameliorated with any common GDM therapies, and also in pre-eclampsia patients. Data from previous chapters may also be of relevance to this emerging field as review articles are now making the case for autologous Tregs as a pre-conception treatment for pre-eclampsia in at-risk women (Robertson et al., 2019).

Collectively data from this thesis show that the surface phenotype of Tregs dictates the functional properties of Treg subsets and that naïve Tregs may have more potent suppressive capacities and more favourable expansion properties than memory Tregs. Additionally, our findings which show a skewed memory Treg phenotype in GDM patients warrants further research into the Tregs as a driver of this disease.

8 References

Adeegbe, D. O., & Nishikawa, H. (2013). Natural and induced T regulatory cells in cancer. *Frontiers in Immunology*, *4*, 190. https://doi.org/10.3389/FIMMU.2013.00190/XML/NLM

Afzali, B., Mitchell, P. J., Edozie, F. C., Povoleri, G. A. M., Dowson, S. E., Demandt, L., … Lombardi, G. (2013). CD161 expression characterizes a subpopulation of human regulatory T cells that produces IL-17 in a STAT3-dependent manner. *European Journal of Immunology*, *43*(8), 2043–2054. https://doi.org/10.1002/EJI.201243296

Ahmed, R., Roger, L., Costa del Amo, P., Miners, K. L., Jones, R. E., Boelen, L., … Ladell, K. (2016). Human Stem Cell-like Memory T Cells Are Maintained in a State of Dynamic Flux. *Cell Reports*, *17*(11), 2811–2818. https://doi.org/10.1016/j.celrep.2016.11.037

Akimova, T., Beier, U. H., Wang, L., Levine, M. H., & Hancock, W. W. (2011). Helios Expression Is a Marker of T Cell Activation and Proliferation. *PLOS ONE*, *6*(8), e24226. https://doi.org/10.1371/JOURNAL.PONE.0024226

Alam, M. S., Kurtz, C. C., Rowlett, R. M., Reuter, B. K., Wiznerowicz, E., Das, S., … Ernst, P. B. (2009). CD73 Is Expressed by Human Regulatory T Helper Cells and Suppresses Proinflammatory Cytokine Production and Helicobacter felis–Induced Gastritis in Mice. *The Journal of Infectious Diseases*, *199*(4), 494–504. https://doi.org/10.1086/596205

American Diabetes Association. (2017). 13. Management of Diabetes in Pregnancy. *Diabetes Care*, *40*(Supplement_1), S114–S119. https://doi.org/10.2337/DC17-S016

Amini, L., Greig, J., Schmueck-Henneresse, M., Volk, H. D., Bézie, S., Reinke, P., … Anegon, I. (2020). Super-Treg: Toward a New Era of Adoptive Treg Therapy Enabled by Genetic Modifications. *Frontiers in Immunology*, *11*, 611638. https://doi.org/10.3389/FIMMU.2020.611638

Amir, E. D., Davis, K. L., Tadmor, M. D., Simonds, E. F., Levine, J. H., Bendall, S. C., … Pe'er, D. (2013). viSNE enables visualization of high dimensional single-cell data and reveals phenotypic heterogeneity of leukemia. *Nature Biotechnology*, *31*(6), 545–552. https://doi.org/10.1038/nbt.2594

Apostolou, I., & Von Boehmer, H. (2004). In Vivo Instruction of Suppressor Commitment in Naive T Cells. *Journal of Experimental Medicine*, *199*(10), 1401–1408. https://doi.org/10.1084/JEM.20040249

Arroyo Hornero, R., Georgiadis, C., Hua, P., Trzupek, D., He, L. Z., Qasim, W., … Hester, J. (2020). CD70 expression determines the therapeutic efficacy of expanded human regulatory T cells. *Communications Biology*, *3*(1), 375. https://doi.org/10.1038/s42003-020-1097-8

Asano, M., Toda, M., Sakaguchi, N., & Sakaguchi, S. (1996). *Autoimmune Disease as a Consequence of Developmental Abnormality of a T Cell Subpopulation*. Retrieved from https://www.ncbi.nlm.nih.gov/pmc/articles/PMC2192701/pdf/je1842387.pdf

Asseman, C., Mauze, S., Leach, M. W., Coffman, R. L., & Powrie, F. (1999). An Essential Role for Interleukin 10 in the Function of Regulatory T Cells That Inhibit Intestinal Inflammation. *Journal of Experimental Medicine*, *190*(7), 995–1004. https://doi.org/10.1084/JEM.190.7.995

Atègbo, J. M., Grissa, O., Yessoufou, A., Hichami, A., Dramane, K. L., Moutairou, K., … Khan, N. A. (2006). Modulation of adipokines and cytokines in gestational diabetes and macrosomia. *The Journal of Clinical Endocrinology and Metabolism*, *91*(10), 4137–4143. https://doi.org/10.1210/JC.2006-0980

Baecher-Allan, C., Brown, J. A., Freeman, G. J., & Hafler, D. A. (2001). CD4+CD25high Regulatory Cells in Human Peripheral Blood. *The Journal of Immunology*, *167*(3), 1245–1253. https://doi.org/10.4049/JIMMUNOL.167.3.1245

Baecher-Allan, C., Viglietta, V., & Hafler, D. A. (2002). Inhibition of Human CD4+CD25+high Regulatory T Cell Function. *The Journal of Immunology*, *169*(11), 6210–6217. https://doi.org/10.4049/JIMMUNOL.169.11.6210

Baecher-Allan, C., Wolf, E., & Hafler, D. A. (2006a). MHC class II expression identifies functionally distinct human regulatory T cells. *Journal of Immunology (Baltimore, Md. : 1950)*, *176*(8), 4622–4631. https://doi.org/10.4049/jimmunol.176.8.4622

Baecher-Allan, C., Wolf, E., & Hafler, D. A. (2006b). MHC Class II Expression Identifies Functionally Distinct Human Regulatory T Cells. *The Journal of Immunology*, *176*(8), 4622–4631. https://doi.org/10.4049/JIMMUNOL.176.8.4622

Bailey-Bucktrout, S. L., Martinez-Llordella, M., Zhou, X., Anthony, B., Rosenthal, W., Luche, H., … Bluestone, J. A. (2013). Self-antigen driven activation induces instability of regulatory T cells during an inflammatory autoimmune response. *Immunity*, *39*(5), 949–962. https://doi.org/10.1016/J.IMMUNI.2013.10.016

Balint, B., Haas, J., Schwarz, A., Jarius, S., Fürwentsches, A., Engelhardt, K., … Wildemann, B. (2013). T-cell homeostasis in pediatric multiple sclerosis: old cells in young patients. *Neurology*, *81*(9), 784–792. https://doi.org/10.1212/WNL.0B013E3182A2CE0E

Banz, A., Pontoux, C., & Papiernik, M. (2002). Modulation of Fas-Dependent Apoptosis: A Dynamic Process Controlling Both the Persistence and Death of CD4 Regulatory T Cells and Effector T Cells. *The Journal of Immunology*, *169*(2), 750–757. https://doi.org/10.4049/JIMMUNOL.169.2.750

Baron, U., Floess, S., Wieczorek, G., Baumann, K., Grützkau, A., Dong, J., … Huehn, J. (2007). DNA demethylation in the human FOXP3 locus discriminates regulatory T cells from activated FOXP3+ conventional T cells. *European Journal of Immunology*, *37*(9), 2378–2389. https://doi.org/https://doi.org/10.1002/eji.200737594

Barrett, J. C., Clayton, D. G., Concannon, P., Akolkar, B., Cooper, J. D., Erlich, H. A., … Zhang, Q. (2009). Genome-wide association study and meta-analysis finds over 40 loci affect risk of type 1 diabetes. *Nature Genetics*, *41*(6), 703–707. https://doi.org/10.1038/NG.381

Barron, L., Dooms, H., Hoyer, K. K., Kuswanto, W., Hofmann, J., O'Gorman, W. E., & Abbas, A. K. (2010). Mechanisms of IL-2–dependent maintenance of functional regulatory T cells. *Journal of Immunology*, *185*(11), 6426–6430. https://doi.org/10.4049/JIMMUNOL.0903940

Barthlott, T., Moncrieffe, H., Veldhoen, M., Atkins, C. J., Christensen, J., O'Garra, A., & Stockinger, B. (2005). CD25+CD4+ T cells compete with naive CD4+ T cells for IL-2 and exploit it for the induction of IL-10 production. *International Immunology*, *17*(3), 279–288. https://doi.org/10.1093/INTIMM/DXH207

Bastian, J., Law, S., Vogler, L., Lawton, A., Herrod, H., Anderson, S., … Hong, R. (1989). Prediction of persistent immunodeficiency in the DiGeorge anomaly. *The Journal of Pediatrics*, *115*(3), 391–396. https://doi.org/10.1016/S0022-3476(89)80837-6

Battaglia, M., Stabilini, A., Migliavacca, B., Horejs-Hoeck, J., Kaupper, T., & Roncarolo, M.-G. (2006). Rapamycin Promotes Expansion of Functional CD4+CD25+FOXP3+ Regulatory T Cells of Both Healthy Subjects and Type 1 Diabetic Patients. *The Journal of Immunology*, *177*(12), 8338–8347. https://doi.org/10.4049/JIMMUNOL.177.12.8338

Bautista, J. L., Lio, C. W., Lathrop, S. K., Forbush, K., Liang, Y., Luo, J., Rudensky, A. Y., & Hsieh, C. S. (2009). Intraclonal competition limits the fate determination of regulatory T cells in the thymus. Nature immunology, 10(6), 610–617. https://doi.org/10.1038/ni.1739

Bayer, A. L., Yu, A., Adeegbe, D., & Malek, T. R. (2005). Essential role for interleukin-2 for CD4+CD25+ T regulatory cell development during the neonatal period. *Journal of Experimental Medicine*, *201*(5), 769–777. https://doi.org/10.1084/JEM.20041179

Bennett, C. L., Christie, J., Ramsdell, F., Brunkow, M. E., Ferguson, P. J., Whitesell, L., … Ochs, H. D. (2001). The immune dysregulation, polyendocrinopathy, enteropathy, X-linked syndrome (IPEX) is caused by mutations of FOXP3. *Nature Genetics*, *27*(1), 20–21. https://doi.org/10.1038/83713

Bensinger, S. J., Walsh, P. T., Zhang, J., Carroll, M., Parsons, R., Rathmell, J. C., … Turka, L. A. (2004). Distinct IL-2 Receptor Signaling Pattern in CD4+CD25+ Regulatory T Cells. *Journal of Immunology (Baltimore, Md. : 1950)*, *172*(9), 5287–5296. https://doi.org/10.4049/JIMMUNOL.172.9.5287

Bernaldo-de-Quirós, E., Cózar, B., López-Esteban, R., Clemente, M., Gil-Jaurena, J. M., Pardo, C., … Correa-Rocha, R. (2022). A Novel GMP Protocol to Produce High-Quality Treg Cells From the Pediatric Thymic Tissue to Be Employed as Cellular Therapy. *Frontiers in Immunology*, *13*, 893576. https://doi.org/10.3389/FIMMU.2022.893576

Bernasconi, A., Marino, R., Ribas, A., Rossi, J., Ciaccio, M., Oleastro, M., … Belgorosky, A. (2006). Characterization of Immunodeficiency in a Patient With Growth Hormone Insensitivity Secondary to a Novel STAT5b Gene Mutation. *Pediatrics*, *118*(5), e1584–e1592. https://doi.org/10.1542/PEDS.2005-2882

Biasco, L., Scala, S., Ricci, L. B., Dionisio, F., Baricordi, C., Calabria, A., … Aiuti, A. (2015). In vivo tracking of T cells in humans unveils decade-long survival and activity of genetically modified T memory stem cells. *Science Translational Medicine*, *7*(273), 273ra13-273ra13. https://doi.org/10.1126/SCITRANSLMED.3010314

Blom, B, Res, P., Noteboom, E., Weijer, K., & Spits, H. (1997). Prethymic CD34+ progenitors capable of developing into T cells are not committed to the T cell lineage. *The Journal of*

Immunology, *158*(8).
Blom, Bianca, Verschuren, M. C. M., Heemskerk, M. H. M., Bakker, A. Q., van Gastel-Mol, E. J., Wolvers-Tettero, I. L. M., … Spits, H. (1999). TCR Gene Rearrangements and Expression of the Pre-T Cell Receptor Complex During Human T-Cell Differentiation. *Blood*, *93*(9), 3033–3043. https://doi.org/10.1182/BLOOD.V93.9.3033
Bluestone, J. A., Buckner, J. H., Fitch, M., Gitelman, S. E., Gupta, S., Hellerstein, M. K., … Tang, Q. (2015a). Type 1 diabetes immunotherapy using polyclonal regulatory T cells. *Science Translational Medicine*, *7*(315), 315ra189. https://doi.org/10.1126/scitranslmed.aad4134
Bluestone, J. A., Buckner, J. H., Fitch, M., Gitelman, S. E., Gupta, S., Hellerstein, M. K., … Tang, Q. (2015b). Type 1 diabetes immunotherapy using polyclonal regulatory T cells. *Science Translational Medicine*, *7*(315), 315ra189. https://doi.org/10.1126/SCITRANSLMED.AAD4134/SUPPL_FILE/7-315RA189_SM.PDF
Boardman, D. A., Wong, M. Q., Rees, W. D., Wu, D., Himmel, M. E., Orban, P. C., Vent-Schmidt, J., Zachos, N. C., Steiner, T. S., & Levings, M. K. (2023). Flagellin-specific human CAR Tregs for immune regulation in IBD. Journal of autoimmunity, 134, 102961. https://doi.org/10.1016/j.jaut.2022.102961
Boij, R., Mjösberg, J., Svensson-Arvelund, J., Hjorth, M., Berg, G., Matthiesen, L., … Ernerudh, J. (2015). Regulatory T-cell Subpopulations in Severe or Early-onset Preeclampsia. *American Journal of Reproductive Immunology*, *74*(4), 368–378. https://doi.org/10.1111/AJI.12410
Boissonnas, A., Scholer-Dahirel, A., Simon-Blancal, V., Pace, L., Valet, F., Kissenpfennig, A., … Amigorena, S. (2010). Foxp3+ T Cells Induce Perforin-Dependent Dendritic Cell Death in Tumor-Draining Lymph Nodes. *Immunity*, *32*(2), 266–278. https://doi.org/10.1016/j.immuni.2009.11.015
Booth, N. J., McQuaid, A. J., Sobande, T., Kissane, S., Agius, E., Jackson, S. E., … Vukmanovic-Stejic, M. (2010). Different proliferative potential and migratory characteristics of human CD4+ regulatory T cells that express either CD45RA or CD45RO. *Journal of Immunology (Baltimore, Md. : 1950)*, *184*(8), 4317–4326. https://doi.org/10.4049/jimmunol.0903781
Borrione, P., Peola, S., Mariani, S., Besostri, B., Mallone, R., Malavasi, F., Pileri, A., & Massaia, M. (1999). CD38 stimulation lowers the activation threshold and enhances the alloreactivity of cord blood T cells by activating the phosphatidylinositol 3-kinase pathway and inducing CD73 expression. Journal of immunology (Baltimore, Md. : 1950), 162(10), 6238–6246.
Borsellino, G., Kleinewietfeld, M., Di Mitri, D., Sternjak, A., Diamantini, A., Giometto, R., … Falk, K. (2007). Expression of ectonucleotidase CD39 by Foxp3+ Treg cells: hydrolysis of extracellular ATP and immune suppression. *Blood*, *110*(4), 1225–1232. https://doi.org/10.1182/BLOOD-2006-12-064527
Bouneaud, C., Kourilsky, P., & Bousso, P. (2000). Impact of negative selection on the T cell repertoire reactive to a self-peptide: a large fraction of T cell clones escapes clonal deletion. *Immunity*, *13*(6), 829–840. https://doi.org/10.1016/S1074-7613(00)00080-7
Bours, M. J. L., Swennen, E. L. R., Di Virgilio, F., Cronstein, B. N., & Dagnelie, P. C. (2006). Adenosine 5′-triphosphate and adenosine as endogenous signaling molecules in immunity and inflammation. *Pharmacology & Therapeutics*, *112*(2), 358–404. https://doi.org/10.1016/J.PHARMTHERA.2005.04.013
Boyman, O., & Sprent, J. (2012). The role of interleukin-2 during homeostasis and activation of the immune system. *Nature Reviews Immunology*, *12*(3), 180–190. https://doi.org/10.1038/nri3156
Brandhuber, B. J., Boone, T., Kenney, W. C., & McKay, D. B. (1987). Three-dimensional structure of interleukin-2. *Science*, *238*(4834), 1707–1709. https://doi.org/10.1126/SCIENCE.3500515
Brunkow, M. E., Jeffery, E. W., Hjerrild, K. A., Paeper, B., Clark, L. B., Yasayko, S. A., … Ramsdell, F. (2001). Disruption of a new forkhead/winged-helix protein, scurfin, results in the fatal lymphoproliferative disorder of the scurfy mouse. *Nature Genetics*, *27*(1), 68–73. https://doi.org/10.1038/83784
Brunstein, C. G., Miller, J. S., Cao, Q., McKenna, D. H., Hippen, K. L., Curtsinger, J., … Wagner, J. E. (2011). Infusion of ex vivo expanded T regulatory cells in adults transplanted with umbilical cord blood: safety profile and detection kinetics. *Blood*, *117*(3), 1061–1070. https://doi.org/10.1182/BLOOD-2010-07-293795

Brusko, T. M., Wasserfall, C. H., Clare-Salzler, M. J., Schatz, D. A., & Atkinson, M. A. (2005). Functional defects and the influence of age on the frequency of CD4+ CD25+ T-cells in type 1 diabetes. *Diabetes*, *54*(5), 1407–1414. https://doi.org/10.2337/DIABETES.54.5.1407

Burton, P. R., Clayton, D. G., Cardon, L. R., Craddock, N., Deloukas, P., Duncanson, A., … Compston, A. (2007). Genome-wide association study of 14,000 cases of seven common diseases and 3,000 shared controls. *Nature*, *447*(7145), 661–678. https://doi.org/10.1038/NATURE05911

Buurma, A., Cohen, D., Veraar, K., Schonkeren, D., Claas, F. H., Bruijn, J. A., … Baelde, H. J. (2012). Preeclampsia is characterized by placental complement dysregulation. *Hypertension*, *60*(5), 1332–1337. https://doi.org/10.1161/HYPERTENSIONAHA.112.194324/-/DC1

Camu, W., Mickunas, M., Veyrune, J. L., Payan, C., Garlanda, C., Locati, M., … Bensimon, G. (2020). Repeated 5-day cycles of low dose aldesleukin in amyotrophic lateral sclerosis (IMODALS): A phase 2a randomised, double-blind, placebo-controlled trial. *EBioMedicine*, *59*, 102844. https://doi.org/10.1016/J.EBIOM.2020.102844

Canavan, J. B., Afzali, B., Scottà, C., Fazekasova, H., Edozie, F. C., Macdonald, T. T., … Lord, G. M. (2012). A rapid diagnostic test for human regulatory T-cell function to enable regulatory T-cell therapy. *Blood*, *119*(8), e57–e66. https://doi.org/10.1182/BLOOD-2011-09-380048

Canavan, J. B., Scottà, C., Vossenkämper, A., Goldberg, R., Elder, M. J., Shoval, I., … Lord, G. M. (2016). Original article: Developing in vitro expanded CD45RA+ regulatory T cells as an adoptive cell therapy for Crohn's disease. *Gut*, *65*(4), 584–594. https://doi.org/10.1136/GUTJNL-2014-306919

Cao, W., Wang, X., Chen, T., Xu, W., Feng, F., Zhao, S., … Xie, B. (2018). Maternal lipids, BMI and IL-17/IL-35 imbalance in concurrent gestational diabetes mellitus and preeclampsia. *Experimental and Therapeutic Medicine*, *16*(1), 427–435. https://doi.org/10.3892/ETM.2018.6144

Care, A. S., Bourque, S. L., Morton, J. S., Hjartarson, E. P., Robertson, S. A., & Davidge, S. T. (2018). Reduction in regulatory t cells in early pregnancy causes uterine artery dysfunction in mice. *Hypertension*, *72*(1), 177–187. https://doi.org/10.1161/HYPERTENSIONAHA.118.10858/-/DC1

Chen, W. J., Jin, W., Hardegen, N., Lei, K. J., Li, L., Marinos, N., … Wahl, S. M. (2003). Conversion of Peripheral CD4+CD25− Naive T Cells to CD4+CD25+ Regulatory T Cells by TGF-β Induction of Transcription Factor Foxp3. *The Journal of Experimental Medicine*, *198*(12), 1875–1886. https://doi.org/10.1084/JEM.20030152

Cheng, G., Yu, A., & Malek, T. R. (2011). T cell tolerance and the multi-functional role of IL-2R signaling in T regulatory cells. *Immunological Reviews*, *241*(1), 63–76. https://doi.org/10.1111/J.1600-065X.2011.01004.X

Cianciotti, B. C., Ruggiero, E., Campochiaro, C., Oliveira, G., Magnani, Z. I., Baldini, M., … Bonini, C. (2020). CD4+ Memory Stem T Cells Recognizing Citrullinated Epitopes Are Expanded in Patients With Rheumatoid Arthritis and Sensitive to Tumor Necrosis Factor Blockade. *Arthritis & Rheumatology*, *72*(4), 565–575. https://doi.org/10.1002/ART.41157

Ciccocioppo, F., Lanuti, P., Pierdomenico, L., Simeone, P., Bologna, G., Ercolino, E., … Marchisio, M. (2019). The Characterization of Regulatory T-Cell Profiles in Alzheimer's Disease and Multiple Sclerosis. *Scientific Reports*, *9*(1), 8788. https://doi.org/10.1038/S41598-019-45433-3

Coenen, J. J. A., Koenen, H. J. P. M., Van Rijssen, E., Hilbrands, L. B., & Joosten, I. (2006). Rapamycin, and not cyclosporin A, preserves the highly suppressive CD27+ subset of human CD4+CD25+ regulatory T cells. *Blood*, *107*(3), 1018–1023. https://doi.org/10.1182/BLOOD-2005-07-3032

Cohen, A. C., Nadeau, K. C., Tu, W., Hwa, V., Dionis, K., Bezrodnik, L., … Lewis, D. B. (2006). Cutting Edge: Decreased Accumulation and Regulatory Function of CD4+CD25high T Cells in Human STAT5b Deficiency. *The Journal of Immunology*, *177*(5), 2770–2774. https://doi.org/10.4049/JIMMUNOL.177.5.2770

Collier, A. ris Y., Smith, L. A., & Karumanchi, S. A. (2021). Review of the immune mechanisms of preeclampsia and the potential of immune modulating therapy. *Human Immunology*, *82*(5), 362–370. https://doi.org/10.1016/J.HUMIMM.2021.01.004

Collison, L. W., Chaturvedi, V., Henderson, A. L., Giacomin, P. R., Guy, C., Bankoti, J., … Vignali, D. A. A. (2010). Interleukin-35-mediated induction of a novel regulatory T cell

population. *Nature Immunology*, *11*(12), 1093–1101. https://doi.org/10.1038/NI.1952
Collison, L. W., & Vignali, D. A. A. (2011). In vitro Treg suppression assays. *Methods in Molecular Biology (Clifton, N.J.)*, *707*, 21–37. https://doi.org/10.1007/978-1-61737-979-6_2
Collison, L. W., Workman, C. J., Kuo, T. T., Boyd, K., Wang, Y., Vignali, K. M., … Vignali, D. A. A. (2007). The inhibitory cytokine IL-35 contributes to regulatory T-cell function. *Nature*, *450*(7169), 566–569. https://doi.org/10.1038/nature06306
Coombes, J. L., Siddiqui, K. R. R., Arancibia-Cárcamo, C. V., Hall, J., Sun, C. M., Belkaid, Y., & Powrie, F. (2007). A functionally specialized population of mucosal CD103+ DCs induces Foxp3+ regulatory T cells via a TGF-β– and retinoic acid–dependent mechanism. *The Journal of Experimental Medicine*, *204*(8), 1757–1764. https://doi.org/10.1084/JEM.20070590
Cossarizza, A., Chang, H., Radbruch, A., Acs, A., Adam, D., Adam-Klages, S., … Zychlinsky, A. (2019). Guidelines for the use of flow cytometry and cell sorting in immunological studies (second edition). *European Journal of Immunology*, *49*(10), 1457–1973. https://doi.org/10.1002/eji.201970107
Courville, E. L., & Lawrence, M. G. (2021). Characteristic CD45RA/CD45RO maturation pattern by flow cytometry associated with the CD45 C77G polymorphism. *Cytometry Part B: Clinical Cytometry*, *100*(5), 602–605. https://doi.org/10.1002/CYTO.B.21993
Cozzo Picca, C., Simons, D. M., Oh, S., Aitken, M., Perng, O. A., Mergenthaler, C., Kropf, E., Erikson, J., & Caton, A. J. (2011). $CD4^+CD25^+Foxp3^+$ regulatory T cell formation requires more specific recognition of a self-peptide than thymocyte deletion. Proceedings of the National Academy of Sciences of the United States of America, 108(36), 14890–14895. https://doi.org/10.1073/pnas.1103810108
Crellin, N. K., Garcia, R. V., & Levings, M. K. (2007). Altered activation of AKT is required for the suppressive function of human CD4+CD25+ T regulatory cells. *Blood*, *109*(5), 2014–2022. https://doi.org/10.1182/BLOOD-2006-07-035279
Cuadrado, E., van den Biggelaar, M., de Kivit, S., Chen, Y., Slot, M., Doubal, I., … Amsen, D. (2018). Proteomic Analyses of Human Regulatory T Cells Reveal Adaptations in Signaling Pathways that Protect Cellular Identity. *Immunity*, *48*(5), 1046-1059.e6. https://doi.org/10.1016/j.immuni.2018.04.008
Cuende, J., Liénart, S., Dedobbeleer, O., Van Der Woning, B., De Boeck, G., Stockis, J., … Lucas, S. (2015). Monoclonal antibodies against GARP/TGF-β1 complexes inhibit the immunosuppressive activity of human regulatory T cells in vivo. *Science Translational Medicine*, *7*(284), 284ec65. https://doi.org/10.1126/SCITRANSLMED.AAA1983/SUPPL_FILE/7-284RA56_SM.PDF
Curiel, T. J., Coukos, G., Zou, L., Alvarez, X., Cheng, P., Mottram, P., … Zou, W. (2004). Specific recruitment of regulatory T cells in ovarian carcinoma fosters immune privilege and predicts reduced survival. *Nature Medicine*, *10*(9), 942–949. https://doi.org/10.1038/NM1093
Curti, A., Pandolfi, S., Valzasina, B., Aluigi, M., Isidori, A., Ferri, E., … Lemoli, R. M. (2007). Modulation of tryptophan catabolism by human leukemic cells results in the conversion of CD25- into CD25+ T regulatory cells. *Blood*, *109*(7), 2871–2877. https://doi.org/10.1182/BLOOD-2006-07-036863
Dandona, P., Ghanim, H., Green, K., Sia, C. L., Abuaysheh, S., Kuhadiya, N., … Chaudhuri, A. (2013). Insulin infusion suppresses while glucose infusion induces Toll-like receptors and high-mobility group-B1 protein expression in mononuclear cells of type 1 diabetes patients. *American Journal of Physiology. Endocrinology and Metabolism*, *304*(8), E810-818. https://doi.org/10.1152/AJPENDO.00566.2012
Danke, N. A., Koelle, D. M., Yee, C., Beheray, S., & Kwok, W. W. (2004). Autoreactive T cells in healthy individuals. *Journal of Immunology*, *172*(10), 5967–5972. https://doi.org/10.4049/jimmunol.172.10.5967
de la Rosa, M., Rutz, S., Dorninger, H., & Scheffold, A. (2004). Interleukin-2 is essential for CD4+CD25+ regulatory T cell function. *European Journal of Immunology*, *34*(9), 2480–2488. https://doi.org/10.1002/EJI.200425274
De Rosa, S. C., Herzenberg, L. A., Herzenberg, L. A., & Roederer, M. (2001). 11-color, 13-parameter flow cytometry: Identification of human naive T cells by phenotype, function, and T-cell receptor diversity. *Nature Medicine*, *7*(2), 245–248. https://doi.org/10.1038/84701
Deaglio, S., Dwyer, K. M., Gao, W., Friedman, D., Usheva, A., Erat, A., … Robson, S. C. (2007). Adenosine generation catalyzed by CD39 and CD73 expressed on regulatory T

cells mediates immune suppression. *Journal of Experimental Medicine*, *204*(6), 1257–1265. https://doi.org/10.1084/JEM.20062512
Derbinski, J., Schulte, A., Kyewski, B., & Klein, L. (2001). Promiscuous gene expression in medullary thymic epithelial cells mirrors the peripheral self. *Nature Immunology*, *2*(11), 1032–1039. https://doi.org/10.1038/ni723
Dieckmann, D., Plottner, H., Berchtold, S., Berger, T., & Schuler, G. (2001). Ex Vivo Isolation and Characterization of Cd4+Cd25+ T Cells with Regulatory Properties from Human Blood. *The Journal of Experimental Medicine*, *193*(11), 1303–1310. https://doi.org/10.1084/JEM.193.11.1303
Dixon, K. O., van der Kooij, S. W., Vignali, D. A. A., & van Kooten, C. (2015). Human tolerogenic dendritic cells produce IL-35 in the absence of other IL-12 family members. *European Journal of Immunology*, *45*(6), 1736–1747. https://doi.org/10.1002/EJI.201445217
Dong, S., Hiam-Galvez, K. J., Mowery, C. T., Herold, K. C., Gitelman, S. E., Esensten, J. H., … Bluestone, J. A. (2021). The effect of low-dose IL-2 and Treg adoptive cell therapy in patients with type 1 diabetes. *JCI Insight*, *6*(18), e147474. https://doi.org/10.1172/JCI.INSIGHT.147474
Donnelly, C., Dykstra, B., Mondal, N., Huang, J., Kaskow, B. J., Griffin, R., … Baecher-Allan, C. (2018). Optimizing human Treg immunotherapy by Treg subset selection and E-selectin ligand expression. *Scientific Reports*, *8*(1), 1–14. https://doi.org/10.1038/s41598-017-17981-z
Duggleby, R. C., Shaw, T. N. F., Jarvis, L. B., Kaur, G., & Hill Gaston, J. S. (2007). CD27 expression discriminates between regulatory and non-regulatory cells after expansion of human peripheral blood CD4+ CD25+ cells. *Immunology*, *121*(1), 129–139. https://doi.org/https://doi.org/10.1111/j.1365-2567.2006.02550.x
Duggleby, R., Danby, R. D., Madrigal, J. A., & Saudemont, A. (2018). Clinical Grade Regulatory CD4+ T Cells (Tregs): Moving Toward Cellular-Based Immunomodulatory Therapies. *Frontiers in Immunology*, *9*, 252. https://doi.org/10.3389/fimmu.2018.00252
Duhen, T., Duhen, R., Lanzavecchia, A., Sallusto, F., & Campbell, D. J. (2012). Functionally distinct subsets of human FOXP3+ Treg cells that phenotypically mirror effector Th cells. *Blood*, *119*(19), 4430–4440. https://doi.org/10.1182/blood-2011-11-392324
Edwards, J. P., Fujii, H., Zhou, A. X., Creemers, J., Unutmaz, D., & Shevach, E. M. (2013). Regulation of the expression of GARP/latent-TGF-β1 complexes on mouse T cells and their role in Regulatory T Cell and Th17 differentiation. *Journal of Immunology (Baltimore, Md. : 1950)*, *190*(11), 5506–5515. https://doi.org/10.4049/JIMMUNOL.1300199
Edwards, J. P., Hand, T. W., Morais da Fonseca, D., Glass, D. D., Belkaid, Y., & Shevach, E. M. (2016). The GARP/Latent TGF-β1 complex on Treg cells modulates the induction of peripherally derived Treg cells during oral tolerance. *European Journal of Immunology*, *46*(6), 1480–1489. https://doi.org/10.1002/EJI.201546204
Efthymiou, A., Mureanu, N., Pemberton, R., Tai-MacArthur, S., Mastronicola, D., Scottà, C., … Shangaris, P. (2022). Isolation and freezing of human peripheral blood mononuclear cells from pregnant patients. *STAR Protocols*, *3*(1), 101204. https://doi.org/10.1016/J.XPRO.2022.101204
Egerton, M., Scollay, R., & Shortman, K. (1990). Kinetics of mature T-cell development in the thymus. *Proceedings of the National Academy of Sciences of the United States of America*, *87*(7), 2579–2582. https://doi.org/10.1073/PNAS.87.7.2579
Eggenhuizen, P. J., Ng, B. H., & Ooi, J. D. (2020). Treg Enhancing Therapies to Treat Autoimmune Diseases. *International Journal of Molecular Sciences*, *21*(19), 1–18. https://doi.org/10.3390/IJMS21197015
Eksteen, B., Miles, A., Curbishley, S. M., Tselepis, C., Grant, A. J., Walker, L. S. K., & Adams, D. H. (2006). Epithelial Inflammation Is Associated with CCL28 Production and the Recruitment of Regulatory T Cells Expressing CCR10. *The Journal of Immunology*, *177*(1), 593–603. https://doi.org/10.4049/JIMMUNOL.177.1.593
Eller, K., Wolf, D., Huber, J. M., Metz, M., Mayer, G., McKenzie, A. N. J., … Wolf, A. M. (2011). IL-9 production by regulatory T cells recruits mast cells that are essential for regulatory T cell-induced immune-suppression. *Journal of Immunology*, *186*(1), 83–91. https://doi.org/10.4049/JIMMUNOL.1001183
Elyaman, W., Bradshaw, E. M., Uyttenhove, C., Dardalhon, V., Awasthi, A., Imitola, J., … Khoury, S. J. (2009). IL-9 induces differentiation of TH17 cells and enhances function of FoxP3+ natural regulatory T cells. *Proceedings of the National Academy of Sciences of*

the United States of America, *106*(31), 12885–12890. https://doi.org/10.1073/PNAS.0812530106
Ernst, P. B., Garrison, J. C., & Thompson, L. F. (2010). Much Ado about Adenosine: Adenosine Synthesis and Function in Regulatory T Cell Biology. *Journal of Immunology (Baltimore, Md. : 1950)*, *185*(4), 1993–1998. https://doi.org/10.4049/JIMMUNOL.1000108
Fagninou, A., Nekoua, M. P., Sossou, D., Moutairou, K., Fievet, N., & Yessoufou, A. (2020). Th2-Immune Polarizing and Anti-Inflammatory Properties of Insulin Are Not Effective in Type 2 Diabetic Pregnancy. *Journal of Immunology Research*, 2038746. https://doi.org/10.1155/2020/2038746
Fahlén, L., Read, S., Gorelik, L., Hurst, S. D., Coffman, R. L., Flavell, R. A., & Powrie, F. (2005). T cells that cannot respond to TGF-β escape control by CD4+CD25+ regulatory T cells. *The Journal of Experimental Medicine*, *201*(5), 737–746. https://doi.org/10.1084/JEM.20040685
Fallarino, F., Grohmann, U., You, S., McGrath, B. C., Cavener, D. R., Vacca, C., … Puccetti, P. (2006). The combined effects of tryptophan starvation and tryptophan catabolites down-regulate T cell receptor zeta-chain and induce a regulatory phenotype in naive T cells. *Journal of Immunology (Baltimore, Md. : 1950)*, *176*(11), 6752–6761. https://doi.org/10.4049/JIMMUNOL.176.11.6752
Feuerer, M., Hill, J. A., Kretschmer, K., Von Boehmer, H., Mathis, D., & Benoist, C. (2010). Genomic definition of multiple ex vivo regulatory T cell subphenotypes. *Proceedings of the National Academy of Sciences of the United States of America*, *107*(13), 5919–5924. https://doi.org/10.1073/PNAS.1002006107
Fiorentino, D F, Zlotnik, A., Mosmann, T. R., Howard, M., & O'Garra, A. (1991). IL-10 inhibits cytokine production by activated macrophages. *The Journal of Immunology*, *147*(11), 3815–3822.
Fiorentino, David F., Bond, M. W., & Mosmann, T. R. (1989). Two types of mouse T helper cell. IV. Th2 clones secrete a factor that inhibits cytokine production by Th1 clones. *The Journal of Experimental Medicine*, *170*(6), 2081–2095. https://doi.org/10.1084/JEM.170.6.2081
Fischbach, M. A., Bluestone, J. A., & Lim, W. A. (2013). Cell-Based Therapeutics: The Next Pillar of Medicine. *Science Translational Medicine*, *5*(179), 179ps7. https://doi.org/10.1126/SCITRANSLMED.3005568
Flores-Borja, F., Jury, E. C., Mauri, C., & Ehrenstein, M. R. (2008). Defects in CTLA-4 are associated with abnormal regulatory T cell function in rheumatoid arthritis. *Proceedings of the National Academy of Sciences of the United States of America*, *105*(49), 19396–19401. https://doi.org/10.1073/PNAS.0806855105/SUPPL_FILE/0806855105SI.PDF
Fonseca, V. R., Agua-Doce, A., Maceiras, A. R., Pierson, W., Ribeiro, F., Romão, V. C., … Graca, L. (2017). Human blood Tfr cells are indicators of ongoing humoral activity not fully licensed with suppressive function. *Science Immunology*, *2*(14), eaan1487. https://doi.org/10.1126/sciimmunol.aan1487
Fontenot, J. D., Gavin, M. A., & Rudensky, A. Y. (2003). Foxp3 programs the development and function of CD4+CD25+ regulatory T cells. *Nature Immunology 2003 4:4*, *4*(4), 330–336. https://doi.org/10.1038/ni904
Fontenot, J. D., Rasmussen, J. P., Gavin, M. A., & Rudensky, A. Y. (2005). A function for interleukin 2 in Foxp3-expressing regulatory T cells. *Nature Immunology*, *6*(11), 1142–1151. https://doi.org/10.1038/ni1263
Franke, A., Balschun, T., Karlsen, T. H., Sventoraityte, J., Nikolaus, S., Mayr, G., … Schreiber, S. (2008). Sequence variants in IL10, ARPC2 and multiple other loci contribute to ulcerative colitis susceptibility. *Nature Genetics*, *40*(11), 1319–1323. https://doi.org/10.1038/ng.221
Fraser, H., Safinia, N., Grageda, N., Thirkell, S., Lowe, K., Fry, L. J., … Lombardi, G. (2018). A Rapamycin-Based GMP-Compatible Process for the Isolation and Expansion of Regulatory T Cells for Clinical Trials. *Molecular Therapy - Methods and Clinical Development*, *8*, 198–209. https://doi.org/10.1016/j.omtm.2018.01.006
Fritzsching, B., Oberle, N., Eberhardt, N., Quick, S., Haas, J., Wildemann, B., … Suri-Payer, E. (2005). Cutting Edge: In Contrast to Effector T Cells, CD4+CD25+FoxP3+ Regulatory T Cells Are Highly Susceptible to CD95 Ligand- but Not to TCR-Mediated Cell Death. *The Journal of Immunology*, *175*(1), 32–36. https://doi.org/10.4049/JIMMUNOL.175.1.32
Fritzsching, B., Oberle, N., Pauly, E., Geffers, R., Buer, J., Poschl, J., … Suri-Payer, E. (2006). Naive regulatory T cells: a novel subpopulation defined by resistance toward CD95L-

mediated cell death. *Blood*, *108*(10), 3371–3378. https://doi.org/10.1182/BLOOD-2006-02-005660
Fuertes Marraco, S. A., Soneson, C., Cagnon, L., Gannon, P. O., Allard, M., Maillard, S. A., … Speiser, D. E. (2015). Long-lasting stem cell-like memory CD8+ T cells with a naïve-like profile upon yellow fever vaccination. *Science Translational Medicine*, *7*(282), 282ra48. https://doi.org/10.1126/SCITRANSLMED.AAA3700/SUPPL_FILE/7-282RA48_TABLE_S3.ZIP
Fuhrman, C. A., Yeh, W.-I., Seay, H. R., Lakshmi, P. S., Chopra, G., Zhang, L., … Brusko, T. M. (2015). Divergent phenotypes of human regulatory T cells expressing the receptors TIGIT and CD226. *Journal of Immunology*, *195*(1), 145–155. https://doi.org/10.4049/JIMMUNOL.1402381
Gaffen, S. L. (2001). SIGNALING DOMAINS OF THE INTERLEUKIN 2 RECEPTOR. *Cytokine*, *14*(2), 63–77. https://doi.org/10.1006/CYTO.2001.0862
Gattinoni, L., Lugli, E., Ji, Y., Pos, Z., Paulos, C. M., Quigley, M. F., … Restifo, N. P. (2011a). A human memory T cell subset with stem cell–like properties. *Nature Medicine*, *17*(10), 1290–1297. https://doi.org/10.1038/nm.2446
Gattinoni, L., Lugli, E., Ji, Y., Pos, Z., Paulos, C. M., Quigley, M. F., … Restifo, N. P. (2011b). A human memory T cell subset with stem cell–like properties. *Nature Medicine*, *17*(10), 1290–1297. https://doi.org/10.1038/nm.2446
Gershon, R. K., & Kondo, K. (1970). Cell interactions in the induction of tolerance: the role of thymic lymphocytes. *Immunology*, *18*(5), 723–737. Retrieved from /pmc/articles/PMC1455602/?report=abstract
Gianchecchi, E., & Fierabracci, A. (2018). Inhibitory Receptors and Pathways of Lymphocytes: The Role of PD-1 in Treg Development and Their Involvement in Autoimmunity Onset and Cancer Progression. *Frontiers in Immunology*, *9*, 2374. https://doi.org/10.3389/FIMMU.2018.02374
Giganti, G., Atif, M., Mohseni, Y., Mastronicola, D., Grageda, N., Povoleri, G. A. M., … Scottà, C. (2021). Treg cell therapy: How cell heterogeneity can make the difference. *European Journal of Immunology*, *51*(1), 39–55. https://doi.org/https://doi.org/10.1002/eji.201948131
Gillis, S., Ferm, M. M., Ou, W., & Smith, K. A. (1978). T Cell Growth Factor: Parameters of Production and a Quantitative Microassay for Activity. *The Journal of Immunology*, *120*(6), 2027–2032.
Glatigny, S., Duhen, R., Oukka, M., & Bettelli, E. (2011). Loss of alpha4 integrin expression differentially affects the homing of Th1 and Th17 cells. *Journal of Immunology*, *187*(12), 6176–6179. https://doi.org/10.4049/JIMMUNOL.1102515
Gomez-Lopez, N., Arenas-Hernandez, M., Romero, R., Sanchez-Torres, C., Done, B., & Tarca Correspondence, A. L. (2020). Regulatory T Cells Play a Role in a Subset of Idiopathic Preterm Labor/Birth and Adverse Neonatal Outcomes. *Cell Reports*, *32*(1), 107874. https://doi.org/10.1016/j.celrep.2020.107874
Gorelik, L., & Flavell, R. A. (2000). Abrogation of TGFβ signaling in T cells leads to spontaneous T cell differentiation and autoimmune disease. *Immunity*, *12*(2), 171–181. https://doi.org/10.1016/S1074-7613(00)80170-3
Gottschalk, R. A., Corse, E., & Allison, J. P. (2012). Expression of Helios in Peripherally Induced Foxp3+ Regulatory T Cells. *The Journal of Immunology*, *188*(3), 976–980. https://doi.org/10.4049/JIMMUNOL.1102964
Graesser, D., Solowiej, A., Bruckner, M., Osterweil, E., Juedes, A., Davis, S., … Madri, J. A. (2002). Altered vascular permeability and early onset of experimental autoimmune encephalomyelitis in PECAM-1–deficient mice. *The Journal of Clinical Investigation*, *109*(3), 383–392. https://doi.org/10.1172/JCI13595
Grant, C. R., Liberal, R., Holder, B. S., Cardone, J., Ma, Y., Robson, S. C., … Longhi, M. S. (2014). DYSFUNCTIONAL CD39POS REGULATORY T CELLS AND ABERRANT CONTROL OF T HELPER TYPE 17 CELLS IN AUTOIMMUNE HEPATITIS. *Hepatology*, *59*(3), 1007–1015. https://doi.org/10.1002/HEP.26583
Green, S., Politis, M., Rallis, K. S., Saenz de Villaverde Cortabarria, A., Efthymiou, A., Mureanu, N., … Shangaris, P. (2021). Regulatory T Cells in Pregnancy Adverse Outcomes: A Systematic Review and Meta-Analysis. *Frontiers in Immunology*, *12*, 737862. https://doi.org/10.3389/FIMMU.2021.737862/FULL
Gregori, S., Tomasoni, D., Pacciani, V., Scirpoli, M., Battaglia, M., Magnani, C. F., … Roncarolo, M. G. (2010). Differentiation of type 1 T regulatory cells (Tr1) by tolerogenic DC-10 requires the IL-10–dependent ILT4/HLA-G pathway. *Blood*, *116*(6), 935–944.

https://doi.org/10.1182/BLOOD-2009-07-234872
Grohmann, U., Orabona, C., Fallarino, F., Vacca, C., Calcinaro, F., Falorni, A., … Puccetti, P. (2002). CTLA-4–Ig regulates tryptophan catabolism in vivo. *Nature Immunology*, *3*(11), 1097–1101. https://doi.org/10.1038/ni846
Grossman, W. J., Verbsky, J. W., Barchet, W., Colonna, M., Atkinson, J. P., & Ley, T. J. (2004). Human T regulatory cells can use the perforin pathway to cause autologous target cell death. *Immunity*, *21*(4), 589–601. https://doi.org/10.1016/j.immuni.2004.09.002
Gubser, C., Schmaler, M., Rossi, S. W., & Palmer, E. (2016). Monoclonal regulatory T cells provide insights into T cell suppression. *Scientific Reports 2016 6:1*, *6*(1), 25758. https://doi.org/10.1038/srep25758
Guo, H., Zheng, M., Zhang, K., Yang, F., Zhang, X., Han, Q., … Zhu, P. (2016). Functional defects in CD4+ CD25high FoxP3+ regulatory cells in ankylosing spondylitis. *Scientific Reports*, *6*, 37559. https://doi.org/10.1038/srep37559
Gutcher, I., Donkor, M. K., Ma, Q., Rudensky, A. Y., Flavell, R. A., & Li, M. O. (2011). Autocrine Transforming Growth Factor-β1 Promotes in vivo Th17 Cell Differentiation. *Immunity*, *34*(3), 396–408. https://doi.org/10.1016/J.IMMUNI.2011.03.005
Haas, J., Fritzsching, B., Trübswetter, P., Korporal, M., Milkova, L., Fritz, B., … Wildemann, B. (2007a). Prevalence of Newly Generated Naive Regulatory T Cells (T reg) Is Critical for T reg Suppressive Function and Determines T reg Dysfunction in Multiple Sclerosis. *The Journal of Immunology*, *179*(2), 1322–1330. https://doi.org/10.4049/jimmunol.179.2.1322
Haas, J., Fritzsching, B., Trübswetter, P., Korporal, M., Milkova, L., Fritz, B., … Wildemann, B. (2007b). Prevalence of Newly Generated Naive Regulatory T Cells (Treg) Is Critical for Treg Suppressive Function and Determines Treg Dysfunction in Multiple Sclerosis. *The Journal of Immunology*, *179*(2), 1322–1330. https://doi.org/10.4049/JIMMUNOL.179.2.1322
Haas, J., Fritzsching, B., Trübswetter, P., Korporal, M., Milkova, L., Fritz, B., … Wildemann, B. (2007c). Prevalence of Newly Generated Naive Regulatory T Cells (Treg) Is Critical for Treg Suppressive Function and Determines Treg Dysfunction in Multiple Sclerosis. *The Journal of Immunology*, *179*(2), 1322–1330. https://doi.org/10.4049/JIMMUNOL.179.2.1322
Halim, L., Romano, M., McGregor, R., Correa, I., Pavlidis, P., Grageda, N., … Lombardi, G. (2017). An Atlas of Human Regulatory T Helper-like Cells Reveals Features of Th2-like Tregs that Support a Tumorigenic Environment. *Cell Reports*, *20*(3), 757–770. https://doi.org/10.1016/j.celrep.2017.06.079
Haribhai, D., Williams, J. B., Jia, S., Nickerson, D., Schmitt, E. G., Edwards, B., … Williams, C. B. (2011). A requisite role for induced regulatory T cells in tolerance based on expanding antigen receptor diversity. *Immunity*, *35*(1), 109–122. https://doi.org/10.1016/j.immuni.2011.03.029
Harlev, A., & Wiznitzer, A. (2010). New insights on glucose pathophysiology in gestational diabetes and insulin resistance. *Current Diabetes Reports*, *10*(3), 242–247. https://doi.org/10.1007/S11892-010-0113-7/FIGURES/2
Hatakeyama, M., Tsudo, M., Minamoto, S., Kono, T., Doi, T., Miyata, T., … Taniguchi, T. (1989). Interleukin-2 Receptor β Chain Gene: Generation of Three Receptor Forms by Cloned Human α and β Chain cDNA's. *Science*, *244*(4904), 551–556. https://doi.org/10.1126/SCIENCE.2785715
Haynes, B. F., & Heinly, C. S. (1995). Early human T cell development: analysis of the human thymus at the time of initial entry of hematopoietic stem cells into the fetal thymic microenvironment. *The Journal of Experimental Medicine*, *181*(4), 1445–1458. https://doi.org/10.1084/JEM.181.4.1445
Heim, L., Yang, Z., Tausche, P., Hohenberger, K., Chiriac, M. T., Koelle, J., … Finotto, S. (2022). IL-9 Producing Tumor-Infiltrating Lymphocytes and Treg Subsets Drive Immune Escape of Tumor Cells in Non-Small Cell Lung Cancer. *Frontiers in Immunology*, *13*, 859738. https://doi.org/10.3389/FIMMU.2022.859738/FULL
Henshall, T. L., Jones, K. L., Wilkinson, R., & Jackson, D. E. (2001). Src homology 2 domain-containing protein-tyrosine phosphatases, SHP-1 and SHP-2, are required for platelet endothelial cell adhesion molecule-1/CD31-mediated inhibitory signaling. *Journal of Immunology*, *166*(5), 3098–3106. https://doi.org/10.4049/JIMMUNOL.166.5.3098
Hill, J. A., Feuerer, M., Tash, K., Haxhinasto, S., Perez, J., Melamed, R., … Benoist, C. (2007). Foxp3 Transcription-Factor-Dependent and -Independent Regulation of the Regulatory T Cell Transcriptional Signature. *Immunity*, *27*(5), 786–800.

https://doi.org/10.1016/j.immuni.2007.09.010
Himmel, M. E., MacDonald, K. G., Garcia, R. V., Steiner, T. S., & Levings, M. K. (2013). Helios+ and Helios− Cells Coexist within the Natural FOXP3+ T Regulatory Cell Subset in Humans. *The Journal of Immunology*, *190*(5), 2001–2008. https://doi.org/10.4049/JIMMUNOL.1201379
Hinterberger, M., Aichinger, M., Prazeres da Costa, O., Voehringer, D., Hoffmann, R., & Klein, L. (2010). Autonomous role of medullary thymic epithelial cells in central CD4(+) T cell tolerance. Nature immunology, 11(6), 512–519. https://doi.org/10.1038/ni.1874
Hippen, K. L., Merkel, S. C., Schirm, D. K., Sieben, C. M., Sumstad, D., Kadidlo, D. M., … Blazar, B. R. (2011). Massive ex vivo expansion of human natural regulatory T cells (Tregs) with minimal loss of in vivo functional activity. *Science Translational Medicine*, *3*(83), 83ra41. https://doi.org/10.1126/SCITRANSLMED.3001809
Hirota, K., Yoshitomi, H., Hashimoto, M., Maeda, S., Teradaira, S., Sugimoto, N., … Sakaguchi, S. (2007). Preferential recruitment of CCR6-expressing Th17 cells to inflamed joints via CCL20 in rheumatoid arthritis and its animal model. *The Journal of Experimental Medicine*, *204*(12), 2803–2812. https://doi.org/10.1084/JEM.20071397
Hoffmann, P., Boeld, T. J., Eder, R., Huehn, J., Floess, S., Wieczorek, G., … Edinger, M. (2009). Loss of FOXP3 expression in natural human CD4+CD25+ regulatory T cells upon repetitive in vitro stimulation. *European Journal of Immunology*, *39*(4), 1088–1097. https://doi.org/10.1002/EJI.200838904
Hoffmann, P., Eder, R., Boeld, T. J., Doser, K., Piseshka, B., Andreesen, R., & Edinger, M. (2006). Only the CD45RA+ subpopulation of CD4+CD25high T cells gives rise to homogeneous regulatory T-cell lines upon in vitro expansion. *Blood*, *108*(13), 4260–4267. https://doi.org/10.1182/BLOOD-2006-06-027409
Höllbacher, B., Duhen, T., Motley, S., Klicznik, M. M., Gratz, I. K., & Campbell, D. J. (2020). Transcriptomic profiling of human effector and regulatory T cell subsets identifies predictive population signatures. *ImmunoHorizons*, *4*(10), 585–596. https://doi.org/10.4049/IMMUNOHORIZONS.2000037
Hori, S., Nomura, T., & Sakaguchi, S. (2003). Control of regulatory T cell development by the transcription factor Foxp3. *Science*, *299*(5609), 1057–1061. https://doi.org/10.1126/SCIENCE.1079490
Hornero, R. A., Betts, G. J., Sawitzki, B., Vogt, K., Harden, P. N., & Wood, K. J. (2017). CD45RA Distinguishes CD4+CD25+CD127−/low TSDR Demethylated Regulatory T Cell Subpopulations With Differential Stability and Susceptibility to Tacrolimus-Mediated Inhibition of Suppression. *Transplantation*, *101*(2), 302–309. https://doi.org/10.1097/TP.0000000000001278
Hosokawa, K., Muranski, P., Feng, X., Townsley, D. M., Liu, B., Knickelbein, J., … Young, N. S. (2016). Memory Stem T Cells in Autoimmune Disease: High Frequency of Circulating CD8+ Memory Stem Cells in Acquired Aplastic Anemia. *Journal of Immunology*, *196*(4), 1568–1578. https://doi.org/10.4049/JIMMUNOL.1501739
Hou, T. Z., Qureshi, O. S., Wang, C. J., Baker, J., Young, S. P., Walker, L. S. K., & Sansom, D. M. (2015). A Transendocytosis model of CTLA-4 function predicts its suppressive behaviour on regulatory T cells. *Journal of Immunology*, *194*(5), 2148–2159. https://doi.org/10.4049/JIMMUNOL.1401876
Hou, Z., Ye, Q., Qiu, M., Hao, Y., Han, J., & Zeng, H. (2017). Increased activated regulatory T cells proportion correlate with the severity of idiopathic pulmonary fibrosis. *Respiratory Research*, *18*(1), 170. https://doi.org/10.1186/s12931-017-0653-3
Hozumi, N., & Tonegawa, S. (1976). Evidence for somatic rearrangement of immunoglobulin genes coding for variable and constant regions. *Proceedings of the National Academy of Sciences of the United States of America*, *73*(10), 3628–3632. https://doi.org/10.1073/PNAS.73.10.3628
Hsieh, C. S., Liang, Y., Tyznik, A. J., Self, S. G., Liggitt, D., & Rudensky, A. Y. (2004). Recognition of the peripheral self by naturally arising CD25+ CD4+ T cell receptors. *Immunity*, *21*(2), 267–277. https://doi.org/10.1016/J.IMMUNI.2004.07.009/ATTACHMENT/0DD657DF-735E-411B-9506-E396FAD8D075/MMC1.PDF
Hsieh, C. S., Liang, Y., Tyznik, A. J., Self, S. G., Liggitt, D., & Rudensky, A. Y. (2004). Recognition of the peripheral self by naturally arising CD25+ CD4+ T cell receptors. Immunity, 21(2), 267–277. https://doi.org/10.1016/j.immuni.2004.07.009
Hsu, P., Santner-Nanan, B., Dahlstrom, J. E., Fadia, M., Chandra, A., Peek, M., & Nanan, R.

(2012). Altered decidual DC-SIGN+ antigen-presenting cells and impaired regulatory T-cell induction in preeclampsia. *The American Journal of Pathology*, *181*(6), 2149–2160. https://doi.org/10.1016/J.AJPATH.2012.08.032

Hu, D., Chen, Y., Zhang, W., Wang, H., Wang, Z., & Dong, M. (2008). Alteration of peripheral CD4+CD25+ regulatory T lymphocytes in pregnancy and pre-eclampsia. *Acta Obstetricia et Gynecologica Scandinavica*, *87*(2), 190–194. https://doi.org/10.1080/00016340701823991

Hu, M., Wang, C., Zhang, G. Y., Saito, M., Wang, Y. M., Fernandez, M. A., … Alexander, S. I. (2013). Infiltrating Foxp3(+) regulatory T cells from spontaneously tolerant kidney allografts demonstrate donor-specific tolerance. *American Journal of Transplantation*, *13*(11), 2819–2830. https://doi.org/10.1111/AJT.12445

Huang, L., Zheng, Y., Yuan, X., Ma, Y., Xie, G., Wang, W., … Shen, L. (2017). Decreased frequencies and impaired functions of the CD31 + subpopulation in T reg cells associated with decreased FoxP3 expression and enhanced T reg cell defects in patients with coronary heart disease. *Clinical & Experimental Immunology*, *187*(3), 441–454. https://doi.org/10.1111/cei.12897

Huang, S., Apasov, S., Koshiba, M., & Sitkovsky, M. (1997). Role of A2a Extracellular Adenosine Receptor-Mediated Signaling in Adenosine-Mediated Inhibition of T-Cell Activation and Expansion. *Blood*, *90*(4), 1600–1610. https://doi.org/10.1182/BLOOD.V90.4.1600

Huber, S., Gagliani, N., Esplugues, E., O'Connor, W., Huber, F. J., Chaudhry, A., … Flavell, R. A. (2011). Th17 cells express interleukin-10 receptor and are controlled by Foxp3− and Foxp3+ regulatory CD4+ T cells in an interleukin-10 dependent manner. *Immunity*, *34*(4), 554–565. https://doi.org/10.1016/J.IMMUNI.2011.01.020

Huehn, J., Siegmund, K., Lehmann, J. C. U., Siewert, C., Haubold, U., Feuerer, M., … Hamann, A. (2004). Developmental Stage, Phenotype, and Migration Distinguish Naive- and Effector/Memory-like CD4+ Regulatory T Cells. *The Journal of Experimental Medicine*, *199*(3), 303–313. https://doi.org/10.1084/JEM.20031562

Iellem, A., Colantonio, L., & D'Ambrosio, D. (2003). Skin-versus gut-skewed homing receptor expression and intrinsic CCR4 expression on human peripheral blood CD4+CD25+ suppressor T cells. *European Journal of Immunology*, *33*(6), 1488–1496. https://doi.org/10.1002/EJI.200323658

Iikuni, N., Lourenço, E. V., Hahn, B. H., & Cava, A. La. (2009). Cutting Edge: Regulatory T Cells Directly Suppress B Cells in Systemic Lupus Erythematosus. *Journal of Immunology*, *183*(3), 1518–1522. https://doi.org/10.4049/JIMMUNOL.0901163

Ito, T., Hanabuchi, S., Wang, Y.-H., Park, W. R., Arima, K., Bover, L., … Liu, Y.-J. (2008). Two Functional Subsets of FOXP3+ Regulatory T Cells in Human Thymus and Periphery. *Immunity*, *28*(6), 870–880. https://doi.org/10.1016/J.IMMUNI.2008.03.018

Itoh, M., Takahashi, T., Sakaguchi, N., Kuniyasu, Y., Shimizu, J., Otsuka, F., & Sakaguchi, S. (1999). Thymus and Autoimmunity: Production of CD25+CD4+ Naturally Anergic and Suppressive T Cells as a Key Function of the Thymus in Maintaining Immunologic Self-Tolerance. *Journal of Immunology*, *162*(9), 5317–5326.

Jacquemin, C., Augusto, J. F., Scherlinger, M., Gensous, N., Forcade, E., Douchet, I., … Blanco, P. (2018). OX40L/OX40 axis impairs follicular and natural Treg function in human SLE. *JCI Insight*, *3*(24), e122167. https://doi.org/10.1172/JCI.INSIGHT.122167

Jarvis, L. B., Rainbow, D. B., Coppard, V., Howlett, S. K., Georgieva, Z., Davies, J. L., … Jones, J. L. (2021). Therapeutically expanded human regulatory T-cells are super-suppressive due to HIF1A induced expression of CD73. *Communications Biology*, *4*(1), 1186. https://doi.org/10.1038/s42003-021-02721-x

Joffre, O., Santolaria, T., Calise, D., Saati, T. Al, Hudrisier, D., Romagnoli, P., & Van Meerwijk, J. P. M. (2008). Prevention of acute and chronic allograft rejection with CD4+CD25+Foxp3+ regulatory T lymphocytes. *Nature Medicine*, *14*(1), 88–92. https://doi.org/10.1038/NM1688

Joller, N., Lozano, E., Burkett, P. R., Patel, B., Xiao, S., Zhu, C., … Kuchroo, V. K. (2014). Treg cells expressing the co-inhibitory molecule TIGIT selectively inhibit pro-inflammatory Th1 and Th17 cell responses. *Immunity*, *40*(4), 569–581. https://doi.org/10.1016/J.IMMUNI.2014.02.012

Jones, B. E., Maerz, M. D., & Buckner, J. H. (2018). IL-6: a cytokine at the crossroads of autoimmunity. *Current Opinion in Immunology*, *55*, 9–14. https://doi.org/10.1016/J.COI.2018.09.002

Jonuleit, H., Schmitt, E., Stassen, M., Tuettenberg, A., Knop, J., & Enk, A. H. (2001). Identification and Functional Characterization of Human Cd4+Cd25+ T Cells with Regulatory Properties Isolated from Peripheral Blood. *The Journal of Experimental Medicine*, *193*(11), 1285–1294. https://doi.org/10.1084/JEM.193.11.1285

Jordan, M. S., Boesteanu, A., Reed, A. J., Petrone, A. L., Holenbeck, A. E., Lerman, M. A., Naji, A., & Caton, A. J. (2001). Thymic selection of CD4+CD25+ regulatory T cells induced by an agonist self-peptide. Nature immunology, 2(4), 301–306. https://doi.org/10.1038/86302

Kälble, F., Wu, L., Lorenz, H. M., Zeier, M., Schaier, M., & Steinborn, A. (2021). Impaired Differentiation of Highly Proliferative ICOS +-Tregs Is Involved in the Transition from Low to High Disease Activity in Systemic Lupus Erythematosus (SLE) Patients. *International Journal of Molecular Sciences*, *22*(17), 9501. https://doi.org/10.3390/IJMS22179501

Karaaslan, Z., Kahraman, Ö. T., Şanlı, E., Ergen, H. A., Ulusoy, C., Bilgiç, B., … Küçükali, C. İ. (2021). Inflammation and regulatory T cell genes are differentially expressed in peripheral blood mononuclear cells of Parkinson's disease patients. *Scientific Reports*, *11*(1), 2316. https://doi.org/10.1038/S41598-021-81961-7

Kekäläinen, E., Tuovinen, H., Joensuu, J., Gylling, M., Franssila, R., Pöntynen, N., … Arstila, T. P. (2007). A Defect of Regulatory T Cells in Patients with Autoimmune Polyendocrinopathy-Candidiasis-Ectodermal Dystrophy. *The Journal of Immunology*, *178*(2), 1208–1215. https://doi.org/10.4049/JIMMUNOL.178.2.1208

Kim, J. M., Rasmussen, J. P., & Rudensky, A. Y. (2007). Regulatory T cells prevent catastrophic autoimmunity throughout the lifespan of mice. *Nature Immunology*, *8*(2), 191–197. https://doi.org/10.1038/ni1428

Kimmig, S., Przybylski, G. K., Schmidt, C. A., Laurisch, K., Möwes, B., Radbruch, A., & Thiel, A. (2002). Two subsets of naive T helper cells with distinct T cell receptor excision circle content in human adult peripheral blood. *The Journal of Experimental Medicine*, *195*(6), 789–794. https://doi.org/10.1084/jem.20011756

Kindler, V., Matthes, T., Jeannin, P., & Zubler, R. H. (1995). Interleukin-2 secretion by human B lymphocytes occurs as a late event and requires additional stimulation after CD40 cross-linking. *European Journal of Immunology*, *25*(5), 1239–1243. https://doi.org/10.1002/EJI.1830250516

Kisielewicz, A., Schaier, M., Schmitt, E., Hug, F., Haensch, G. M., Meuer, S., … Steinborn, A. (2010). A distinct subset of HLA-DR+-regulatory T cells is involved in the induction of preterm labor during pregnancy and in the induction of organ rejection after transplantation. *Clinical Immunology*, *137*(2), 209–220. https://doi.org/10.1016/J.CLIM.2010.07.008

Kitagawa, Y., Ohkura, N., Kidani, Y., Vandenbon, A., Hirota, K., Kawakami, R., … Sakaguchi, S. (2017). Guidance of regulatory T cell development by Satb1-dependent super-enhancer establishment. *Nature Immunology*, *18*(2), 173–183. https://doi.org/10.1038/ni.3646

Klatzmann, D., & Abbas, A. K. (2015). The promise of low-dose interleukin-2 therapy for autoimmune and inflammatory diseases. *Nature Reviews Immunology*, *15*(5), 283–294. https://doi.org/10.1038/nri3823

Klein, L., Kyewski, B., Allen, P. M., & Hogquist, K. A. (2014). Positive and negative selection of the T cell repertoire: what thymocytes see (and don't see). *Nature Reviews Immunology 2014 14:6*, *14*(6), 377–391. https://doi.org/10.1038/nri3667

Kleinewietfeld, M., Starke, M., Di Mitri, D., Borsellino, G., Battistini, L., Rötzschke, O., & Falk, K. (2009). CD49d provides access to "untouched" human Foxp3+ Treg free of contaminating effector cells. *Blood*, *113*(4), 827–836. https://doi.org/10.1182/blood-2008-04-150524

Kluger, M. A., Melderis, S., Nosko, A., Goerke, B., Luig, M., Meyer, M. C., … Steinmetz, O. M. (2016). Treg17 cells are programmed by Stat3 to suppress Th17 responses in systemic lupus. *Kidney International*, *89*(1), 158–166. https://doi.org/10.1038/KI.2015.296

Kobayashi, S., Yoshida, K., Ward, J. M., Letterio, J. J., Longenecker, G., Yaswen, L., … Kulkarni, A. B. (1999). β2-Microglobulin-Deficient Background Ameliorates Lethal Phenotype of the TGF-β1 Null Mouse. *The Journal of Immunology*, *163*(7), 4013–4019.

Koch, M. A., Tucker-Heard, G., Perdue, N. R., Killebrew, J. R., Urdahl, K. B., & Campbell, D. J. (2009). The transcription factor T-bet controls regulatory T cell homeostasis and function during type 1 inflammation. *Nature Immunology*, *10*(6), 595–602. https://doi.org/10.1038/ni.1731

Koenen, H. J. P. M., Fasse, E., & Joosten, I. (2005). CD27/CFSE-based ex vivo selection of highly suppressive alloantigen-specific human regulatory T cells. *Journal of Immunology*, *174*(12), 7573–7583. https://doi.org/10.4049/JIMMUNOL.174.12.7573

Koga, T., Ichinose, K., Mizui, M., Crispín, J. C., & Tsokos, G. C. (2012). Calcium/calmodulin-dependent protein kinase IV suppresses IL-2 production and regulatory T cell activity in lupus. *Journal of Immunology (Baltimore, Md. : 1950)*, *189*(7), 3490–3496. https://doi.org/10.4049/JIMMUNOL.1201785

Kohm, A. P., Carpentier, P. A., Anger, H. A., & Miller, S. D. (2002). Cutting edge: CD4+CD25+ regulatory T cells suppress antigen-specific autoreactive immune responses and central nervous system inflammation during active experimental autoimmune encephalomyelitis. *Journal of Immunology*, *169*(9), 4712–4716. https://doi.org/10.4049/JIMMUNOL.169.9.4712

Kojima, A., & Prehn, R. T. (1981). Genetic susceptibility to post-thymectomy autoimmune diseases in mice. *Immunogenetics*, *14*(1), 15–27. https://doi.org/10.1007/BF00344296

Komatsu, N., Okamoto, K., Sawa, S., Nakashima, T., Oh-Hora, M., Kodama, T., … Takayanagi, H. (2013). Pathogenic conversion of Foxp3+ T cells into TH17 cells in autoimmune arthritis. *Nature Medicine 2013 20:1*, *20*(1), 62–68. https://doi.org/10.1038/nm.3432

Kordasti, S., Costantini, B., Seidl, T., Perez Abellan, P., Martinez Llordella, M., McLornan, D., … Mufti, G. J. (2016). Deep phenotyping of Tregs identifies an immune signature for idiopathic aplastic anemia and predicts response to treatment. *Blood*, *128*(9), 1193–1205. https://doi.org/10.1182/blood-2016-03-703702

Kornete, M., Sgouroudis, E., & Piccirillo, C. A. (2012). ICOS-Dependent Homeostasis and Function of Foxp3+ Regulatory T Cells in Islets of Nonobese Diabetic Mice. *The Journal of Immunology*, *188*(3), 1064–1074. https://doi.org/10.4049/JIMMUNOL.1101303

Kraczyk, B., Remus, R., & Hardt, C. (2014). CD49d- Treg Cells with High Suppressive Capacity are Remarkably Less Efficient on Activated CD45RA- than on Naive CD45RA+ Teff Cells. *Cellular Physiology and Biochemistry*, *34*(2), 346–355. https://doi.org/10.1159/000363004

Kühn, R., Löhler, J., Rennick, D., Rajewsky, K., & Müller, W. (1993). Interleukin-10-deficient mice develop chronic enterocolitis. *Cell*, *75*(2), 263–274. https://doi.org/10.1016/0092-8674(93)80068-P

Kulkarni, A. B., Huh, C. G., Becker, D., Geiser, A., Lyght, M., Flanders, K. C., … Karlsson, S. (1993). Transforming growth factor beta 1 null mutation in mice causes excessive inflammatory response and early death. *Proceedings of the National Academy of Sciences of the United States of America*, *90*(2), 770–774. https://doi.org/10.1073/PNAS.90.2.770

Kullberg, M. C., Hay, V., Cheever, A. W., Mamura, M., Sher, A., Letterio, J. J., … Piccirillo, C. A. (2005). TGF-β1 production by CD4+CD25+ regulatory T cells is not essential for suppression of intestinal inflammation. *European Journal of Immunology*, *35*(10), 2886–2895. https://doi.org/10.1002/EJI.200526106

Lafaille, M. A. C. de, Lino, A. C., Kutchukhidze, N., & Lafaille, J. J. (2004). CD25− T Cells Generate CD25+Foxp3+ Regulatory T Cells by Peripheral Expansion. *The Journal of Immunology*, *173*(12), 7259–7268. https://doi.org/10.4049/JIMMUNOL.173.12.7259

Landuyt, A. E., Klocke, B. J., Colvin, T. B., Schoeb, T. R., & Maynard, C. L. (2019). Cutting Edge: ICOS-Deficient Regulatory T Cells Display Normal Induction of Il10 but Readily Downregulate Expression of Foxp3. *The Journal of Immunology*, *202*(4), 1039–1044. https://doi.org/10.4049/JIMMUNOL.1801266/-/DCSUPPLEMENTAL

Landwehr-Kenzel, S., Zobel, A., Hoffmann, H., Landwehr, N., Schmueck-Henneresse, M., Schachtner, T., … Reinke, P. (2018). Ex vivo expanded natural regulatory T cells from patients with end-stage renal disease or kidney transplantation are useful for autologous cell therapy. *Kidney International*, *93*(6), 1452–1464. https://doi.org/10.1016/J.KINT.2018.01.021

Lathrop, S. K., Bloom, S. M., Rao, S. M., Nutsch, K., Lio, C.-W., Santacruz, N., … Hsieh, C.-S. (2011). Peripheral education of the immune system by colonic commensal microbiota. *Nature*, *478*(7368), 250–254. https://doi.org/10.1038/nature10434

Lawson, J. M., Tremble, J., Dayan, C., Beyan, H., Leslie, R. D. G., Peakman, M., & Tree, T. I. M. (2008). Increased resistance to CD4+CD25hi regulatory T cell-mediated suppression in patients with type 1 diabetes. *Clinical and Experimental Immunology*, *154*(3), 353–359. https://doi.org/10.1111/J.1365-2249.2008.03810.X

Lee, J. H., Ulrich, B., Cho, J., Park, J., & Kim, C. H. (2011). Progesterone promotes differentiation of human cord blood fetal T cells into T regulatory cells but suppresses their differentiation into Th17 cells. *Journal of Immunology*, *187*(4), 1778–1787. https://doi.org/10.4049/JIMMUNOL.1003919

Lee, K., Nguyen, V., Lee, K. M., Kang, S. M., & Tang, Q. (2014). Attenuation of donor-reactive T cells allows effective control of allograft rejection using regulatory T cell therapy. *American*

Journal of Transplantation, *14*(1), 27–38. https://doi.org/10.1111/AJT.12509
Lee, S. Y., Lee, S. H., Yang, E. J., Kim, E. K., Kim, J. K., Shin, D. Y., & Cho, M. La. (2015). Metformin Ameliorates Inflammatory Bowel Disease by Suppression of the STAT3 Signaling Pathway and Regulation of the between Th17/Treg Balance. *PloS One*, *10*(9), e0135858. https://doi.org/10.1371/JOURNAL.PONE.0135858
Legorreta-Haquet, M. V., Chávez-Rueda, K., Chávez-Sánchez, L., Cervera-Castillo, H., Zenteno-Galindo, E., Barile-Fabris, L., … Blanco-Favela, F. (2016). Function of Treg Cells Decreased in Patients With Systemic Lupus Erythematosus Due To the Effect of Prolactin. *Medicine*, *95*(5), e2384. https://doi.org/10.1097/MD.0000000000002384
Lekva, T., Norwitz, E. R., Aukrust, P., & Ueland, T. (2016). Impact of Systemic Inflammation on the Progression of Gestational Diabetes Mellitus. *Current Diabetes Reports*, *16*(4), 1–11. https://doi.org/10.1007/S11892-016-0715-9/FIGURES/1
Letterio, J. J., Geiser, A. G., Kulkarni, A. B., Dang, H., Kong, L., Nakabayashi, T., … Roberts, A. B. (1996). Autoimmunity associated with TGF-beta1-deficiency in mice is dependent on MHC class II antigen expression. *Journal of Clinical Investigation*, *98*(9), 2109–2119. https://doi.org/10.1172/JCI119017
Leung, M. W., Shen, S., & Lafaille, J. J. (2009). TCR-dependent differentiation of thymic Foxp3+ cells is limited to small clonal sizes. The Journal of experimental medicine, 206(10), 2121–2130. https://doi.org/10.1084/jem.20091033
Levings, M. K., Sangregorio, R., & Roncarolo, M. G. (2001). Human Cd25+Cd4+ T Regulatory Cells Suppress Naive and Memory T Cell Proliferation and Can Be Expanded in Vitro without Loss of Function. *The Journal of Experimental Medicine*, *193*(11), 1295–1302. https://doi.org/10.1084/JEM.193.11.1295
Li, M. O., Wan, Y. Y., & Flavell, R. A. (2007). T Cell-Produced Transforming Growth Factor-β1 Controls T Cell Tolerance and Regulates Th1- and Th17-Cell Differentiation. *Immunity*, *26*(5), 579–591. https://doi.org/10.1016/j.immuni.2007.03.014
Li, W., Deng, C., Yang, H., & Wang, G. (2019). The regulatory T cell in active systemic lupus erythematosus patients: A systemic review and meta-analysis. *Frontiers in Immunology*, *10*, 159. https://doi.org/10.3389/FIMMU.2019.00159/BIBTEX
Li, X., Mai, J., Virtue, A., Yin, Y., Gong, R., Sha, X., … Yang, X. F. (2012). IL-35 Is a Novel Responsive Anti-inflammatory Cytokine — A New System of Categorizing Anti-inflammatory Cytokines. *PLoS ONE*, *7*(3), e33628. https://doi.org/10.1371/JOURNAL.PONE.0033628
Liang, B., Workman, C., Lee, J., Chew, C., Dale, B. M., Colonna, L., … Clynes, R. (2008). Regulatory T Cells Inhibit Dendritic Cells by Lymphocyte Activation Gene-3 Engagement of MHC Class II. *The Journal of Immunology*, *180*(9), 5916–5926. https://doi.org/10.4049/JIMMUNOL.180.9.5916
Lindheimer, M. D., & Chesley, L. C. (1987). Early onset pre-eclampsia: recognition of underlying renal disease. *British Medical Journal (Clinical Research Ed.)*, *294*(6586), 1547–1548. https://doi.org/10.1136/bmj.294.6586.1547-b
Lindley, S., Dayan, C. M., Bishop, A., Roep, B. O., Peatman, M., & Tree, T. I. M. (2005). Defective Suppressor Function in CD4+CD25+ T-Cells From Patients With Type 1 Diabetes. *Diabetes*, *54*(1), 92–99. https://doi.org/10.2337/DIABETES.54.1.92
Lio, C. W. J., & Hsieh, C. S. (2008). A two-step process for thymic regulatory T cell development. *Immunity*, *28*(1), 100–111. https://doi.org/10.1016/J.IMMUNI.2007.11.021
Liu, W., Putnam, A. L., Xu-Yu, Z., Szot, G. L., Lee, M. R., Zhu, S., … Bluestone, J. A. (2006). CD127 expression inversely correlates with FoxP3 and suppressive function of human CD4+ T reg cells. *The Journal of Experimental Medicine*, *203*(7), 1701–1711. https://doi.org/10.1084/jem.20060772
Lobo, T. F., Borges, C. de M., Mattar, R., Gomes, C. P., de Angelo, A. G. S., Pendeloski, K. P. T., & Daher, S. (2018). Impaired Treg and NK cells profile in overweight women with gestational diabetes mellitus. *American Journal of Reproductive Immunology*, *79*(3), e12810. https://doi.org/10.1111/AJI.12810
Long, A. E., Tatum, M., Mikacenic, C., & Buckner, J. H. (2017). A novel and rapid method to quantify Treg mediated suppression of CD4 T cells. *Journal of Immunological Methods*, *449*, 15–22. https://doi.org/10.1016/j.jim.2017.06.009
Long, S. A., Cerosaletti, K., Bollyky, P. L., Tatum, M., Shilling, H., Zhang, S., … Buckner, J. H. (2010). Defects in IL-2R Signaling Contribute to Diminished Maintenance of FOXP3 Expression in CD4+CD25+ Regulatory T-Cells of Type 1 Diabetic Subjects. *Diabetes*, *59*(2), 407–415. https://doi.org/10.2337/DB09-0694

Loza, M. J., Shane Anderson, A., O'Rourke, K. S., Wood, J., & Khan, I. U. (2011). T –cell specific defect in expression of the NTPDase CD39 as a biomarker for lupus. *Cellular Immunology*, *271*(1), 110–117. https://doi.org/10.1016/J.CELLIMM.2011.06.010

Lugli, E., Dominguez, M. H., Gattinoni, L., Chattopadhyay, P. K., Bolton, D. L., Song, K., … Roederer, M. (2013). Superior T memory stem cell persistence supports long-lived T cell memory. *The Journal of Clinical Investigation*, *123*(2), 594–599. https://doi.org/10.1172/JCI66327

Lugli, E., Gattinoni, L., Roberto, A., Mavilio, D., Price, D. A., Restifo, N. P., & Roederer, M. (2013). Identification, isolation and in vitro expansion of human and nonhuman primate T stem cell memory cells. *Nature Protocols*, *8*(1), 33–42. https://doi.org/10.1038/nprot.2012.143

Luo, Y., Xu, C., Wang, B., Niu, Q., Su, X., Bai, Y., … Feng, X. (2021). Single-cell transcriptomic analysis reveals disparate effector differentiation pathways in human Treg compartment. *Nature Communications*, *12*(1), 3913. https://doi.org/10.1038/S41467-021-24213-6

Ma, L., Mauro, C., Cornish, G. H., Chai, J.-G., Coe, D., Fu, H., … Marelli-Berg, F. M. (2010). Ig gene-like molecule CD31 plays a nonredundant role in the regulation of T-cell immunity and tolerance. *Proceedings of the National Academy of Sciences of the United States of America*, *107*(45), 19461–19466. https://doi.org/10.1073/pnas.1011748107

MacDonald, K. N., Ivison, S., Hippen, K. L., Hoeppli, R. E., Hall, M., Zheng, G., … Levings, M. K. (2019). Cryopreservation timing is a critical process parameter in a thymic regulatory T-cell therapy manufacturing protocol. *Cytotherapy*, *21*(12), 1216–1233. https://doi.org/10.1016/J.JCYT.2019.10.011

Mahmoud, F., Abul, H., Omu, A., & Haines, D. (2005). Lymphocyte Sub-populations in Gestational Diabetes. *American Journal of Reproductive Immunology*, *53*(1), 21–29. https://doi.org/10.1111/J.1600-0897.2004.00241.X

Malek, T. R., Yu, A., Vincek, V., Scibelli, P., & Kong, L. (2002). CD4 regulatory T cells prevent lethal autoimmunity in IL-2Rbeta-deficient mice. Implications for the nonredundant function of IL-2. *Immunity*, *17*(2), 167–178. https://doi.org/10.1016/S1074-7613(02)00367-9

Mandapathil, M., Hilldorfer, B., Szczepanski, M. J., Czystowska, M., Szajnik, M., Ren, J., … Whiteside, T. L. (2010). Generation and accumulation of immunosuppressive adenosine by human CD4+CD25highFOXP3+ regulatory T cells. *The Journal of Biological Chemistry*, *285*(10), 7176–7186. https://doi.org/10.1074/jbc.M109.047423

Mandapathil, M., Lang, S., Gorelik, E., & Whiteside, T. L. (2009). Isolation of functional human regulatory T cells (Treg) from the peripheral blood based on the CD39 expression. *Journal of Immunological Methods*, *346*(1–2), 55–63. https://doi.org/10.1016/J.JIM.2009.05.004

Marek-Trzonkowska, N., Myśliwiec, M., Dobyszuk, A., Grabowska, M., Derkowska, I., Juścińska, J., … Trzonkowski, P. (2014). Therapy of type 1 diabetes with CD4+CD25highCD127-regulatory T cells prolongs survival of pancreatic islets — Results of one year follow-up. *Clinical Immunology*, *153*(1), 23–30. https://doi.org/10.1016/J.CLIM.2014.03.016

Marek, N., Bieniaszewska, M., Krzystyniak, A., Juścińska, J., Myśliwska, J., Witkowski, P., … Trzonkowski, P. (2011). The Time is Crucial for Ex Vivo Expansion of T Regulatory Cells for Therapy: *Http://Dx.Doi.Org/10.3727/096368911X566217*, *20*(11–12), 1747–1758. https://doi.org/10.3727/096368911X566217

Marelli-Berg, F. M., Clement, M., Mauro, C., & Caligiuri, G. (2013). An immunologist's guide to CD31 function in T-cells. *Journal of Cell Science*, *126*(Pt 11), 2343–2352. https://doi.org/10.1242/jcs.124099

Marie, J. C., Letterio, J. J., Gavin, M., & Rudensky, A. Y. (2005). TGF-β1 maintains suppressor function and Foxp3 expression in CD4+CD25+ regulatory T cells. *The Journal of Experimental Medicine*, *201*(7), 1061–1067. https://doi.org/10.1084/JEM.20042276

Markert, M. L., Boeck, A., Hale, L. P., Kloster, A. L., McLaughlin, T. M., Batchvarova, M. N., … Mahaffey, S. M. (1999). Transplantation of Thymus Tissue in Complete DiGeorge Syndrome. *Http://Dx.Doi.Org/10.1056/NEJM199910143411603*, *341*(16), 1180–1189. https://doi.org/10.1056/NEJM199910143411603

Mason, G. M., Lowe, K., Melchiotti, R., Ellis, R., de Rinaldis, E., Peakman, M., … Tree, T. I. M. (2015). Phenotypic Complexity of the Human Regulatory T Cell Compartment Revealed by Mass Cytometry. *Journal of Immunology (Baltimore, Md. : 1950)*, *195*(5), 2030–2037. https://doi.org/10.4049/jimmunol.1500703

Massaia, M., Perrin, L., Bianchi, A., Ruedi, J., Attisano, C., Altieri, D., Rijkers, G. T., & Thompson, L. F. (1990). Human T cell activation. Synergy between CD73 (ecto-5'-

nucleotidase) and signals delivered through CD3 and CD2 molecules. Journal of immunology (Baltimore, Md. : 1950), 145(6), 1664–1674.
Mathew, J. M., H.-Voss, J., LeFever, A., Konieczna, I., Stratton, C., He, J., … Leventhal, J. R. (2018). A Phase I Clinical Trial with Ex Vivo Expanded Recipient Regulatory T cells in Living Donor Kidney Transplants. *Scientific Reports*, *8*(1), 7428. https://doi.org/10.1038/s41598-018-25574-7
Maude, S. L., Laetsch, T. W., Buechner, J., Rives, S., Boyer, M., Bittencourt, H., … Grupp, S. A. (2018). Tisagenlecleucel in Children and Young Adults with B-Cell Lymphoblastic Leukemia. *The New England Journal of Medicine*, *378*(5), 439–448. https://doi.org/10.1056/NEJMOA1709866
McClymont, S. A., Putnam, A. L., Lee, M. R., Esensten, J. H., Liu, W., Hulme, M. A., … Brusko, T. M. (2011). Plasticity of human regulatory T cells in healthy subjects and patients with type 1 diabetes. *Journal of Immunology*, *186*(7), 3918–3926. https://doi.org/10.4049/jimmunol.1003099
Mekie, M., Mekonnen, W., & Assegid, M. (2020). Cohabitation duration, obstetric, behavioral and nutritional factors predict preeclampsia among nulliparous women in West Amhara Zones of Ethiopia: Age matched case control study. *PLoS ONE*, *15*(1), e0228127. https://doi.org/10.1371/JOURNAL.PONE.0228127
Miyao, T., Floess, S., Setoguchi, R., Luche, H., Fehling, H. J., Waldmann, H., … Hori, S. (2012). Plasticity of Foxp3(+) T cells reflects promiscuous Foxp3 expression in conventional T cells but not reprogramming of regulatory T cells. *Immunity*, *36*(2), 262–275. https://doi.org/10.1016/J.IMMUNI.2011.12.012
Miyara, M., Chader, D., Sage, E., Sugiyama, D., Nishikawa, H., Bouvry, D., … Gorochov, G. (2015). Sialyl Lewis x (CD15s) identifies highly differentiated and most suppressive FOXP3high regulatory T cells in humans. *Proceedings of the National Academy of Sciences of the United States of America*, *112*(23), 7225–7230. https://doi.org/10.1073/pnas.1508224112
Miyara, M., Yoshioka, Y., Kitoh, A., Shima, T., Wing, K., Niwa, A., … Sakaguchi, S. (2009). Functional Delineation and Differentiation Dynamics of Human CD4+ T Cells Expressing the FoxP3 Transcription Factor. *Immunity*, *30*(6), 899–911. https://doi.org/10.1016/J.IMMUNI.2009.03.019
Mjösberg, J., Berg, G., Ernerudh, J., & Ekerfelt, C. (2007). CD4+ CD25+ regulatory T cells in human pregnancy: development of a Treg-MLC-ELISPOT suppression assay and indications of paternal specific Tregs. *Immunology*, *120*(4), 456–466. https://doi.org/10.1111/J.1365-2567.2006.02529.X
Moradi, B., Schnatzer, P., Hagmann, S., Rosshirt, N., Gotterbarm, T., Kretzer, J. P., … Tretter, T. (2014). CD4+CD25+/highCD127low/- regulatory T cells are enriched in rheumatoid arthritis and osteoarthritis joints-analysis of frequency and phenotype in synovial membrane, synovial fluid and peripheral blood. *Arthritis Research and Therapy*, *16*(2), R97. https://doi.org/10.1186/AR4545/FIGURES/3
Moran, A. E., Holzapfel, K. L., Xing, Y., Cunningham, N. R., Maltzman, J. S., Punt, J., & Hogquist, K. A. (2011). T cell receptor signal strength in Treg and iNKT cell development demonstrated by a novel fluorescent reporter mouse. The Journal of experimental medicine, 208(6), 1279–1289. https://doi.org/10.1084/jem.20110308
Moran, C. J., Walters, T. D., Guo, C. H., Kugathasan, S., Klein, C., Turner, D., … Muise, A. M. (2013). IL-10R Polymorphisms are Associated with Very Early-Onset Ulcerative Colitis. *Inflammatory Bowel Diseases*, *19*(1), 115–123. https://doi.org/10.1002/IBD.22974
Morgan, D. A., Ruscetti, F. W., & Gallo, R. (1976). Selective in vitro growth of T lymphocytes from normal human bone marrows. *Science*, *193*(4257), 1007–1008. https://doi.org/10.1126/SCIENCE.181845
Morgan, M. E., Flierman, R., Van Duivenvoorde, L. M., Witteveen, H. J., Van Ewijk, W., Van Laar, J. M., … Toes, R. E. M. (2005). Effective treatment of collagen-induced arthritis by adoptive transfer of CD25+ regulatory T cells. *Arthritis and Rheumatism*, *52*(7), 2212–2221. https://doi.org/10.1002/ART.21195
Morrissey, P. J., Charrier, K., Braddy, S., Liggitt, D., & Watson, J. D. (1993). CD4+ T cells that express high levels of CD45RB induce wasting disease when transferred into congenic severe combined immunodeficient mice. Disease development is prevented by cotransfer of purified CD4+ T cells. *The Journal of Experimental Medicine*, *178*(1), 237–244. https://doi.org/10.1084/JEM.178.1.237
Murai, M., Turovskaya, O., Kim, G., Cheroutre, H., Kronenberg, M., & Madan, R. (2009).

Interleukin 10 acts on regulatory T cells to maintain expression of the transcription factor Foxp3 and suppressive function in mice with colitis. *Nature Immunology*, *10*(11), 1178–1184. https://doi.org/10.1038/NI.1791

Nadkarni, S., Smith, J., Sferruzzi-Perri, A. N., Ledwozyw, A., Kishore, M., Haas, R., … Perretti, M. (2016). Neutrophils induce proangiogenic T cells with a regulatory phenotype in pregnancy. *Proceedings of the National Academy of Sciences of the United States of America*, *113*(52), E8415–E8424. https://doi.org/10.1073/PNAS.1611944114/-/DCSUPPLEMENTAL

Naganuma, M., Wiznerowicz, E. B., Lappas, C. M., Linden, J., Worthington, M. T., & Ernst, P. B. (2006). Cutting Edge: Critical Role for A2A Adenosine Receptors in the T Cell-Mediated Regulation of Colitis. *The Journal of Immunology*, *177*(5), 2765–2769. https://doi.org/10.4049/JIMMUNOL.177.5.2765

Nakagawa, H., Sido, J. M., Reyes, E. E., Kiers, V., Cantor, H., & Kim, H. J. (2016). Instability of Helios-deficient Tregs is associated with conversion to a T-effector phenotype and enhanced antitumor immunity. *Proceedings of the National Academy of Sciences of the United States of America*, *113*(22), 6248–6253. https://doi.org/10.1073/PNAS.1604765113/-/DCSUPPLEMENTAL

Nakamura, K., Kitani, A., Fuss, I., Pedersen, A., Harada, N., Nawata, H., & Strober, W. (2004). TGF-beta 1 plays an important role in the mechanism of CD4+CD25+ regulatory T cell activity in both humans and mice. *Journal of Immunology (Baltimore, Md. : 1950)*, *172*(2), 834–842. https://doi.org/10.4049/JIMMUNOL.172.2.834

Negrotto, L., Farez, M. F., & Correale, J. (2016). Immunologic Effects of Metformin and Pioglitazone Treatment on Metabolic Syndrome and Multiple Sclerosis. *JAMA Neurology*, *73*(5), 520–528. https://doi.org/10.1001/JAMANEUROL.2015.4807

Newton-Nash, D. K., & Newman, P. J. (1999). A New Role for Platelet-Endothelial Cell Adhesion Molecule-1 (CD31): Inhibition of TCR-Mediated Signal Transduction. *The Journal of Immunology*, *163*(2), 682–688. Retrieved from http://www.jimmunol.org/content/163/2/682.abstract

Niedbala, W., Wei, X. Q., Cai, B., Hueber, A. J., Leung, B. P., McInnes, I. B., & Liew, F. Y. (2007). IL-35 is a novel cytokine with therapeutic effects against collagen-induced arthritis through the expansion of regulatory T cells and suppression of Th17 cells. *European Journal of Immunology*, *37*(11), 3021–3029. https://doi.org/10.1002/EJI.200737810

Nolte, M. A., Van Olffen, R. W., Van Gisbergen, K. P. J. M., & Van Lier, R. A. W. (2009). Timing and tuning of CD27–CD70 interactions: the impact of signal strength in setting the balance between adaptive responses and immunopathology. *Immunological Reviews*, *229*(1), 216–231. https://doi.org/https://doi.org/10.1111/j.1600-065X.2009.00774.x

Nosko, A., Kluger, M. A., Diefenhardt, P., Melderis, S., Wegscheid, C., Tiegs, G., … Steinmetz, O. M. (2017). T-bet enhances regulatory T cell fitness and directs control of th1 responses in Crescentic GN. *Journal of the American Society of Nephrology*, *28*(1), 185–196. https://doi.org/10.1681/ASN.2015070820/-/DCSUPPLEMENTAL

Noval Rivas, M., Burton, O. T., Wise, P., Charbonnier, L.-M., Georgiev, P., Oettgen, H. C., … Chatila, T. A. (2015). Regulatory T Cell Reprogramming toward a Th2-Cell-like Lineage Impairs Oral Tolerance and Promotes Food Allergy. *Immunity*, *42*(3), 512–523. https://doi.org/10.1016/J.IMMUNI.2015.02.004

Oberle, N., Eberhardt, N., Falk, C. S., Krammer, P. H., & Suri-Payer, E. (2007). Rapid Suppression of Cytokine Transcription in Human CD4+CD25− T Cells by CD4+Foxp3+ Regulatory T Cells: Independence of IL-2 Consumption, TGF-β, and Various Inhibitors of TCR Signaling. *The Journal of Immunology*, *179*(6), 3578–3587. https://doi.org/10.4049/JIMMUNOL.179.6.3578

Ohkura, N., Hamaguchi, M., Morikawa, H., Sugimura, K., Tanaka, A., Ito, Y., … Sakaguchi, S. (2012). T Cell Receptor Stimulation-Induced Epigenetic Changes and Foxp3 Expression Are Independent and Complementary Events Required for Treg Cell Development. *Immunity*, *37*(5), 785–799. https://doi.org/10.1016/J.IMMUNI.2012.09.010

Ohkura, N., & Sakaguchi, S. (2020). Transcriptional and epigenetic basis of Treg cell development and function: its genetic anomalies or variations in autoimmune diseases. *Cell Research*, *30*(6), 465–474. https://doi.org/10.1038/s41422-020-0324-7

Onizuka, S., Tawara, I., Shimizu, J., Sakaguchi, S., Fujita, T., & Nakayama, E. (1999). Tumor Rejection by in Vivo Administration of Anti-CD25 (Interleukin-2 Receptor α) Monoclonal Antibody1. *Cancer Research*, *59*(13), 3128–3133.

Ono, M., Yaguchi, H., Ohkura, N., Kitabayashi, I., Nagamura, Y., Nomura, T., … Sakaguchi, S.

(2007). Foxp3 controls regulatory T-cell function by interacting with AML1/Runx1. *Nature*, *446*(7136), 685–689. https://doi.org/10.1038/nature05673

Ou, K., Hamo, D., Schulze, A., Roemhild, A., Kaiser, D., Gasparoni, G., … Polansky, J. K. (2021). Strong Expansion of Human Regulatory T Cells for Adoptive Cell Therapy Results in Epigenetic Changes Which May Impact Their Survival and Function. *Frontiers in Cell and Developmental Biology*, *9*, 751590. https://doi.org/10.3389/FCELL.2021.751590/FULL

Ouyang, W., Beckett, O., Ma, Q., & Li, M. O. (2010). Transforming Growth Factor-β Signaling Curbs Thymic Negative Selection Promoting Regulatory T Cell Development. *Immunity*, *32*(5), 642–653. https://doi.org/10.1016/J.IMMUNI.2010.04.012

Pacholczyk, R., Ignatowicz, H., Kraj, P., & Ignatowicz, L. (2006). Origin and T cell receptor diversity of Foxp3+CD4+CD25+ T cells. *Immunity*, *25*(2), 249–259. https://doi.org/10.1016/J.IMMUNI.2006.05.016

Paeschke, S., Chen, F., Horn, N., Fotopoulou, C., Zambon-Bertoja, A., Sollwedel, A., … Zenclussen, A. C. (2005). Pre-eclampsia is not associated with changes in the levels of regulatory T cells in peripheral blood. *American Journal of Reproductive Immunology*, *54*(6), 384–389. https://doi.org/10.1111/J.1600-0897.2005.00334.X

Pandiyan, P., Zheng, L., Ishihara, S., Reed, J., & Lenardo, M. J. (2007). CD4+CD25+Foxp3+ regulatory T cells induce cytokine deprivation–mediated apoptosis of effector CD4+ T cells. *Nature Immunology*, *8*(12), 1353–1362. https://doi.org/10.1038/ni1536

Paolino, M., Koglgruber, R., Cronin, S. J. F., Uribesalgo, I., Rauscher, E., Harreiter, J., … Penninger, J. M. (2021). RANK links thymic regulatory T cells to fetal loss and gestational diabetes in pregnancy. *Nature*, *589*(7842), 442–447. https://doi.org/10.1038/S41586-020-03071-0

Paterson, A. M., Lovitch, S. B., Sage, P. T., Juneja, V. R., Lee, Y., Trombley, J. D., … Sharpe, A. H. (2015). Deletion of CTLA-4 on regulatory T cells during adulthood leads to resistance to autoimmunity. *Journal of Experimental Medicine*, *212*(10), 1603–1621. https://doi.org/10.1084/JEM.20141030

Pendeloski, K. P. T., Mattar, R., Torloni, M. R., Gomes, C. P., Alexandre, S. M., & Daher, S. (2015). Immunoregulatory molecules in patients with gestational diabetes mellitus. *Endocrine*, *50*(1), 99–109. https://doi.org/10.1007/S12020-015-0567-0/FIGURES/4

Penhale, W. J., Stumbles, P. A., Huxtable, C. R., Sutherlanld, R. J., & Pethick, D. W. (1990). Induction of Diabetes in PVG/c Strain Rats by Manipulation of the Immune System. *Autoimmunity*, *7*(2–3), 169–179. https://doi.org/10.3109/08916939008993389

Pennington, D. J., Silva-Santos, B., Silberzahn, T., Escórcio-Correia, M., Woodward, M. J., Roberts, S. J., Smith, A. L., Dyson, P. J., & Hayday, A. C. (2006). Early events in the thymus affect the balance of effector and regulatory T cells. Nature, 444(7122), 1073–1077. https://doi.org/10.1038/nature06051

Pesenacker, A. M., Bending, D., Ursu, S., Wu, Q., Nistala, K., & Wedderburn, L. R. (2013). CD161 defines the subset of FoxP3+ T cells capable of producing proinflammatory cytokines. *Blood*, *121*(14), 2647–2658. https://doi.org/10.1182/BLOOD-2012-08-443473

Powrie, F., Leach, M. W., Mauze, S., Caddie, L. B., & Coffman, R. L. (1993). Phenotypically distinct subsets of CD4+ T cells induce or protect from chronic intestinal inflammation in C. B-17 scid mice. *International Immunology*, *5*(11), 1461–1471. https://doi.org/10.1093/INTIMM/5.11.1461

Powrie, F., & Mason, D. (1990). OX-22high CD4+ T cells induce wasting disease with multiple organ pathology: prevention by the OX-22low subset. *The Journal of Experimental Medicine*, *172*(6), 1701–1708. https://doi.org/10.1084/JEM.172.6.1701

Putnam, A. L., Brusko, T. M., Lee, M. R., Liu, W., Szot, G. L., Ghosh, T., … Bluestone, J. A. (2009). Expansion of Human Regulatory T-Cells From Patients With Type 1 Diabetes. *Diabetes*, *58*(3), 652. https://doi.org/10.2337/DB08-1168

Qiao, Y. L., Jiao, W. E., Xu, S., Kong, Y. G., Deng, Y. Q., Yang, R., … Chen, S. M. (2022). Allergen immunotherapy enhances the immunosuppressive effects of Treg cells to alleviate allergic rhinitis by decreasing PU-1+ Treg cell numbers. *International Immunopharmacology*, *112*, 109187. https://doi.org/10.1016/J.INTIMP.2022.109187

Qureshi, O. S., Zheng, Y., Nakamura, K., Attridge, K., Manzotti, C., Schmidt, E. M., … Sansom, D. M. (2011). Trans-endocytosis of CD80 and CD86: a molecular basis for the cell extrinsic function of CTLA-4. *Science*, *332*(6029), 600–603. https://doi.org/10.1126/SCIENCE.1202947

Raffin, C., Vo, L. T., & Bluestone, J. A. (2019). Treg cell-based therapies: challenges and perspectives. *Nature Reviews Immunology*, *20*(3), 158–172.

https://doi.org/10.1038/s41577-019-0232-6
Read, S., Malmström, V., & Powrie, F. (2000). Cytotoxic T Lymphocyte–Associated Antigen 4 Plays an Essential Role in the Function of Cd25+Cd4+ Regulatory Cells That Control Intestinal Inflammation. *The Journal of Experimental Medicine*, *192*(2), 295–302. https://doi.org/10.1084/JEM.192.2.295
Reading, J. L., Roobrouck, V. D., Hull, C. M., Becker, P. D., Beyens, J., Valentin-Torres, A., … Tree, T. (2021). Augmented Expansion of Treg Cells From Healthy and Autoimmune Subjects via Adult Progenitor Cell Co-Culture. *Frontiers in Immunology*, *12*, 716606. https://doi.org/10.3389/FIMMU.2021.716606/FULL
Reddi Rani, P., & Begum, J. (2016). Screening and Diagnosis of Gestational Diabetes Mellitus, Where Do We Stand. *Journal of Clinical and Diagnostic Research*, *10*(4), QE01–QE04. https://doi.org/10.7860/JCDR/2016/17588.7689
Reif, K., Burgering, B. M. T., & Cantrell, D. A. (1997). Phosphatidylinositol 3-Kinase Links the Interleukin-2 Receptor to Protein Kinase B and p70 S6 Kinase *. *Journal of Biological Chemistry*, *272*(22), 14426–14433. https://doi.org/10.1074/JBC.272.22.14426
Ren, X., Ye, F., Jiang, Z., Chu, Y., Xiong, S., & Wang, Y. (2007). Involvement of cellular death in TRAIL/DR5-dependent suppression induced by CD4+CD25+ regulatory T cells. *Cell Death & Differentiation 2007 14:12*, *14*(12), 2076–2084. https://doi.org/10.1038/sj.cdd.4402220
Robertson, S. A., Green, E. S., Care, A. S., Moldenhauer, L. M., Prins, J. R., Louise Hull, M., … Dekker, G. (2019). Therapeutic potential of regulatory T cells in preeclampsia-opportunities and challenges. *Frontiers in Immunology*, *10*, 478. https://doi.org/10.3389/FIMMU.2019.00478/BIBTEX
Roth, T. L., Puig-Saus, C., Yu, R., Shifrut, E., Carnevale, J., Li, P. J., … Marson, A. (2018). Reprogramming human T cell function and specificity with non-viral genome targeting. *Nature*, *559*(7714), 405–409. https://doi.org/10.1038/S41586-018-0326-5
Rowan, J. A., Hague, W. M., Gao, W., Battin, M. R., & Moore, M. P. (2008). Metformin versus Insulin for the Treatment of Gestational Diabetes. *New England Journal of Medicine*, *358*(19), 2003–2015. https://doi.org/10.1056/NEJMOA0707193/SUPPL_FILE/NEJM_ROWAN_2003SA1.PDF
Rubtsov, Y. P., Rasmussen, J. P., Chi, E. Y., Fontenot, J., Castelli, L., Ye, X., … Rudensky, A. Y. (2008). Regulatory T cell-derived interleukin-10 limits inflammation at environmental interfaces. *Immunity*, *28*(4), 546–558. https://doi.org/10.1016/J.IMMUNI.2008.02.017
Ruprecht, C. R., Gattorno, M., Ferlito, F., Gregorio, A., Martini, A., Lanzavecchia, A., & Sallusto, F. (2005). Coexpression of CD25 and CD27 identifies FoxP3+ regulatory T cells in inflamed synovia. *The Journal of Experimental Medicine*, *201*(11), 1793–1803. https://doi.org/10.1084/JEM.20050085
Russell, S. M., Johnston, J. A., Noguchi, M., Kawamura, M., Bacon, C. M., Friedmann, M., … Leonard, W. J. (1994). Interaction of IL-2Rβ and γc Chains with Jak1 and Jak3: Implications for XSCID and XCID. *Science*, *266*(5187), 1042–1045. https://doi.org/10.1126/SCIENCE.7973658
Sabatini, D. M., Erdjument-Bromage, H., Lui, M., Tempst, P., & Snyder, S. H. (1994). RAFT1: A mammalian protein that binds to FKBP12 in a rapamycin-dependent fashion and is homologous to yeast TORs. *Cell*, *78*(1), 35–43. https://doi.org/10.1016/0092-8674(94)90570-3
Sadlack, B., Merz, H., Schorle, H., Schimpl, A., Feller, A. C., & Horak, I. (1993). Ulcerative colitis-like disease in mice with a disrupted interleukin-2 gene. *Cell*, *75*(2), 253–261. https://doi.org/10.1016/0092-8674(93)80067-O
Safinia, N., Vaikunthanathan, T., Fraser, H., Thirkell, S., Lowe, K., Blackmore, L., … Lombardi, G. (2016). Successful expansion of functional and stable regulatory T cells for immunotherapy in liver transplantation. *Oncotarget*, *7*(7), 7563–7577. https://doi.org/10.18632/oncotarget.6927
Sage, P. T., Francisco, L. M., Carman, C. V, & Sharpe, A. H. (2013). The receptor PD-1 controls follicular regulatory T cells in the lymph nodes and blood. *Nature Immunology*, *14*(2), 152–161. https://doi.org/10.1038/ni.2496
Saito, T., Nishikawa, H., Wada, H., Nagano, Y., Sugiyama, D., Atarashi, K., … Sakaguchi, S. (2016). Two FOXP3+CD4+ T cell subpopulations distinctly control the prognosis of colorectal cancers. *Nature Medicine*, *22*(6), 679–684. https://doi.org/10.1038/nm.4086
Sakaguchi, S. (2011). Regulatory T Cells: History and Perspective. In *Regulatory T Cells. Methods in Molecular Biology (Methods and Protocols)* (pp. 3–17).

https://doi.org/10.1007/978-1-61737-979-6_1
Sakaguchi, S., Fukuma, K., Kuribayashi, K., & Masuda, T. (1985). Organ-specific autoimmune diseases induced in mice by elimination of T cell subset. I. Evidence for the active participation of T cells in natural self-tolerance; deficit of a T cell subset as a possible cause of autoimmune disease. *The Journal of Experimental Medicine*, *161*(1), 72–87. https://doi.org/10.1084/JEM.161.1.72
Sakaguchi, S., Sakaguchi, N., Asano, M., Itoh, M., & Toda, M. (1995). Immunologic self-tolerance maintained by activated T cells expressing IL-2 receptor alpha-chains (CD25). Breakdown of a single mechanism of self-tolerance causes various autoimmune diseases. *Journal of Immunology*, *155*(3), 1151–1164. Retrieved from http://www.ncbi.nlm.nih.gov/pubmed/7636184
Sakaguchi, S., Takahashi, T., & Nishizuka, Y. (1982a). Study on cellular events in post-thymectomy autoimmune oophoritis in mice. II. Requirement of Lyt-1 cells in normal female mice for the prevention of oophoritis. *The Journal of Experimental Medicine*, *156*(6), 1577–1586. https://doi.org/10.1084/JEM.156.6.1577
Sakaguchi, S., Takahashi, T., & Nishizuka, Y. (1982b). Study on cellular events in postthymectomy autoimmune oophoritis in mice. I. Requirement of Lyt-1 effector cells for oocytes damage after adoptive transfer. *The Journal of Experimental Medicine*, *156*(6), 1565–1576. https://doi.org/10.1084/JEM.156.6.1565
Salam, N., Rane, S., Das, R., Faulkner, M., Gund, R., Kandpal, U., … Bal, V. (2013). T cell ageing: Effects of age on development, survival & function. *The Indian Journal of Medical Research*, *138*(5), 595–608. Retrieved from /pmc/articles/PMC3928693/
Salomon, B., Lenschow, D. J., Rhee, L., Ashourian, N., Singh, B., Sharpe, A., & Bluestone, J. A. (2000). B7/CD28 costimulation is essential for the homeostasis of the CD4+CD25+ immunoregulatory T cells that control autoimmune diabetes. *Immunity*, *12*(4), 431–440. https://doi.org/10.1016/S1074-7613(00)80195-8
Sambucci, M., Gargano, F., De Rosa, V., De Bardi, M., Picozza, M., Placido, R., … Borsellino, G. (2018). FoxP3 isoforms and PD-1 expression by T regulatory cells in multiple sclerosis. *Scientific Reports 2018 8:1*, *8*(1), 1–9. https://doi.org/10.1038/s41598-018-21861-5
Samstein, R. M., Josefowicz, S. Z., Arvey, A., Treuting, P. M., & Rudensky, A. Y. (2012). Extrathymic generation of regulatory T cells in placental mammals mitigates maternal-fetal conflict. *Cell*, *150*(1), 29–38. https://doi.org/10.1016/j.cell.2012.05.031
Sánchez-Fueyo, A., Whitehouse, G., Grageda, N., Cramp, M. E., Lim, T. Y., Romano, M., … Lombardi, G. (2020). Applicability, safety, and biological activity of regulatory T cell therapy in liver transplantation. *American Journal of Transplantation*, *20*(4), 1125–1136. https://doi.org/10.1111/AJT.15700
Santner-Nanan, B., Peek, M. J., Khanam, R., Richarts, L., Zhu, E., Fazekas de St Groth, B., & Nanan, R. (2009). Systemic increase in the ratio between Foxp3+ and IL-17-producing CD4+ T cells in healthy pregnancy but not in preeclampsia. *Journal of Immunology*, *183*(11), 7023–7030. https://doi.org/10.4049/JIMMUNOL.0901154
Sasada, T., Kimura, M., Yoshida, Y., Kanai, M., & Takabayashi, A. (2003). CD4+CD25+ regulatory T cells in patients with gastrointestinal malignancies: possible involvement of regulatory T cells in disease progression. *Cancer*, *98*(5), 1089–1099. https://doi.org/10.1002/CNCR.11618
Sasaki, Y., Darmochwal-Kolarz, D., Suzuki, D., Sakai, M., Ito, M., Shima, T., … Saito, S. (2007). Proportion of peripheral blood and decidual CD4+ CD25bright regulatory T cells in pre-eclampsia. *Clinical and Experimental Immunology*, *149*(1), 139–145. https://doi.org/10.1111/J.1365-2249.2007.03397.X
Sasaki, Y., Sakai, M., Miyazaki, S., Higuma, S., Shiozaki, A., & Saito, S. (2004). Decidual and peripheral blood CD4+CD25+ regulatory T cells in early pregnancy subjects and spontaneous abortion cases. *Molecular Human Reproduction*, *10*(5), 347–353. https://doi.org/10.1093/MOLEHR/GAH044
Sather, B. D., Treuting, P., Perdue, N., Miazgowicz, M., Fontenot, J. D., Rudensky, A. Y., & Campbell, D. J. (2007). Altering the distribution of Foxp3+ regulatory T cells results in tissue-specific inflammatory disease. *The Journal of Experimental Medicine*, *204*(6), 1335–1347. https://doi.org/10.1084/JEM.20070081
Saunders, J. A. H., Estes, K. A., Kosloski, L. M., Allen, H. E., Dempsey, K. M., Torres-Russotto, D. R., … Gendelman, H. E. (2012). CD4+ Regulatory and Effector/Memory T Cell Subsets Profile Motor Dysfunction in Parkinson's Disease. *Journal of Neuroimmune Pharmacology*, *7*(4), 927–938. https://doi.org/10.1007/S11481-012-9402-Z

Sawitzki, B., Harden, P. N., Reinke, P., Moreau, A., Hutchinson, J. A., Game, D. S., … Geissler, E. K. (2020). Regulatory cell therapy in kidney transplantation (The ONE Study): a harmonised design and analysis of seven non-randomised, single-arm, phase 1/2A trials. *The Lancet*, *395*(10237), 1627–1639. https://doi.org/10.1016/S0140-6736(20)30167-7

Schaefer, C., Kim, G. G., Albers, A., Hoermann, K., Myers, E. N., & Whiteside, T. L. (2005). Characteristics of CD4+CD25+ regulatory T cells in the peripheral circulation of patients with head and neck cancer. *British Journal of Cancer*, *92*(5), 913–920. https://doi.org/10.1038/SJ.BJC.6602407

Schaier, M., Seissler, N., Schmitt, E., Meuer, S., Hug, F., Zeier, M., & Steinborn, A. (2012). DRhigh+CD45RA−-Tregs Potentially Affect the Suppressive Activity of the Total Treg Pool in Renal Transplant Patients. *PLoS ONE*, *7*(3), e34208. https://doi.org/10.1371/JOURNAL.PONE.0034208

Schatz, D. G., & Ji, Y. (2011). Recombination centres and the orchestration of V(D)J recombination. *Nature Reviews Immunology 2011 11:4*, *11*(4), 251–263. https://doi.org/10.1038/nri2941

Scheffold, A., Hühn, J., & Höfer, T. (2005). Regulation of CD4+CD25+ regulatory T cell activity: it takes (IL-)two to tango. *European Journal of Immunology*, *35*(5), 1336–1341. https://doi.org/10.1002/EJI.200425887

Schlossberger, V., Schober, L., Rehnitz, J., Schaier, M., Zeier, M., Meuer, S., … Steinborn, A. (2013). The success of assisted reproduction technologies in relation to composition of the total regulatory T cell (Treg) pool and different Treg subsets. *Human Reproduction*, *28*(11), 3062–3073. https://doi.org/10.1093/HUMREP/DET316

Schmidt, A., Oberle, N., Weiß, E. M., Vobis, D., Frischbutter, S., Baumgrass, R., … Krammer, P. H. (2011). Human regulatory T cells rapidly suppress T cell receptor-induced Ca 2+, NF-κB, and NFAT signaling in conventional T cells. *Science Signaling*, *4*(204), ra90. https://doi.org/10.1126/SCISIGNAL.2002179/SUPPL_FILE/4_RA90_SM.PDF

Schmidt, A. M., Lu, W., Sindhava, V. J., Huang, Y., Burkhardt, J. K., Yang, E., Riese, M. J., Maltzman, J. S., Jordan, M. S., & Kambayashi, T. (2015). Regulatory T cells require TCR signaling for their suppressive function. Journal of immunology (Baltimore, Md. : 1950), 194(9), 4362–4370. https://doi.org/10.4049/jimmunol.1402384

Schneider, A., & Buckner, J. H. (2011). Assessment of suppressive capacity by human regulatory T cells using a reproducible, bi-directional CFSE-based in vitro assay. *Methods in Molecular Biology*, *707*, 233–241. https://doi.org/10.1007/978-1-61737-979-6_15/FIGURES/1

Schneider, A., Long, S. A., Cerosaletti, K., Ni, C. T., Samuels, P., Kita, M., & Buckner, J. H. (2013). In active relapsing-remitting multiple sclerosis, effector T cell resistance to adaptive Tregs involves IL-6-mediated signaling. *Science Translational Medicine*, *5*(170), 170ra15. https://doi.org/10.1126/SCITRANSLMED.3004970/SUPPL_FILE/5-170RA15_SM.PDF

Schober, L., Radnai, D., Spratte, J., Kisielewicz, A., Schmitt, E., Mahnke, K., … Steinborn, A. (2014). The role of regulatory T cell (Treg) subsets in gestational diabetes mellitus. *Clinical and Experimental Immunology*, *177*(1), 76–85. https://doi.org/10.1111/CEI.12300

Scholz, G., Jandus, C., Zhang, L., Grandclément, C., Lopez-Mejia, I. C., Soneson, C., … Romero, P. (2016). Modulation of mTOR Signalling Triggers the Formation of Stem Cell-like Memory T Cells. *EBioMedicine*, *4*, 50–61. https://doi.org/10.1016/J.EBIOM.2016.01.019

Schubert, D., Bode, C., Kenefeck, R., Hou, T. Z., Wing, J. B., Kennedy, A., … Grimbacher, B. (2014). Autosomal-dominant immune dysregulation syndrome in humans with CTLA4 mutations. *Nature Medicine*, *20*(12), 1410–1416. https://doi.org/10.1038/NM.3746

Schuiveling, M., Vazirpanah, N., Radstake, T. R. D. J., Zimmermann, M., & Broen, J. C. A. (2018). Metformin, A New Era for an Old Drug in the Treatment of Immune Mediated Disease? *Current Drug Targets*, *19*(8), 945–959. https://doi.org/10.2174/1389450118666170613081730

Schuler, P. J., Saze, Z., Hong, C.-S., Muller, L., Gillespie, D. G., Cheng, D., … Whiteside, T. L. (2014). Human CD4+ CD39+ regulatory T cells produce adenosine upon co-expression of surface CD73 or contact with CD73+ exosomes or CD73+ cells. *Clinical and Experimental Immunology*, *177*(2), 531–543. https://doi.org/10.1111/cei.12354

Scottà, C., Esposito, M., Fazekasova, H., Fanelli, G., Edozie, F. C., Ali, N., … Lombardi, G. (2013). Differential effects of rapamycin and retinoic acid on expansion, stability and suppressive qualities of human CD4+CD25+FOXP3+ T regulatory cell subpopulations.

Haematologica, *98*(8), 1291–1299. https://doi.org/10.3324/HAEMATOL.2012.074088
Seay, H. R., Putnam, A. L., Cserny, J., Posgai, A. L., Rosenau, E. H., Wingard, J. R., … Brusko, T. M. (2016). Expansion of Human Tregs from Cryopreserved Umbilical Cord Blood for GMP-Compliant Autologous Adoptive Cell Transfer Therapy. *Molecular Therapy - Methods and Clinical Development*, *4*, 178–191. https://doi.org/10.1016/j.omtm.2016.12.003
Seddiki, N., Santner-Nanan, B., Tangye, S. G., Alexander, S. I., Solomon, M., Lee, S., … Fazekas De Saint Groth, B. (2006). Persistence of naive CD45RA+ regulatory T cells in adult life. *Blood*, *107*(7), 2830–2838. https://doi.org/10.1182/BLOOD-2005-06-2403
Seddon, B., & Mason, D. (1999). Peripheral autoantigen induces regulatory T cells that prevent autoimmunity. The Journal of experimental medicine, 189(5), 877–882. https://doi.org/10.1084/jem.189.5.877
Seng, A., Krausz, K. L., Pei, D., Koestler, D. C., Fischer, R. T., Yankee, T. M., & Markiewicz, M. A. (2020). Coexpression of FOXP3 and a Helios isoform enhances the effectiveness of human engineered regulatory T cells. *Blood Advances*, *4*(7), 1325–1339. https://doi.org/10.1182/BLOODADVANCES.2019000965
Setoguchi, R., Hori, S., Takahashi, T., & Sakaguchi, S. (2005). Homeostatic maintenance of natural Foxp3+ CD25+ CD4+ regulatory T cells by interleukin (IL)-2 and induction of autoimmune disease by IL-2 neutralization. *Journal of Experimental Medicine*, *201*(5), 723–735. https://doi.org/10.1084/JEM.20041982
Sharfe, N., Dadi, H. K., Shahar, M., & Roifman, C. M. (1997). Human immune disorder arising from mutation of the α chain of the interleukin-2 receptor. *Proceedings of the National Academy of Sciences of the United States of America*, *94*(7), 3168–3171. https://doi.org/10.1073/PNAS.94.7.3168
Shen, P., Roch, T., Lampropoulou, V., O'Connor, R. A., Stervbo, U., Hilgenberg, E., … Fillatreau, S. (2014). IL-35-producing B cells are critical regulators of immunity during autoimmune and infectious diseases. *Nature*, *507*(7492), 366–370. https://doi.org/10.1038/nature12979
Sheu, A., Chan, Y., Ferguson, A., Bakhtyari, M. B., Hawke, W., White, C., … Lau, S. M. (2018). A proinflammatory CD4 + T cell phenotype in gestational diabetes mellitus. *Diabetologia*, *61*(7), 1633–1643. https://doi.org/10.1007/S00125-018-4615-1
Shevach, E. M. (2018a). Foxp3+ T Regulatory Cells: Still Many Unanswered Questions-A Perspective After 20 Years of Study. *Frontiers in Immunology*, *9*, 1048. https://doi.org/10.3389/fimmu.2018.01048
Shevach, E. M. (2018b). Foxp3+ T regulatory cells: Still many unanswered Questions-A perspective after 20 years of study. *Frontiers in Immunology*, *9*, 1048. https://doi.org/10.3389/FIMMU.2018.01048/BIBTEX
Shigeta, N., Kumasawa, K., Tanaka, A., Badger Wing, J., Nakamura, H., Sakaguchi, S., & Kimura, T. (2020). Dynamics of effector and naïve Regulatory T cells throughout pregnancy. *Journal of Reproductive Immunology*, *140*, 103135. https://doi.org/10.1016/J.JRI.2020.103135
Shimizu, J., Yamazaki, S., & Sakaguchi, S. (1999). Induction of Tumor Immunity by Removing CD25+CD4+T Cells: A Common Basis Between Tumor Immunity and Autoimmunity. *The Journal of Immunology*, *163*(10), 5211–5218. Retrieved from http://www.jimmunol.org/content/163/10/5211.abstract
Sifnaios, E., Mastorakos, G., Psarra, K., Panagopoulos, N. D., Panoulis, K., Vitoratos, N., … Creatsas, G. (2019). Gestational Diabetes and T-cell (Th1/Th2/Th17/Treg) Immune Profile. *In Vivo*, *33*(1), 31–40. https://doi.org/10.21873/INVIVO.11435
Smyth, L. A., Ratnasothy, K., Tsang, J. Y. S., Boardman, D., Warley, A., Lechler, R., & Lombardi, G. (2013). CD73 expression on extracellular vesicles derived from CD4+CD25+Foxp3+ T cells contributes to their regulatory function. *European Journal of Immunology*, *43*(9), 2430–2440. https://doi.org/10.1002/EJI.201242909
Snir, O., Rieck, M., Gebe, J. A., Yue, B. B., Rawlings, C. A., Nepom, G., … Buckner, J. H. (2011). Identification and functional characterization of T cells reactive to citrullinated vimentin in HLA-DRB1*0401-positive humanized mice and rheumatoid arthritis patients. *Arthritis and Rheumatism*, *63*(10), 2873–2883. https://doi.org/10.1002/ART.30445
Sojka, D. K., Hughson, A., Sukiennicki, T. L., & Fowell, D. J. (2005). Early Kinetic Window of Target T Cell Susceptibility to CD25+ Regulatory T Cell Activity. *The Journal of Immunology*, *175*(11), 7274–7280. https://doi.org/10.4049/JIMMUNOL.175.11.7274
Somerset, D. A., Zheng, Y., Kilby, M. D., Sansom, D. M., & Drayson, M. T. (2004a). Normal human pregnancy is associated with an elevation in the immune suppressive CD25+

CD4+ regulatory T-cell subset. *Immunology*, *112*(1), 38–43. https://doi.org/10.1111/J.1365-2567.2004.01869.X

Somerset, D. A., Zheng, Y., Kilby, M. D., Sansom, D. M., & Drayson, M. T. (2004b). Normal human pregnancy is associated with an elevation in the immune suppressive CD25+ CD4+ regulatory T-cell subset. *Immunology*, *112*(1), 38–43. https://doi.org/10.1111/J.1365-2567.2004.01869.X

Stagg, J., Divisekera, U., McLaughlin, N., Sharkey, J., Pommey, S., Denoyer, D., … Smyth, M. J. (2010). Anti-CD73 antibody therapy inhibits breast tumor growth and metastasis. *Proceedings of the National Academy of Sciences of the United States of America*, *107*(4), 1547–1552. https://doi.org/10.1073/PNAS.0908801107

Steinborn, A., Schmitt, E., Kisielewicz, A., Rechenberg, S., Seissler, N., Mahnke, K., … Sohn, C. (2012). Pregnancy-associated diseases are characterized by the composition of the systemic regulatory T cell (Treg) pool with distinct subsets of Tregs. *Clinical and Experimental Immunology*, *167*(1), 84–98. https://doi.org/10.1111/J.1365-2249.2011.04493.X

Stephens, L. A., Mottet, C., Mason, D., & Powrie, F. (2001). Human CD4(+)CD25(+) thymocytes and peripheral T cells have immune suppressive activity in vitro. *European Journal of Immunology*, *31*(4), 1247–1254. https://doi.org/10.1002/1521-4141(200104)31:4<1247::AID-IMMU1247gt;3.0.CO;2-M

Strauss, L., Czystowska, M., Szajnik, M., Mandapathil, M., & Whiteside, T. L. (2009). Differential Responses of Human Regulatory T Cells (Treg) and Effector T Cells to Rapamycin. *PLoS ONE*, *4*(6), e5994. https://doi.org/10.1371/JOURNAL.PONE.0005994

Strauss, L., Whiteside, T. L., Knights, A., Bergmann, C., Knuth, A., & Zippelius, A. (2007). Selective Survival of Naturally Occurring Human CD4+CD25+Foxp3+ Regulatory T Cells Cultured with Rapamycin. *The Journal of Immunology*, *178*(1), 320–329. https://doi.org/10.4049/JIMMUNOL.178.1.320

Sugiyama, D., Nishikawa, H., Maeda, Y., Nishioka, M., Tanemura, A., Katayama, I., … Sakaguchi, S. (2013). Anti-CCR4 mAb selectively depletes effector-type FoxP3+CD4+ regulatory T cells, evoking antitumor immune responses in humans. *Proceedings of the National Academy of Sciences*, *110*(44), 17945–17950. https://doi.org/10.1073/PNAS.1316796110

Sun, T., Meng, F., Zhao, H., Yang, M., Zhang, R., Yu, Z., … Zang, S. (2020). Elevated First-Trimester Neutrophil Count Is Closely Associated With the Development of Maternal Gestational Diabetes Mellitus and Adverse Pregnancy Outcomes. *Diabetes*, *69*(7), 1401–1410. https://doi.org/10.2337/DB19-0976

Sun, Y., Tian, T., Gao, J., Liu, X., Hou, H., Cao, R., … Guo, L. (2016). Metformin ameliorates the development of experimental autoimmune encephalomyelitis by regulating T helper 17 and regulatory T cells in mice. *Journal of Neuroimmunology*, *292*, 58–67. https://doi.org/10.1016/J.JNEUROIM.2016.01.014

Sung, J. L., Lin, J. T., & Gorham, J. D. (2003). CD28 co-stimulation regulates the effect of transforming growth factor-β1 on the proliferation of naïve CD4+ T cells. *International Immunopharmacology*, *3*(2), 233–245. https://doi.org/10.1016/S1567-5769(02)00276-X

Suzuki, H., Kündig, T. M., Furlonger, C., Wakeham, A., Timms, E., Matsuyama, T., … Mak, T. W. (1995). Deregulated T cell activation and autoimmunity in mice lacking interleukin-2 receptor beta. *Science*, *268*(5216), 1472–1476. https://doi.org/10.1126/SCIENCE.7770771

Szymczak-Workman, A. L., Delgoffe, G. M., Green, D. R., & Vignali, D. A. A. (2011). Cutting Edge: Regulatory T Cells Do Not Mediate Suppression via Programmed Cell Death Pathways. *The Journal of Immunology*, *187*(9), 4416–4420. https://doi.org/10.4049/JIMMUNOL.1100548

Taams, L. S., Smith, J., Rustin, M. H., Salmon, M., Poulter, L. W., & Akbar, A. N. (2001). Human anergic/suppressive CD4+CD25+ T cells: a highly differentiated and apoptosis-prone population. *European Journal of Immunology*, *31*(4), 1122–1131. https://doi.org/10.1002/1521-4141(200104)31:4<1122::AID-IMMU1122>3.0.CO;2-P

Taams, L. S., Vukmanovic-Stejic, M., Smith, J., Dunne, P. J., Fletcher, J. M., Plunkett, F. J., … Akbar, A. N. (2002). Antigen-specific T cell suppression by human CD4+CD25+ regulatory T cells. *European Journal of Immunology*, *32*(6), 1621–1630. https://doi.org/https://doi.org/10.1002/1521-4141(200206)32:6<1621::AID-IMMU1621>3.0.CO;2-Q

Takahashi, T., Kuniyasu, Y., Toda, M., Sakaguchi, N., Itoh, M., Iwata, M., … Sakaguchi, S. (1998). Immunologic self-tolerance maintained by CD25+CD4+ naturally anergic and

suppressive T cells: induction of autoimmune disease by breaking their anergic/suppressive state. *International Immunology*, *10*(12), 1969–1980. https://doi.org/10.1093/INTIMM/10.12.1969
Takahashi, T., Tagami, T., Yamazaki, S., Uede, T., Shimizu, J., Sakaguchi, N., … Sakaguchi, S. (2000). Immunologic Self-Tolerance Maintained by Cd25+Cd4+Regulatory T Cells Constitutively Expressing Cytotoxic T Lymphocyte–Associated Antigen 4. *The Journal of Experimental Medicine*, *192*(2), 303–310. https://doi.org/10.1084/JEM.192.2.303
Takeshita, T., Asao, H., Ohtani, K., Ishii, N., Kumaki, S., Tanaka, N., … Sugamura, K. (1992). Cloning of the γ Chain of the Human IL-2 Receptor. *Science*, *257*(5068), 379–382. https://doi.org/10.1126/SCIENCE.1631559
Tan, T. G., Mathis, D., & Benoist, C. (2016). Singular role for T-BET + CXCR3 + regulatory T cells in protection from autoimmune diabetes. *Proceedings of the National Academy of Sciences*, *113*(49), 14103–14108. https://doi.org/10.1073/pnas.1616710113
Tanaka, A., & Sakaguchi, S. (2019). Targeting Treg cells in cancer immunotherapy. *European Journal of Immunology*, *49*(8), 1140–1146. https://doi.org/10.1002/EJI.201847659
Tanaka, M., Tsujimoto, Y., Goto, K., Kumahara, K., Onishi, S., Iwanari, S., … Takeoka, H. (2015). Preeclampsia before 20 weeks of gestation: a case report and review of the literature. *CEN Case Reports*, *4*(1), 55–60. https://doi.org/10.1007/s13730-014-0140-3
Tang, Q., Henriksen, K. J., Bi, M., Finger, E. B., Szot, G., Ye, J., … Bluestone, J. A. (2004). In Vitro–expanded Antigen-specific Regulatory T Cells Suppress Autoimmune Diabetes. *The Journal of Experimental Medicine*, *199*(11), 1455–1465. https://doi.org/10.1084/JEM.20040139
Thornton, A. M., Donovan, E. E., Piccirillo, C. A., & Shevach, E. M. (2004). Cutting Edge: IL-2 Is Critically Required for the In Vitro Activation of CD4+CD25+ T Cell Suppressor Function. *The Journal of Immunology*, *172*(11), 6519–6523. https://doi.org/10.4049/JIMMUNOL.172.11.6519
Thornton, A. M., Korty, P. E., Tran, D. Q., Wohlfert, E. A., Murray, P. E., Belkaid, Y., & Shevach, E. M. (2010). Expression of Helios, an Ikaros transcription factor family member, differentiates thymic-derived from peripherally induced Foxp3+ T regulatory cells. *Journal of Immunology (Baltimore, Md. : 1950)*, *184*(7), 3433–3441. https://doi.org/10.4049/jimmunol.0904028
Thornton, A. M., Lu, J., Korty, P. E., Kim, Y. C., Martens, C., Sun, P. D., & Shevach, E. M. (2019). Helios+ and Helios− Treg subpopulations are phenotypically and functionally distinct and express dissimilar TCR repertoires. *European Journal of Immunology*, *49*(3), 398–412. https://doi.org/https://doi.org/10.1002/eji.201847935
Thornton, A. M., & Shevach, E. M. (1998). CD4+CD25+ Immunoregulatory T Cells Suppress Polyclonal T Cell Activation In Vitro by Inhibiting Interleukin 2 Production. *Journal of Experimental Medicine*, *188*(2), 287–296. https://doi.org/10.1084/JEM.188.2.287
Thornton, A. M., & Shevach, E. M. (2000). Suppressor Effector Function of CD4+CD25+ Immunoregulatory T Cells Is Antigen Nonspecific. *The Journal of Immunology*, *164*(1), 183–190. https://doi.org/10.4049/JIMMUNOL.164.1.183
Tian, Y., Babor, M., Lane, J., Schulten, V., Patil, V. S., Seumois, G., … Peters, B. (2017). Unique phenotypes and clonal expansions of human CD4 effector memory T cells re-expressing CD45RA. *Nature Communications*, *8*(1), 1473. https://doi.org/10.1038/s41467-017-01728-5
Tilburgs, T., Roelen, D. L., van der Mast, B. J., de Groot-Swings, G. M., Kleijburg, C., Scherjon, S. A., & Claas, F. H. (2008). Evidence for a selective migration of fetus-specific CD4+CD25bright regulatory T cells from the peripheral blood to the decidua in human pregnancy. *Journal of Immunology*, *180*(8), 5737–5745. https://doi.org/10.4049/JIMMUNOL.180.8.5737
Tivol, E. A., Borriello, F., Schweitzer, A. N., Lynch, W. P., Bluestone, J. A., & Sharpe, A. H. (1995). Loss of CTLA-4 leads to massive lymphoproliferation and fatal multiorgan tissue destruction, revealing a critical negative regulatory role of CTLA-4. *Immunity*, *3*(5), 541–547. https://doi.org/10.1016/1074-7613(95)90125-6
Todd, J. A., Evangelou, M., Cutler, A. J., Pekalski, M. L., Walker, N. M., Stevens, H. E., … Waldron-Lynch, F. (2016). Regulatory T Cell Responses in Participants with Type 1 Diabetes after a Single Dose of Interleukin-2: A Non-Randomised, Open Label, Adaptive Dose-Finding Trial. *PLoS Medicine*, *13*(10), e1002139. https://doi.org/10.1371/JOURNAL.PMED.1002139
Todd, J. A., Walker, N. M., Cooper, J. D., Smyth, D. J., Downes, K., Plagnol, V., … Clayton, D.

G. (2007). Robust associations of four new chromosome regions from genome-wide analyses of type 1 diabetes. *Nature Genetics*, *39*(7), 857–864. https://doi.org/10.1038/ng2068

Togashi, Y., Shitara, K., & Nishikawa, H. (2019). Regulatory T cells in cancer immunosuppression — implications for anticancer therapy. *Nature Reviews Clinical Oncology*, *16*(6), 356–371. https://doi.org/10.1038/s41571-019-0175-7

Toldi, G., Rigó, J., Stenczer, B., Vásárhelyi, B., & Molvarec, A. (2011). Increased prevalence of IL-17-producing peripheral blood lymphocytes in pre-eclampsia. *American Journal of Reproductive Immunology*, *66*(3), 223–229. https://doi.org/10.1111/J.1600-0897.2011.00987.X

Toldi, G., Saito, S., Shima, T., Halmos, A., Veresh, Z., Vásárhelyi, B., … Molvarec, A. (2012). The frequency of peripheral blood CD4+ CD25high FoxP3+ and CD4+ CD25- FoxP3+ regulatory T cells in normal pregnancy and pre-eclampsia. *American Journal of Reproductive Immunology*, *68*(2), 175–180. https://doi.org/10.1111/J.1600-0897.2012.01145.X

Toldi, G., Švec, P., Vásárhelyi, B., Mészáros, G., Rigó, J., Tulassay, T., & Treszl, A. (2008). Decreased number of FoxP3+ regulatory T cells in preeclampsia. *Acta Obstetricia et Gynecologica Scandinavica*, *87*(11), 1229–1233. https://doi.org/10.1080/00016340802389470

Toldi, G., Vásárhelyi, Z. E., Rigó, J., Orbán, C., Tamássy, Z., Bajnok, A., … Molvarec, A. (2015). Prevalence of Regulatory T-Cell Subtypes in Preeclampsia. *American Journal of Reproductive Immunology*, *74*(2), 110–115. https://doi.org/10.1111/AJI.12380

Tran, D. Q., Glass, D. D., Uzel, G., Darnell, D. A., Spalding, C., Holland, S. M., & Shevach, E. M. (2009). Analysis of adhesion molecules, target cells and role of interleukin-2 in human FOXP3+ regulatory T cell suppressor function. *Journal of Immunology*, *182*(5), 2929–2938. https://doi.org/10.4049/JIMMUNOL.0803827

Trigueros, C., Ramiro, A. R., Carrasco, Y. R., De Yebenes, V. G., Albar, J. P., & Toribio, M. L. (1998). Identification of a Late Stage of Small Noncycling pTα− Pre-T Cells as Immediate Precursors of T Cell Receptor α/β+ Thymocytes. *The Journal of Experimental Medicine*, *188*(8), 1401–1412. https://doi.org/10.1084/JEM.188.8.1401

Tsuda, H., Michimata, T., Hayakawa, S., Tanebe, K., Sakai, M., Fujimura, M., … Saito, S. (2002). A Th2 chemokine, TARC, produced by trophoblasts and endometrial gland cells, regulates the infiltration of CCR4+ T lymphocytes into human decidua at early pregnancy. *American Journal of Reproductive Immunology*, *48*(1), 1–8. https://doi.org/10.1034/J.1600-0897.2002.01117.X

Tsuda, S., Nakashima, A., Shima, T., & Saito, S. (2019). New paradigm in the role of regulatory T cells during pregnancy. *Frontiers in Immunology*, *10*, 573. https://doi.org/10.3389/FIMMU.2019.00573/BIBTEX

Tsuda, S., Zhang, X., Hamana, H., Shima, T., Ushijima, A., Tsuda, K., … Saito, S. (2018). Clonally Expanded Decidual Effector Regulatory T Cells Increase in Late Gestation of Normal Pregnancy, but Not in Preeclampsia, in Humans. *Frontiers in Immunology*, *9*, 1934. https://doi.org/10.3389/FIMMU.2018.01934

Turner, J. A., Stephen-Victor, E., Wang, S., Rivas, M. N., Abdel-Gadir, A., Harb, H., … Chatila, T. A. (2020). Regulatory T cell-derived TGF-β1 Controls Multiple Checkpoints Governing Allergy and Autoimmunity. *Immunity*, *53*(6), 1202–1214. https://doi.org/10.1016/J.IMMUNI.2020.10.002

Ueno, T., Saito, F., Gray, D. H. D., Kuse, S., Hieshima, K., Nakano, H., … Takahama, Y. (2004). CCR7 Signals Are Essential for Cortex–Medulla Migration of Developing Thymocytes. *The Journal of Experimental Medicine*, *200*(4), 493-505. https://doi.org/10.1084/JEM.20040643

Uhlig, H. H., Coombes, J., Mottet, C., Izcue, A., Thompson, C., Fanger, A., … Powrie, F. (2006). Characterisation of Foxp3+CD4+CD25+ and IL-10 secreting CD4+CD25+ T cells during cure of colitis1. *Journal of Immunology*, *177*(9), 5852–5860. https://doi.org/10.4049/JIMMUNOL.177.9.5852

Valencia, X., Yarboro, C., Illei, G., & Lipsky, P. E. (2007). Deficient CD4+CD25high T Regulatory Cell Function in Patients with Active Systemic Lupus Erythematosus. *The Journal of Immunology*, *178*(4), 2579–2588. https://doi.org/10.4049/JIMMUNOL.178.4.2579

Valmori, D., Merlo, A., Souleimanian, N. E., Hesdorffer, C. S., & Ayyoub, M. (2005). A peripheral circulating compartment of natural naive CD4 Tregs. *The Journal of Clinical*

Investigation, *115*(7), 1953–1962. https://doi.org/10.1172/JCI23963
Valmori, D., Tosello, V., Souleimanian, N. E., Godefroy, E., Scotto, L., Wang, Y., & Ayyoub, M. (2006). Rapamycin-Mediated Enrichment of T Cells with Regulatory Activity in Stimulated CD4+ T Cell Cultures Is Not Due to the Selective Expansion of Naturally Occurring Regulatory T Cells but to the Induction of Regulatory Functions in Conventional CD4+ T Cells. *The Journal of Immunology*, *177*(2), 944–949. https://doi.org/10.4049/JIMMUNOL.177.2.944
Van Der Merwe, P. A., Bodian, D. L., Daenke, S., Linsley, P., & Davis, S. J. (1997). CD80 (B7-1) Binds Both CD28 and CTLA-4 with a Low Affinity and Very Fast Kinetics. *The Journal of Experimental Medicine*, *185*(3), 393–404. https://doi.org/10.1084/JEM.185.3.393
Van Gassen, S., Callebaut, B., Van Helden, M. J., Lambrecht, B. N., Demeester, P., Dhaene, T., & Saeys, Y. (2015). FlowSOM: Using self-organizing maps for visualization and interpretation of cytometry data. *Cytometry Part A*, *87*(7), 636–645. https://doi.org/10.1002/cyto.a.22625
Van Zeebroeck, L., Arroyo Hornero, R., Côrte-Real, B. F., Hamad, I., Meissner, T. B., & Kleinewietfeld, M. (2021). Fast and Efficient Genome Editing of Human FOXP3+ Regulatory T Cells. *Frontiers in Immunology*, *12*, 655122. https://doi.org/10.3389/FIMMU.2021.655122/BIBTEX
Veerapathran, A., Pidala, J., Beato, F., Yu, X. Z., & Anasetti, C. (2011). Ex vivo expansion of human Tregs specific for alloantigens presented directly or indirectly. *Blood*, *118*(20), 5671–5680. https://doi.org/10.1182/BLOOD-2011-02-337097
Venken, K., Hellings, N., Thewissen, M., Somers, V., Hensen, K., Rummens, J. L., … Stinissen, P. (2008). Compromised CD4+ CD25(high) regulatory T-cell function in patients with relapsing-remitting multiple sclerosis is correlated with a reduced frequency of FOXP3-positive cells and reduced FOXP3 expression at the single-cell level. *Immunology*, *123*(1), 79–89. https://doi.org/10.1111/J.1365-2567.2007.02690.X
Venken, K., Thewissen, M., Hellings, N., Somers, V., Hensen, K., Rummens, J. L., & Stinissen, P. (2007). A CFSE based assay for measuring CD4+CD25+ regulatory T cell mediated suppression of auto-antigen specific and polyclonal T cell responses. *Journal of Immunological Methods*, *322*(1–2), 1–11. https://doi.org/10.1016/J.JIM.2007.01.025
Vent-Schmidt, J., Han, J. M., Macdonald, K. G., & Levings, M. K. (2014). The Role of FOXP3 in Regulating Immune Responses. *International Reviews of Immunology*, *33*(2), 110–128. https://doi.org/10.3109/08830185.2013.811657
Venturi, G. M., Conway, R. M., Steeber, D. A., & Tedder, T. F. (2007). CD25+CD4+ regulatory T cell migration requires L-selectin expression: L-selectin transcriptional regulation balances constitutive receptor turnover. *Journal of Immunology*, *178*(1), 291–300. https://doi.org/10.4049/JIMMUNOL.178.1.291
Verma, N. D., Lam, A. D., Chiu, C., Tran, G. T., Hall, B. M., & Hodgkinson, S. J. (2021). Multiple sclerosis patients have reduced resting and increased activated CD4 + CD25 + FOXP3 + T regulatory cells. *Scientific Reports*, *11*(1), 10476. https://doi.org/10.1038/S41598-021-88448-5
Wagner, M. I., Jöst, M., Spratte, J., Schaier, M., Mahnke, K., Meuer, S., … Steinborn, A. (2016). Differentiation of ICOS+ and ICOS−recent thymic emigrant regulatory T cells (RTE Tregs) during normal pregnancy, pre-eclampsia and HELLP syndrome. *Clinical & Experimental Immunology*, *183*(1), 129–142. https://doi.org/10.1111/cei.12693
Wagner, M., Mai, C., Schmitt, E., Mahnke, K., Meuer, S., Eckstein, V., … Steinborn, A. (2015). The role of recent thymic emigrant-regulatory T-cell (RTE-Treg) differentiation during pregnancy. *Immunology and Cell Biology*, *93*(10), 858–867. https://doi.org/10.1038/ICB.2015.51
Wagner, Miriam I, Mai, C., Schmitt, E., Mahnke, K., Meuer, S., Eckstein, V., … Steinborn, A. (2015). The role of recent thymic emigrant-regulatory T-cell (RTE-Treg) differentiation during pregnancy. *Immunology & Cell Biology*, *93*(10), 858–867. https://doi.org/10.1038/icb.2015.51
Wakkach, A., Fournier, N., Brun, V., Breittmayer, J. P., Cottrez, F., & Groux, H. (2003). Characterization of dendritic cells that induce tolerance and T regulatory 1 cell differentiation in vivo. *Immunity*, *18*(5), 605–617. https://doi.org/10.1016/S1074-7613(03)00113-4
Walsh, P. T., Buckler, J. L., Zhang, J., Gelman, A. E., Dalton, N. M., Taylor, D. K., … Turka, L. A. (2006). PTEN inhibits IL-2 receptor–mediated expansion of CD4+ CD25+ Tregs. *Journal of Clinical Investigation*, *116*(9), 2521–2531. https://doi.org/10.1172/JCI28057

Wang, J., Ioan-Facsinay, A., van der Voort, E. I. H., Huizinga, T. W. J., & Toes, R. E. M. (2007). Transient expression of FOXP3 in human activated nonregulatory CD4+ T cells. *European Journal of Immunology*, *37*(1), 129–138. https://doi.org/10.1002/eji.200636435

Wang, Y. Y., Wang, Q., Sun, X. H., Liu, R. Z., Shu, Y., Kanekura, T., … Xiao, R. (2014). DNA hypermethylation of the forkhead box protein 3 (FOXP3) promoter in CD4+ T cells of patients with systemic sclerosis. *British Journal of Dermatology*, *171*(1), 39–47. https://doi.org/10.1111/BJD.12913

Webber, A. B., & Vincenti, F. (2016). An update on calcineurin inhibitor-free regimens: The need persists, but the landscape has changed. *Transplantation*, *100*(4), 836–843. https://doi.org/10.1097/TP.0000000000000872

Weiss, E.-M., Schmidt, A., Vobis, D., Garbi, N., Lahl, K., Mayer, C. T., … Krammer, P. H. (2011). Foxp3-mediated suppression of CD95L expression confers resistance to activation-induced cell death in regulatory T cells. *Journal of Immunology (Baltimore, Md. : 1950)*, *187*(4), 1684–1691. https://doi.org/10.4049/jimmunol.1002321

Wendering, D. J., Amini, L., Schlickeiser, S., Reinke, P., Volk, H. D., & Schmueck-Henneresse, M. (2019). The value of a rapid test of human regulatory T cell function needs to be revised. *Frontiers in Immunology*, *10*, 150. https://doi.org/10.3389/FIMMU.2019.00150/FULL

Whangbo, J. S., Kim, H. T., Mirkovic, N., Leonard, L., Poryanda, S., Silverstein, S., … Koreth, J. (2019). Dose-escalated interleukin-2 therapy for refractory chronic graft-versus-host disease in adults and children. *Blood Advances*, *3*(17), 2550–2561. https://doi.org/10.1182/BLOODADVANCES.2019000631

Whangbo, J. S., Kim, H. T., Nikiforow, S., Koreth, J., Alho, A. C., Falahee, B., … Ritz, J. (2019). Functional analysis of clinical response to low-dose IL-2 in patients with refractory chronic graft-versus-host disease. *Blood Advances*, *3*(7), 984–994. https://doi.org/10.1182/BLOODADVANCES.2018027474

Wilkinson, R., Bruce Lyons, A., Roberts, D., Wong, M. X., Bartley, P. A., & Jackson, D. E. (2002). Platelet endothelial cell adhesion molecule-1 (PECAM-1/CD31) acts as a regulator of B-cell development, B-cell antigen receptor (BCR)–mediated activation, and autoimmune disease. *Blood*, *100*(1), 184–193. https://doi.org/10.1182/BLOOD-2002-01-0027

Willerford, D. M., Chen, J., Ferry, J. A., Davidson, L., Ma, A., & Alt, F. W. (1995). Interleukin-2 receptor alpha chain regulates the size and content of the peripheral lymphoid compartment. *Immunity*, *3*(4), 521–530. https://doi.org/10.1016/1074-7613(95)90180-9

Williams, L. M., & Rudensky, A. Y. (2007). Maintenance of the Foxp3-dependent developmental program in mature regulatory T cells requires continued expression of Foxp3. *Nature Immunology*, *8*(3), 277–284. https://doi.org/10.1038/ni1437

Wollenberg, I., Agua-Doce, A., Hernández, A., Almeida, C., Oliveira, V. G., Faro, J., & Graca, L. (2011). Regulation of the Germinal Center Reaction by Foxp3+ Follicular Regulatory T Cells. *The Journal of Immunology*, *187*(9), 4553–4560. https://doi.org/10.4049/JIMMUNOL.1101328

Wong, M. X., Hayball, J. D., Hogarth, P. M., & Jackson, D. E. (2005). The Inhibitory Co-Receptor, PECAM-1 Provides a Protective Effect in Suppression of Collagen-Induced Arthritis. *Journal of Clinical Immunology*, *25*(1), 19–28. https://doi.org/10.1007/S10875-005-0354-7

Yamazaki, T., Yang, X. O., Chung, Y., Fukunaga, A., Nurieva, R., Pappu, B., … Dong, C. (2008). CCR6 Regulates the Migration of Inflammatory and Regulatory T Cells. *Journal of Immunology*, *181*(12), 8391–8401. https://doi.org/10.4049/JIMMUNOL.181.12.8391

Yang, H., Qiu, L., Chen, G., Ye, Z., Lü, C., & Lin, Q. (2008). Proportional change of CD4+CD25+ regulatory T cells in decidua and peripheral blood in unexplained recurrent spontaneous abortion patients. *Fertility and Sterility*, *89*(3), 656–661. https://doi.org/10.1016/J.FERTNSTERT.2007.03.037

Yang, J. H. M., Cutler, A. J., Ferreira, R. C., Reading, J. L., Cooper, N. J., Wallace, C., … Tree, T. I. M. (2015). Natural variation in IL-2 sensitivity influences regulatory T cell frequency and function in individuals with long-standing type 1 diabetes. *Diabetes*, *64*(11), 3891–3902. https://doi.org/10.2337/DB15-0516

Yang, Y., Liu, L., Liu, B., Li, Q., Wang, Z., Fan, S., … Wang, L. (2018). Functional Defects of Regulatory T Cell Through Interleukin 10 Mediated Mechanism in the Induction of Gestational Diabetes Mellitus. *DNA and Cell Biology*, *37*(3), 278–285. https://doi.org/10.1089/DNA.2017.4005

Ye, C., Brand, D., & Zheng, S. G. (2018). Targeting IL-2: an unexpected effect in treating immunological diseases. *Signal Transduction and Targeted Therapy*, *3*(2). https://doi.org/10.1038/s41392-017-0002-5

Yu, A., Snowhite, I., Vendrame, F., Rosenzwajg, M., Klatzmann, D., Pugliese, A., & Malek, T. R. (2015). Selective IL-2 Responsiveness of Regulatory T Cells Through Multiple Intrinsic Mechanisms Supports the Use of Low-Dose IL-2 Therapy in Type 1 Diabetes. *Diabetes*, *64*(6), 2172–2183. https://doi.org/10.2337/DB14-1322

Yu, X., Harden, K., Gonzalez, L. C., Francesco, M., Chiang, E., Irving, B., … Grogan, J. L. (2009). The surface protein TIGIT suppresses T cell activation by promoting the generation of mature immunoregulatory dendritic cells. *Nature Immunology*, *10*(1), 48–57. https://doi.org/10.1038/ni.1674

Zare, M., Namavar Jahromi, B., & Gharesi-Fard, B. (2019). Analysis of the frequencies and functions of CD4 + CD25 + CD127 low/neg, CD4 + HLA-G +, and CD8 + HLA-G + regulatory T cells in pre-eclampsia. *Journal of Reproductive Immunology*, *133*, 43–51. https://doi.org/10.1016/J.JRI.2019.06.002

Zarnitsyna, V. I., Evavold, B. D., Schoettle, L. N., Blattman, J. N., & Antia, R. (2013). Estimating the Diversity, Completeness, and Cross-Reactivity of the T Cell Repertoire. *Frontiers in Immunology*, *4*(DEC). https://doi.org/10.3389/FIMMU.2013.00485

Zhang, N., Schröppel, B., Lal, G., Jakubzick, C., Mao, X., Chen, D., … Bromberg, J. S. (2009a). Regulatory T cells sequentially migrate from inflamed tissues to draining lymph nodes to suppress the alloimmune response. *Immunity*, *30*(3), 458–469. https://doi.org/10.1016/J.IMMUNI.2008.12.022

Zhang, N., Schröppel, B., Lal, G., Jakubzick, C., Mao, X., Chen, D., … Bromberg, J. S. (2009b). Regulatory T cells sequentially migrate from the site of tissue inflammation to the draining LN to suppress the alloimmune response. *Immunity*, *30*(3), 458–469. https://doi.org/10.1016/J.IMMUNI.2008.12.022

Zhang, X., Zhang, X., Zhuang, L., Xu, C., Li, T. A. O., Zhang, G., & Liu, Y. (2018). Decreased regulatory T-cell frequency and interleukin-35 levels in patients with rheumatoid arthritis. *Experimental and Therapeutic Medicine*, *16*(6), 5366. https://doi.org/10.3892/ETM.2018.6885

Zhang, Y., Joe, G., Hexner, E., Zhu, J., & Emerson, S. G. (2005). Host-reactive CD8+ memory stem cells in graft-versus-host disease. *Nature Medicine*, *11*(12), 1299–1305. https://doi.org/10.1038/nm1326

Zhang, Z., Gothe, F., Pennamen, P., James, J. R., McDonald, D., Mata, C. P., … Lenardo, M. J. (2019). Human interleukin-2 receptor β mutations associated with defects in immunity and peripheral tolerance. *Journal of Experimental Medicine*, *216*(6), 1311–1327. https://doi.org/10.1084/JEM.20182304

Zhao, Y., Zhang, X., Du, N., Sun, H., Chen, L., Bao, H., … Wang, W. J. (2020). Immune checkpoint molecules on T cell subsets of pregnancies with preeclampsia and gestational diabetes mellitus. *Journal of Reproductive Immunology*, *142*, 103208. https://doi.org/10.1016/J.JRI.2020.103208

Zheng, Y., Josefowicz, S., Chaudhry, A., Peng, X. P., Forbush, K., & Rudensky, A. Y. (2010). Role of conserved non-coding DNA elements in the Foxp3 gene in regulatory T-cell fate. *Nature*, *463*(7282), 808–812. https://doi.org/10.1038/nature08750

Zhong, W., Jiang, Y., Ma, H., Wu, J., Jiang, Z., & Zhao, L. (2017). Elevated levels of CCR6+ T helper 22 cells correlate with skin and renal impairment in systemic lupus erythematosus. *Scientific Reports*, *7*(1), 12962. https://doi.org/10.1038/s41598-017-13344-w

Zhou, X., Bailey-Bucktrout, S. L., Jeker, L. T., Penaranda, C., Martínez-Llordella, M., Ashby, M., … Bluestone, J. A. (2009). Instability of the transcription factor Foxp3 leads to the generation of pathogenic memory T cells in vivo. *Nature Immunology*, *10*(9), 1000–1007. https://doi.org/10.1038/ni.1774

Zhu, Y., & Zhang, C. (2016). Prevalence of Gestational Diabetes and Risk of Progression to Type 2 Diabetes: a Global Perspective. *Current Diabetes Reports*, *16*(1), 7. https://doi.org/10.1007/S11892-015-0699-X/FIGURES/3

Zhuang, Y., Zhang, J., Li, Y., Gu, H., Zhao, J., Sun, Y., … Xu, X. (2019). B Lymphocytes Are Predictors of Insulin Resistance in Women with Gestational Diabetes Mellitus. *Endocrine, Metabolic & Immune Disorders Drug Targets*, *19*(3), 358–366. https://doi.org/10.2174/1871530319666190101130300